Queen Mary
University of London

Peripheral blood immune profile in patients with pancreatic cancer

Konstantinos Stasinos MBBS, MRCS, MSc

Candidate no: 200006239

Supervisors: Professor Hemant M Kocher and Professor Claude Chelala

In memory of my dad

Acknowledgements

I would like to express my heartfelt gratitude to Professor Kocher and Professor Chelala, my dedicated supervisors, for their constant support and valuable guidance throughout this Ph.D. journey. Their patience and encouragement have been essential in shaping my research and improving my skills as a scientist.

I am incredibly grateful to the PCRFTB tissue bank for their collaboration, which made this research possible. Access to their extensive tissue repository has been a crucial aspect of my investigations, and I want to thank the whole team for their commitment to advancing scientific knowledge.

A special thank you goes to Amina Saad, whose compassionate work with the patients and donors associated with the tissue bank has been crucial to this study. Her dedication to medical progress has been an inspiration to me.

I want to extend my sincere appreciation to the patients and donors who selflessly contributed to the tissue bank. Their participation has been instrumental in advancing our understanding of a complex disease, and I am deeply grateful for their generosity.

My family deserves a special mention for their support throughout this journey. To my parents and brother, thank you for always believing in me and providing a strong foundation to pursue my academic goals.

I am also indebted to the mentors and colleagues who have contributed to my growth as a researcher. Their collaboration and feedback have enriched my work and motivated me to excel.

I would like to express my gratitude to the Barts Cancer Institute and the Tumor Biology Group in particular, whose support made this study possible both in terms of expertise and emotional support. I will fondly remember being part of this lovely group of people.

Lastly, I want to thank my friends for their companionship and for being a source of joy and support during challenging times.

Completing this MD thesis has been a transformative experience, and I am excited about the possibilities that lie ahead. I am grateful to everyone who has been part of this journey and contributed to its success. Thank you all!

1 CONTENTS

Abbreviations' Table

CAR	Chimeric antigen receptor
CCR7	c-c chemokine receptor 7
CD	Cluster of differentiation
CFSE	Carboxyfluorescein succinimidyl ester
CTL	Cytotoxic T cells
CXCR	CXC motif chemokine receptor
DMSO	Dimethylsulfoxide
EOMES	Eomesodermin
FDR	False discovery rate
FoxP3	Forkhead box protein 3
gag	Group specific antigen
HBV	Hepatitis B virus
HIV	Human immunodeficiency virus
IL-10	Interleukin 10
IL-2	Interleukin 2
IL7Ra	Interleukin 7 receptor a
INF-γ	Interferon gamma
KLRG1	Killer cell lectin-like receptor subfamily G member 1
LAG-3	Lymphocyte activation gene 3
LCMV	Leukocyte choriomeningitis virus
MHCII	Major histocompatibility complex II
MFI	Mean fluorescence intensity
NFAT	Nuclear factor of activated T cells
NR4A	Nuclear receptor subfamily 4A
PBMCs	Peripheral blood mononuclear cells
PD-1	Programmed cell death protein 1
SEB	Staphylococcal enterotoxin B
T-bet	t-box transcription factor
TCF1	T cell factor 1
TCR	T cell receptor
Th	Helper T cell
TILs	Tumour infiltrating lymphocytes
TGF-β	Tumour growth factor beta
TNF-α	Tumour necrosis factor alpha
TSST	Toxic shock syndrome toxin-1
TOX	Thymocyte selection-associated high mobility group box protein
SEB	Staphylococcal enterotoxin B
V2β	Variable 2β domain

Figures

Figure 1	Hypothetical changes in antigen experienced and exhausted T cells before and after surgical de-bulking. The existence of pre-exhausted populations defined by TCF1(Tcf7) expression before the operation may be a valuable signal for recovery of the immune system after removal of the primary focus which would act as a persistent stimulatory signal and therefore a niche of systemic exhaustion. This reversal may be dependent on the presence of sub-clinical metastatic foci even if the initial surgical removal of the tumour was complete.
Figure 2	Experimental set up for the analysis and spectral unmixing of the PDAC samples.
Figure 3	Gating strategy for identification and analysis of T cell subsets.
Figure 4	a) Phred score values showing 3.39% reads following below score of 30. b) Average base quality score per position showing small drop at 5' and 3' ends. c) Bioinformatics analysis pipeline for gene deferential expression of bulk RNA sequencing samples from PDAC patients as implemented on Partek® Flow® suite.
Figure 5	Percentage of memory and effector subsets and expression of inhibitory receptors for CD4 and CD8 T cells who have undergone the exhaustion protocol. A) Representative flow cytometry sub-gating on a CD4 subset (T_{naive}: $CD45RA^+CCR7^+$, $T_{central\ memory}$: $CD45RA^-CCR7^+$, $T_{effectors}$: $CD45RA^-CCR7^-$, TEMRA: $CD45RA^+CCR7^-$). B) Comparison of the exhausted and expanded populations based on memory subsets. C) Comparison of the exhausted and expanded population base on the expression of inhibitory receptors. Results are representative of 4 independent experiments. Statistical analysis performed with Mann-Whitney test. Line represents median. (* $p \leq 0.05$, ** $p \leq 0.01$, *** $p \leq 0.001$)
Figure 6	Comparison of proliferation index between $T_{exhausted}$ and expanded populations, based on memory subsets and expression of inhibitory receptors. A) Representative CFSE plots for CD8 T cells from an exhausted and expanded population. B) Proliferation index comparison of functional subsets between exhausted and expanded T cells. (Comparison was performed for the subsets that would be present on both populations). C) Proliferation index comparison based on the expression of inhibitory receptors. Results are representative of 3 independent experiments. Statistical analysis performed with Mann-Whitney test. Bars present median with interquartile range. (* $p \leq 0.05$, ** $p \leq 0.01$, *** $p \leq 0.001$)
Figure 7	CD8 subsets based on CD45RA and CCR7 sub-gating. Each dot represents a patient with PDAC and separate technical repeats as control from the *in vitro* exhausted and expanded populations. A) Percentage of CD8 naïve cells ($CD45RA^+CCR7^+$). B) Percentage of CD8 central memory cells ($CD45RA^-CCR7^+$). C) Percentage of CD8 effector cells ($CD45RA^-CCR7^-$). D) Percentage of CD8 effector memory cells ($CD45RA^+CCR7^-$). Statistical analysis performed with Kruskal-Wallis test with Dunn's test for multiple comparisons. Bars present median with whiskers representing interquartile range. (* $p \leq 0.05$, ** $p \leq 0.01$, *** $p \leq 0.001$)
Figure 8	CD8 expression of PD1, TIM3 and TCF1. Each dot represents a patient with PDAC and separate technical repeats as control from the *in vitro* exhausted and expanded populations. A) Percentage of CD8 PD1 expressing cells. B) Percentage of CD8 TIM3 expressing cells. C) Percentage of CD8 PD1 and TIM3 expressing cells. D) Percentage of CD8 TCF1 expressing cells. Statistical analysis performed with Kruskal-Wallis test with Dunn's test for multiple comparisons. Bars present median with whiskers representing interquartile range. (* $p \leq 0.05$, ** $p \leq 0.01$, *** $p \leq 0.001$)
Figure 9	CD4 subsets based on CD45RA and CCR7 sub-gating. Each dot represents a patient with PDAC and separate technical repeats as control from the *in vitro* exhausted and expanded populations. A) Percentage of CD4 naïve cells ($CD45RA^+CCR7^+$). B) Percentage of CD4 central memory cells ($CD45RA^-CCR7^+$). C) Percentage of CD4 effector cells ($CD45RA^-CCR7^-$). D) Percentage of CD4 effector memory cells ($CD45RA^+CCR7^-$). Statistical

	analysis performed with Kruskal-Wallis test with Dunn's test for multiple comparisons. Bars present median with whiskers representing interquartile range. (* $p \leq 0.05$, ** $p \leq 0.01$, *** $p \leq 0.001$)
Figure 10	CD4 expression of PD1, TIM3 and TCF1. Each dot represents a patient with PDAC and separate technical repeats as control from the *in vitro* exhausted and expanded populations. A) Percentage of CD4 PD1 expressing cells. B) Percentage of CD4 TIM3 expressing cells. C) Percentage of CD4 PD1 and TIM3 expressing cells. D) Percentage of CD4 TCF1 expressing cells. Statistical analysis performed with Kruskal-Wallis test with Dunn's test for multiple comparisons. Bars present median with whiskers representing interquartile range. (* $p \leq 0.05$, ** $p \leq 0.01$, *** $p \leq 0.001$)
Figure 11	CD4 memory subsets based on CXCR3 and CCR6 expression. Each dot represents a patient with PDAC and separate technical repeats as control from the *in vitro* exhausted and expanded populations. A) Percentage of CD4 Th1 cells ($CXCR3^+CCR6^-$). B) Percentage of CD4 Th2 cells ($CXCR3^-CCR6^-$). C) Percentage of CD4 Th17 cells ($CXCR3^-CCR6^+$). D) Percentage of CD4 Th1Th17 cells ($CXCR3^+CCR6^+$). Statistical analysis performed with Kruskal-Wallis test with Dunn's test for multiple comparisons. Bars present median with whiskers representing interquartile range. (* $p \leq 0.05$, ** $p \leq 0.01$, *** $p \leq 0.001$)
Figure 12	T regulatory cells based on FoxP3 and CD25 expression. Each dot represents a patient with PDAC and separate technical repeats as control from the *in vitro* exhausted and expanded populations. A) Percentage of CD4 T regulatory cells ($FoxP3^+CD25^+$). B) Percentage of CD4 memory T regulatory cells ($FoxP3^+CD25^+CD45RO^+$). Statistical analysis performed with Kruskal-Wallis test with Dunn's test for multiple comparisons. Bars present median with whiskers representing interquartile range. (* $p \leq 0.05$, ** $p \leq 0.01$, *** $p \leq 0.001$)
Figure 13	CD8 subsets based on CD45RA and CCR7 sub-gating. Each dot represents a patient with PDAC and separate technical repeats as control from the *in vitro* exhausted and expanded populations. A) Percentage of CD8 naïve cells ($CD45RA^+CCR7^+$). B) Percentage of CD8 central memory cells ($CD45RA^-CCR7^+$). C) Percentage of CD8 effector cells ($CD45RA^-CCR7^-$). D) Percentage of CD8 effector memory cells ($CD45RA^+CCR7^-$). Statistical analysis performed with Kruskal-Wallis test with Dunn's test for multiple comparisons. Bars present median with whiskers representing interquartile range. (* $p \leq 0.05$, ** $p \leq 0.01$, *** $p \leq 0.001$)
Figure 14	CD8 expression of PD1, TIM3 and TCF1 post-stimulation. Each dot represents a patient with PDAC and separate technical repeats as control from the *in vitro* exhausted and expanded populations. A) Percentage of CD8 PD1 expressing cells. B) Percentage of CD8 TIM3 expressing cells. C) Percentage of CD8 PD1 and TIM3 expressing cells. D) Percentage of CD8 TCF1 expressing cells. Statistical analysis performed with Kruskal-Wallis test with Dunn's test for multiple comparisons. Bars present median with whiskers representing interquartile range. (* $p \leq 0.05$, ** $p \leq 0.01$, *** $p \leq 0.001$)
Figure 15	CD4 subsets based on CD45RA and CCR7 sub-gating. Each dot represents a patient with PDAC and separate technical repeats as control from the *in vitro* exhausted and expanded populations. A) Percentage of CD4 naïve cells ($CD45RA^+CCR7^+$). B) Percentage of CD4 central memory cells ($CD45RA^-CCR7^+$). C) Percentage of CD4 effector cells ($CD45RA^-CCR7^-$). D) Percentage of CD4 effector memory cells ($CD45RA^+CCR7^-$). Statistical analysis performed with Kruskal-Wallis test with Dunn's test for multiple comparisons. Bars present median with whiskers representing interquartile range. (* $p \leq 0.05$, ** $p \leq 0.01$, *** $p \leq 0.001$)

Figure 16	CD4 expression of PD1, TIM3 and TCF1. Each dot represents a patient with PDAC and separate technical repeats as control from the *in vitro* exhausted and expanded populations. A) Percentage of CD4 PD1 expressing cells. B) Percentage of CD4 TIM3 expressing cells. C) Percentage of CD4 PD1 and TIM3 expressing cells. D) Percentage of CD4 TCF1 expressing cells. Statistical analysis performed with Kruskal-Wallis test with Dunn's test for multiple comparisons. Bars present median with whiskers representing interquartile range. (* $p \leq 0.05$, ** $p \leq 0.01$, *** $p \leq 0.001$)
Figure 17	Comparison of unstimulated versus stimulated phenotype of CD8 T cells isolated from patients with PDAC. T cells where stimulated post-thaw for 48h with CD3/CD28 beads in RPMI. Percentages of CD8 cells were compared with paired two-tailed Wilcoxon test. (* $p \leq 0.05$, ** $p \leq 0.01$, *** $p \leq 0.001$)
Figure 18	Comparison of unstimulated versus stimulated phenotype of CD4 T cells isolated from patients with PDAC. T cells where stimulated post-thaw for 48h with CD3/CD28 beads in RPMI. Percentages of CD4 cells were compared with paired two-tailed Wilcoxon test. (* $p \leq 0.05$, ** $p \leq 0.01$, *** $p \leq 0.001$)
Figure 19	Comparison of proliferation index amongst PDAC, T exhausted and expanded populations, based on memory subsets. a) Representative CFSE plots for CD4 (black) & CD8 (purple) T cells from a PDAC patient. b) Proliferation index comparison of functional subsets amongst CD8 T cells [CM: central memory ($CD45RA^-CCR7^+$), effectors ($CD45RA^-CCR7^-$), TEMRA ($CD45RA^+CCR7^-$)]. c) Proliferation index comparison of functional subsets amongst CD4 T cells [CM: central memory ($CD45RA^-CCR7^+$), effectors ($CD45RA^-CCR7^-$), TEMRA ($CD45RA^+CCR7^-$)]. Statistical analysis performed with Kruskal-Wallis test with Dunn's test for multiple comparisons. Violin plots present median with interquartile range. (* $p \leq 0.05$, ** $p \leq 0.01$, *** $p \leq 0.001$)
Figure 20	Comparison of proliferation index amongst PDAC, T exhausted and expanded populations, based on expression of inhibitory receptors. a) Representative CFSE plots for $CD4PD1^+$ (left) & $CD4TIM3^+$ (Right) T cells from a PDAC patient. b) Proliferation index comparison based on the expression of inhibitory receptors on CD8 T cells. c) Proliferation index comparison based on the expression of inhibitory receptors on CD4 T cells. Statistical analysis performed with Kruskal-Wallis test with Dunn's test for multiple comparisons. Violin plots present median with interquartile range. (* $p \leq 0.05$, ** $p \leq 0.01$, *** $p \leq 0.001$)
Figure 21	Comparison of proliferation index amongst PDAC patients based on functional subsets and expression of inhibitory receptors. a) Comparison of functional subsets from 6 PDAC patients. b) Comparison of proliferation index based on inhibitory receptor expression from 6 PDAC patients. Statistical analysis performed with Kruskal-Wallis test with Dunn's test for multiple comparisons. (* $p \leq 0.05$, ** $p \leq 0.01$, *** $p \leq 0.001$)
Figure 22	Phenotypic profile of CD4 & CD8 subtypes present in the peripheral blood of PDAC patients before (blue) and after (red) the operation. a) CD4 subsets (Tnaive: $CD45RA^+CCR7^+$, T central memory: $CD45RA^-CCR7^+$, T effectors: $CD45RA^-CCR7^-$, TEMRA: $CD45RA^+CCR7^-$, Treg: $FOXP3^+CD25^+$, Th1:$CXCR3^+CCR6^-$, Th2: $CXCR3^-CCR6^-$, Th17:$CXCR3^-CCR6^+$), b) CD8 subsets (Tnaive: $CD45RA^+CCR7^+$, T central memory: $CD45RA^-CCR7^+$, T effectors: $CD45RA^-CCR7^-$, TEMRA: $CD45RA^+CCR7^-$, Treg: $FOXP3^+CD25^+$, Tc1:$CXCR3^+CCR6^-$, Tc2: $CXCR3^-CCR6^-$, Tc17:$CXCR3^-CCR6^+$).
Figure 23	CD4 & CD8 subset expression of inhibitory receptors and TCF1 present in the peripheral blood of PDAC patients before (blue) and after (red) the operation. a) CD4 $PD1^+$, $TIM3^+$, double positive ($PD1^+TIM3^+$), negative ($PD1^-TIM3^-$) and $TCf1^+$. b) CD8 $PD1^+$, $TIM3^+$, double positive ($PD1^+TIM3^+$), negative ($PD1^-TIM3^-$) and $TCF1^+$.

Figure 24	Comparison T cell response to 72h stimulation with CD3/CD28 beads before (a,b) and after the operation (c,d). a) Representative plot of preoperative CD8 memory/effector subsets upon stimulation with overlay expression of PD1 (red), TIM3 (green) and TCF1 (yellow). b) Representative plot of CD8 inhibitory receptor expression upon stimulation preoperatively with overlay expression of TCF1 (yellow). c) Representative plot of postoperative CD8 memory subsets upon stimulation with overlay expression of PD1 (red), TIM3 (green) and TCF1 (yellow). d) Representative plot of CD8 inhibitory receptor expression upon stimulation postoperatively with overlay expression of TCF1 (yellow).
Figure 25	Percentage differences in memory subsets (a, b) and expression of inhibitory receptors and TCF1 (c, d) for CD4 & CD8 subsets. a) Percentage difference in CD4 memory subsets before (blue) and after (red) operation. b) Percentage difference in CD8 memory subsets before (blue) and after (red) operation. c) Percentage difference in CD4 subsets expressing the inhibitory receptors PD1 and TIM3 and the transcription factor TCF1 before (blue) and after (red) operation. d) Percentage difference in CD8 subsets expressing the inhibitory receptors PD1 and TIM3 and the transcription factor TCF1 before (blue) and after (red) operation. Bars represent mean difference in percentages of different subsets from 3 independent experiments (n=3). (Tnaive: $CD45RA^+CCR7^+$, T central memory: $CD45RA^-CCR7^+$, T effectors: $CD45RA^-CCR7^-$, TEMRA: $CD45RA^+CCR7$
Figure 26	Proliferation index differences per memory (a, b), inhibitory receptor expression and TCF1 subsets (c, d) for CD4 & CD8 T cells before and after operation. a) Proliferation index of CD8 memory subsets before (blue) and after (red) operation. b) proliferation index in CD8 subsets expressing the inhibitory receptors PD1 and TIM3 and the transcription factor TCF1 before (blue) and after (red) operation. c) Proliferation index in CD4 memory subsets before (blue) and after (red) operation. d) Proliferation index in CD4 subsets expressing the inhibitory receptors PD1 and TIM3 and the transcription factor TCF1 before (blue) and after (red) operation. Median and values of different subsets from 3 independent experiments (n=3). (Tnaive: $CD45RA^+CCR7^+$, T central memory: $CD45RA^-CCR7^+$, T effectors: $CD45RA^-CCR7^-$, TEMRA: $CD45RA^+CCR7^-$)
Figure 27	Transcriptomics of peripheral blood mononuclear cells at quiescence before (yellow) and after (green) operation. a) PCA showing limited clustering of samples preoperatively (red) and loose clustering of postoperative samples (blue). b) Volcano plot showing significantly upregulated genes (FDR<0.05 & log_2Fc >=1) postoperative compared to preoperative (red) and significantly downregulated genes (FDR<0.05 & log_2Fc <=-1) in blue (Total number of differentially expressed genes= 563). c) Hierarchical clustering of preoperative (yellow) and postoperative (green) transcriptomic profiles showing discrete clustering amongst preoperative and postoperative samples.
Figure 28	T cell specific gene set by genome ontology filter on peripheral mononuclear cells before (yellow) and after (green) operation. a) Volcano plot showing significantly upregulated genes (FDR<0.05 & log_2Fc >=1) postoperative compared to preoperative (red) and significantly downregulated genes (FDR<0.05 & log_2Fc <=-1) in blue. b) Top KEGG enriched pathways using the T cell specific list. Th17 and TCR signalling are the top 2 enriched pathways with enrichment scores of 71 and 47.7 respectively (p<0.01) c) Hierarchical clustering of preoperative (yellow) and postoperative (green) transcriptomic profiles for the T cell specific list with loss of the previously observed sub clustering based on operation status.
Figure 29	Transcriptomic analysis of T cell stimulation before and after operation showing divergent response. a) ¬PCA of paired samples bases on operation and stimulation status showing main effect of stimulation on PC1 and effect of operation on PC2. b) Volcano plot showing differentially expressed genes based on operation effect under a generalized linear model taking into consideration the effect of stimulation (FDR<0.05, & log2Fc >=1 or & log2Fc <=-1). c) Hierarchical clustering of the genes differentially expressed due to operation

Tables

Appendixes

2 ABSTRACT

Aims

Evaluate the T cell phenotypic subsets and functional responses in paired blood samples from patients undergoing surgical debulking for pancreatic adenocarcinoma (PDAC).

Methods

Preoperative and postoperative samples from patients with PDAC provided by the PCRFTB (2019/09/QM/HK/P/Blood) after ethical approval for the processing and handling of human tissue samples with the informed consent of the participants. Specimens have been collected at Barts Health NHS trust. T cells were stained with fluorescent antibodies to characterise memory subsets (CD45RA, CCR7), inhibitory receptors (PD-1, TIM3) and the functional transcription factor TCF1. T cells were also stimulated in vitro with CD3/CD28 beads (Dynabeads, Gibco) to assess phenotypic changes and functional responses under T cell receptor (TCR) stimulatory conditions. The samples were acquired using a spectral flow cytometer (Cytek Aurora) and part of the samples was used for bulk transcriptomics analysis. The analysis of the flow cytometry acquisition panels was performed using FCS Express (DeNovo Software 7th edition). Descriptive statistics were performed using GraphPad Prism (8th edition). Transcriptomics analysis was performed using PartekFlow.

Results

There is no percentage difference in the memory subsets of T cells or the expression of inhibitory receptors at rest. After TCR stimulation we observe a divergence to effector subsets in the preoperative samples compared to the postoperative samples which maintain a better equilibrium amongst all memory subsets. Similarly, there is no percentage difference in the expression of inhibitory receptors (PD1, TIM3) at rest but under stimulatory conditions TIM3 expression is increasing in postoperative samples. Finally, we can see high upregulation of TCF1 in the postoperative samples after stimulation which can explain the equilibrium maintenance in the postoperative samples. Similarly, divergent stimulatory response has been observed in the transcriptomic analysis supporting the expression of less effector phenotype.

Conclusions

This study shows divergent functionality of T cells associated with surgical debulking of PDAC with increased expression of TCF1. Although our results cannot support causality related to the presence of PDAC, they support the presence of offsite effects in T cells by PDAC which are altered by surgical debulking. These observations may partially explain the higher survival observed in the operated population and might support the use of adjuvant immunotherapies targeted at T cells in the perioperative period.

3 INTRODUCTION

T cells are at the centre of adaptive immunity by communicating with antigen presenting cells regarding the specific antigen that has triggered an inflammatory process and consequently by implementing an antigen specific response.[1] T cells, identified by surface expression of CD3 (cluster of differentiation), achieve a measured foreign (non-self) antigen-specific response by orchestrating different T cell subsets, each of which possesses a specific role(s) in mounting a precise response, maintaining a response in continued presence of foreign antigen, toning down the response after removal of antigen and re-mounting a response upon repeat exposure. The Helper T cells (Th), expressing the accessory molecule CD4, are important in recognizing the antigen expressed by MHCII (major histocompatibility complex) on dendritic cells, and consequently providing help in the full activation of B cells and antibody production by co-stimulatory ligands and by maintaining a pro-inflammatory milieu through the production of cytokines appropriate for the type of antigen encountered.[2,3]

On the contrary Cytotoxic T cells (CTL), identified by CD8 expression, have a more direct role in recognising and killing cells which express a foreign antigen on their MHCI. This characteristic makes these cells ideal for recognition of intracellular pathogens such as viruses but also for identifying cancer cells which may express altered antigens in their surface and therefore making them susceptible to direct cytotoxic mediated apoptosis.[4]

More recently, the role of a subset of Th cells in mediating resolution of inflammation and maintaining tolerance to self- antigens has been discovered. These Th cells, named T regulatory cells (T_{regs}), are characterized by expression of the master transcription factor FoxP3 (Forkhead box protein 3) and the expression of immunosuppressive cytokines such as IL-10 and TGF-β.[5] The role of these cells is mainly in suppressing the immune response to avoid an uncontrolled over-activation. Whether antigen presenting cells or T effector cells are the main target is still debatable, they can achieve this response through different mechanisms.[6,7]

3.1 T CELL MEMORY DEVELOPMENT IN ACUTE INFECTION

Development of immunological memory has been one of the differentiating factors of the adaptive immune system. It describes the ability of the immune system to mount a response rapidly and effectively to a previously encountered antigen. The development of a spectrum of $CD8^+$ T cell subpopulations, from short-lived effectors (T_{eff}) to long-term central memory (T_{CM}) cells[8], during acute inflammation may be explained by different models. These models are not mutually exclusive and aim to provide an explanation of the diversity of T cell sub-populations.[9,10]

A) **Decreasing potential model**

This model supports that "memory T cells can only arise under conditions in which the antigenic load is limited and the stimulation of precursors ceases before a point of no return" (Ahmed and Gray, 1996).[9] The model is supported by adoptive transfer experiments of transgenic mice infected with Leukocyte choriomeningitis virus (LCMV), or recombinant vaccinia virus. In these models of acute infection $CD8^+$ T cells are separated into killer cell lectin-like receptor subfamily G member 1^{high}/Cluster of Differentiation 127^{Low} ($KLRG1^{High}CD127^{Low}$) and $KLRG1^{Int/Low}CD127^{High}$, with the latter describing a memory precursor population. Although, both of these populations maintain their effector cytotoxic ability *ex vivo* and have similar expression of granzyme B, the memory precursors ($KLRG1^{Int/Low}CD127^{High}$) have proliferated to a lesser degree compared to their effector counterparts and also produce increased amounts of interleukin-2 (IL-2).[11] The development of these two distinct populations into memory precursors and effectors seems to be controlled by IL-12, which in turn activates transcription factor T-bet (t-box transcription factor). Although, both populations express T-bet, high expression of T-bet seems to be important for effectors, since knocking-out its expression diverges T cells towards a memory precursor phenotype.[12]

Nevertheless, the transcriptional profile of these populations ($KLRG1^{High}CD127^{Low}$ and $KLRG1^{Int/Low}CD127^{High}$) is not drastically different. As measured by microarray analysis these populations are different from both naïve and memory cells (30 days post infection), while their differences are more subtle both in the number of genes (76) and fold discovery rate (~ FDR: 4).[11] Studies supporting the diminishing potential model investigate in these well-defined populations the effects of decreasing the

duration of inflammation. They show that lower duration of antigenic exposure in the context of inflammatory conditions preferentially supports the precursor memory population.[11,12] Also, they provide evidence that it is the amount of inflammation that is important for leading the terminal effector production rather than the amount of antigen.[12] In particular, they show that with similar antigenic quantities, an inflammatory milieu would most likely promote the production of terminal effectors and it is the resolution of that environment which will allow the generation of memory precursors.

B) **Progressive differentiation model**

This model suggests that "as a function of the level of signal that is accumulated, T cells progress through hierarchical thresholds for proliferation and differentiation" (Lanzavecchia, A. et al 2002).[13] This model in contrast to the diminishing potential model describes a signal dependent development of a spectrum of T cells fates during initial antigenic stimulation, by the random strength of activation of the T cell receptor (TCR) along with co-stimulatory signals and cytokines, and a subsequent selection of the fittest T cells to enrich the memory pool after the resolution of infection.[14]

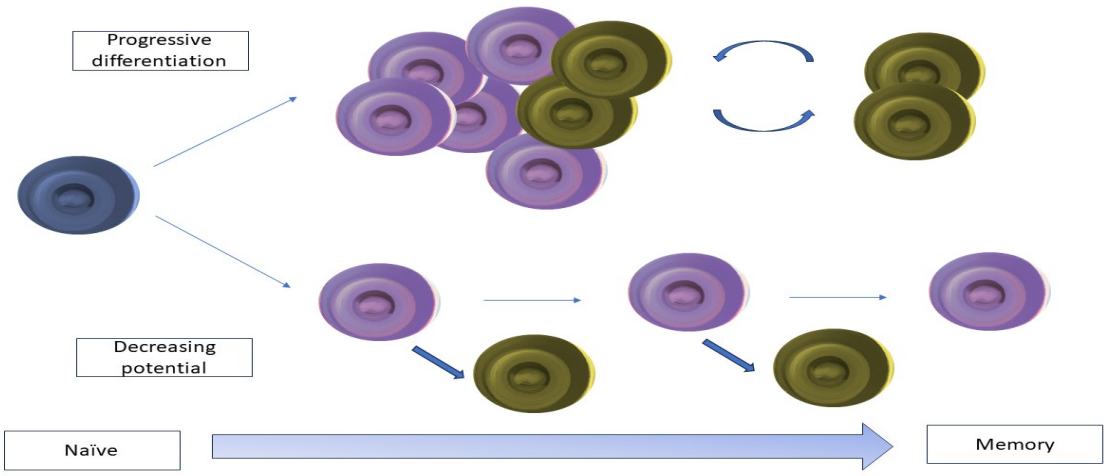

In support of the progressive differentiation model *ex vivo* stimulation of naïve $CD4^+$ T cells with Toxic shock syndrome toxin (TSST) primed dendritic cells (DCs) has shown that the avidity of the variable 2β domain (V2β) TCR chain, the degree of DCs priming and the length of interaction between DCs and T cells is important for the T cells to acquire an effector phenotype, defined as loss of c-c chemokine receptor 7 (CCR7) expression and increased production of interferon-γ (INF-γ) and IL-2. The same study

proved that identical clones of the V2β chain can be discovered both in the non-effector and effector populations suggesting that cell fate is not clone-dependent.[15]

4 T CELL EXHAUSTION

4.1 THE MODEL OF CHRONIC INFECTION

T cell exhaustion is described as a state of T cell dysfunction that arises during many chronic infections and cancer.[16] This state has been initially described in murine models of chronic LCMV infection and subsequently proven to exist in other chronic viral infections such as human immunodeficiency virus (HIV), Hepatitis B virus (HBV) and human cancer.[17]

The use of the LCMV model has been based on the pleiotropic tropism of the virus and the CD8-based relation to the control of the acute infection. Wherry et al.[18] have shown that by comparing the acute with chronic LCMV infection there is clonal selection of the CD8 antigen specific cells in the spleen of mice. This finding has since been reaffirmed in different murine models of chronic LCMV infection and has been expanded to the CD4 virus specific T cells.[19]

The preserved CD8, antigen specific T cells have different tissue tropism during chronic infection with increased frequency and numbers of tetramer stained $CD44^+$ T cells specific to the chronic LCMV strain found in the liver, kidney and brain of mice compared to the acute infection. Further evaluation of the model of chronic LCMV infection shows that there is a hierarchical loss of T cell function in the antigen specific CD8 cells that are not eliminated early in the chronic infection.[18] This loss of function is more prominent in the absence of CD4 co-stimulation,[20] and progresses from initial loss of production of IL-2 and TNF-α, to the subsequent loss of INF-γ.[18] Similar, to the loss of the ability to produce inflammatory mediators there is loss of the lytic ability of T cells as early as from the 8^{th} day after the acute infection.[18,20] Nevertheless, it is evident that the continuous presence of antigen is important to promote an exhausted phenotype and this has been observed in human with CMV and EBV chronic infections.

4.2 PHENOTYPE OF EXHAUSTED T CELLS

The phenotype of exhausted T cells is characterized the expression of inhibitory receptors. One of the main receptors expressed is programmed cell death-1 (PD-1) who is member of the B7-cluster of differentiation 28 (B7-CD28) family of co-inhibitory molecules.[21] PD-1 contains an extracellular immunoglobulin like domain, and two intracellular immunoreceptor tyrosine-based motifs, an inhibitory (ITIM) and a switch motif (ITSM).[21,22] In both murine and human T cells the interaction of PD-1 with its ligand has been shown *in vitro* to abrogate TCR dependent proliferation, and cytokine production (INF-γ, IL-10 and IL-2).[23] This effect could be reversed by CD28 dependent co-stimulation under sub-par T cell receptor (TCR) engagement or annulled under TCR saturating conditions.[23]

Barber et al. using the model of chronic LCMV infection compared memory CD8 T cells with antigen specific exhausted T cells and found that, while PD-1 is upregulated early during infection in CD8 effectors, there is persistent expression in exhausted CD8 T cells. As an adjunct proof of PD-1 being responsible for some aspects of the dysfunctional state of exhausted T cells, they found that the splenocytes of chronically infected mice showed expression of the PD-L1. Finally, by blocking the PD-1 ligand they were able to revert the exhausted state of CD8 cells which showed increased proliferation in different tissues, increased production of INF-γ and TNF-α and finally clearance of the chronic infection.[24] The dynamics of PD-1 expression during acute or chronic viral infection were further elucidated by investigating the methylation status of regulatory elements for the *Pdcd1* locus which is responsible for the transcription of PD-1. It was shown that during the 8th day of an acute LCMV infection there is remethylation of regulatory elements for the *Pdcd1* locus in both memory precursors (KLRG1^{lo}IL7Ra^{hi}) or effector cells (KLRG1^{hi}IL7Ra^{lo}) which suppresses the initially increased transcription of PD-1. On the contrary, from the 8th day of a chronic LCMV infection the regulatory elements of *Pdcd1* locus are unmethylated and remain as such for over than 30 days. This epigenetic programming was proven to be TCR stimulation dependent as it was indicated by the difference in the methylation status of regulatory elements for the *Pdcd1* locus in naïve, antigen responsive CD8 effectors and chronically infected CD8 exhausted cells.[25] Furthermore, during infection with different viral loads it was shown that not only is TCR dependent but also the duration of TCR engagement is important. In particular, for the same viral load there was difference between LMCV clone-13 (which produces chronic infection) versus clone Armstrong

(which produces acute infection). Similarly, for the same clone decreasing viral loads have been shown to correlate with decreasing demethylation status of regulatory elements for the *Pdcd1* locus.

In conjunction with this dysfunctional state denoted by PD-1 the progressive loss of function may be related with the expression of T-cell immunoglobulin and mucin domain-3 (TIM3)[26]. TIM3 was initially described as expressed by Th1 but not Th2 cells and its activation would cause exacerbation of an experimental autoimmune encephalomyelitis murine model.[27] This effect was subsequently shown to be related to increase macrophage activation rather than the initially thought Th1 related response.[27] Subsequent to the identification of galectin-9 as the ligand for TIM3 and the associated Th1 mediated apoptosis, TIM3 has been considered as an important molecule in regulating Th1 responses.[28] Nevertheless, the first evidence that TIM3 could in fact play a role in T cell exhaustion came from recognition of a highly dysfunctional CD8 population expressing TIM3 in patients with HIV (Human Immunodeficiency virus) infection.[29] This CD8 population was HIV specific and was increased in acute HIV infected individuals and chronic progressors compared to uninfected and non-progressors. The dysfunctional state of the TIM3 positive population was further described by assessing peptide sorted T cells from HIV infected individuals.[29] These cells were T-bet positive concise with a Th1/CTL differentiation and had impaired production of INF-γ after both specific gag peptide and non-specific staphylococcal enterotoxin B (SEB) stimulation.[29] Corroborating with an exhausted population, $CD8^{+}TIM3^{hi}$ sorted cell from HIV infected individual showed limited proliferation assessed by CFSE staining.[29]

In order to provide better insight in the dynamics of TIM-3 in exhausted T cells, Ji et al. showed that during chronic LCMV infection $PD1^{+}TIM3^{+}$ cells showed signs of more severe exhaustion compared to $PD\text{-}1^{+}TIM3^{-}$ CD8 cells.[30] $PD1^{+}TIM3^{+}$ cells showed decreased INF-γ compared to the $PD1^{+}TIM3^{-}$ counterparts, limited proliferation and increased production of the immunosuppressive cytokine Il-10.[30] Consequently, TIM3 possibly denotes a terminally exhausted T cell population. Since the central role of PD1 upregulation in exhausted T cells has been described in the literature the search for other molecules with inhibitory function, expressed along with PD1 in the subset of exhausted T cells has been fruitful.[31] One of the molecules that has been shown to be co-expressed in PD1 during chronic LCMV infection is

lymphocyte activation gene-3 (LAG-3) and along with other inhibitory receptors as CD160 and CD244 seems to denote a functionally exhausted population of T cells. Although, LAG-3 blockade did not improve the cytolytic activity of exhausted cells expressing a combination of at least three inhibitory receptors, *in vivo* experiments of co-blockade of PD-L1 and LAG-3 improved antigen specific T cell frequency in established chronic LCMV infection and their functional phenotype as assessed by CD107 and INF-γ expression.[32] This might be explained by the need for a stable peptide – MHC expression for LAG-3 to exert its inhibitory activity during the activation of CD4 T cells.[33]

One of the main transcription factors involved in the initiation of the exhaustion program is the Thymocyte selection-associated high mobility group box protein (TOX). TOX is induced downstream of the nuclear factor of activated T cells (NFAT) in conjunction with nuclear receptor subfamily 4A (NR4A) and its deletion in chimeric antigen receptor (CAR) tumour infiltrating lymphocytes (TILs) seems to promote improved effector function measured by supressing tumour growth and improved survival in a murine model.[34] Similarly, TOX is implicated in diminishing PD-1 degradation on the surface of tumour infiltrating CD8 cells and is associated with decreased survival in patients with hepatocellular carcinoma.[34] Finally, using the LCMV model at a single cell level TOX has been associated with the commitment to early exhausted progenitors which can be differentiated by early memory precursors.[35,36] Neverthless, the expression of TOX is not specific in exhausted T cells and it has been reported in effector memory cells and effector cells in HIV patients who have achieved viral load control.[37]

Similar to the importance of TOX in the maintenance of the exhaustion program is the action of T cell factor 1 (TCF1) in maintenance of the pre-exhausted T cells (T_{pex}).[38] TCF1 has been identified as an important factor for lymphopoiesis in the bone marrow and lineage commitment.[39] In the context of chronic infection it has been associated with improved viral control and it has also been identified in the CXC motif receptor 5 (CXCR5) expressing CD8 T cells in the LCMV model. [40,41] The same subset of CXCR5 expressing cells has also been identified as being responsive to PD-1 blockade by expansion and differentiation after adoptive cell transfer in a murine model of chronic infection.[42] Concurrent with the examples provided by chronic infection TCF1+ CD8 T cells seems to maintain the capacity to recirculate

between the tumour microenvironment and the draining lymph nodes bridging systemic and intratumoral immune responses.[43]

4.3 T CELL EXHAUSTION IN CANCER AND ITS EFFECT ON IMMUNOTHERAPY RESPONSE

Immunotherapy has emerged as a promising approach for cancer treatment in recent years. It involves the use of immune system components to fight cancer cells. One of the major players in this approach is the CD8 T cells, due to their cytotoxic abilities. However, despite their potential, immunotherapy treatments and in particular inhibitory receptor blockade does not always work in all patients with one of the reasons being T cell exhaustion and the lack of functional subsets which would establish a prolonged immune response.[44–46] T cell exhaustion can occur during the initial stages of cancer development but has been broadly confirmed in the tumour microenvironment.[47] The presence of T cell exhaustion in cancer patients has been associated with poor prognosis[48,49,50,] and reduced response to immunotherapy.[51,52] In fact, the response rate to immunotherapy is often lower in patients with T cell exhaustion than in those without it. This has led to the development of new approaches to overcome T cell exhaustion and improve the efficacy of immunotherapy.[46,53–55]

One of the most promising approaches is the use of checkpoint inhibitors, such as anti-PD-1 and anti-CTLA-4 antibodies. These antibodies can block the inhibitory signals mediated by PD-1 and CTLA-4 receptors on T cells, allowing them to regain their effector functions and attack cancer cells. Although, alternative mechanisms have been supported in the literature, including alternate regulation of T_{reg} or aberrant changes in the TCR receptor activity.[56,57,58] Checkpoint inhibitors have shown remarkable clinical benefits in a variety of cancers, including melanoma, non-small cell lung cancer, and renal cell carcinoma, with 93 clinical trials involving the use of PD-1 inhibitors in solid malignancies being completed at clinicaltrials.gov and 28 involving the use of CTLA-4 inhibitors. (clinicaltrials.gov accessed 30/05/2023)

The biological effects of immunotherapy on exhausted subsets are mainly supported by proof of concept studies mainly in melanoma where the $T_{exhausted}$ are clonally enriched for neoantigen responsive TCRs.[59] The identification of clonally specific responsive T cells in patients responsive to immunotherapy has

been reported in skin, lung and renal cancers and depicts the importance of replenishing the pool of exhausted T cells encountered both in the tumour, adjacent normal tissue and blood as a consequence.[60,61] Finally, it has been reported that immunotherapy responses are driven by a subset of $T_{exhausted}$ precursors which are able to maintain a sustained immunosurveillance measured by improved survival in patients with high $TCF1^+$ ratio amongst $PD1^+CD8^+$ cells.[34]

In summary, T cell exhaustion is a state of T cell dysfunction that occurs in chronic infections and cancer, which can impair the efficacy of immunotherapy. The presence of T cell exhaustion has been associated with poor prognosis and reduced response to immunotherapy. However, the use of checkpoint inhibitors, combination therapies, and new targets for immunotherapy has shown promise in overcoming T cell exhaustion and improving the efficacy of immunotherapy in cancer patients.

4.4 T CELLS IN PANCREATIC CANCER

Although, the advent of immunotherapies has been successful in multiple solid malignancies the results in pancreatic cancer have been underwhelming.[62] Similarly, efforts to delineate the immune system response have not been able to delineate intrinsic relationships to the presence of the primary tumour, but rather try to relate immune subsets with survival.[63–65] The presence of proven immune-suppressive microenvironment nevertheless may explain both the treatment failures and the lack of actionable immune subsets.[66,67] The tumour microenvironment plays a critical role in shaping T cell responses within pancreatic tumours. Pancreatic tumours create an immunosuppressive milieu through the recruitment of immunosuppressive cells, secretion of inhibitory cytokines, and upregulation of immune checkpoint molecules.[68] Myeloid-derived suppressor cells (MDSCs), immunosuppressive macrophages and regulatory T cells (T_{regs}) are among the immunosuppressive cells that infiltrate pancreatic tumours and hinder T cell function.[69,70,71] Moreover, cytokines like transforming growth factor-beta (TGF-β) and interleukin-10 (IL-10), along with arginase contribute to T cell dysfunction by suppressing their effector functions.[69,72,73,74] Understanding and targeting these immunosuppressive mechanisms hold promise for restoring T cell function and unleashing their anti-tumour potential.[75]

The presence of tumour-infiltrating lymphocytes (TILs), including T cells, within pancreatic tumours has been associated with better patient prognosis. Particularly, high densities of cytotoxic CD8+ T cells have been correlated with improved survival.[76–78] Nevertheless, the immunosuppressive milieu would still impede dendritic cell presentation and effective cytotoxicity.[79] Strategies aimed at enhancing the recruitment, activation, and survival of TILs hold promise for improving patient outcomes,[79] but the presence of dysfunctional / exhausted subsets of T cells in the tumour microenvironment has been suggested by the presence of inhibitory receptors and their ligands.[64,80,81]

In a recent study, Jainarayanan et al using pseudotime dynamics suggests a more diverse image of T cells from PDAC samples with the presence of effector and even central memory cells. Similarly Xu et al. suggest an intricate regulation program with the presence of Th1 and Th17 interactions amongst T cells and different types of ductal malignant cells.[70,82] Such subsets have not been identified in the peripheral blood of PDAC patients to our knowledge but reactive T cell clones have been isolated from the blood of PDAC patients opening the avenue to search for the phenotypic and functional characteristics of such subsets in more detail.[83–85]

The phenotype and clonal aspects of reactive T cells in the circulation of PDAC patients has tangentially been investigated in limited cohorts. Meng et al. in an effort to produce primed T cells using autologous organoids from PDAC patients have shown that it is possible to generate unique T cell responses with a different combination of inhibitory receptors and a specific clonal expansion which can cause Fas ligand or granzyme B dependent tumour killing.[86] Despite the aforementioned results *in vitro,* Stromnes et al. report limited clonal expansion despite activation signatures in TILs from 9 PDAC patients and comparison with blood clonality showed no significant difference. Furthermore, using a cutoff of tumours with clonality index above 0.1 they found that the T cells from these tumours expressed markers of recently activated T cells along with inhibitory receptors but were mostly T-bet positive and rather than Eomesodermin (EOMES) positive suggesting a reactive phenotype rather than an exhausted one.[87] Nevertheless, when investigating the T cells of the peripheral blood from pancreatic cancer compared to other pancreatic diseases oligoclonal TCRβ repertoires where found but with limited overlapping amongst patients. Similarly, the same team identified decreased Simpson diversity index (a measure of diverse

TCR profiles which would correlate with clonal expansion) for pancreatic cancer patients which might suggest the presence of reactive T cells in the blood or could at least reflect the immune status of pancreatic cancer.[88]

Similar to the results of Stromnes et al. the diversity index of T cells from pancreatic cancer and the blood of patients is similar and also has no difference to the blood of healthy controls. Nevertheless, there is overlap of TCR repertoires amongst patients' tumour samples and blood samples compared to healthy controls but there is no clonotype expansion with the blood showing higher percentage of more frequent clonotypes (0.001 to 0.01%) compared to the tumour where clonotypes with less than 0.001% frequency were most abundant. This could still support the presence of reactive clonotypes especially considering the clonal evolution of tumours but would not be able to explain the difference observed with healthy controls.[88]

Finally, to further support the existence of selected clonotypes in PDAC samples Pan et al. performed single cell RNA sequencing and compared the results from 5 patients with healthy controls. They found the increased incidence of CD8 cytotoxic subsets and tissue resident/activated subsets but also lower inverse Simpson index in PDAC samples in the aforementioned subsets. They were also able to show that using mass cytometry the increased expression of soluble TIM-3 in the plasma of PDAC patients which correlated with decreased survival.[89]

5 HYPOTHESIS & AIMS

If we consider the prerequisites for the development of an exhausted T cell population as depicted by Wherry et al.[90] needing a continuous TCR stimulation, in the presence of sub-par co-stimulation and immunosuppressive mediators, it is possible to consider the tumour microenvironment as a generator of exhausted T cell populations. In addition, the emerging hallmarks of avoiding immune destruction, tumour-promoting inflammation, genome instability and mutational burden (as a persistent neo-antigenic stimulus)[91], we may consider deviation of the immune response to exhaustion as a mechanism allowing tumour growth alongside sub-par immune surveillance. Building on this hypothesis, we may consider surgical de-bulking of the primary malignancy as an intervention to limit generation of exhausted populations and partially reconstitute immune surveillance. This would be true if sub-clinical metastatic foci have not been established by that time point since these metastatic foci may provide new niches for generation of exhausted populations. (Fig. 1)

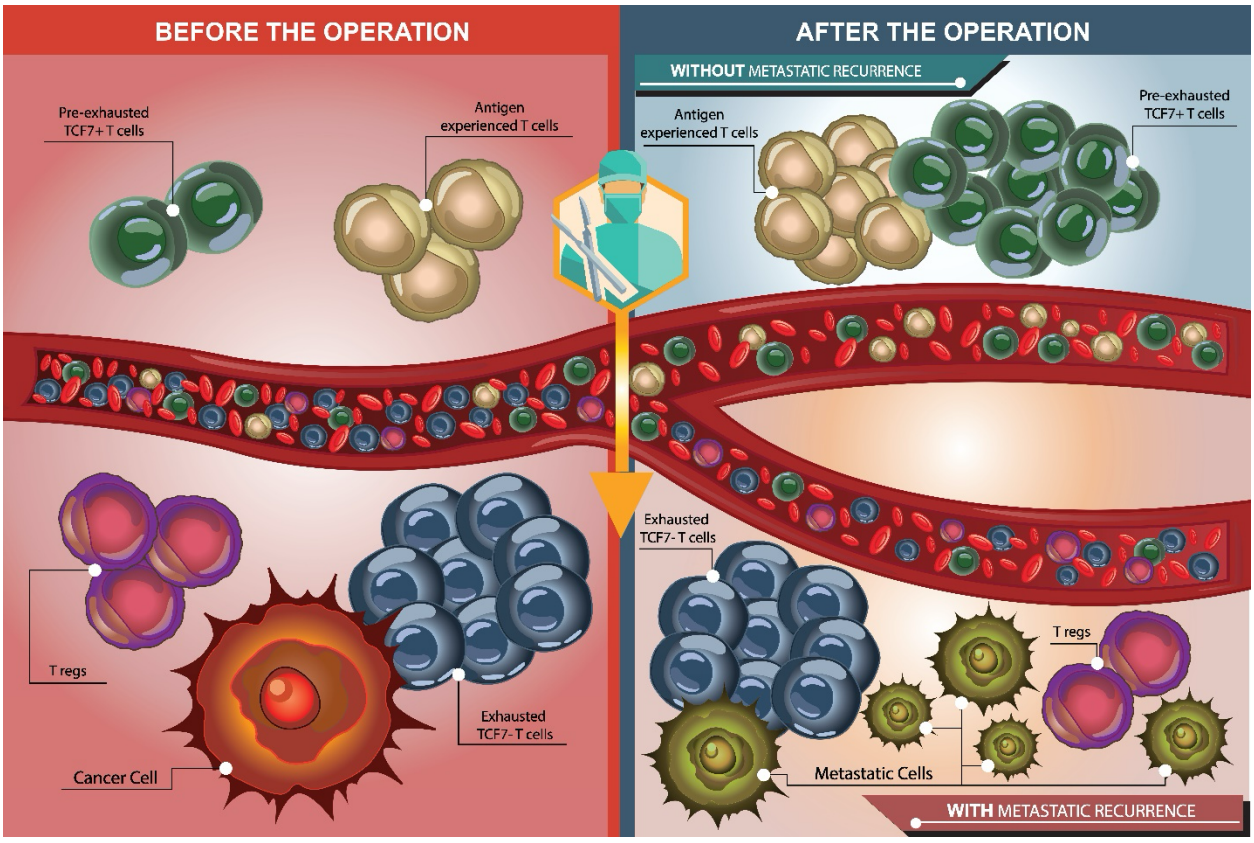

Figure 2. Hypothetical changes in antigen experienced and exhausted T cells before and after surgical de-bulking. The existence of pre-exhausted populations defined by TCF1(Tcf7)[92] expression before the

operation may be a valuable signal for recovery of the immune system after removal of the primary focus which would act as a persistent stimulatory signal and therefore a niche of systemic exhaustion. This reversal may be dependent on the presence of sub-clinical metastatic foci even if the initial surgical removal of the tumour was complete.

5.1 AIMS

A. Describe the phenotype of T cells from the blood of patients with PDAC.

B. Evaluate possible alterations in immunological memory development.

C. Evaluate the presence of exhausted T cells (expressing PD1/TIM3).

D. Evaluate the stimulatory response of T cells compared to an *in vitro* expanded/exhausted population.

E. Evaluate phenotypic changes in the composition of T cells' sub-sets before and after surgical de-bulking of the primary pancreatic malignancy.

F. Assess changes in the transcriptomic profile of peripheral blood mononuclear cells (PBMCs) before and after surgical de-bulking and correlate with T cell sub-sets.

6 METHODS

6.1 SAMPLE PROCESSING

Samples have been provided by the Barts Pancreas Tissue Bank (BPTB application number 2019/09/QM/HK/P/Blood) after ethical approval for the processing and handling of human tissue samples with the informed consent of the participants. Specimens were collected at Barts Health NHS trust.

Patients' peripheral blood was collected at two time points before and at an interval after surgery to allow for resolution of the surgical associated inflammatory process (~ 4 weeks). The samples were processed fresh and PBMCs were isolated by Ficoll® Paque Plus (Cytiva, 17144002, Germany), according to the protocol provided by Cossarizza et al. with an addition of initial centrifugation to allow plasma isolation for BPTB.[93] The PBMCs were split to a sample to be cryopreserved in 10% DMSO (Sigma-Aldrich, D8418, Germany) solution for subsequent flow cytometric analysis and a sample kept in RNA protect Cell Reagent® (Qiagen, 76526, UK) in -80ºC for RNA extraction and transcriptomic analysis.

PBMCs were stimulated with CD3/CD28 beads (Dynabeads™ Human T-Activator CD3/CD28 for T Cell Expansion, Thermofisher, 11131D, Lithuania) every 48h for a period of 12 days thus inducing repetitive stimulation and promoting T cell exhaustion. PBMCs remained in culture in complete RPMI (RPMI 1960 with 10% FBS, Sigma-Aldrich, F7524, Germany) with penicillin/streptomycin but no added cytokines. After the first period of 72h a set of cells was frozen in DMEM with 10% DMSO to act as an expanded ($T_{expanded}$) population, while the rest of the cells were re-stimulated for subsequent 2 more times to complete 12 days of continuous stimulation. After completion of the 12 days of continuous stimulation the T cells were considered exhausted ($T_{exhausted}$)[94] were frozen with DMEM and 10% DMSO (See Appendix 11.3 for schematic).

6.2 FLOW CYTOMETRY STAINING & ANALYSIS

Thawed samples were stained immediately after thawing/harvesting for surface markers (see Appendix A: Panel of antibodies) according to the manufacturer's protocol (Biolegend). Intracellular staining was

performed using True-Nuclear™ Transcription Factor Buffer Set (Biolegend) according to the manufacturer's protocol. Stained and fixated samples were acquired using the Cytek Aurora spectral flow cytometer (4-laser configuration UV/Blue/Violet/Red). Spectral unmixing was performed using single stained beads (UltraComp eBeads™ Plus Compensation Beads, Invitrogen, 01-2222-41) and unstained samples as control (Fig. 2). Flow cytometry analysis was conducted using FCS Express 7 research edition (7.12.0005). The common flow cytometry gating strategy used for subsets can be seen in figure 3 and is based on the markers suggested by Human Immunology Project Consortium (HIPC) to allow for direct comparison with published literature.

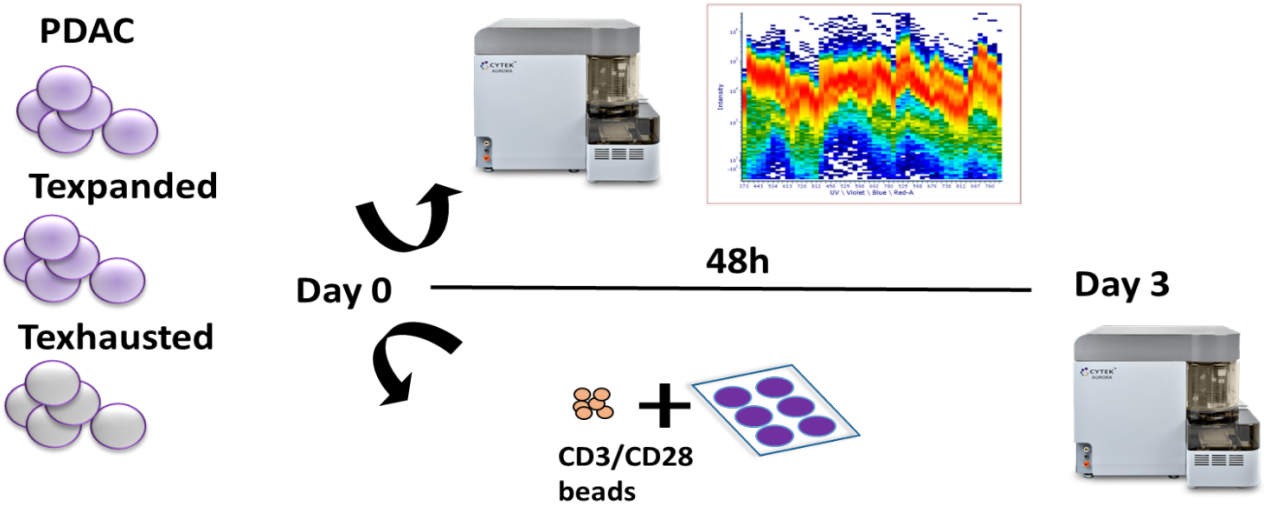

Figure 2. Experimental set up for the analysis and spectral unmixing of the PDAC samples.

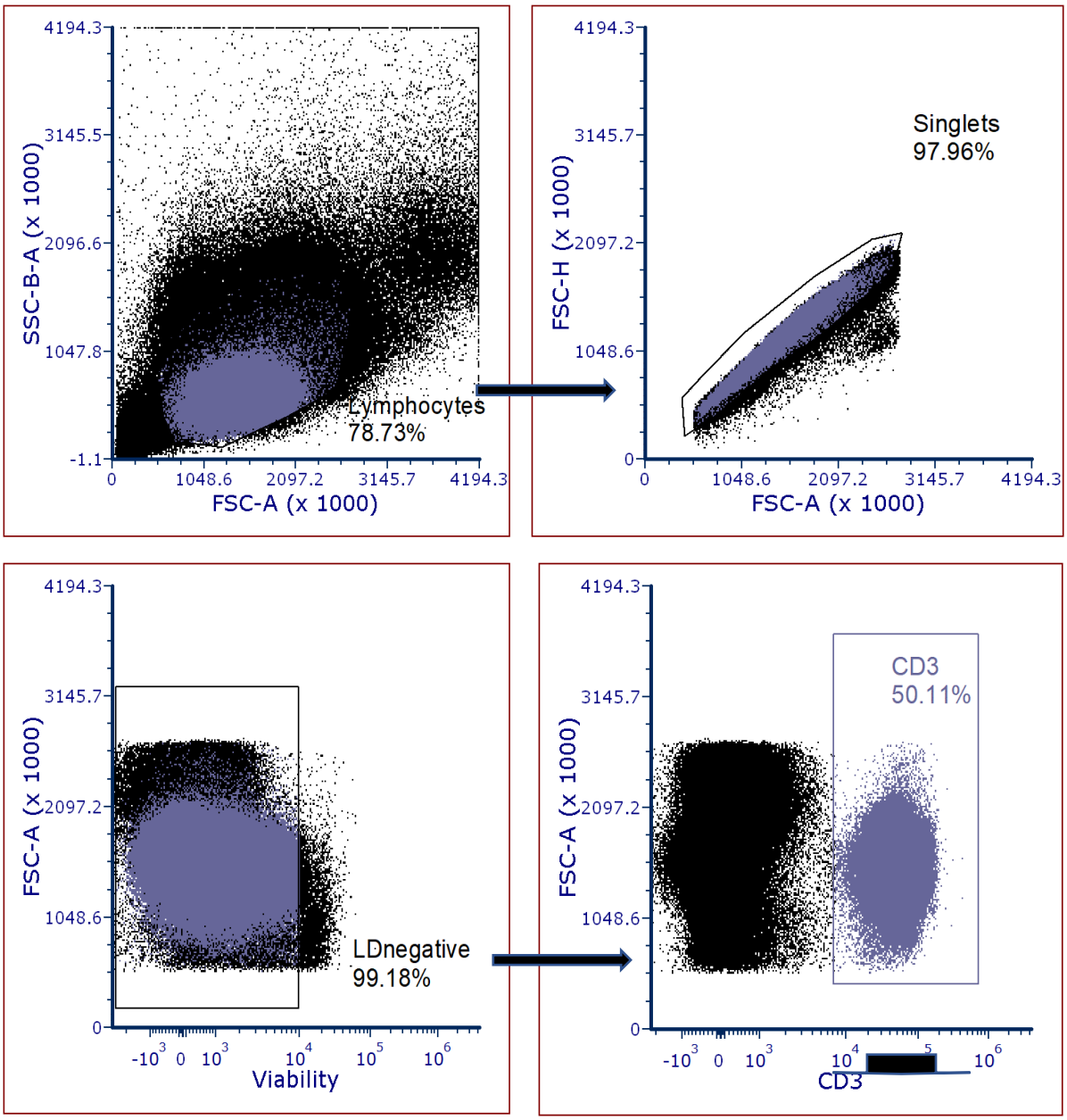
4194.3
3145.5
2096.6
1047.8
-1.1
SSC-B-A (x 1000)
Lymphocytes
78.73%
0
1048.6
2097.2
3145.7
4194.3
FSC-A (x 1000)
4194.3
3145.7
2097.2
1048.6
0
FSC-H (x 1000)
Singlets
97.96%
0
1048.6
2097.2
3145.7
4194.3
FSC-A (x 1000)
4194.3
3145.7
2097.2
1048.6
0
FSC-A (x 1000)
LDnegative
99.18%
-10^3 0 10^3 10^4 10^5 10^6
Viability
4194.3
3145.7
2097.2
1048.6
0
FSC-A (x 1000)
CD3
50.11%
-10^3 0 10^3 10^4 10^5 10^6
CD3

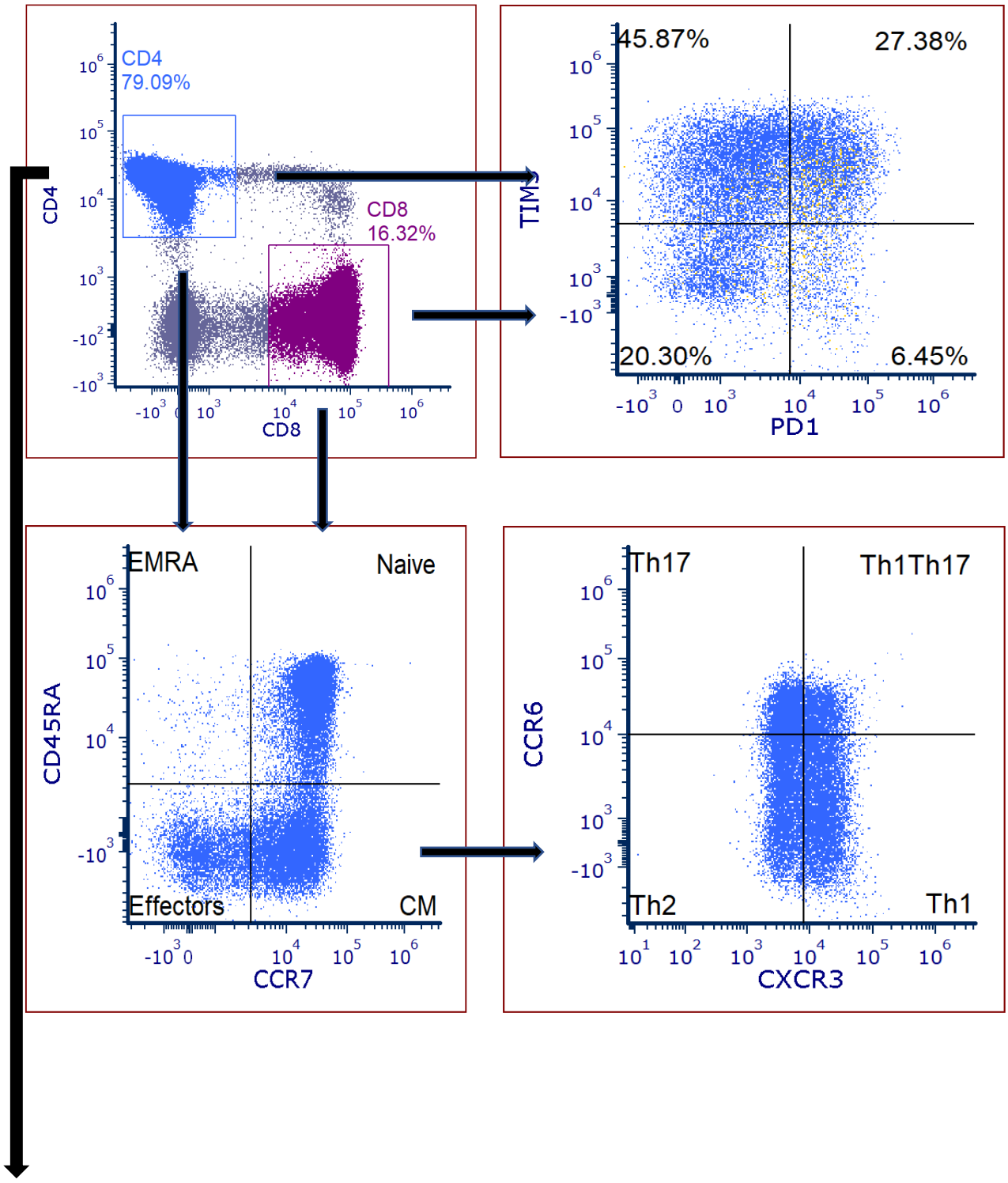
CD4
79.09%
CD8
16.32%
CD4
CD8
45.87%
27.38%
20.30%
6.45%
TIM3
PD1
EMRA
Naive
Effectors
CM
CD45RA
CCR7
Th17
Th1Th17
Th2
Th1
CCR6
CXCR3

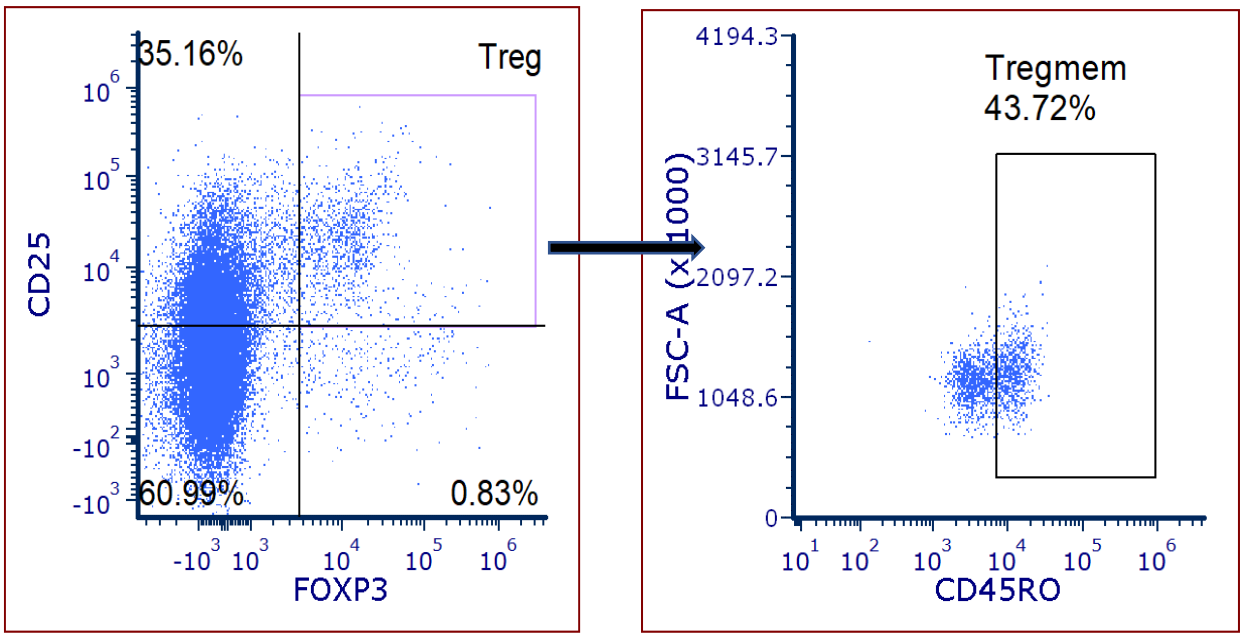

Figure 3. Gating strategy for identification and analysis of T cell subsets.

6.3 PROLIFERATION ASSAY

Thawed PBMCs, $T_{exhausted}$ and $T_{expanded}$ cells are stained with CFSE as per protocol suggested by Quah et al.[95] with the alterations suggested for small number of cells in order to account for possible toxicity such as by adding fetal bovine serum during staining step. Subsequently, cells are stimulated with CD3/CD28 beads (Dynabeads™ Human T-Activator CD3/CD28 for T Cell Expansion, Thermofisher, 11131D, Lithuania) for a period of 48h in complete RPMI. After the stimulation period the cells are harvested, beads are removed, and the samples are stained for flow cytometry. During flow cytometric acquisition an unstimulated CFSE stained control is used to adjust the fitting algorithm for the starting generation. The proliferation index is calculated according to the following formula:

$$\frac{\sum_{i=0}^{p-1} N_i}{\sum_{i=0}^{p-1} \frac{N_i}{2^i}}$$

where N is the number of cells in a generation and p is the number of peaks.

6.4 STATISTICAL ANALYSIS

The statistical analysis was performed using GraphPad prism (8.4.3). Kruskal-Wallis or Mann-Whitney U test was performed depending on the number of groups for comparison and Dunn's correction was performed for statistically significant results to elucidate intergroup differences.

The analysis of the paired samples was performed by calculating the sum of differences for the 3 patients This is the sum of differences for the 3 patients before/after: Σ(χ1+...x3) - Σ(y1+...+y3) = (χ1-y1)+(x2-y2)+(x3-y3). Then the sum of the differences of the 3 patients was calculated to show the trend for each operation status. In this way the calculated percentages are normalized to the preoperative percentage in order to make comparison between operation status.

6.5 TRANSCRIPTOMICS ANALYSIS

6.5.1 Library preparation

Library was prepared from the samples maintained at RNA protect Cell Reagent®. The use of quality metrics of RIN above 7 and at least 100ng of RNA resulted in 4 samples failing QC with additional extraction for the 3 samples which improved RIN numbers to above 7 but with still decreased useable RNA quantity for 2 samples (Average: 381.0972222ng, range: 17.9 -1027ng, see Appendix 12.1). Based on these results the SMART-Seq® v4 Ultra® Low Input RNA Kit for Sequencing (Cat. 634892, Takara Bio) as per manufacturer's instructions was used with a prior step for gDNA clearance and polyA selection. Next Generation Sequencing was performed on NextSeq550 (Illumina) with 22million paired end reads sequencing depth. The average sequencing depth was 23,920,577.67 reads (range: 13,474,315 – 29,995,757 reads, see Appendix 12.2) with an average of 77.13% unique paired reads mapped (range: 63.8 – 83.7%, see Appendix 12.3)

6.5.2 Bioinformatics analysis

The analysis was conducted using the Partek® Flow® suite for next generation sequencing.

Contaminants were removed using Bowtie2 [96] and pre-alignment Phred Score below 30 was observed for 3.39% of the sequences. (Fig. 4a) Alignment was performed using STAR RNA-seq aligner (version 2.7.3a)[97] with unique paired reads reaching >70% of reads per sample for all samples except one which

was removed from subsequent analysis (see appendix). The quantification was performed using the Expectation-Maximization algorithm[98] of Partek® Flow® with strict paired-end compatibility. Finally, low reads (less than 2 reads) were removed, and deferential expression analysis was performed using the DESeq2 algorithm[99] with levels for operation, stimulation and using the operation*stimulation interaction as factor for the paired samples. (Fig. 4c)

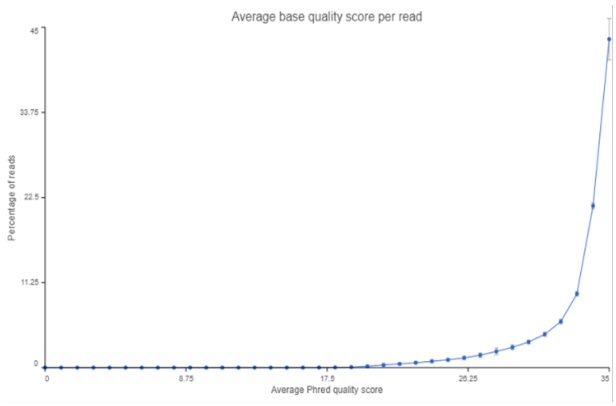

a)

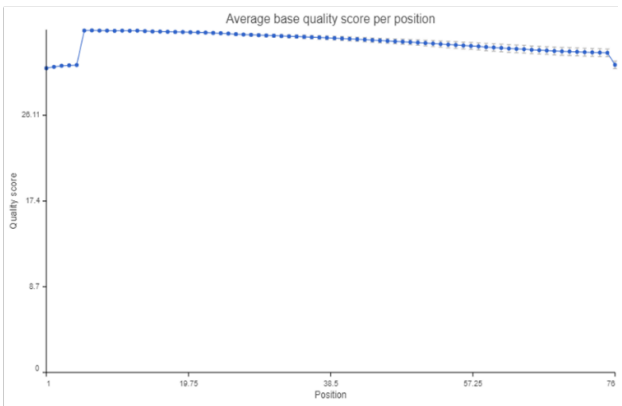

b)

c)

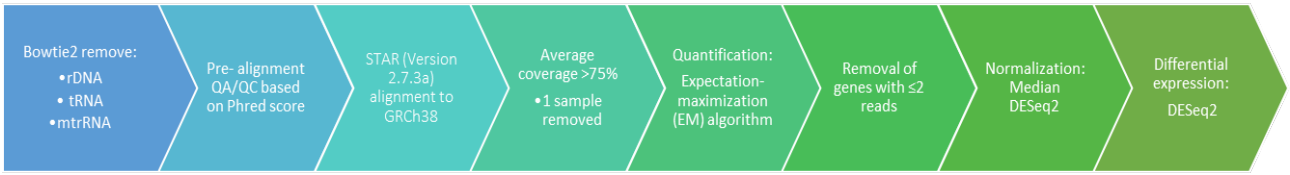

Figure 4. a) Phred score values showing 3.39% reads following below score of 30. B) Average base quality score per position showing small drop at 5' and 3' ends. c) Bioinformatics analysis pipeline for gene deferential expression of bulk RNA sequencing samples from PDAC patients as implemented on Partek® Flow® suite.

7 RESULTS

7.1 PHENOTYPIC AND FUNCTIONAL CHARACTERISTICS OF THE IN VITRO EXHAUSTION MODEL

7.1.1 Phenotypic comparison of exhausted population with an expanded population

a)

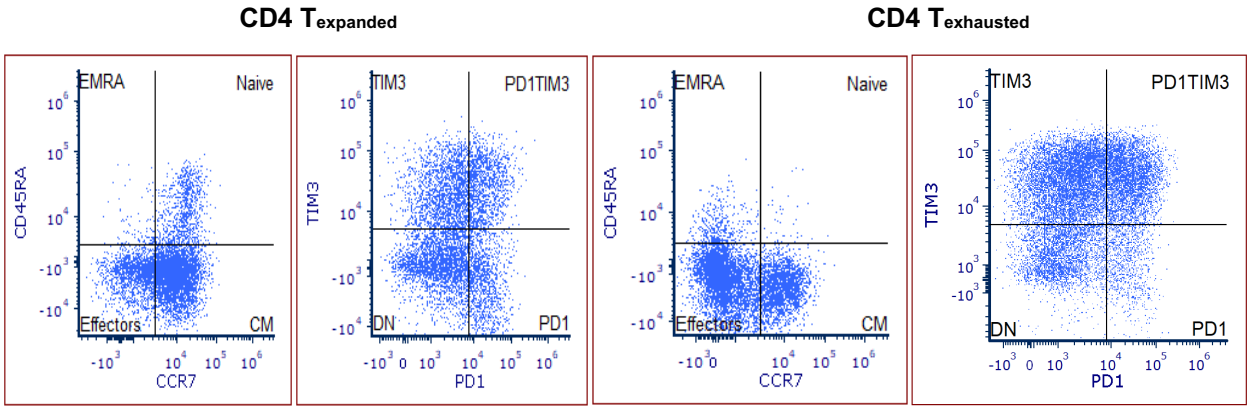

b)

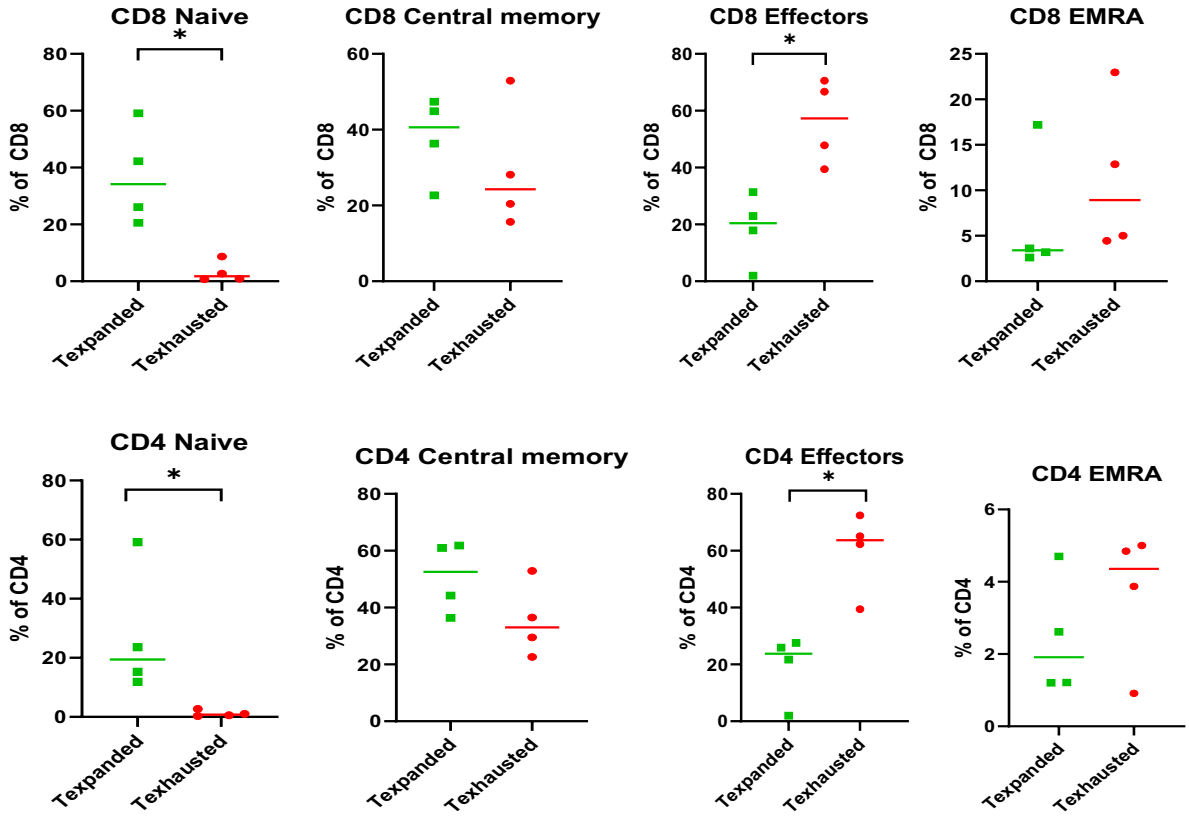

c)

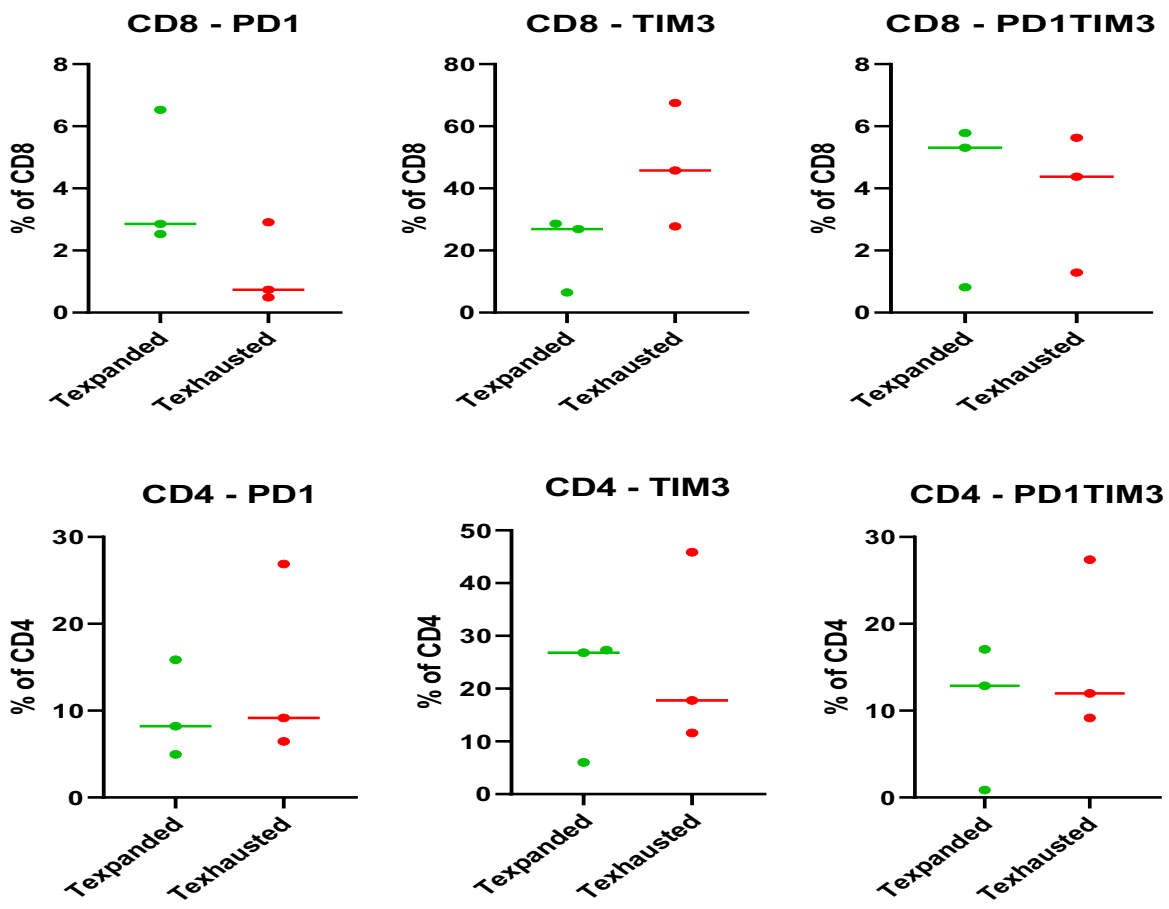

Figure 5. Percentage of memory and effector subsets and expression of inhibitory receptors for CD4 and CD8 T cells who have undergone the exhaustion protocol. a) Representative flow cytometry sub-gating on a CD4 subset (T_{naive}: $CD45RA^{+}CCR7^{+}$, $T_{central\ memory}$: $CD45RA^{-}CCR7^{+}$, $T_{effectors}$: $CD45RA^{-}CCR7^{-}$, TEMRA: $CD45RA^{+}CCR7^{-}$). b) Comparison of the exhausted and expanded populations based on subsets identified by the expression of CD45RA and CCR7. c) Comparison of the exhausted and expanded population base on the expression of inhibitory receptors. Results are representative of 4 independent experiments but the expression of PD1 and TIM3 for one of the experiments was zero and was removed from panel c. Statistical analysis performed with Mann-Whitney test. Line represents median. (* $p \leq 0.05$, ** $p \leq 0.01$, *** $p \leq 0.001$)

On examining the differences among the memory subsets of the exhausted and expanded populations (Fig.5b) we observed expected differences in the naïve and effector compartments due to ongoing re-stimulation of the exhausted population. These differences are consistent for both the CD8 and CD4 populations. On examination of expression of the inhibitory receptors PD1 and TIM3, we were not able to establish a statistically significant difference between the expanded and exhausted population although an increase in the TIM3 expression is observed for the exhausted population in CD8 subsets. (Fig. 5c)

These results show that expression of inhibitory receptors cannot act as a unique identifier of exhausted cells and coincide with similar protocols already published using both murine and human cells.[94,100,101] In particular, Dunsford et al. found a quantitative increase of PD1 and TIM3 along with TOX in their repeatedly stimulated T cells and increase in the mean fluorescence intensity (MFI) values of PD1 and TIM3 along with LAG3. Despite this phenotypic and transcriptomic change, it was mostly the decrease in production of IL-2, INF-γ and the decreased cytotoxicity which would validate the creation of $T_{exhausted}$ cells.[94] Our model probably depicts a spectrum of T cells at different stages of stimulation/exhaustion and would provide an appropriate benchmark for the PDAC blood samples; especially if we consider inter-sample variability and the similar diversity and lower percentage of antigen specific T cells reported in the literature compared to the tumor microenvironment.[102–104]

7.1.2 Comparison of proliferation with an expanded population

As a functional assay, we compared the proliferation index based on the CFSE proliferation assay. We were not able to observe statistically significant difference, although a higher proliferation index was observed for the expanded population in most of the memory subsets. (Fig. 6b) On comparing the proliferation index of subsets based on the expression of inhibitory receptors there is no statistically significant difference amongst the two population. Nevertheless, there is increased proliferation index for the expanded population for PD1 and TIM3 with the exception of $CD4^+PD1^+$. (Fig. 6c) In particular, the expression of TIM3 on the expanded population has not been consistent for all experiments and therefore results are based on limited cell numbers. Our results, again reach the conclusion that the phenotypic response to stimulation involves the upregulation of inhibitory receptors. Nevertheless, the trend of TIM3 subsets to have decreased proliferation could be either be explained by increased activation induced cell death during our assay, or depicts the possibility that TIM3 enhances TCR signalling through the Akt/mTOR pathway which in turn supports short-lived effector cells in murine models.[105] Considering that the dead cell gate population does not express TIM3 the hypothesis for priming short-lived effectors and the overall trend of decreased proliferation noted in the exhausted population irrespective of central memory or effector memory phenotype would better explain our results. (Fig. 6b)

Figure 6. Comparison of proliferation index between $T_{exhausted}$ and expanded populations, based on memory subsets and expression of inhibitory receptors. a) Representative CFSE plots for CD8 T cells from an exhausted and expanded population. b) Proliferation index comparison of functional subsets

between exhausted and expanded T cells. (Comparison was performed for the subsets that would be present on both populations). c) Proliferation index comparison based on the expression of inhibitory receptors. Results are representative of 3 independent experiments but limited due to low TIM3 expression on one of the repeats on the expanded population. Statistical analysis performed with Mann-Whitney test. Bars present median with interquartile range. (* $p \leq 0.05$, ** $p \leq 0.01$, *** $p \leq 0.001$)

a) **Texpanded** **Texhausted**

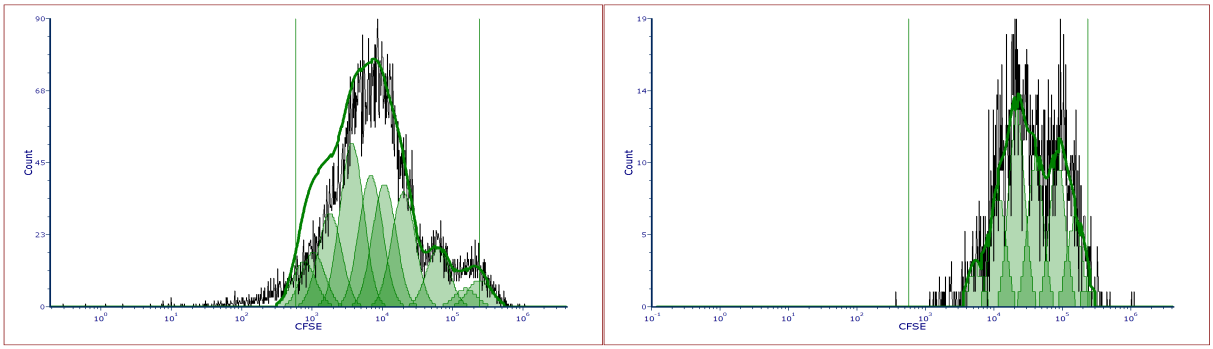

b)

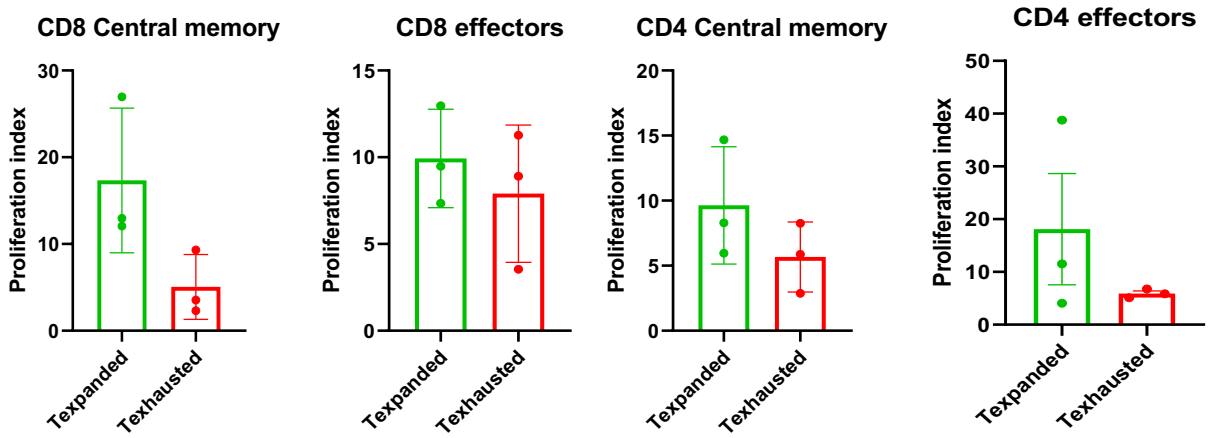

c)

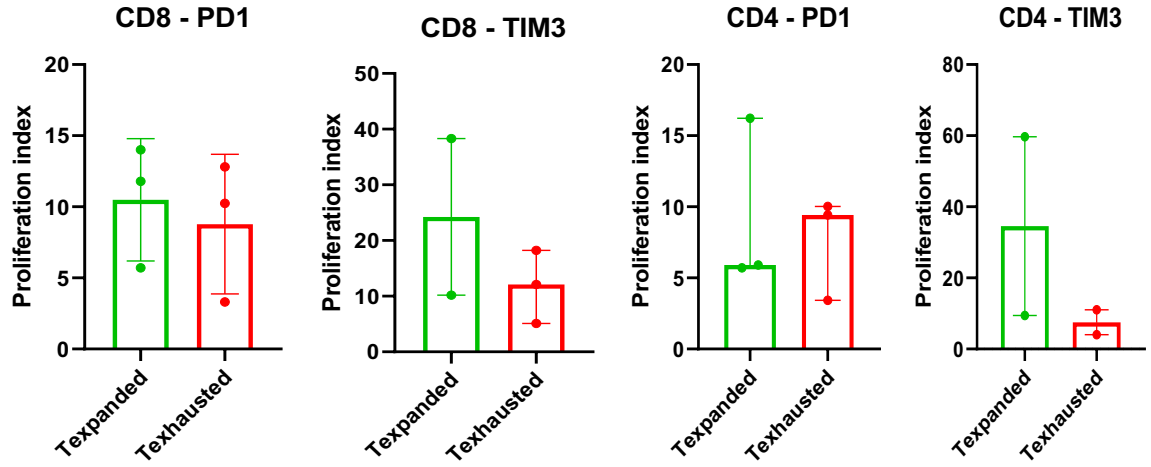

7.2 ASSESSMENT OF PERIPHERAL BLOOD FROM PATIENTS WITH PDAC

7.2.1 Analysis of phenotype post thawing

The PBMC from six patients with PDAC were compared to controls to assess their expanded / exhausted state. The results from this section are described alongside post-simulation results (after Figure 18) to provide a comprehensive picture.

CD8 subsets based on CD45RA/CCR7

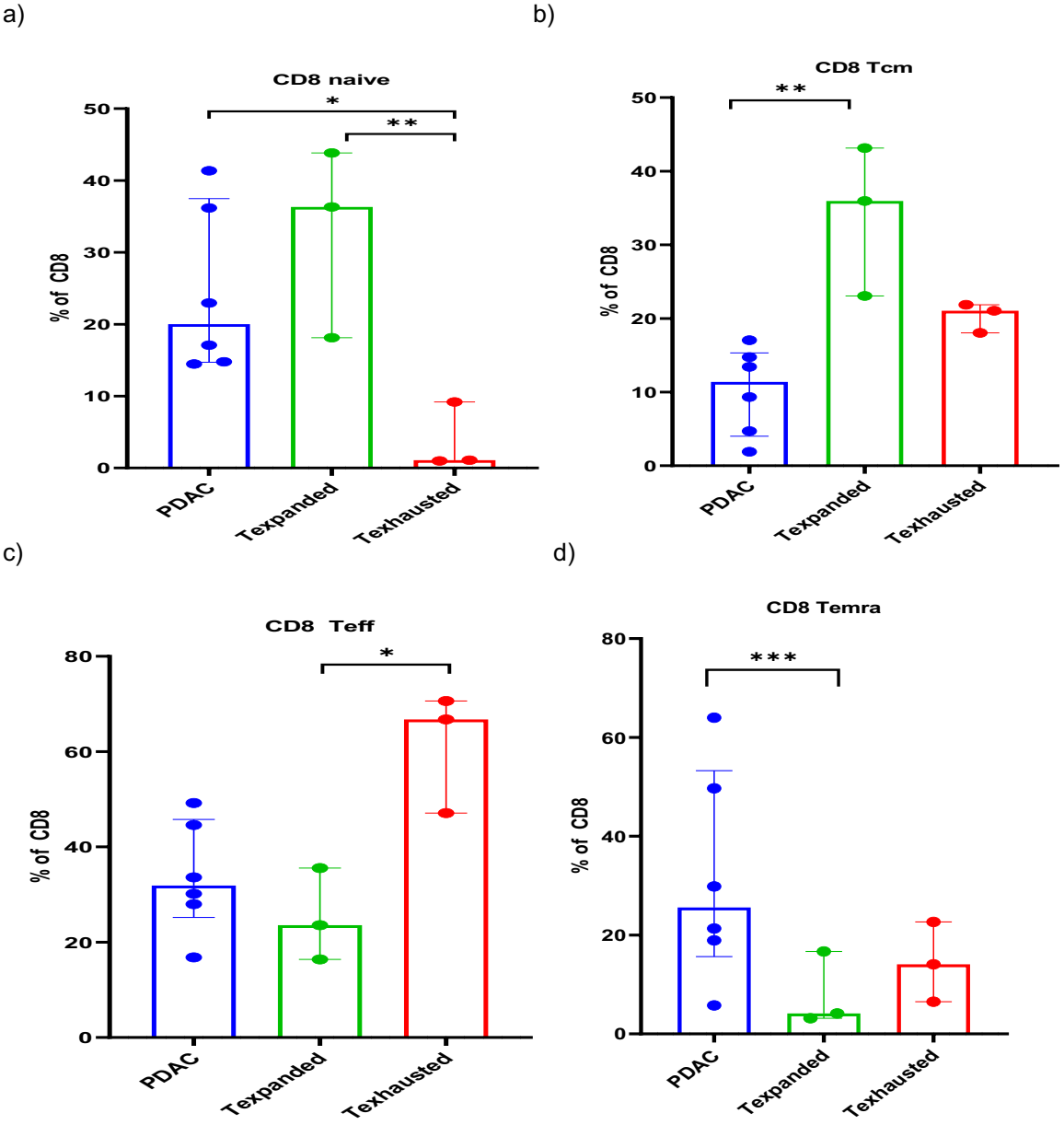

Figure 7. CD8 subsets based on CD45RA and CCR7 sub-gating. Each dot represents a patient with PDAC and separate technical repeats as control from the *in vitro* exhausted and expanded populations. a) Percentage of CD8 naïve cells ($CD45RA^{+}CCR7^{+}$). b) Percentage of CD8 central memory cells ($CD45RA^{-}CCR7^{+}$). c) Percentage of CD8 effector cells ($CD45RA^{-}CCR7^{-}$). d) Percentage of CD8 effector

memory cells (CD45RA^{+}CCR7^{-}). Statistical analysis performed with Kruskal-Wallis test with Dunn's test for multiple comparisons. Bars present median with whiskers representing interquartile range. (* $p \leq 0.05$, ** $p \leq 0.01$, *** $p \leq 0.001$)

CD8 expression of inhibitory receptors and TCF1

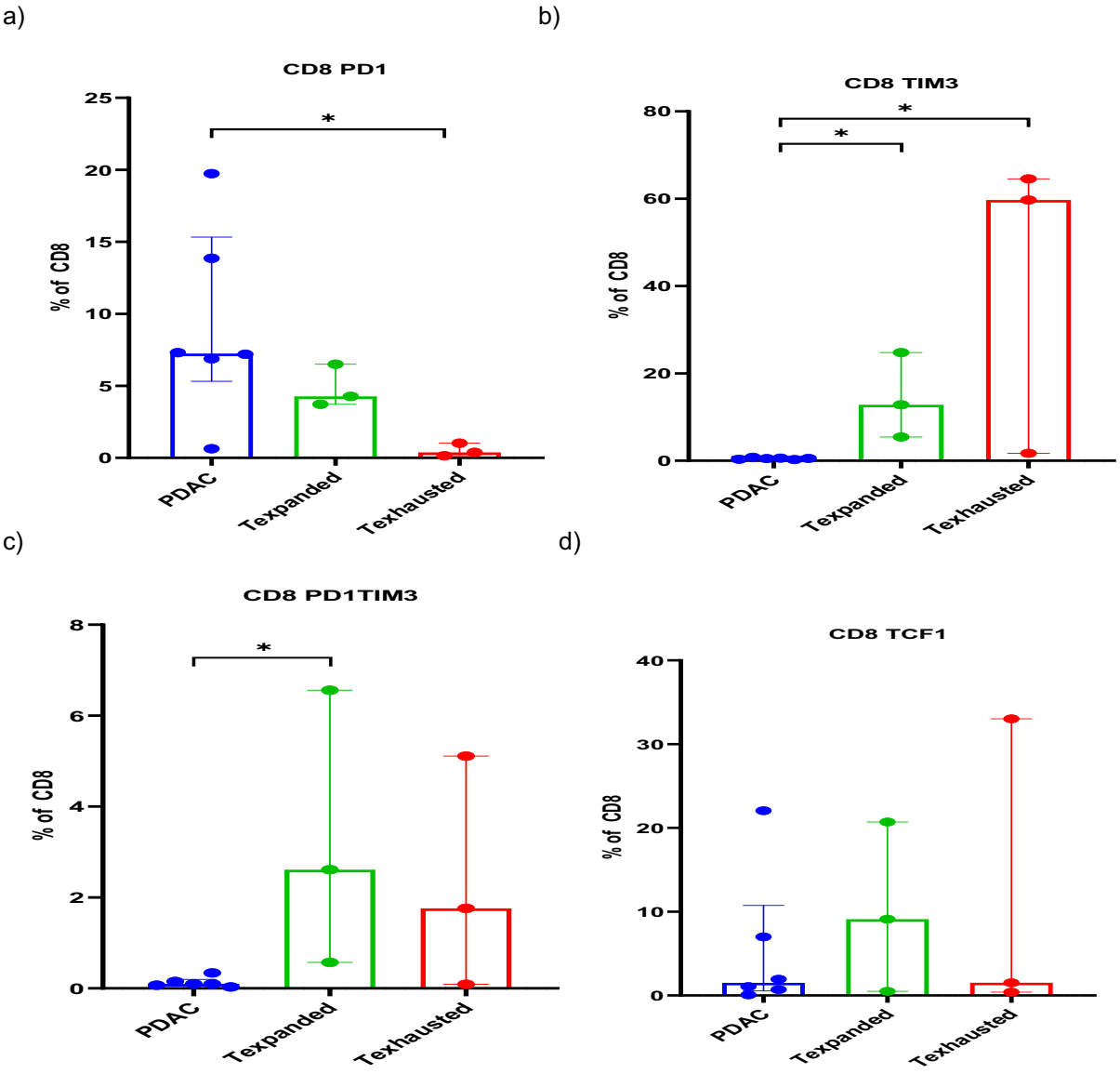

Figure 8. CD8 expression of PD1, TIM3 and TCF1. Each dot represents a patient with PDAC and separate technical repeats as control from the *in vitro* exhausted and expanded populations. a) Percentage of CD8 PD1 expressing cells. b) Percentage of CD8 TIM3 expressing cells. c) Percentage of CD8 PD1 and TIM3 expressing cells. D) Percentage of CD8 TCF1 expressing cells. Statistical analysis performed with Kruskal-Wallis test with Dunn's test for multiple comparisons. Bars present median with whiskers representing interquartile range. (* $p \leq 0.05$, ** $p \leq 0.01$, *** $p \leq 0.001$)

CD4 subsets based on CD45RA/CCR7

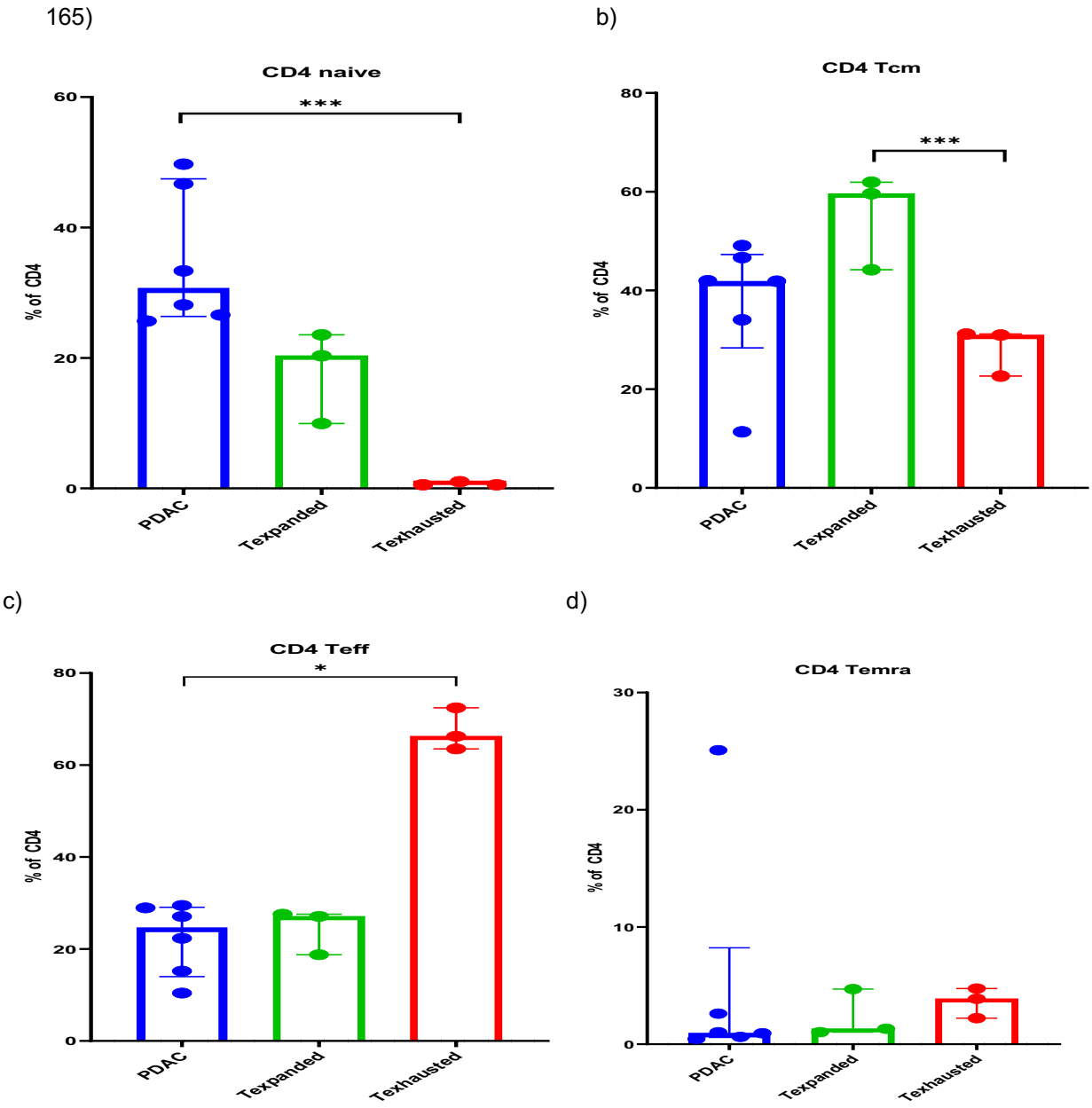

Figure 9. CD4 subsets based on CD45RA and CCR7 sub-gating. Each dot represents a patient with PDAC and separate technical repeats as control from the *in vitro* exhausted and expanded populations. a) Percentage of CD4 naïve cells ($CD45RA^{+}CCR7^{+}$). b) Percentage of CD4 central memory cells ($CD45RA^{-}CCR7^{+}$). c) Percentage of CD4 effector cells ($CD45RA^{-}CCR7^{-}$). d) Percentage of CD4 effector memory cells ($CD45RA^{+}CCR7^{-}$). Statistical analysis performed with Kruskal-Wallis test with Dunn's test for multiple comparisons. Bars present median with whiskers representing interquartile range. (* $p \leq 0.05$, ** $p \leq 0.01$, *** $p \leq 0.001$)

CD4 expression of inhibitory receptors and TCF1

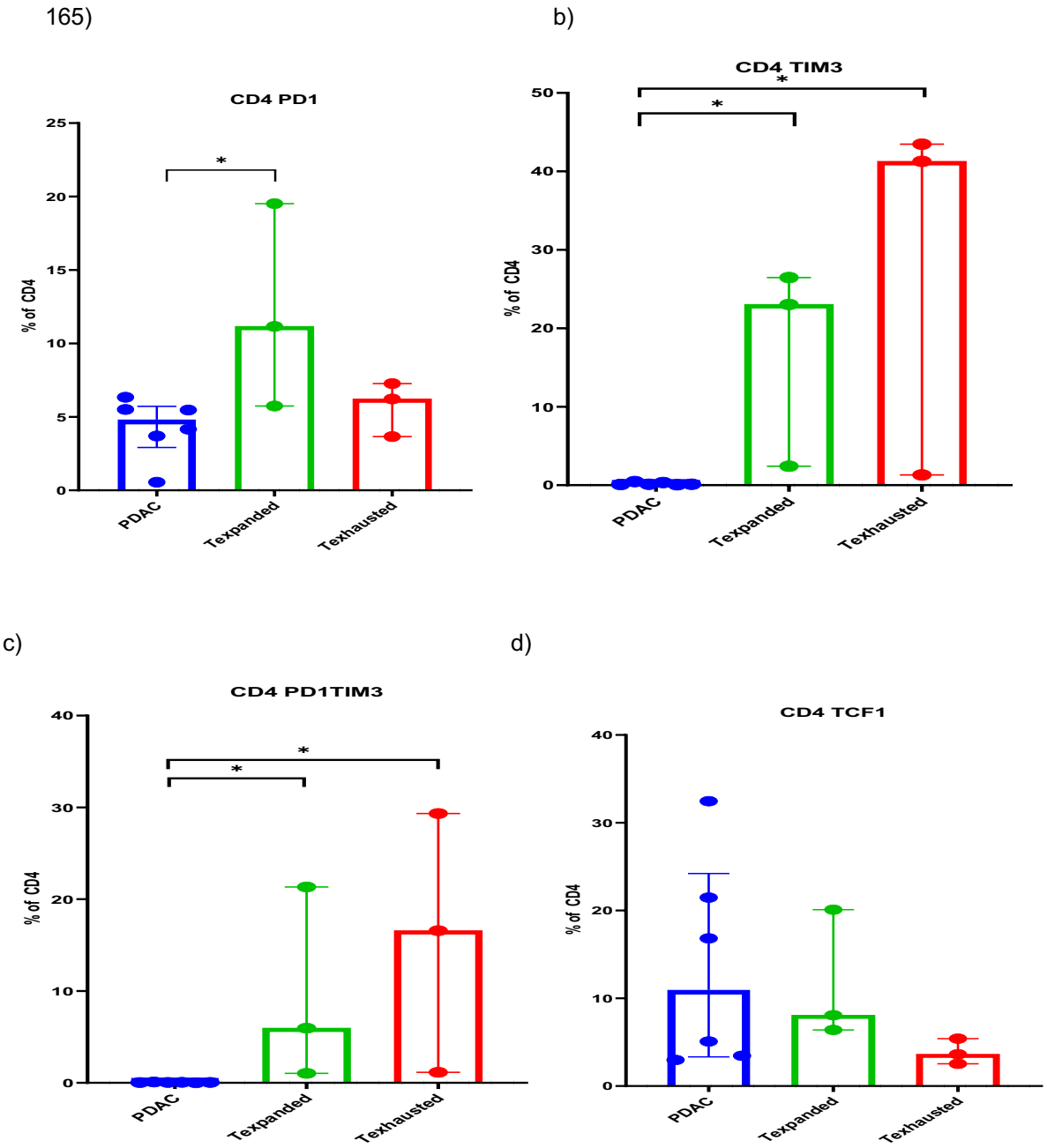

Figure 10. CD4 expression of PD1, TIM3 and TCF1. Each dot represents a patient with PDAC and separate technical repeats as control from the *in vitro* exhausted and expanded populations. a) Percentage of CD4 PD1 expressing cells. b) Percentage of CD4 TIM3 expressing cells. c) Percentage of CD4 PD1 and TIM3 expressing cells. d) Percentage of CD4 TCF1 expressing cells. Statistical analysis performed with Kruskal-Wallis test with Dunn's test for multiple comparisons. Bars present median with whiskers representing interquartile range. (* $p \leq 0.05$, ** $p \leq 0.01$, *** $p \leq 0.001$)

CD4 memory subsets

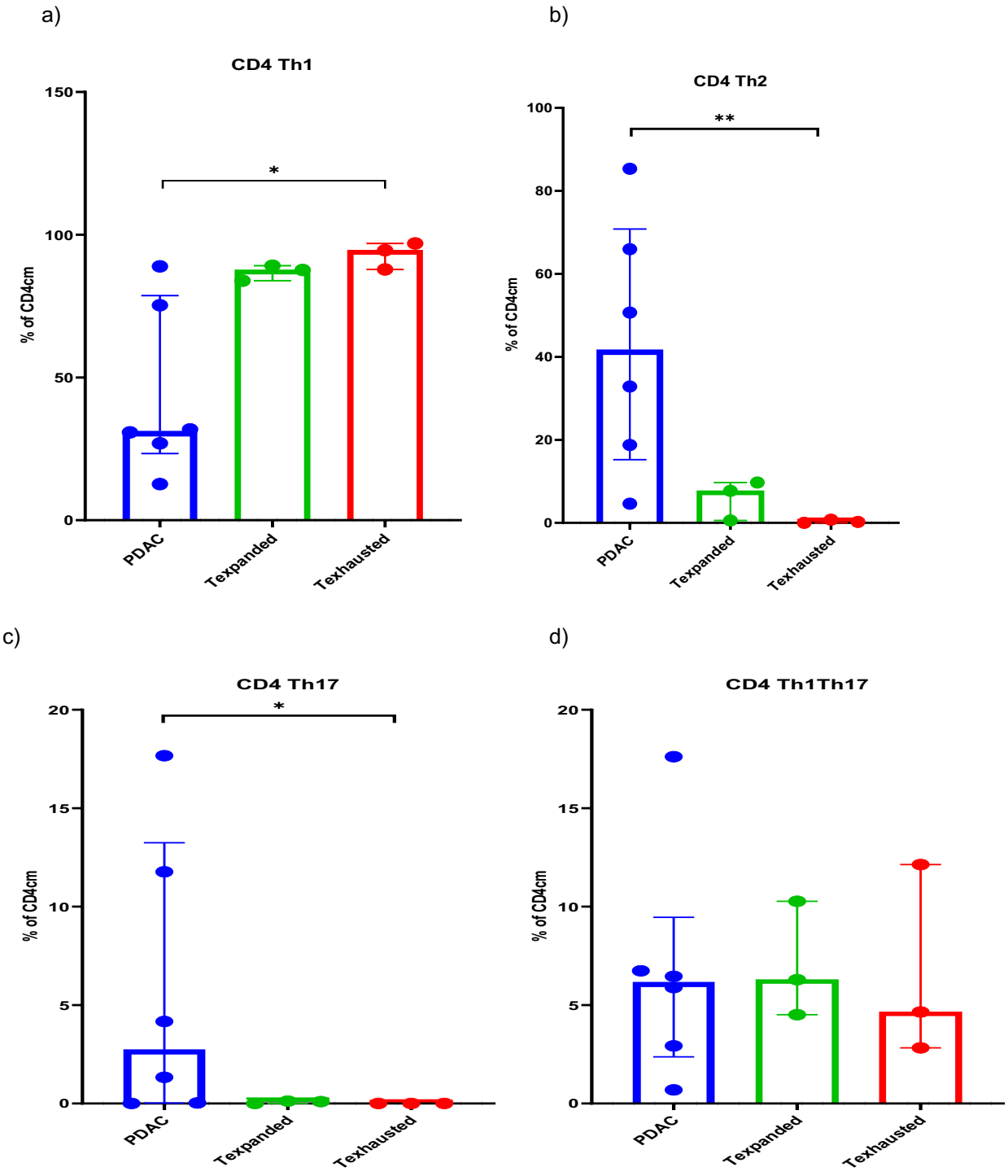

Figure 11. CD4 memory subsets based on CXCR3 and CCR6 expression. Each dot represents a patient with PDAC and separate technical repeats as control from the *in vitro* exhausted and expanded populations. a) Percentage of CD4 Th1 cells ($CXCR3^{+}CCR6^{-}$). b) Percentage of CD4 Th2 cells ($CXCR3^{-}CCR6^{-}$). c) Percentage of CD4 Th17 cells ($CXCR3^{-}CCR6^{+}$). d) Percentage of CD4 Th1Th17 cells ($CXCR3^{+}CCR6^{+}$). Statistical analysis performed with Kruskal-Wallis test with Dunn's test for multiple

comparisons. Bars present median with whiskers representing interquartile range. (* p ≤ 0.05, ** p ≤ 0.01, *** p ≤ 0.001)

T regulatory cells and T regulatory memory cells

165) b)

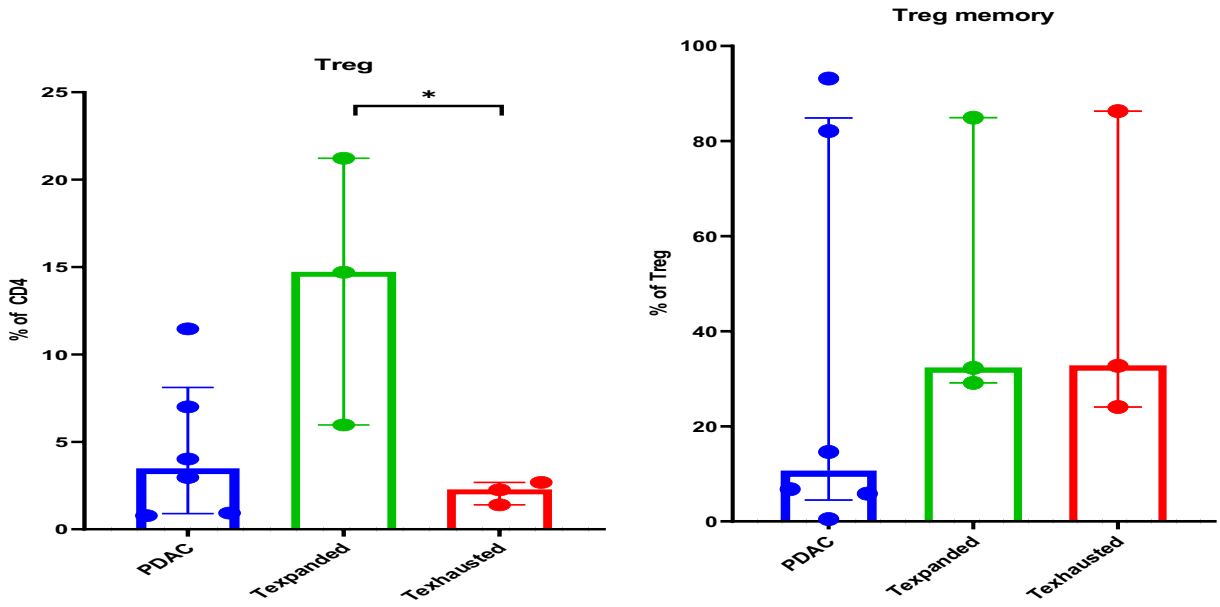

Figure 12. T regulatory cells based on FoxP3 and CD25 expression. Each dot represents a patient with PDAC and separate technical repeats as control from the *in vitro* exhausted and expanded populations. a) Percentage of CD4 T regulatory cells ($FoxP3^+CD25^+$). b) Percentage of CD4 memory T regulatory cells ($FoxP3^+CD25^+CD45RO^+$). Statistical analysis performed with Kruskal-Wallis test with Dunn's test for multiple comparisons. Bars present median with whiskers representing interquartile range. (* p ≤ 0.05, ** p ≤ 0.01, *** p ≤ 0.001)

7.2.2 Analysis of phenotype post stimulation

The PBMC from six patients with PDAC were stimulated with CD3/CD28 beads and compared to controls to assess their expanded / exhausted state.

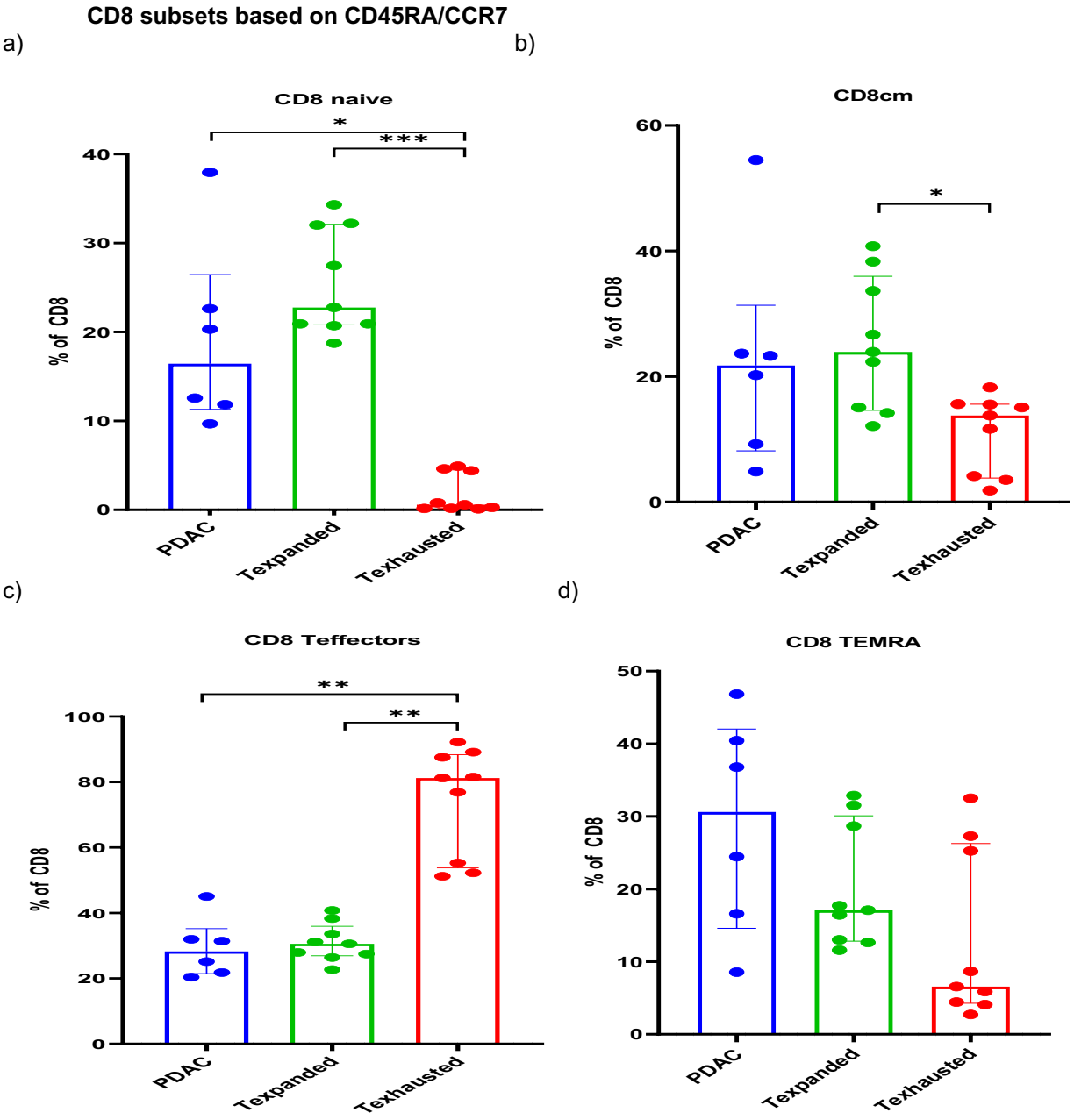

Figure 13. CD8 subsets based on CD45RA and CCR7 sub-gating. Each dot represents a patient with PDAC and 3 separate technical repeats per experiment as control from the *in vitro* exhausted and expanded populations. a) Percentage of CD8 naïve cells ($CD45RA^{+}CCR7^{+}$). b) Percentage of CD8 central memory cells ($CD45RA^{-}CCR7^{+}$). c) Percentage of CD8 effector cells ($CD45RA^{-}CCR7^{-}$). d) Percentage of CD8 effector memory cells ($CD45RA^{+}CCR7^{-}$). Statistical analysis performed with Kruskal-Wallis test with Dunn's test for multiple comparisons. Bars present median with whiskers representing interquartile range. (* $p \leq 0.05$, ** $p \leq 0.01$, *** $p \leq 0.001$)

CD8 expression of inhibitory receptors and TCF1

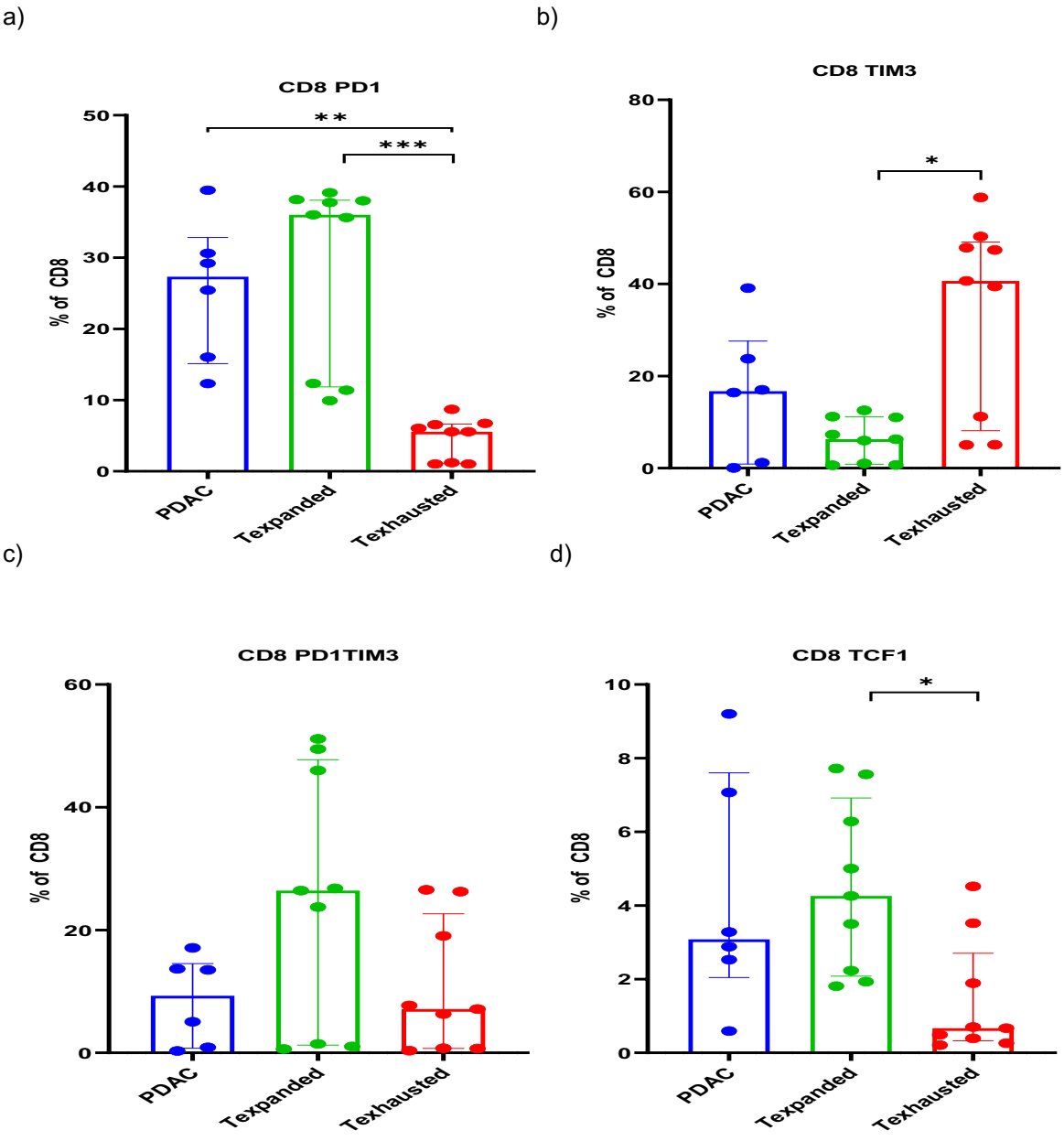

Figure 14. CD8 expression of PD1, TIM3 and TCF1 post-stimulation. Each dot represents a patient with PDAC and 3 separate technical repeats per experiment as control from the *in vitro* exhausted and expanded populations. a) Percentage of CD8 PD1 expressing cells. b) Percentage of CD8 TIM3 expressing cells. c) Percentage of CD8 PD1 and TIM3 expressing cells. d) Percentage of CD8 TCF1 expressing cells. Statistical analysis performed with Kruskal-Wallis test with Dunn's test for multiple comparisons. Bars present median with whiskers representing interquartile range. (* $p \leq 0.05$, ** $p \leq 0.01$, *** $p \leq 0.001$)

CD4 subsets based on CD45RA/CCR7

a)

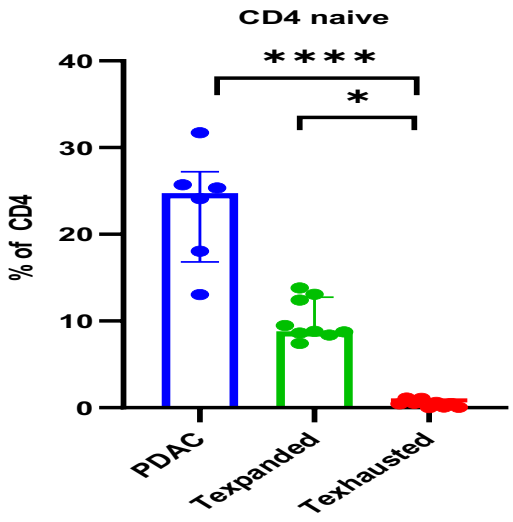

b)

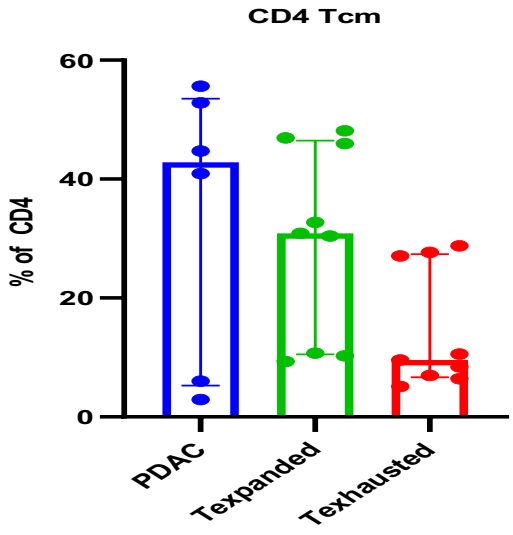

c)

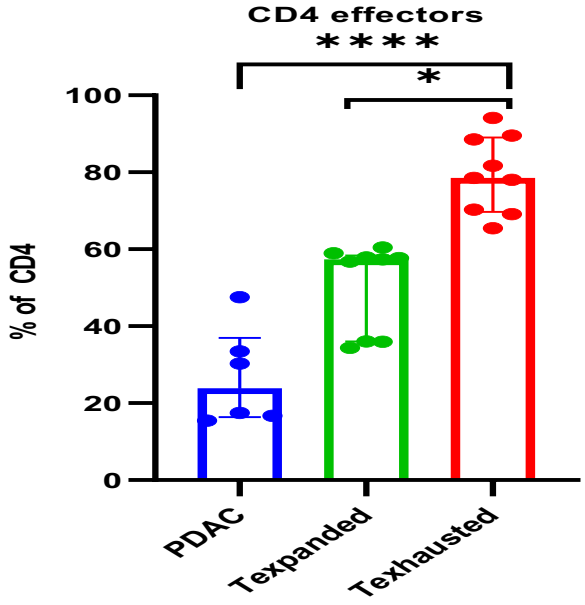

d)

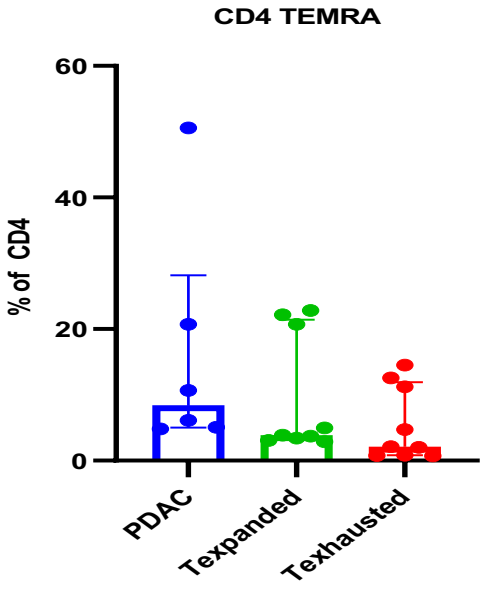

Figure 15. CD4 subsets based on CD45RA and CCR7 sub-gating. Each dot represents a patient with PDAC and 3 separate technical repeats as control per experiment from the *in vitro* exhausted and expanded populations. a) Percentage of CD4 naïve cells ($CD45RA^{+}CCR7^{+}$). b) Percentage of CD4 central memory cells ($CD45RA^{-}CCR7^{+}$). c) Percentage of CD4 effector cells ($CD45RA^{-}CCR7^{-}$). d) Percentage of CD4 effector memory cells ($CD45RA^{+}CCR7^{-}$). Statistical analysis performed with Kruskal-Wallis test with Dunn's test for multiple comparisons. Bars present median with whiskers representing interquartile range. (* $p \leq 0.05$, ** $p \leq 0.01$, *** $p \leq 0.001$)

CD4 expression of inhibitory receptors and TCF1

165)

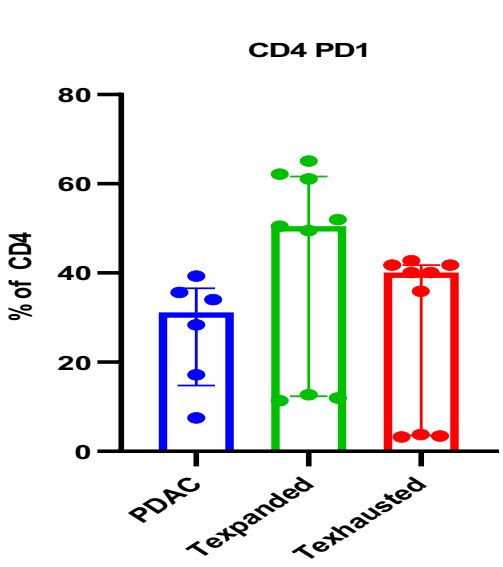

b)

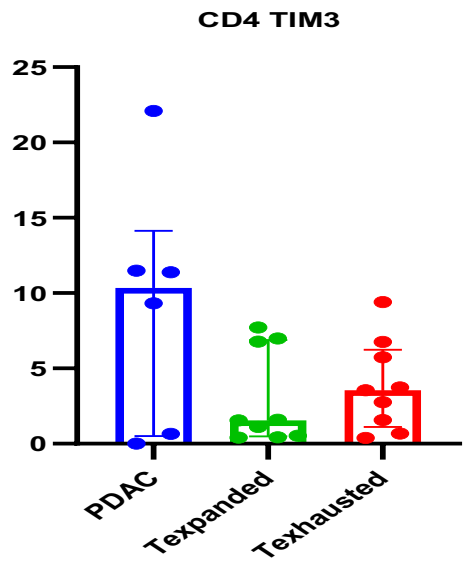

c)

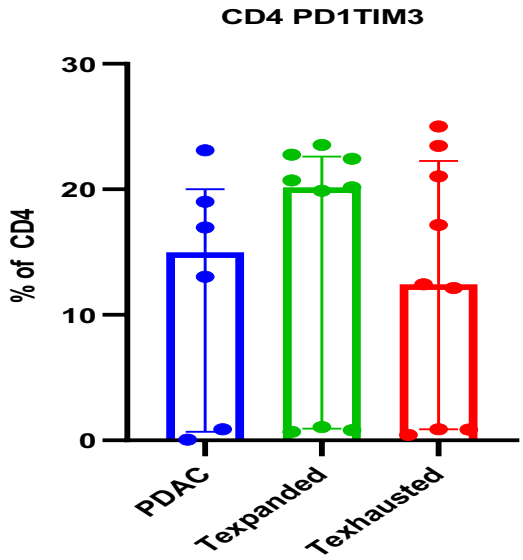

d)

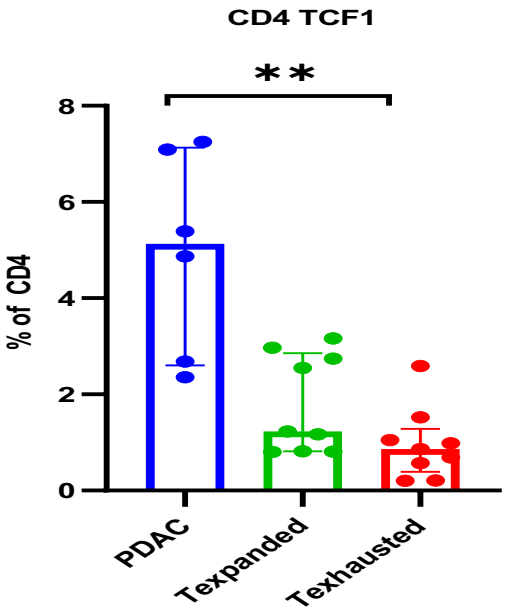

Figure 16. CD4 expression of PD1, TIM3 and TCF1. Each dot represents a patient with PDAC and 3 separate technical repeats as control per experiment from the *in vitro* exhausted and expanded populations. a) Percentage of CD4 PD1 expressing cells. b) Percentage of CD4 TIM3 expressing cells. c) Percentage of CD4 PD1 and TIM3 expressing cells. d) Percentage of CD4 TCF1 expressing cells. Statistical analysis performed with Kruskal-Wallis test with Dunn's test for multiple comparisons. Bars present median with whiskers representing interquartile range. (* $p \leq 0.05$, ** $p \leq 0.01$, *** $p \leq 0.001$)

7.2.3 Phenotypic changes in PDAC samples before and after stimulation

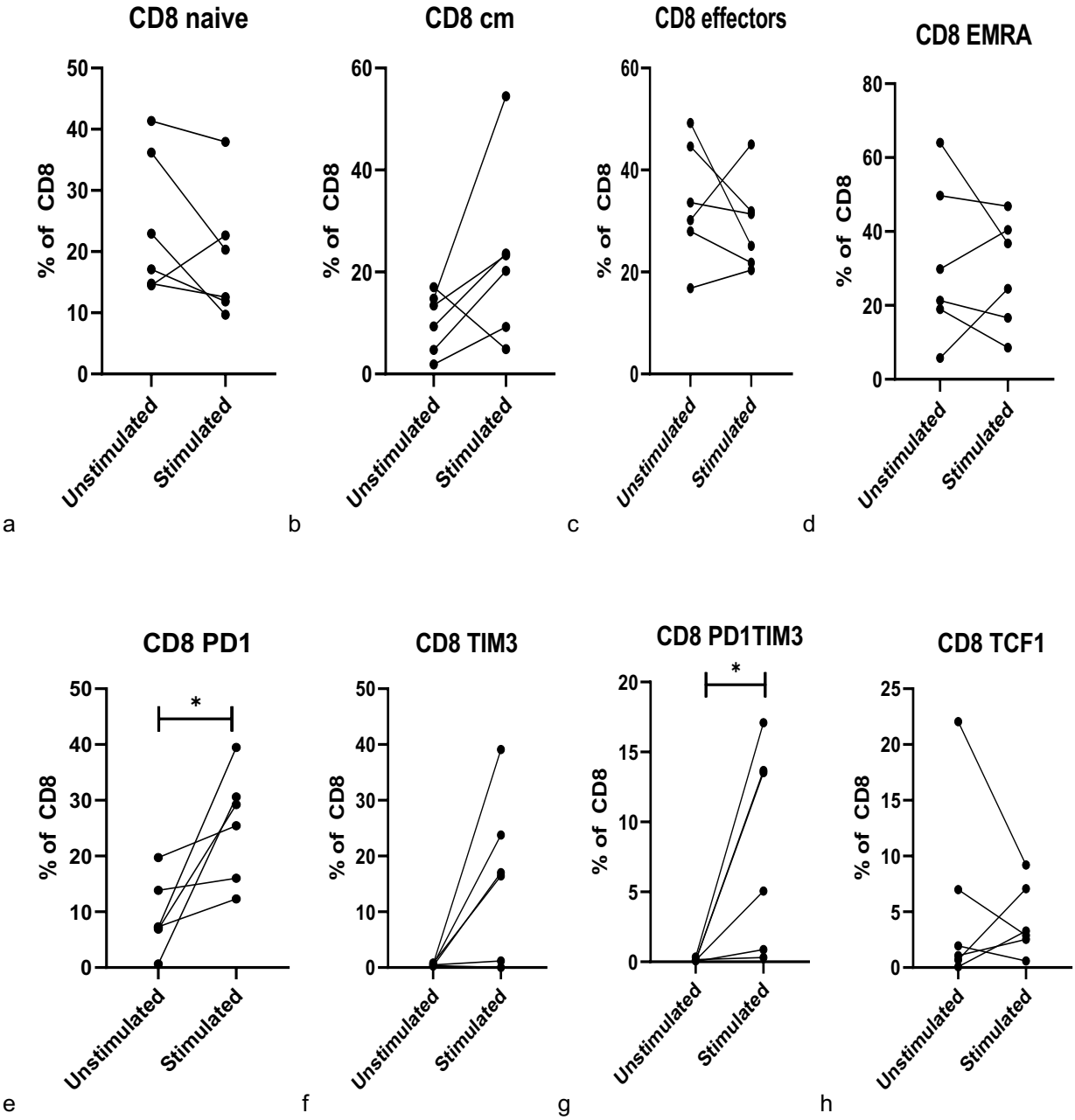

Figure 17. Comparison of unstimulated versus stimulated phenotype of CD8 T cells isolated from patients with PDAC. T cells where stimulated post-thaw for 48h with CD3/CD28 beads in RPMI. Percentages of CD8 cells were compared with paired two-tailed Wilcoxon test. (* $p \leq 0.05$, ** $p \leq 0.01$, *** $p \leq 0.001$)

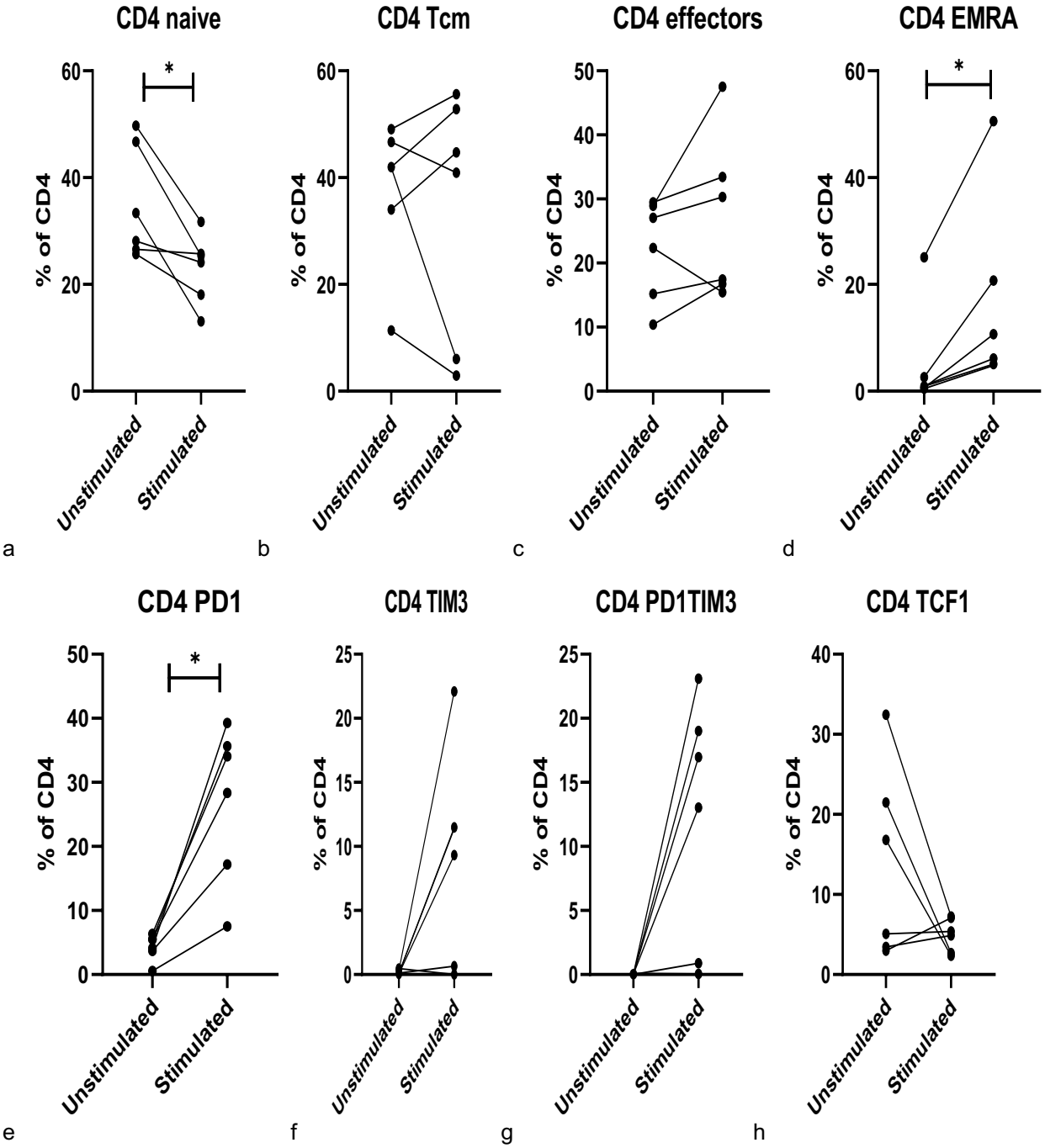

Figure 18. Comparison of unstimulated versus stimulated phenotype of CD4 T cells isolated from patients with PDAC. T cells where stimulated post-thaw for 48h with CD3/CD28 beads in RPMI. Percentages of CD4 cells were compared with paired two-tailed Wilcoxon test. (* $p \leq 0.05$, ** $p \leq 0.01$, *** $p \leq 0.001$)

CD8 results

The use of CD45RA and CCR7 shows that CD8 cells from patients with PDAC have higher percentage of T_{EMRA} cells (median = 25.59%) compared to the *in vitro* expanded population (p= 0.03, mean rank difference= 5.5) a difference which resolves post stimulation (*Fig.7d & Fig.13d*). This change cannot be interpreted by a statistically significant change post-stimulation (median= 30.63%) in the PDAC samples (p=0.84, median difference= -3.79, *Fig.17d*) but is relevant in comparison to control in the unstimulated setting.

Similarly, the CD8 central memory population in PDAC (median = 11.38%) is comparably less to the expanded population. (p= 0.003, mean rank difference= -7.5, *Fig.7b*), a difference which resolves post stimulation (*Fig.13b*). The reduction in CD8 naïve is usually explained by an increase in CD8 central memory population, an aspect we do not observe (p= 0.33, mean rank difference = -2.5, *Fig.7a*). Post stimulation there is no difference in the PDAC central memory CD8 subset (p= 0.15, median difference= 12.09, *Fig.17b*) or naïve population. (p= 0.21, median difference= -4.33, *Fig.17a*).

The expression of inhibitory receptor PD1 in the post-thaw sample is higher in the PDAC (median= 7.25%) compared to T exhausted (p=0.01, mean difference= 6.5, *Fig.8a*). This difference is maintained post-stimulation (p= 0.007, mean difference= 11.33, *Fig.14a*) primarily driven by change in the expression of PD1 in the PDAC samples. (p= 0.03, median difference= 14.02, *Fig.17e*).

On the contrary the expression of TIM3 in the post-thaw sample is minimal (median= 0.5%) compared to both the T exhausted and expanded populations. (p=0.01, mean difference= -6.5, p=0.03 mean difference= -5.5 respectively, *Fig.8b*). These differences are eliminated post stimulation with increase in TIM3 expressing CD8 T cells (median= 16.26%, *Fig.14b*) although this change is not reaching statistical significance (p= 0.06, median difference=16.18, *Fig.17f*).

Finally, we can detect an increase in the double positive population expressing both PD1 and TIM3 (p= 0.03, median difference 9.2, Fig.17g), although similar increase is observed both for the T exhausted and T expanded populations (*Fig.8c & Fig.14c*).

CD4 results

In contrast to the differences observed in the CD8 subsets, the CD4 T cells do not show statistically significant differences to the T exhausted and expanded populations apart from the expected ones in the naïve and effector compartment. (*Fig 9a, 9c*) These phenotypic relationships are maintained post stimulation although there is inherent change in the TEMRA population by a statistically significant increase post stimulation (p= 0.03, median difference= 7.59, *Fig. 18d*) while there is no change in the effector and central memory populations, depicting a deviation of the naïve population to TEMRA in the CD4 compartment post stimulation. (*Fig. 18a-c*)

The memory subsets observed post-thaw are showing a significant proportion of Th2 cells (median= 41.78, *Fig. 11b*) although with a large variation. Similarly, the presence of Th1 memory cells is almost equally evident (median= 31.31, *Fig. 11a*) and a small percentage of Th17 cells could be identified in the peripheral blood. (median= 2.8, *Fig. 11c*). Finally, T_{reg} cells are observed in the periphery of PDAC patients (median= 3.5, *Fig. 12a*) but surprisingly T_{regmem} by expression of CD45RO is low (median= 10.69) with only 2 patients presenting expected levels of CD45RO (~80%) expression in the $CD4^{+}FOXP3^{+}CD25^{+}$.

Contrary to the CD8 population the CD4 expression of PD1 (median= 4.8) in the post-thaw sample is not different from the exhausted (p= 0.43, mean difference= -2, *Fig. 10a*). This lack of difference is subsequently maintained post-stimulation (p >0.9, mean difference= -1.72, *Fig.16a*) although there is statistically significant increase in the expression of PD1. (p=0.03, median differences= 25.27, *Fig.18a*)

Similarly, although the expression of TIM3 in the post-thaw sample is significantly lower compared to both the exhausted and expanded populations, (p= 0.01, mean difference= -6.5, p=0.03 mean difference= -5.5 respectively, *Fig. 10b*) after stimulation this difference is eliminated with CD4 cells from PDAC patients expressing high percentage of TIM3 compared to both the exhausted and expanded controls but this is not reaching statistical significance (median=10.35, p=0.9, p=0.4 respectively, *Fig. 16b*).

Finally, although there is increase in TIM3 and double positive PD1TIM3 CD4 cells post stimulation, there is no statistically significant difference before and after stimulation on the current cohort. (p=0.06 median difference= 10.28, p=0.06 median difference=14.95, *Fig.18f and g*).

Overall, the results depict an expected phenotype distribution amongst patients with PDAC which might deviate during stimulation to the known TEMRA population on the CD4 compartment. The expression of inhibitory receptors after stimulation does not necessarily depict an exhausted phenotype but nevertheless cannot exclude divergent kinetics especially in the expression of TIM3.

7.2.4 Analysis of proliferation index

The proliferation index of CD4 (median= 6.5, p=0.56) and CD8 (median= 5.4, p=0.82) for the PDAC samples is not different in a statistically significant way from the expanded or exhausted population overall. Inspecting the functional memory subset of central memory T cells CD4 and CD8 cells from PDAC patients, their proliferation index is not different from the control populations and similar results occurred when looking at the effectors and EMRA T cells. (*Fig.19b, 19c*)

Similarly, on comparing the CD4-PD1^{+} (median=8.8, p=0.64) and CD8-PD1^{+} (median=4.3, p= 0.35) subsets we do not find difference in the proliferation index amongst the three groups. On evaluating the CD8-TIM3^{+} expressing population on the expanded subset we find an increased proliferation index (median=41.6, p=0.01) compared to the exhausted population. However, these results are based on the limitation that less TIM3 positive cells expanded to provide proliferation index measurements for the expanded population compared to the exhausted and PDAC subsets (n=6) which have a more consistent expression of TIM3. Therefore it is very difficult to appreciate its biological relevance. Similar result can be seen for CD4-TIM3^{+} (median=60, p=0.002). (*Fig. 20b, 20c*)

Comparison of the proliferation index amongst the PDAC samples shows no significant difference based on the functional memory status of CD8 T cells (p=0.96, median(I)= 6.7) and similar is the comparison for the CD4 T cells. (p=0.87, median (naïve) = 5.36, Fig.21a). On the contrary, we are able to show a statistically significant difference between the PD1 and TIM3 expressing subsets which is apparent both on CD4 and CD8 subsets (mean rank difference=-7.17 p=0.039, mean rank difference=-6.53 p=0.047,

respectively, Fig. 21b). This result along with the limited TIM3 expression in the expanded populations suggests a divergent pathway during stimulation for the PDAC patient samples. This may suggest that TIM3 is preferentially expressed in PDAC samples upon activation and this subset is able to sustain a proliferative response in contrast to the TIM3 expressing population in the expanded cells.

7.2.5 Analysis of proliferation index of subsets

a)

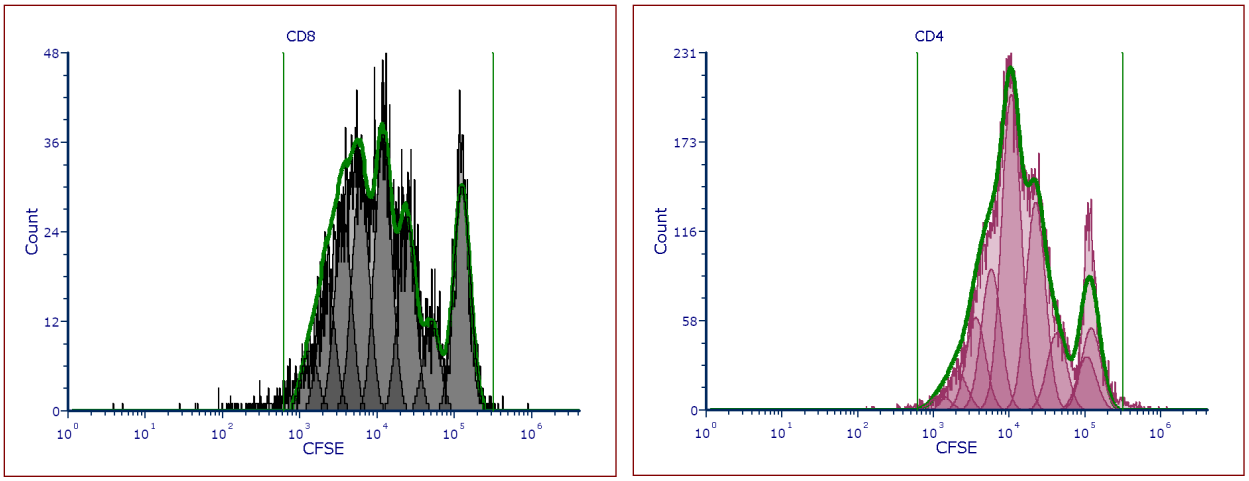

b)

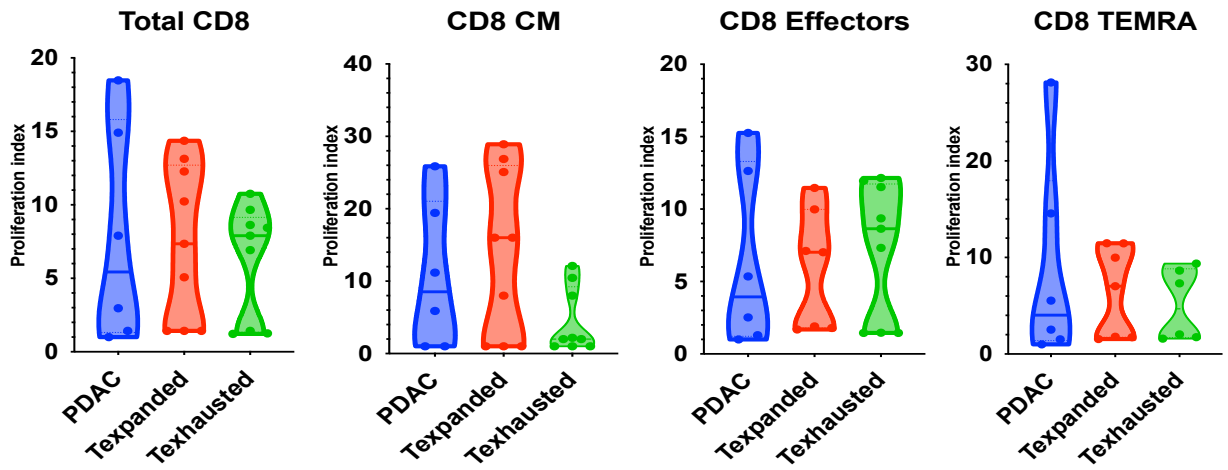

c)

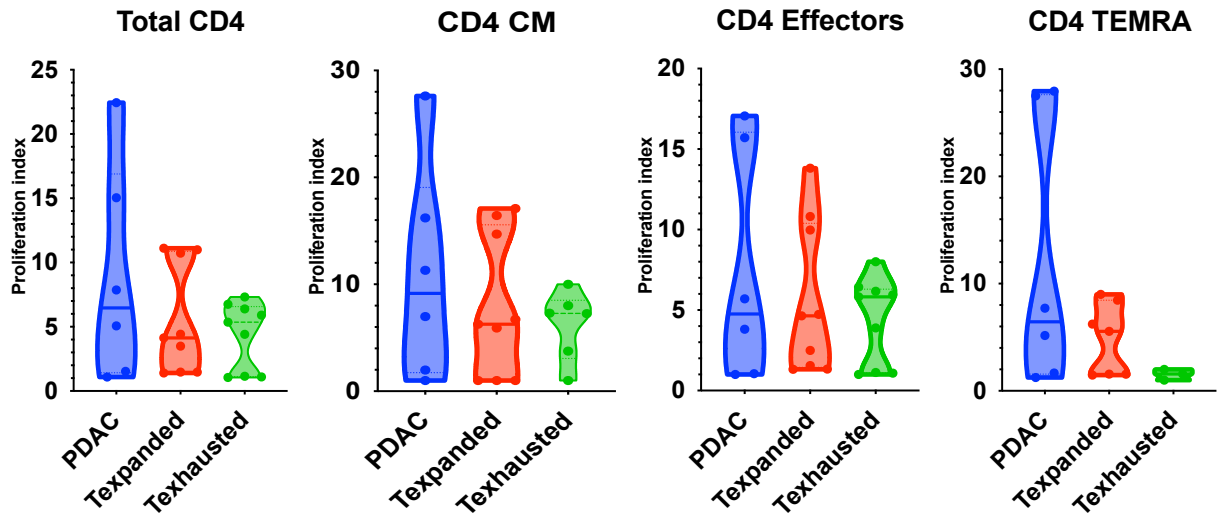

Figure 19. Comparison of proliferation index amongst PDAC, T exhausted and expanded populations, based on memory subsets. a) Representative CFSE plots for CD4 (black) & CD8 (purple) T cells from a PDAC patient. b) Proliferation index comparison of functional subsets amongst CD8 T cells [CM: central memory ($CD45RA^{-}CCR7^{+}$), effectors ($CD45RA^{-}CCR7^{-}$), TEMRA ($CD45RA^{+}CCR7^{-}$)]. c) Proliferation index comparison of functional subsets amongst CD4 T cells [CM: central memory ($CD45RA^{-}CCR7^{+}$), effectors ($CD45RA^{-}CCR7^{-}$), TEMRA ($CD45RA^{+}CCR7^{-}$)]. Statistical analysis performed with Kruskal-Wallis test with Dunn's test for multiple comparisons. Violin plots present median with interquartile range. (* $p \leq 0.05$, ** $p \leq 0.01$, *** $p \leq 0.001$)

a)

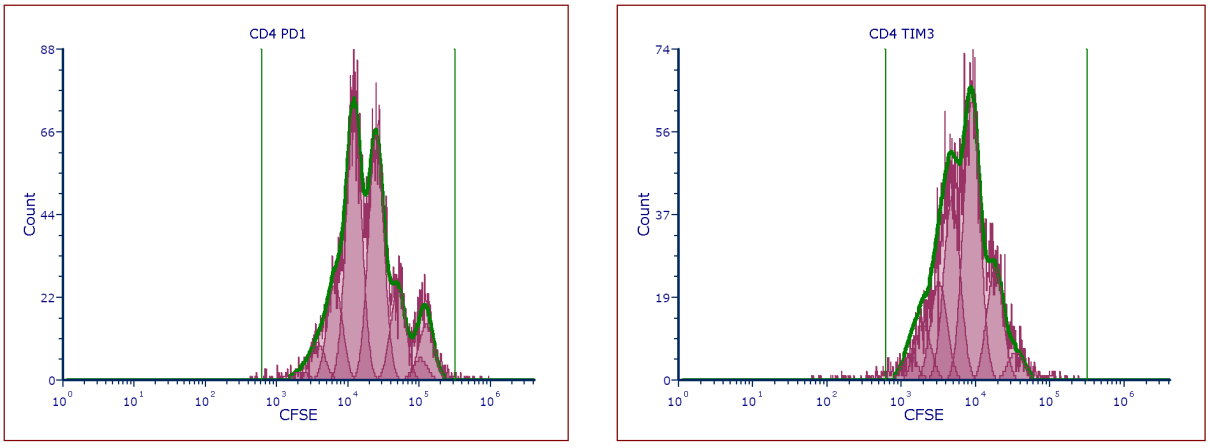

b)

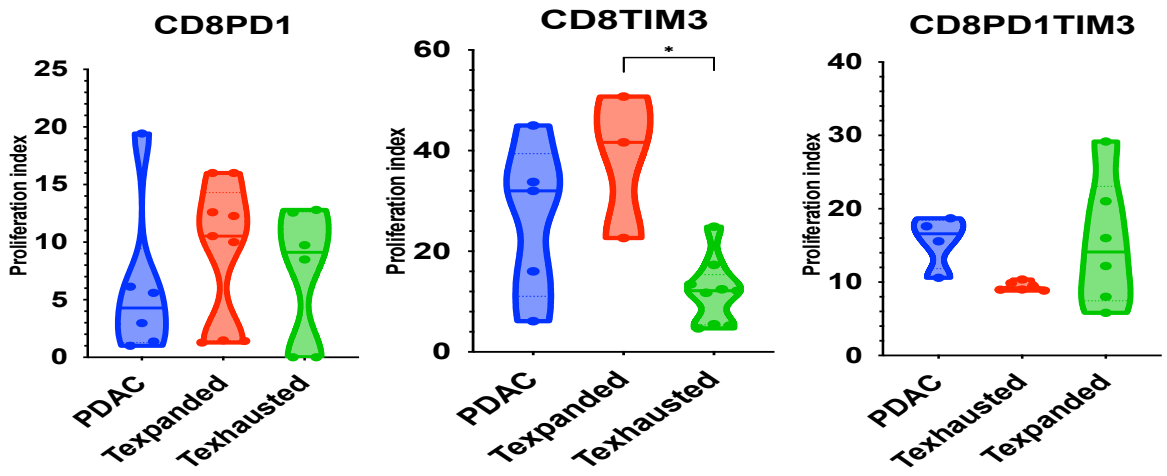

c)

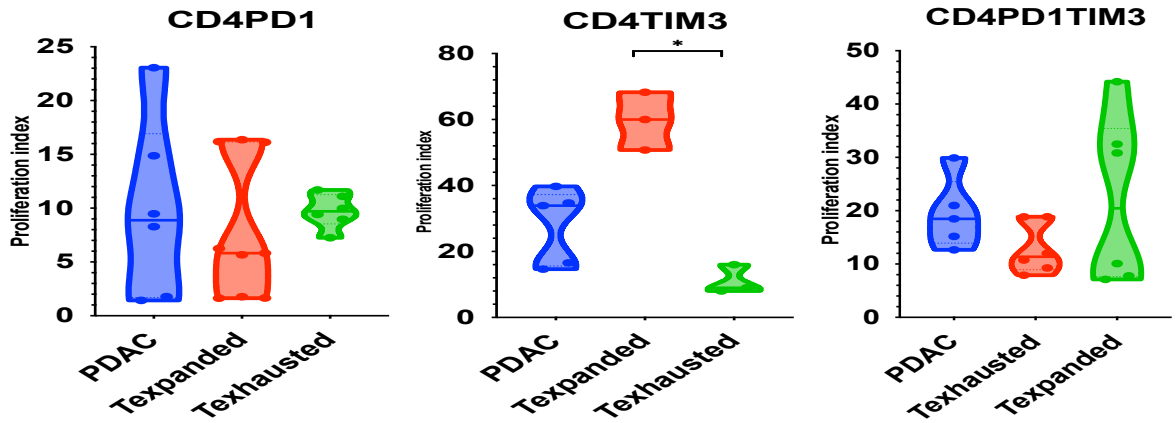

Figure 20. Comparison of proliferation index amongst PDAC, T exhausted and expanded populations, based on expression of inhibitory receptors. a) Representative CFSE plots for $CD4PD1^{+}$ (left) & $CD4TIM3^{+}$ (Right) T cells from a PDAC patient. b) Proliferation index comparison based on the expression of inhibitory receptors on CD8 T cells. c) Proliferation index comparison based on the expression of inhibitory receptors on CD4 T cells. Statistical analysis performed with Kruskal-Wallis test with Dunn's test for multiple comparisons. Violin plots present median with interquartile range. (* $p \leq 0.05$, ** $p \leq 0.01$, *** $p \leq 0.001$)

a)

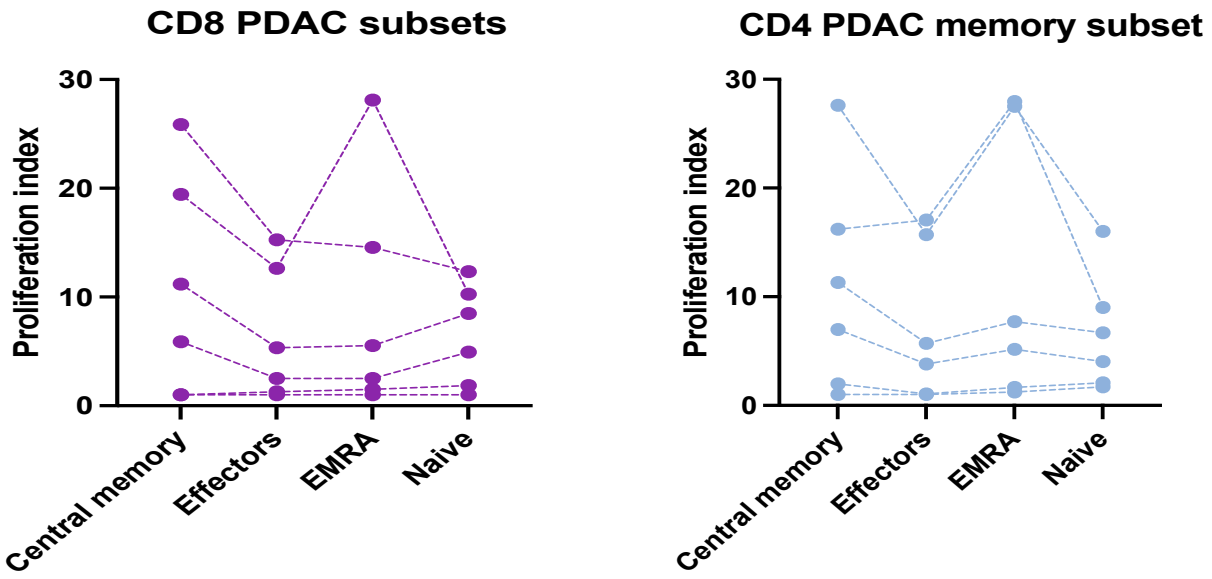

b)

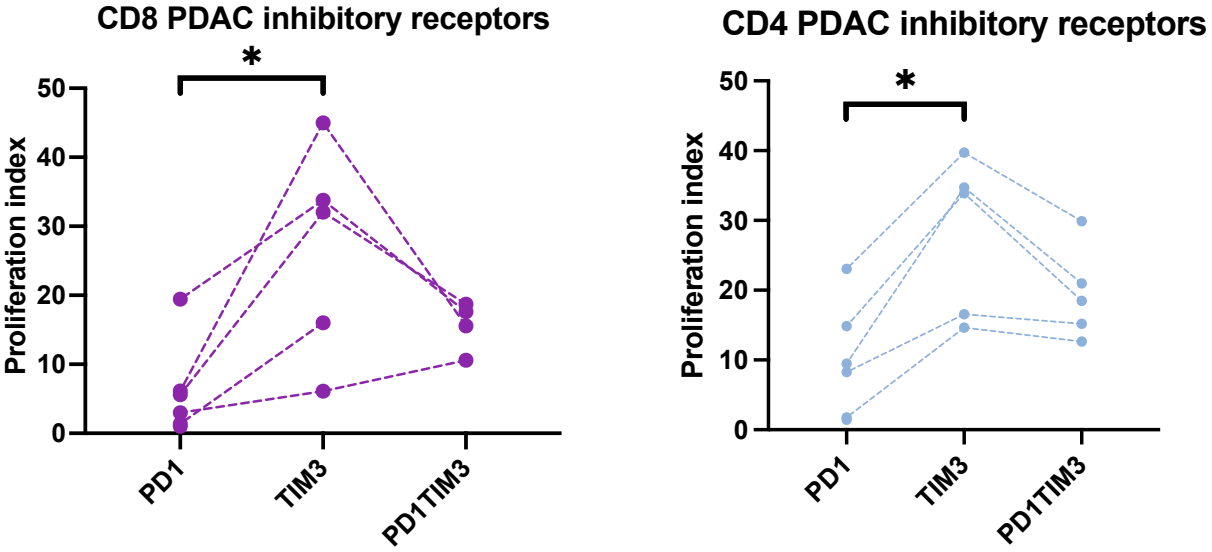

Figure 21. Comparison of proliferation index amongst PDAC patients based on functional subsets and expression of inhibitory receptors. a) Comparison of functional subsets from 6 PDAC patients. b) Comparison of proliferation index based on inhibitory receptor expression from 6 PDAC patients. Statistical analysis performed with Kruskal-Wallis test with Dunn's test for multiple comparisons. (* $p \leq 0.05$, ** $p \leq 0.01$, *** $p \leq 0.001$)

8 COMPARISON OF SAMPLES BEFORE AND AFTER SURGICAL DE-BULKING

8.1 T CELL PHENOTYPIC COMPARISON

The phenotypic analysis of the paired samples before and after surgical de-bulking shows minimal differences which can be attributed to the removal of the pancreatic adenocarcinoma. In particular, the memory subsets of CD4 (Fig. 22a) depict similar median percentages for $T_{naïve}$ (preoperative= 18.6%, postoperative= 26.12%), T_{CM} (preoperative= 15.4%, postoperative= 21.7%), T_{eff} (preoperative= 60.3%, postoperative= 44.5%), T_{EMRA} (preoperative= 5.4%, postoperative= 6.8%) and Treg (preoperative= 4.8%, postoperative= 6.5%). In contrast, we observe a decrease in the Th1($CXCR3^+CCR6^-$) median response (preoperative= 66.8%, postoperative= 39.5%) and an associated increase in the Th2 ($CXCR3^-CCR6^-$) response in the postoperative samples (preoperative= 33.2%, postoperative= 60%). Finally, we observe minimal Th17 presence (preoperative= 0.01%, postoperative= 0.2%) and a Treg memory ($FOXP3^+CD25^+CD45RO^+$) increase postoperatively (preoperative= 2.4, postoperative= 6).

a) b)

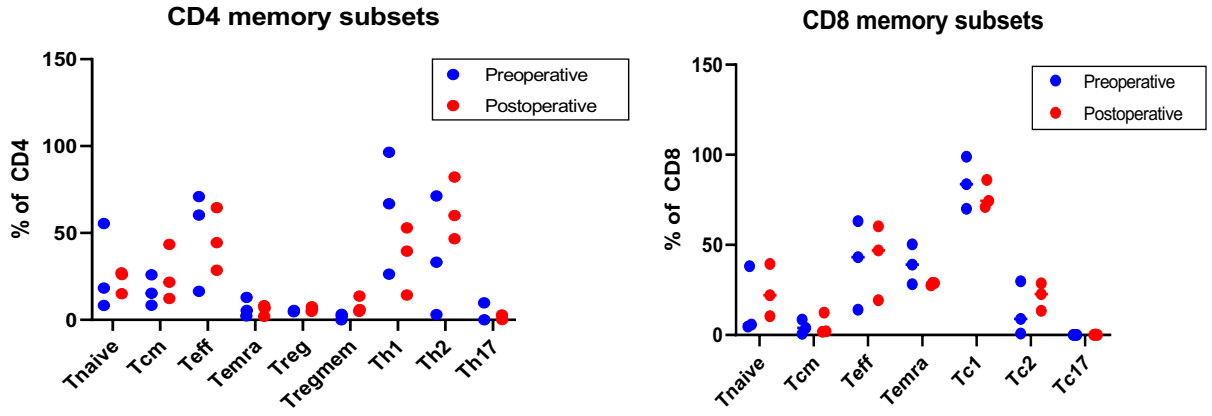

Figure 22. Phenotypic profile of CD4 & CD8 subtypes present in the peripheral blood of PDAC patients before (blue) and after (red) the operation. a) CD4 subsets (Tnaive: $CD45RA^+CCR7^+$, T central memory: $CD45RA^-CCR7^+$, T effectors: $CD45RA^-CCR7^-$, TEMRA: $CD45RA^+CCR7^-$, Treg: $FOXP3^+CD25^+$, Th1:$CXCR3^+CCR6^-$, Th2: $CXCR3^-CCR6^-$, Th17:$CXCR3^-CCR6^+$), b) CD8 subsets (Tnaive: $CD45RA^+CCR7^+$, T central memory: $CD45RA^-CCR7^+$, T effectors: $CD45RA^-CCR7^-$, TEMRA: $CD45RA^+CCR7^-$, Treg: $FOXP3^+CD25^+$, Tc1:$CXCR3^+CCR6^-$, Tc2: $CXCR3^-CCR6^-$, Tc17:$CXCR3^-CCR6^+$).

The results from the CD8 memory subsets (Fig.22b) are like the ones observed for CD4, considering that there is minimal difference in the medians of memory subsets. We observed some variability in Tnaive

(preoperative= 5.85%, postoperative= 22%) which show a trend to increase after the surgical removal of PDAC, while Tcm (preoperative= 4%, postoperative= 2.1%) and Teff (preoperative= 43%, postoperative= 47%) maintain similar medians. Finally, we reaffirm the previously observed high prevalence of TEMRA which is maintained also in the post-operative sample (preoperative= 39 %, postoperative= 28.8%). On further evaluation of the expression of chemokine receptors the type 1 cytotoxic cells ($CXCR3^+CCR6^-$) are the majority of CD8 and maintain that percentage peri-operatively (preoperative= 83.6 %, postoperative= 74.4%) with no inversion to the type 2 phenotype (preoperative= 9.8 %, postoperative= 22.7%) as observed in CD4. Moreover, there are minimal type 17 ($CXCR3^-CCR6^+$) cytotoxic cells (preoperative= 0.01%, postoperative= 0.1%).

a) b)

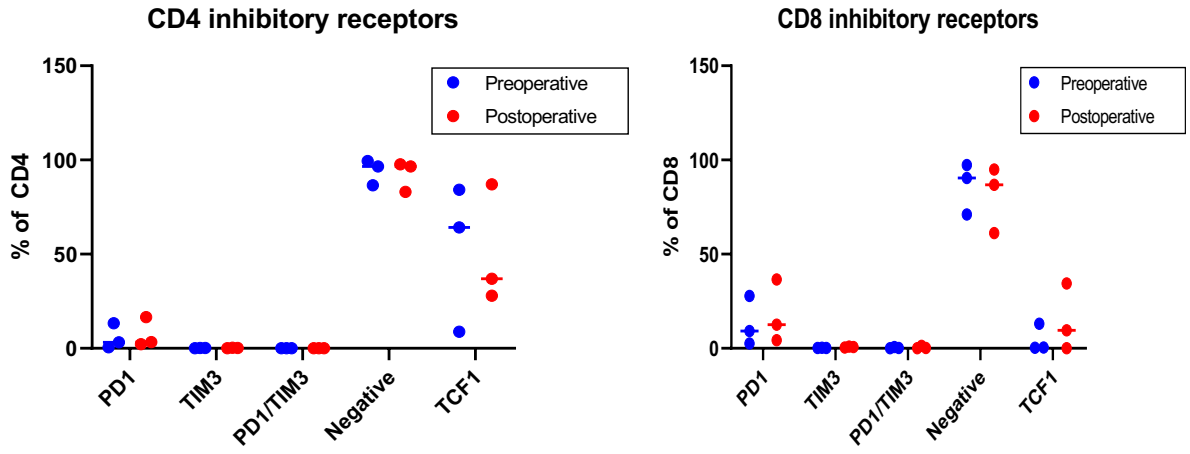

Figure 23. CD4 & CD8 subset expression of inhibitory receptors and TCF1 present in the peripheral blood of PDAC patients before (blue) and after (red) the operation. a) CD4 $PD1^+$, $TIM3^+$, double positive ($PD1^+TIM3^+$), negative ($PD1^-TIM3^-$) and $TCf1^+$. b) CD8 $PD1^+$, $TIM3^+$, double positive ($PD1^+TIM3^+$), negative ($PD1^-TIM3^-$) and $TCF1^+$.

The expression of inhibitory receptors is comparable before and after operation (Fig. 23). In CD4 T cells there is limited expression of PD1 (preoperative=3.15%, postoperative= 3.32%), while higher expression is observed for CD8 (preoperative= 9.2%, postoperative= 12.6%). There is minimal expression of TIM3 expressing CD4 cells (preoperative= 0.13%, postoperative= 0.16%) and double positive PD1/TIM3 cells (preoperative= 0.1%, postoperative= 0.02%). The CD8 cells show a similar pattern of expression for TIM3 (preoperative= 0.2%, postoperative= 0.7%) and PD1/TIM3 (preoperative= 0.14%, postoperative= 0.16%). Finally, the expression of TCF1 in CD4 achieves a higher median preoperatively although with

overlapping variance (preoperative= 64.2 %, postoperative= 37%) while the CD8 cells show higher expression postoperatively (preoperative= 0.5%, postoperative= 9.6%).

8.2 T CELL STIMULATORY RESPONSE

The stimulation of T cells with CD3/CD28 beads *in vitro* was used to depict changes in memory subsets, expression of inhibitory receptors PD-1 and TIM3 and the expression of the transcription factor TFC1. Concurrently, the cells were stained with CFSE as previously described to evaluate the proliferation capacity of different phenotypic subsets.

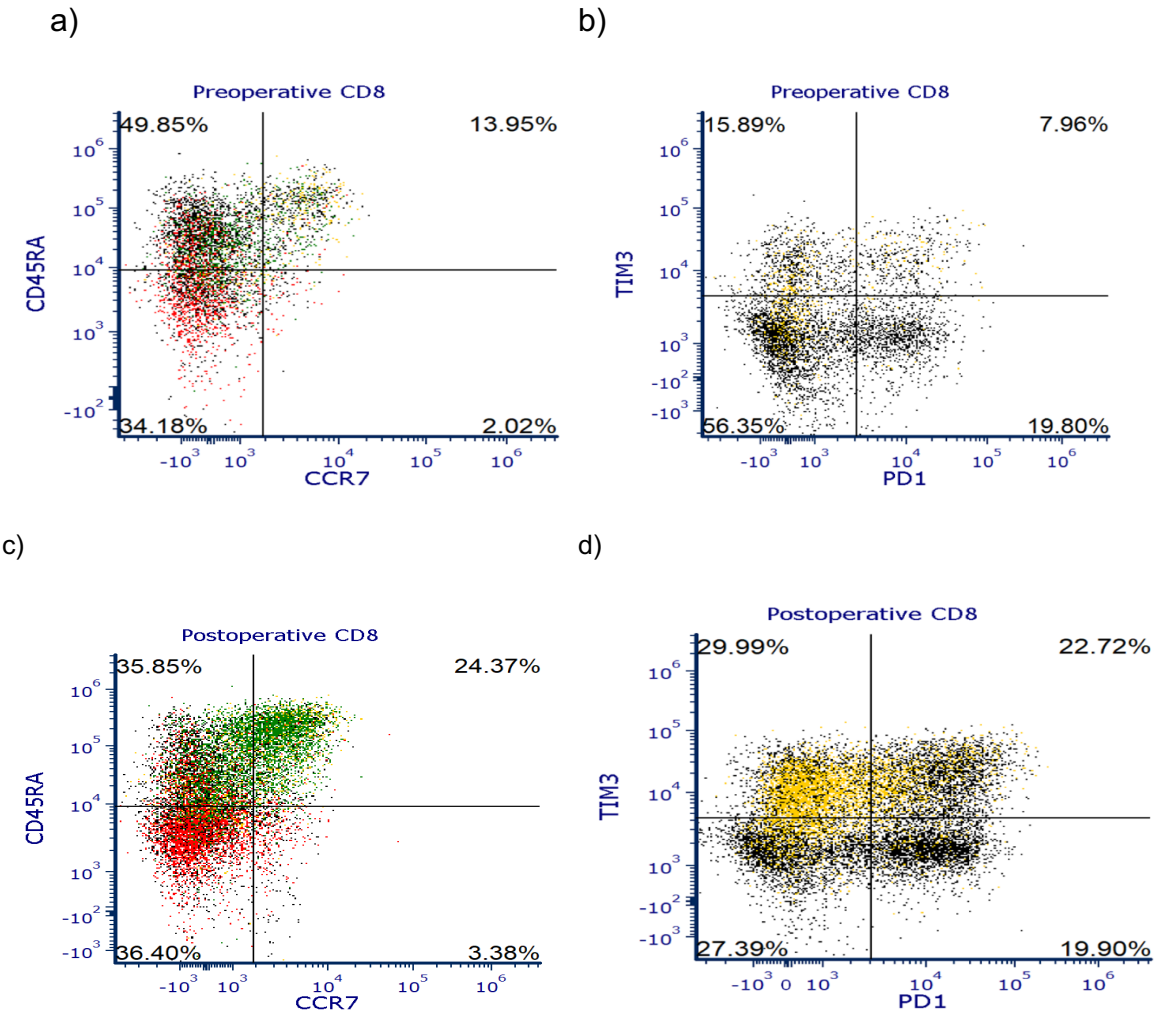

Figure 24. Comparison T cell response to 72h stimulation with CD3/CD28 beads before (a,b) and after the operation (c,d). a) Representative plot of preoperative CD8 memory/effector subsets upon stimulation with overlay expression of PD1 (red), TIM3 (green) and TCF1 (yellow). b) Representative plot of CD8 inhibitory receptor expression upon stimulation preoperatively with overlay expression of TCF1 (yellow). c) Representative plot of postoperative CD8 memory subsets upon stimulation with overlay expression of PD1 (red), TIM3 (green) and TCF1 (yellow). d) Representative plot of CD8 inhibitory receptor expression upon stimulation postoperatively with overlay expression of TCF1 (yellow).

Under stimulation we observe deviation in the response of the memory subsets (Fig. 24 & 25). The CD4 naïve cells in the postoperative samples are increasing (median = +3.61%) while there is decrease in the pre-operative samples (median= -3.52%). Similarly, there is an observable increase in the central memory subset in the postoperative samples (median= +13.7%) compared to a marginal increase in the postoperative samples (median= +1.24%). Similar response is observed for the CD8 naïve with an increase in the postoperative sample (median= +14.3%) compared to the preoperative sample (median= + 1.8%), and a less pronounced difference in central memory compartment (preoperative median= -1.6%, postoperative median= +1.31%).

On the contrary, we may observe the opposite response in the CD4 effector subsets (Fig. 22a) with a reduction in the effectors postoperative (median= -13.6%) and an increase in the preoperative sample (median= +3.6%), while the CD4 EMRA show a more pronounced decrease in the postoperative sample (median= -4.4%). Similar is the response of the CD8 effectors (preoperative median= + 4.8%, postoperative median= -12.7%), while the CD8 EMRA show comparable increase (preoperative median= + 2.9%, postoperative median= +3.7%).

On examining the expression of inhibitory receptors, we observe also altered kinetics with increase in the PD1 and TIM3 expression (Fig.25c) in the postoperative CD4 sample (median = +13.9%, median= +6.3%, respectively) while there is only marginal increase in the PD1 expression on the preoperative sample (median= +4.4%) and minimal expression of TIM3 (median= +0.5%). We also observe an increase in the double positive ($PD1^+/TIM3^+$) in the postoperative sample (median= +3%) and a marginal increase in the preoperative sample (median= +0.4%). The CD8 population shows a significant increase in TIM3 expression postoperatively (median= +29.3%) compared to the preoperative samples (median= +7.9%). The difference in expression of PD1 shows a slight increase preoperatively (median= +1.5%) compared to a decrease postoperatively (median= -1.4%). The increase in the double positive ($PD1^+/TIM3^+$) population is also significant postoperatively (median= +8.34%) compared to the increase observed preoperatively (median= 3.9%). Finally, on evaluating the expression of TCF1 we depict divergent kinetics in the CD4 T cells with significant decrease preoperatively (median= -48%) compared to an increase postoperatively (median= +9.4%). The CD8 T cells show a significant increase in TCF1

expression postoperatively (median= +21.2%) compared to a small increase preoperatively (median= +4.7%). Finally, on examining the TCF1 expression in the cohort of CD4 we observe difference in the proliferation of CD4 preoperatively (median= 0.8) and postoperatively (median= 2.9). This difference is not maintained in the CD8 subsets (preoperative median= 1.31, postoperative median= 3.2) despite having an upwards trend in the proliferation index postoperatively.

b)

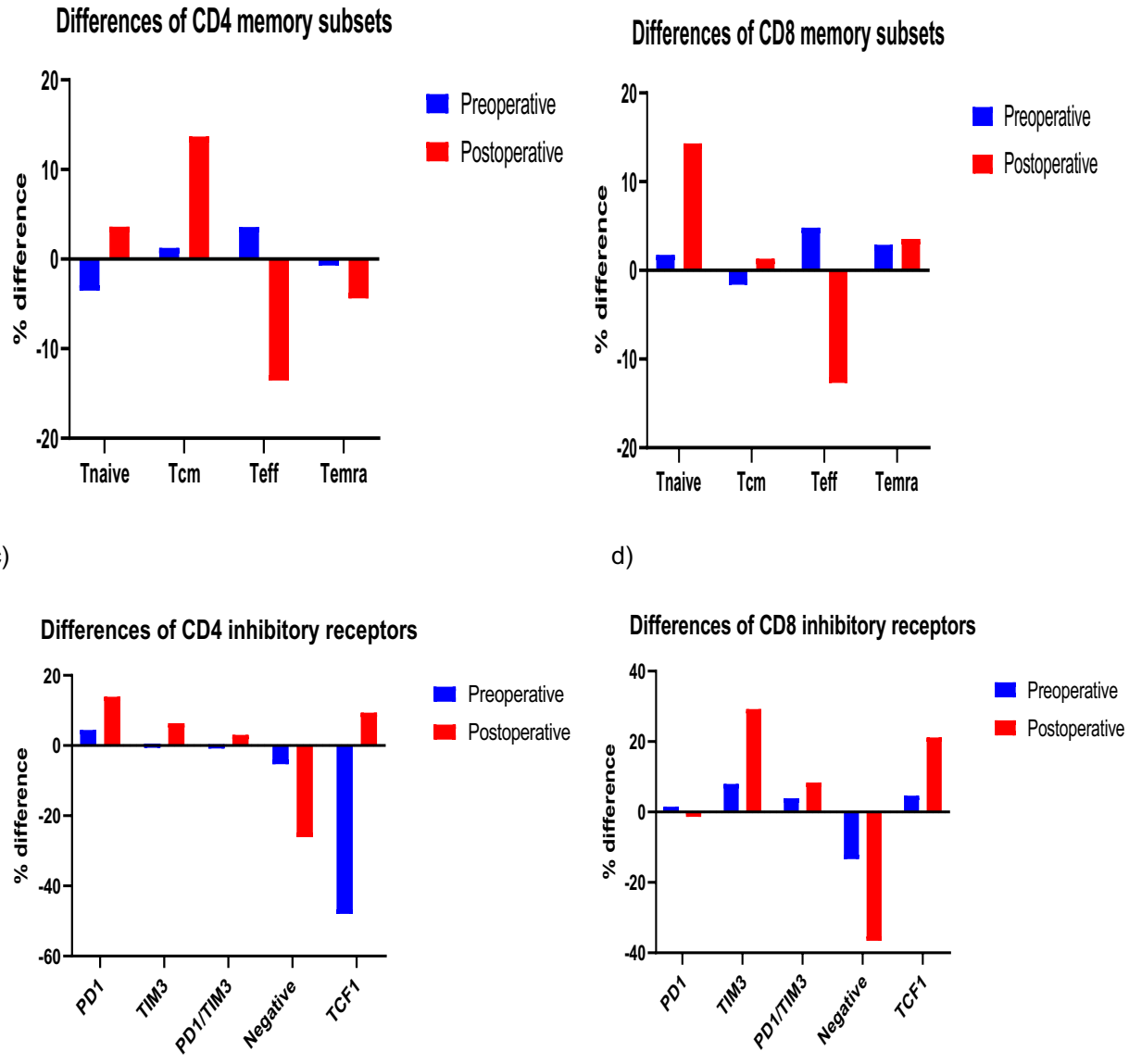

Figure 25. Percentage differences in memory subsets (a, b) and expression of inhibitory receptors and TCF1 (c, d) for CD4 & CD8 subsets. a) Percentage difference in CD4 memory subsets before (blue) and after (red) operation. b) Percentage difference in CD8 memory subsets before (blue) and after (red)

operation. c) Percentage difference in CD4 subsets expressing the inhibitory receptors PD1 and TIM3 and the transcription factor TCF1 before (blue) and after (red) operation. d) Percentage difference in CD8 subsets expressing the inhibitory receptors PD1 and TIM3 and the transcription factor TCF1 before (blue) and after (red) operation. Bars represent mean difference in percentages of different subsets from 3 independent experiments (n=3). (Tnaive: $CD45RA^{+}CCR7^{+}$, T central memory: $CD45RA^{-}CCR7^{+}$, T effectors: $CD45RA^{-}CCR7^{-}$, TEMRA: $CD45RA^{+}CCR7$

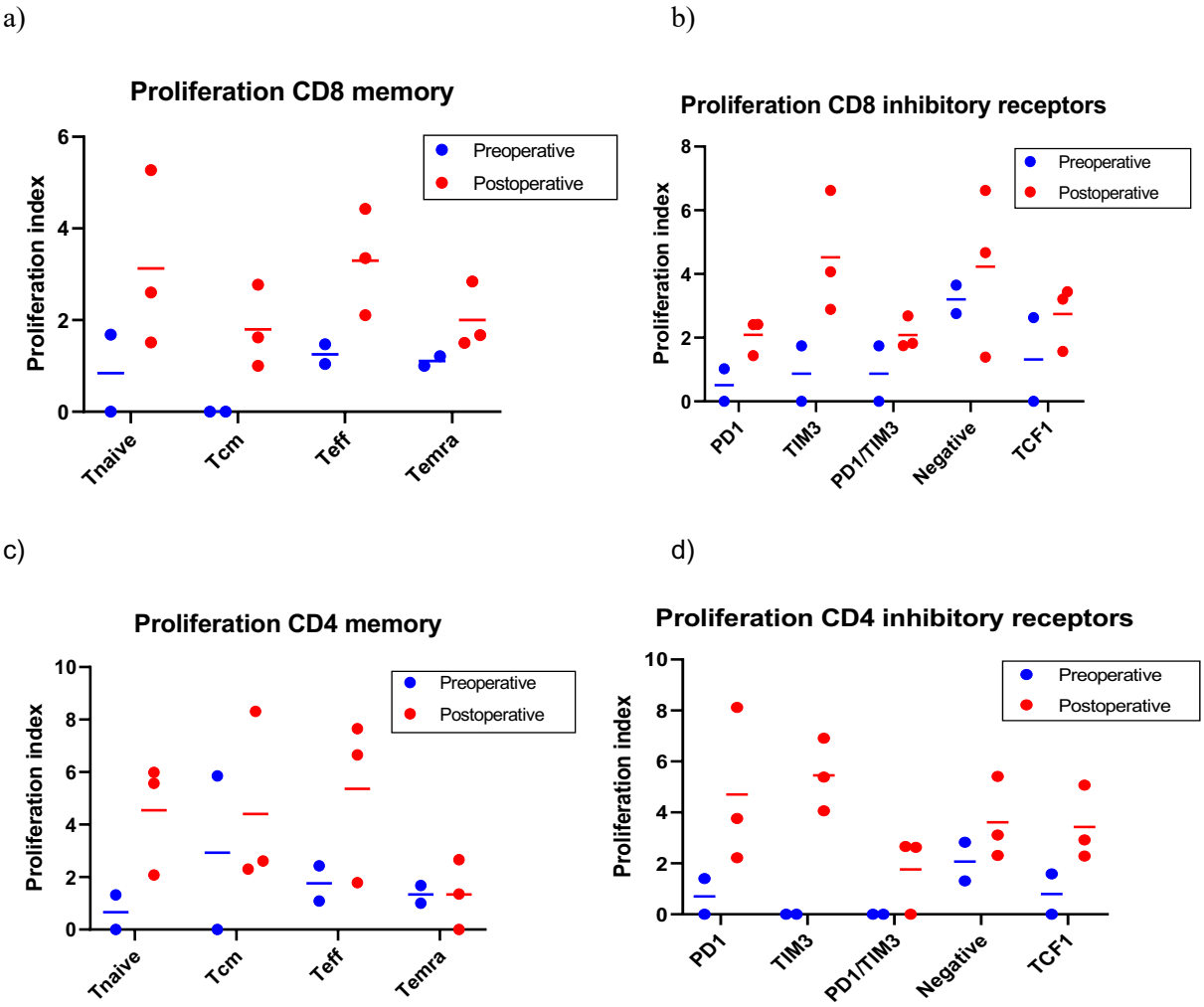

Figure 26. Proliferation index differences per memory (a, b), inhibitory receptor expression and TCF1 subsets (c, d) for CD4 & CD8 T cells before and after operation. a) Proliferation index of CD8 memory subsets before (blue) and after (red) operation. b) proliferation index in CD8 subsets expressing the inhibitory receptors PD1 and TIM3 and the transcription factor TCF1 before (blue) and after (red) operation. c) Proliferation index in CD4 memory subsets before (blue) and after (red) operation. d) Proliferation index in CD4 subsets expressing the inhibitory receptors PD1 and TIM3 and the transcription factor TCF1 before (blue) and after (red) operation. Median and values of different subsets from 3 independent experiments (n=3, one of the proliferation experiments was not successful and was removed from the data). (Tnaive: $CD45RA^{+}CCR7^{+}$, T central memory: $CD45RA^{-}CCR7^{+}$, T effectors: $CD45RA^{-}CCR7^{-}$, TEMRA: $CD45RA^{+}CCR7^{-}$)

The comparison of the proliferation indices for the memory subsets (Fig.26a, c) shows a trend of higher median index per subset for most of the CD4 and CD8 subsets. In particular, we observe significant differences amongst the preoperative and postoperative CD8 central memory cells (median= 0, median= 1.62, respectively) and effector subsets (median= 1.5, median = 3.35, respectively). Similar trend is observed for the CD4 central memory subsets with a preoperative median of 2.93 and a postoperative median of 5.6. The CD4 effectors cells show a higher median postoperatively (median= 6.7) compared to a small proliferation index preoperatively (median= 1.8). Nevertheless, the differences are less pronounced for the CD4 memory and effector subsets since there is higher variance of the values. The naïve CD4 subset shows significant increase in proliferation postoperatively (median= 5.6) compared to preoperatively (median= 0.7) and similar but less pronounced difference is observed for the naïve CD8 cells (preoperative median= 0.8, postoperative median = 2.6). Finally, the CD4 EMRA cells show no difference in their proliferation response but the CD8 EMRA show significant difference (preoperative median= 1.1, postoperative median= 1.8).

Assessing the proliferation indices based on the expression of inhibitory receptors (Fig.23b, d) also shows an increased proliferation trend in the postoperative samples. This trend is noticeable in the TIM3 subset for the CD4 (preoperative median= 0, postoperative median= 5.4) and CD8 (preoperative median= 0.9, postoperative median= 4.1). Similar is the trend observed by the PD1 expressing cells for CD4 (preoperative median= 0.7, postoperative median= 3.8) and CD8 (preoperative median= 0.5, postoperative median= 2.4). The difference in response is less pronounced for the double positive PD1/TIM3 populations for CD4 (preoperative median= 0, postoperative median= 2.63) and CD8 (preoperative median= 0.9, postoperative median= 1.82) mainly due to higher variance of the data.

9 ANALYSIS OF TRANSCRIPTOMICS

9.1 REVIEW OF THE PREOPERATIVE AND POSTOPERATIVE SAMPLES IN QUIESCENCE

To find any differences between the groups of samples, a principal component analysis on the levels of gene expression was performed. This showed loose association of the preoperative samples and more tight clustering for the postoperative samples using a principal components analysis (PCA) with 12 components (Fig. 27a). Comparing the preoperative and postoperative samples at a unstimulated state we found 563 differentially expressed genes (Fig. 27b, Appendix 12.6) using the DESeq2 algorithm and taking into consideration samples sourced from the same patient and the operation state ($p<=0.05$, $\log_2Fc>2$ & $\log_2Fc<-2$). The volcano plot generated by DESeq2 showed in the preoperative sample upregulated genes such as *CXCL2* ($\log_2Fc= -13.3$, FDR= 4.99E-3), *PTGES* ($\log_2Fc= -6.84$, FDR= 0.02), *LPL* ($\log_2Fc= -6.9$, FDR= 0.05), *CXCL1* ($\log_2Fc= -6.33$, FDR= 0.02), while the gene set enrichment showed that multiple genes related with monocyte function have been downregulated in the postoperative period (Appendix 12.5)

On the contrary the postoperative sample shows upregulation of *IFI44* ($\log_2Fc= 2.29$, FDR= 0.02), *IFI44L* ($\log_2Fc= 3.96$, FDR= 0.01), *CMPK2* ($\log_2Fc= 2.28$, FDR=0.01), and *NEFL* ($\log_2Fc= 2.33$, FDR=0.03). Using the filtered subset of 563 differentially upregulated genes we performed average linkage hierarchical clustering (Fig. 27c), which shows that there is identifiable sub-clustering of the preoperative samples versus the postoperative ones. This is mainly driven by a more homogeneous expression pattern of the postoperative samples corroborating with the PCA results. (Fig. 27a). Finally, the gene set enrichment process of the samples shows upregulated chemotactic pathways, and cytokine production pathways mostly orientated towards a humoral immune response (Appendix 12.5)

a)

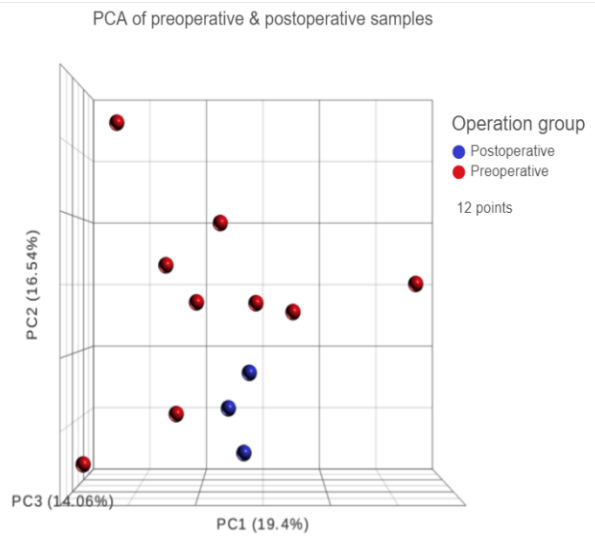

b)

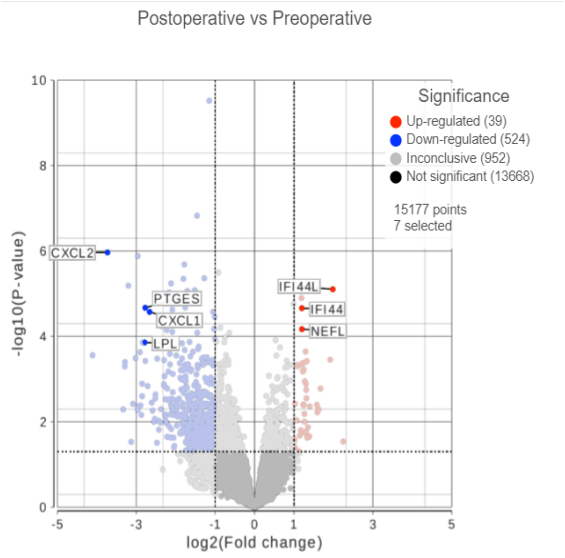

c)

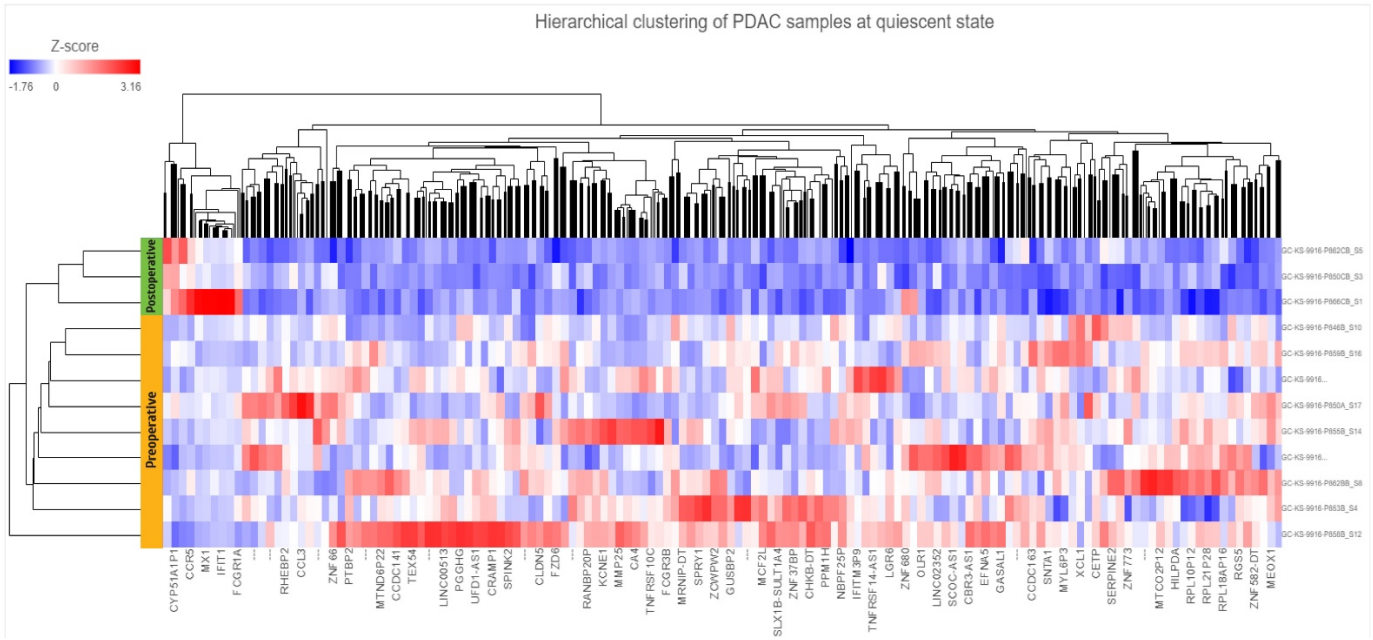

Figure 27. Transcriptomics of peripheral blood mononuclear cells at quiescence before (yellow) and after (green) operation. a) PCA showing limited clustering of samples preoperatively (red) and loose clustering of postoperative samples (blue). b) Volcano plot showing significantly upregulated genes (FDR<0.05 & log_2Fc >=1) postoperative compared to preoperative (red) and significantly downregulated genes (FDR<0.05 & log_2Fc <=-1) in blue (Total number of differentially expressed genes= 563). c) Hierarchical clustering of preoperative (yellow) and postoperative (green) transcriptomic profiles showing discrete clustering amongst preoperative and postoperative samples.

We further aimed to investigate if specific T cell associated genes would be able to maintain the clustering we observed amongst the quiescent samples (Fig. 28). Therefore a curated list of genes from Gene Ontology (GO) was used including 519 genes (Appendix 12.4). Amongst this subset the volcano plot generated by DESeq2 found 399 genes as differentially expressed, which were used for hierarchical clustering. We also found 3 genes with significant differential expression but not meeting our FDR cut off: *RSAD2* (log_2Fc= 2.17, FDR= 0.61), *IL4I1* (log_2Fc= 2.99, FDR= 0.23) and the upregulated in the preoperative sample *ARG1* (log_2Fc= -7.22, FDR= 0.18) and *XCL1* (log_2Fc= -3.1, FDR= 0.35). The hierarchical clustering (Fig. 28c, Appendix 12.7) shows no obvious clustering based on operation status or tendency for clustering on samples stemming from the same patient. This reaffirms to an extent our phenotypic results based on the flow cytometry and provides insight into considering other immune subsets which might be responsible for the previously observed results. Finally, specific gene set enrichment on the T cell genes shows highly enriched scores for Th17 responses without a particular Th1, Th2 polarization and responses more specific to EBV and HTLV-1 (Fig. 28b).

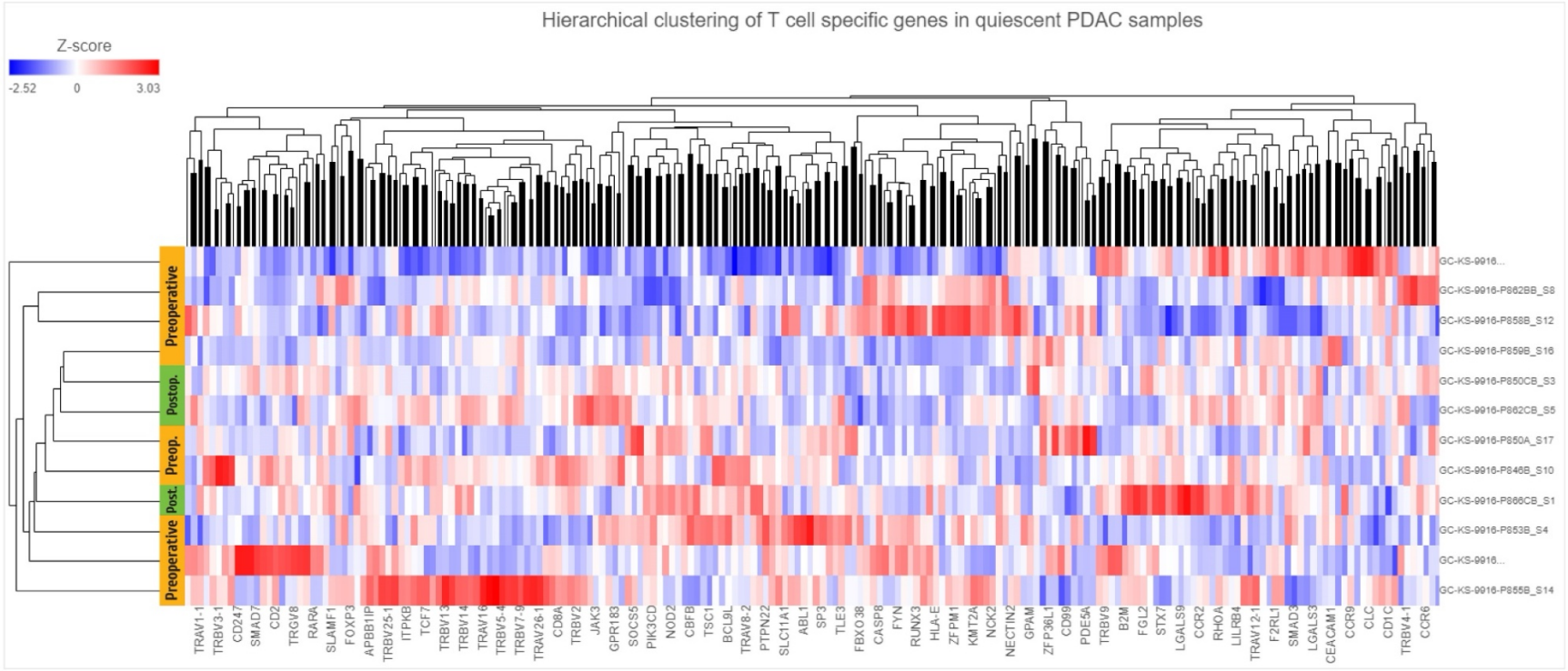

Figure 28. T cell specific gene set by genome ontology filter on peripheral mononuclear cells before (yellow) and after (green) operation. a) Volcano plot showing significantly upregulated genes (FDR<0.05 & $\log_2$Fc >=1) postoperative compared to preoperative (red) and significantly downregulated genes (FDR<0.05 & $\log_2$Fc <=-1) in blue. b) Top KEGG enriched pathways using the T cell specific list. Th17 and TCR signalling are the top 2 enriched pathways with enrichment scores of 71 and 47.7 respectively (p<0.01) c) Hierarchical clustering of preoperative (yellow) and postoperative (green) transcriptomic profiles for the T cell specific list with loss of the previously observed sub clustering based on operation status.

9.2 REVIEW OF THE PREOPERATIVE AND POSTOPERATIVE SAMPLES IN STIMULATION

In order to assess further the response of T cells based on the operation status we stimulated pairs of samples from the patients as before for the flow cytometric analysis and subsequently analysed the transcriptome of these samples. A PCA on the bulk mRNA analysis proved the presence of sub-clustering based on both the operation and stimulation status in the post-operative period (Fig. 29a). The PC1 attributed to the stimulation 34.6% of the clustering, while PC2 12.1% to the operative status. We further proceed to evaluate the differential expression of the samples based on the operation status and taking into account their stimulatory condition. We found 114 differentially expressed genes (Fig. 29b) based on the operation status while considering their stimulatory condition using the DESeq2 algorithm (FDR<=0.05). The hierarchical clustering indeed showed clustering based on the operation status and further sub-clustering based on stimulation status which was further investigated by assessing the differential expression of genes based on the operation status and the differences produced from the stimulatory response. (Fig. 29c, d, Appendix 12.8)

Genes that were upregulated preoperatively were *ZBED2* (log_2Fc= -4.05 FDR= 0.003), *DAPK2* (log_2Fc= -3.98, FDR= 4.7e-5), *Il1R2*(log_2Fc= -3.97, FDR= 1.98e-5), *MYEF2* (log_2Fc= -2.59, FDR= 2.8e-4) while genes the show increased differential expression differences as response to stimulation preoperatively were *PALLD* (log_2Fc= -7.58, FDR= 5.74e-03), *GZMB* (log_2Fc= -4.32, FDR= 0.004), *RGS16* (log_2Fc= -3.89, FDR= 0.004), *TRAF4* (log_2Fc= -2.59, FDR= 0.01) *BATF3* (log_2Fc= -2.64, FDR= 0.004), *CD70* (log_2Fc= -2.52, FDR= 0.004), *ZDHHC14* (log_2Fc= -2.94, FDR= 0.004) and *TNFSF4* (log_2Fc= -2.74, FDR= 0.03). On the contrary genes significantly upregulated postoperatively included *CRYBG3* (log_2Fc= 2.14, FDR= 0.04), *SGSM2* (log_2Fc= 1.83, FDR= 0.03), *LDLRAP1*(log_2Fc= 1.80, FDR= 0.04), *HIVEP2* (log_2Fc= 1.79, FDR= 0.02), and *TCF7* (log_2Fc= 1.77, FDR= 2.36e-4) and increased differential expression differences after stimulation postoperatively were *IATPR* (log_2Fc= 13.17, FDR= 0.003), *CDKN2B* (log_2Fc= 12.18, FDR= 0.001), *EPHA1* (log_2Fc= 7.91, FDR= 0.02), *CCR2* (log_2Fc= 5.97, FDR= 0.001), *PELI2*(log_2Fc= 5.85, FDR= 0.003) *ZBTB10* (log_2Fc= 3.48, FDR= 0.03), *TRIB2* (log_2Fc= 3.79, FDR= 0.006), *SAMHD1*(log_2Fc= 2.12, FDR= 0.004), *LCP1* (log_2Fc= 1.87, FDR= 9.85e-5)

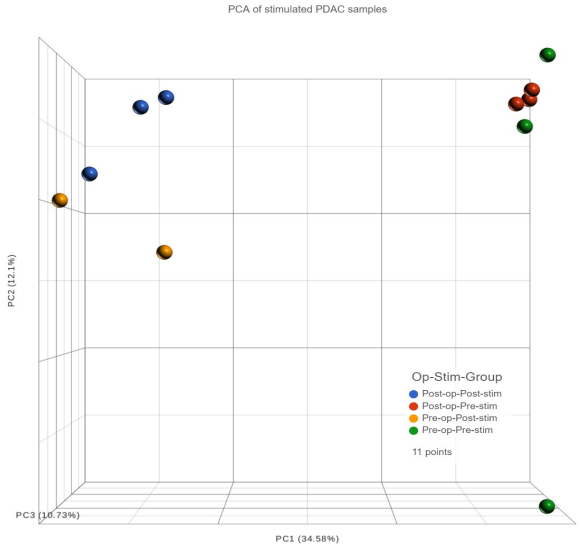
PCA of stimulated PDAC samples
PC2 (12.1%)
PC3 (16.73%)
PC1 (34.58%)
Op-Stim-Group
Post-op-Post-stim
Post-op-Pre-stim
Pre-op-Post-stim
Pre-op-Pre-stim
11 points

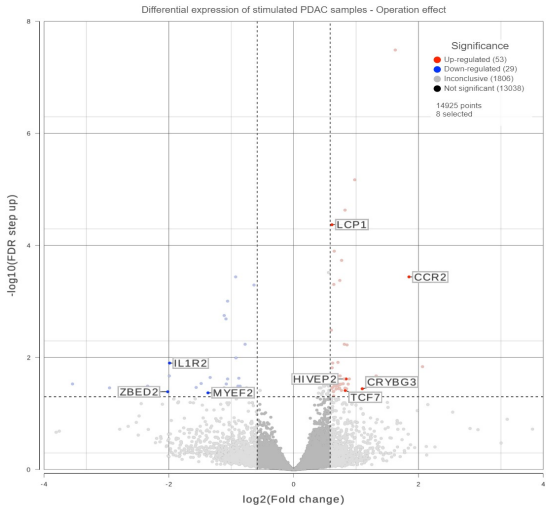
Differential expression of stimulated PDAC samples - Operation effect
Significance
Up-regulated (53)
Down-regulated (29)
Inconclusive (1806)
Not significant (13038)
14925 points
8 selected
-log10(FDR step up)
log2(Fold change)
LCP1
CCR2
IL1R2
ZBED2
MYEF2
HIVEP2
CRYBG3
TCF7

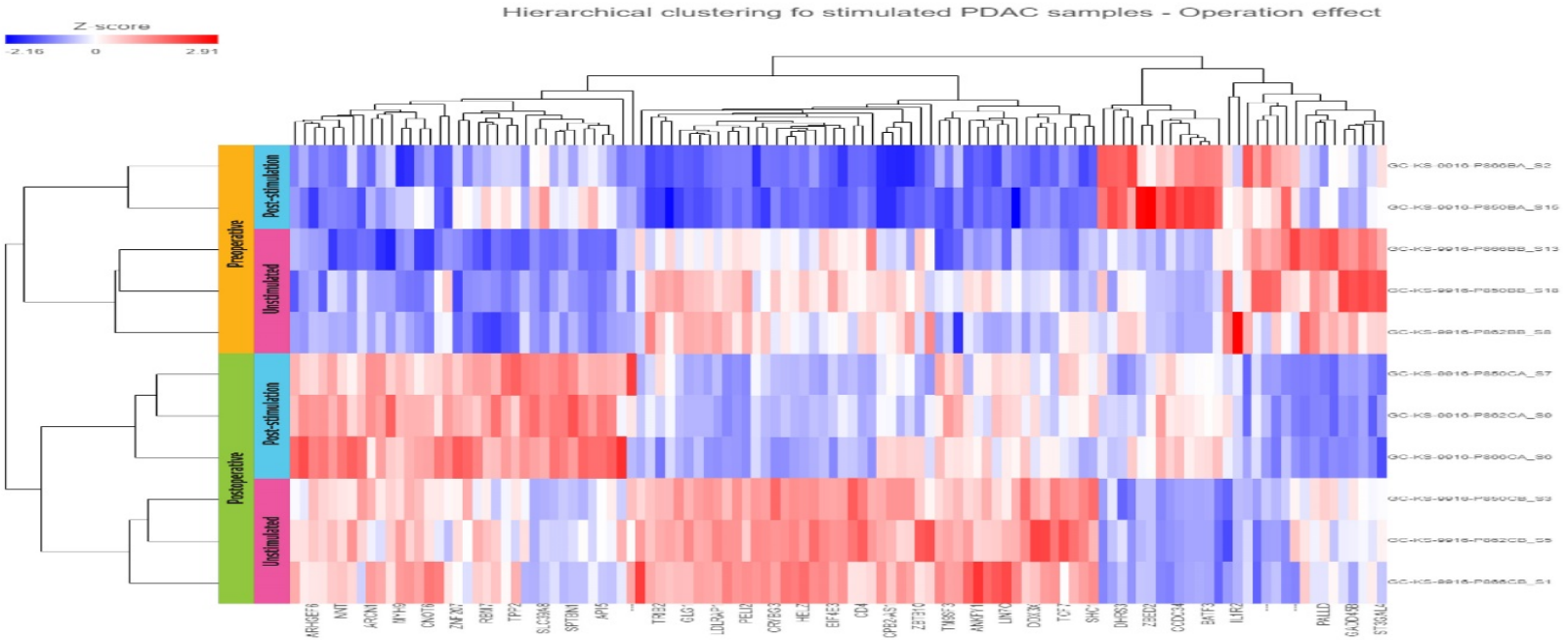
Hierarchical clustering fo stimulated PDAC samples - Operation effect
Z-score
-2.16
0
2.91
Preoperative
Postoperative
Post-stimulation
Unstimulated

d)

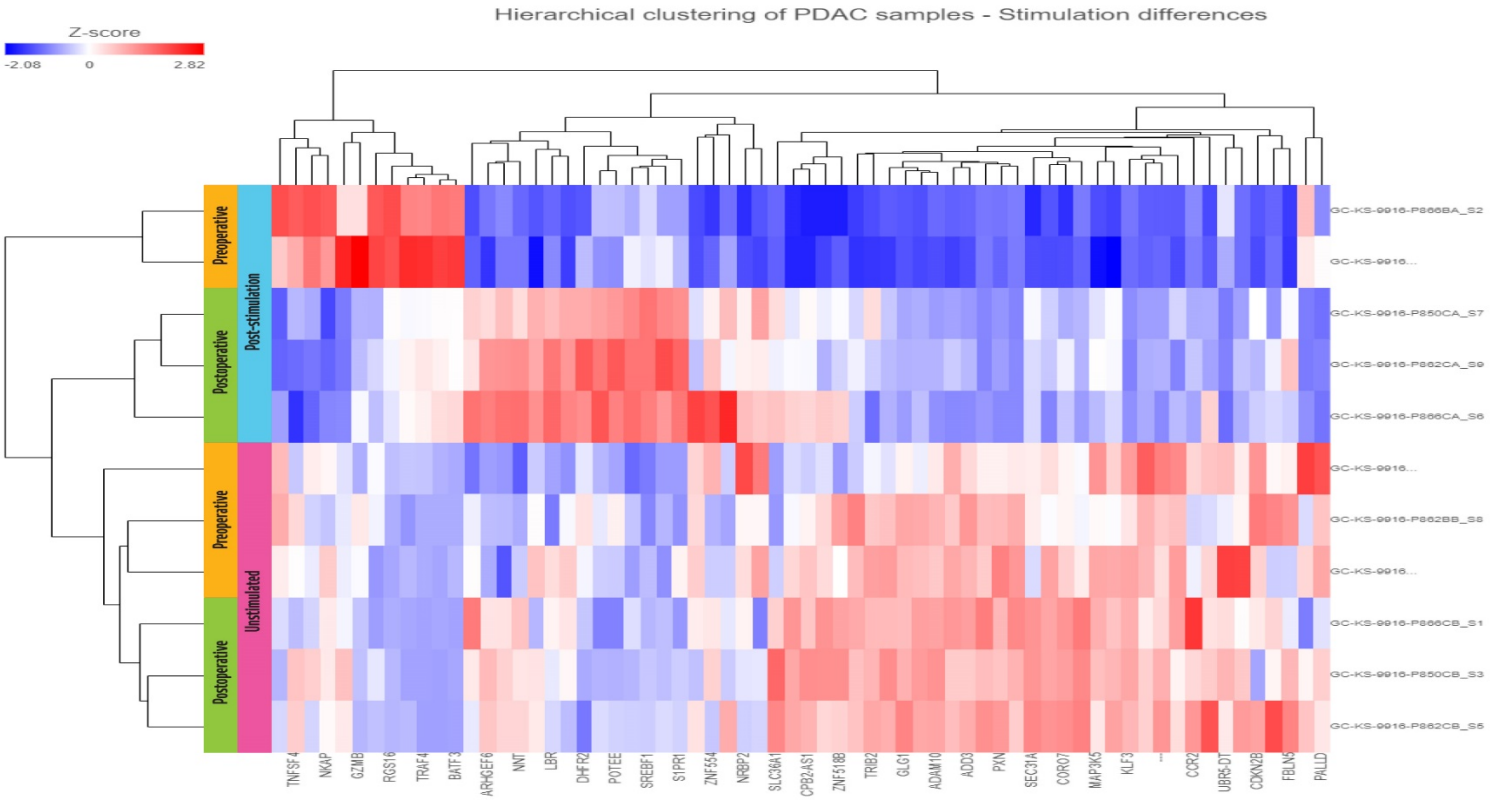

Figure 29. Transcriptomic analysis of T cell stimulation before and after operation showing divergent response. a) PCA of paired samples bases on operation and stimulation status showing main effect of stimulation on PC1 and effect of operation on PC2. b) Volcano plot showing differentially expressed genes based on operation effect under a generalized linear model taking into consideration the effect of stimulation (FDR<0.05, & $\log_2$Fc >=1 or & $\log_2$Fc <=-1). c) Hierarchical clustering of the genes differentially expressed due to operation (green/yellow) showing divergent stimulatory response based on operation status. d) Hierarchical clustering of the genes that have differential expression difference in their response to stimulation (pink/ciel)based on the operation status under the same generalized linear differences. The effect of operation in the difference is more prominent after removal of PDAC as shown on left side dendrogram

10 DISCUSSION

The results of the phenotypic analysis from patients with PDAC have shown that the functional subsets observed are mainly maintaining a normal composition with a preponderance of naïve and central memory subsets and less effectors or EMRA cells. The phenotypic differences that have reached statistical significance mainly with the T exhausted population are probably a result of polarization under the *in vitro* stimulatory conditions that the exhausted population has undergone. We also show a higher presence of T EMRA cells, although with a high degree of variability, in the CD8 compartment which is statistically different from our expanded population. TEMRA are thought to be descendants from central memory cells and in patients with different types of cancers are associated with clonal specific anti-tumour immune responses,[106,107] and responsive to combination immunotherapy with PD1/CTLA4 andtibodies.[108] In these studies the genomic background of TEMRA cells obtained from blood shows distinctions from those derived from tumour tissue, as revealed by NGS evaluation. Additionally, unlike general CD8+ tumour infiltrating lymphocytes, which predominantly comprises exhausted effector cells, TEMRA cells share genetic signature with blood samples from healthy individuals, while also maintaining a distinct signature characterised of 163 upregulated genes.[107] These differences have been evaluated in the context of NSCLC samples which show TCF7 upregulation in tumour infiltrating lymphocytes and TOX in peripheral blood TEMRA and may also support report of TEMRA cells being responsible for immunotherapy response in clinical trial of mesothelioma.[106,108] Similarly, we have shown a high prevalence of CD4 Th2 cells in peripheral blood of patients with PDAC. Although, classically Th2 immune responses have been associated with tumour progression[3] and the presence of Th2 T cells in the tumour microenvironment of breast cancer has been associated with a high proliferation index for cancer cells, and these observations are not related to patient survival.[109] Similarly, a Th2 cytokine profile based on expression of IL-4, although nonspecific, it is associated with worse survival in resectable PDAC patients.[110]

The presence of inhibitory receptors in PDAC samples is shown to be associated with their activation status since PD-1 is upregulated to a statistically significant level post-stimulation and TIM-3 increases its expression post-stimulation. Considering that the presence of inhibitory receptors might also showcase

an exhausted population, it is very difficult to elaborate if the subsets which upregulated the inhibitory receptors are indeed exhausted or activated, especially if we consider that similar expression is seen in the $T_{expanded}$ population. Nevertheless, it is important to mention here the lack of TIM-3 expression in a consistent manner on the $T_{expanded}$ cells compared to both the PDAC and $T_{exhausted}$ populations, which reaches a statistical significance in the CD8 post-stimulation conditions. Although, one explanation would be divergent kinetics of expression in TIM-3 during activation[111,112], TIM-3 is mainly associated with tumour reactive T cells in melanoma murine and human models.[113,114] Conversely, the decrease of TIM-3 on the T exhausted population post activation, considering that it represents mainly an effector population, gives rise to the possibility of post activation death.

Since we already eluded that it is difficult to assume an exhausted state based only on the presence of inhibitory receptors, and our data on proliferation show similar indices amongst different functional T cell subsets, we have to interpret these data with caution. Therefore, although the T cell subsets do not show a change in of proliferation to a different level compared to our *in vitro* controls, it is interesting to see the lack of change in functional subsets after stimulation considering the presence of similar proliferation per functional subset in the unstimulated state. This could be explained, perhaps, by the presence of proliferating subsets which “salvage” the proliferation index for the PDAC samples and the exhausted population. If we investigate the proliferation index amongst the PDAC patients’ functional subsets, we see that there is minimal variability amongst subsets which should have different proliferation capacities, namely increased proliferation for the naïve or central memory subsets and less for effectors/EMRA. Similarly, when looking at the inhibitory receptors, we found that TIM-3 subsets have statistically increased proliferation index compared to PD1. These results may indicate that TIM-3 upregulation may play an important role in controlling the activation of T cells from PDAC patients especially since TIM-3 expression is limited in the T expanded population, which coincides with reports on TIM-3 upregulation on T cells isolated from healthy pancreatic lymph nodes and peripheral blood and activated *in vitro*.[2]

Exploring the responses to stimulation for the paired cohort of samples has demonstrated that there is divergent response under stimulatory conditions. This was mainly observed in the better maintenance of naïve and memory subsets with increase in the expression of TCF1 in the postoperative samples

compared to the response of the preoperative samples which showed a marked effector response with decrease or comparably smaller increase in the expression of TCF1. There is increasing body of literature supporting TCF1 as a transcription factor maintaining naivety[115,116]. Taken together, this would support the possible improvement in the functional response of T cells by removal of the primary PDAC tumour.[45,117] On assessing the expression of inhibitory receptors we observe an increase in both PD1 and TIM3 which is more significant in the postoperative samples, although the TIM3 upregulation is more pronounced in the CD8 subset while concurrent PD1, TIM3 upregulation is observed mostly on the CD4 subset. The expression of TIM3 has been shown to regulate T cell activation in a complementary way with TCR stimulation towards an effector subset through mTOR pathway.[118,119] In the context of persistent antigen through TCR stimulation this effect would hypothetically drive an exhausted response through limiting the production of long-term memory precursors, albeit would support a more robust effector response.[120,121] This has been shown both by the preferential silencing of TIM-3 which seems to decrease NFAT/AP-1 phosphorylation in CD3/CD28 activated Jurkat cells, while its ectopic expression in primary T cells increases INF-γ production. Similarly, in the context of effector function TIM3 seems to improve INFγ production,[122] but its co-expression with PD1 and binding to galectin9 may suppress Th1 responses and promote a dysfunctional response in chronic infection/cancer.[123,124] Specifically, the closed interaction of TCR and TIM3 in the context of cancer specific antigens, has been reported in melanoma with NY-ESO-1 cancer germline mutation specific T cells being responsive to TIM-3 blockade by increased cytokine production and proliferation.[124] All these reports, show that TIM-3 may regulate TCR dependent stimulation which in the context of persistent antigenic response may indeed promote effector functions and exhaustion.

The examination of the proliferation indexes of the paired samples shows an overall upwards trend for most memory subsets, particularly improved on the naïve and effectors for both CD4 and CD8 subsets (Fig. 26). Similarly, there is improved proliferation for PD1, TIM3 or double positive subsets but also for the subsets with no expression of inhibitory receptors (Fig. 26). Of note is the increased improvement in the proliferation index of the TIM3 subset which would probably support an improved expansion of effectors. Considering that TIM3 expression coincides with the naïve T cells and is co-expressed with TCF1 in our cohort, it might represent a population of short-lived effectors which have separate trajectory

to the TCF1$^+$ exhausted precursors previously described in murine models of chronic infection.[125,126,127] In particular, it has been reported that early precursors with transcriptionally distinct signature are observed in the TIM-3$^+$ positive population. These precursors have limited effector potential and although they maintain their proliferative capacity, as we also observe in our PDAC samples, they are poised towards an exhausted trajectory.[36] This would explain the increased proliferation observed in our PDAC samples but the lack of phenotypic difference in an unstimulated state.

The transcriptome before and after operation showed in the postoperative samples the expression of *IF44* & *IF44L* which have been shown in the literature to have anti-viral effects by controlling HIV-1 and RSV replication[128,129] but also has shown to have prognostic value in head & neck and breast cancers.[44,130] Similarly we note the upregulation of NEFL which in the context of the immune system is upregulated in CD4 memory and effector memory cells.[131] Concurrently, the upregulation of *PTGES* and *LPL* preoperatively along with the expression of CXCL1 and CXCL2 depicts an inflammatory response mediated by monocytes or myeloid derived suppressor cells in the presence of the primary malignancy.[132,133]In particular, the expression of prostaglandin E2 has been shown to act as a suppressor of T cell cytotoxicity in chronic viral infections[134] and in a murine model of lung cancer.[135] The expression of CXCL1 and CXCL2 has also been implicated in progression of breast cancer via a Th17 mediated pathway[136] which coincides with our findings from the gene set enrichment of T cell specific genes.

Review of the stimulatory response is showing an increase in *ZBED2,* a zinc finger protein, in the preoperative samples, *ZBED2* has been shown to antagonize with IRF1 for the INF response[137] suggesting a higher threshold for activation. Similarly, the expression of IL1R2 a decoy receptor for IL-1 may hinder an inflammatory response and promote tolerogenic effects.[138–140] Finally, the expression of *DAPK2,* (which is similar in structure with DAPK1 a positive regulator of programmed cell death) negatively regulates T cell activation and germinal cell formation through the NF-κB pathway and its interaction with mTORC1.[141,142] On the contrary, the increase of *LDLRAP1* and *TCF7* in the postoperative sample denotes a signature which has been previously been described as naïve like cell from infiltrating melanoma T cells[143] and the increased expression of *HIVEP2*[144–146] which has implicated in Treg immunosuppression may depict a favourable change in T cell behaviour postoperatively.

Similar to the divergent gene expression noted based on the operation status we also observe a divergent response to stimulation. The preoperative samples show expression of *GZMB* and *RGS16* which are involved in terminally differentiated effector/exhausted subsets, while decreasing TCR related activation.[147–150] Weisshaar et al. have shown in a murine model of GFP reporter that RGS16 potentiates exhaustion in CD8 infiltrating T cells and correlates with PD-1 blockade response in melanoma. This action seems to be related with the ERK1 induced phosphorylation by TCR activation which is abrogated in RGS16$^{-/-}$ mice.[147] We have also observed increased *BATF3* expression in the stimulatory response in the preoperative samples. *BATF3* has been involved in effective recall response and survival of CD8 T cells in murine model of acute infection.[151,152] On the contrary *CD70* expression has been involved in T cell mediated apoptosis on activation and acting as an inhibitory molecule in a colitis model,[153] but also has been shown to enhance the proliferation capacity of isolated CD4 and CD8 cells *in vitro.*[154] Finally, the finding of *TNFSF4* preoperatively supports a deviation to a Th2 response upon stimulation,[155,156] but has also been associated with a terminally exhausted profile in T cells isolated from malignancies at the single cell level.[157]

The stimulatory response shows an increase of *CDKN2B* a CDK4/6 inhibitor which would potentiate T cell activation and memory formation[158,159] albeit decreasing their proliferation,[160] the upregulated expression of *EPHA1* would support again an increased T cell stimulation mainly mediated by PYK2 phosphorylation and cytoskeletal remodeling in both CD4 and CD8 subsets.[161,162] *CCR2* has been already shown to increase T cell infiltration in murine model of PDAC in combination with radiation and PD-1 blockade[163], and also seems to denote a stable CD4 memory population with rapid recall to CMV infection.[164] Concurrently, CCR2 deletion abrogated inflammation in a colitis model both inducing Foxp3^{+} Tregs and attenuating a Th17 effector response.[165] *SAMHD1* has been shown to increase CD8 INFγ production in HIV infection[166] and control viral load while seems to concurrently be less expressed in CD4 memory lymphocytes during HIV viremia.[167] Finally, *LCP1* seems to regulate actin polymerization and improve the immunological synapse along with IL2 production in stimulated CD4 cells.[168]

Our results are limited by increased variability in functional subsets, expression of inhibitory receptors and proliferation indexes. Similarly, our *in vitro* controls although could provide insight into the expansion of

functional subsets and the expression of inhibitory receptors under different stimulatory conditions, they cannot act as a direct comparison with the patient samples especially in the post-thaw phenotypic analysis. Nevertheless, they provide a reproducible background to compare the responses of PDAC samples and find similarities or lineage specific subsets since we already know the exact timings of TCR stimulation that led to their production. There is also possibility that our *in vitro* stimulatory conditions are sub-par to elude responses in T cells (and especially naïve subsets), but this is unlikely because our *in vitro* T cells seem to respond irrespective of the functional subset and the fact that we observe expected up titration of PD1. Furthermore, our *in vitro* stimulation is a combined stimulation of CD4 and CD8 subsets which might not help delineate subset specific differences upon stimulation and concurrently alter their responses compared to in isolation stimulation but considering that such co-existence is part of *in vivo* stimulation might also provide more appropriate model to assess such responses.

The phenotypic analysis of the PDAC samples has not shown subsets of interest which are deviating from phenotypically known expected subsets in the peripheral blood. Nevertheless, under stimulatory conditions we have observed limited change in the functional memory subsets especially in the CD8 population and up titration of inhibitory receptors, PD1 and to a lesser degree TIM3. This in conjunction with the proliferation index of the PDAC samples showing increased proliferation for the TIM3 positive population may indicate a subset which under stimulatory condition may propagate but not effectively differentiate to memory subsets resembling short memory effectors. The increase proliferation may be explained by the co-expression of the TCF1 in this population in our results, but also it has been documented that TIM3 upregulation in early TCR stimulation protects against activation induced death compared to late activation when it promoted cell death.[169] Similarly, in models of chronic infection TIM3 subsets have been associated with a transitory $CX3CR1^{+}CD101^{-}$ population which provided better viral control but resembling an effector phenotype.[46,170] This in fact would also correlate with our finding on the paired operation samples which show marked upregulation of TIM3 after removal of the primary tumour and an overall better proliferation especially for the TIM3 subset.

The transcriptomics of PDAC samples show an upregulated cytokinetic response at quiescence. Although is difficult to elude the direct impact this may have on T cell subsets it provides evidence of an immune

adaptation to the presence of a primary malignancy similar to that of a chronic viral infection which may be viewed in the peripheral blood. Nevertheless, the fact that our data are not deconvoluted to specific immune subsets hinders further assumptions at quiescence. The divergent immune response upon T cell specific stimulation indeed provides further evidence of functional impairment in the presence of PDAC for T cell subsets mainly denoted by impediment in production of long-term immunity both by the downregulation of *TCF1*, and a transcriptional machinery which supports effector functions. This may indeed not pinpoint to dysfunctional/exhausted subsets, but it might encompass an adaptation in order to avoid ongoing resurgence of an inflammatory response in the presence of PDAC which would manifest to dysfunctional trajectories in the tumour microenvironment rather than the periphery and would be TCR specific.

Overall, our results support an altered immune response in the presence of PDAC for T cells and support the immune modulating effects of surgical de-bulking. We have shown that there are signatures both phenotypic and transcriptomic which are associated with the stimulatory response of T cells. The quantification of these responses would be important to act both as a biomarker and support the use of adjuncts which would support immunological control in the perioperative period in order to avoid metastatic disease. Our results are mainly limited by small number of individuals and the use of techniques with high variability, although well established for the evaluation of immune subsets. This problem is compounded on the transcriptomic analysis where is difficult to evaluate if the differences are related to a molecular difference which is unrelated to T cell intrinsic mechanisms. In order to be able to confirm our results a larger cohort of patients would be important and in particular testing if the signature is prevalent among different malignancies would indicate if this was a tumour intrinsic or T cell intrinsic behaviour in the context of malignancy. In particular, establishing a pipeline of comparing the responses of T cells upon TCR stimulation after surgical debulking amongst different malignancies would help confirm and evaluate if there is a certain signature which is universal in how T cells adapt to the presence of primary malignancy, or this is a tumour intrinsic behaviour. Combining such experiments with immune scores targeted at the tumour microenvironment and correlating them with T cell response would help evaluate intra-tumoral characteristics which may contribute to this adaptation. Similarly, we can correlate such features with survival information and responses to other treatments, in order to establish in a more

concrete way what would be a beneficial immunological adaptation to control metastasis after different treatments in correlation with tumoral characteristics. Separate to that endeavour it would be important to understand the gene regulatory networks which alter the T cell memory responses in PDAC and generally in cancer considering that if different therapeutic interventions have different immune-modulatory effects their delineation at the cellular level would provide an avenue to enhance memory response and not only reversal of dysfunctional subsets which is the target of immunotherapy at the moment. In particular, using multiomic single cell techniques instead of bulk transcriptional profiles will be helpful in assessing if this adaptation is established at the genetic or epigenetic level. Subsequently, identification of molecular mechanisms which affect these responses would help alter the responses by more targeted approaches and also would help cross reference these mechanisms in other areas where immune-modulation would be beneficial like chronic inflammatory processes, autoimmunity and vaccination.

11 REFERENCES

1. Janeway's Immunobiology - Google Books. Available at: https://www.google.co.uk/books/edition/Janeway_s_Immunobiology/DmebDwAAQBAJ?hl=en&gbpv=0. (Accessed: 5th March 2022)
2. Hastings, W. D. *et al.* TIM-3 is Expressed on Activated Human CD4+ T Cells and Regulates Th1 and Th17 Cytokines. *Eur. J. Immunol.* **39**, 2492 (2009).
3. Ellyard, J. I., Simson, L. & Parish, C. R. Th2-mediated anti-tumour immunity: friend or foe? *Tissue Antigens* **70**, 1–11 (2007).
4. Lugli, E., Galletti, G., Boi, S. K. & Youngblood, B. A. Stem, Effector, and Hybrid States of Memory CD8+ T Cells. *Trends Immunol.* **41**, 17–28 (2020).
5. Shevach, E. M. Foxp3+ T regulatory cells: Still many unanswered Questions-A perspective after 20 years of study. *Front. Immunol.* **9**, 1048 (2018).
6. Gavin, M. A. *et al.* Foxp3-dependent programme of regulatory T-cell differentiation. *Nature* **445**, 771–775 (2007).
7. Zhao, H., Liao, X. & Kang, Y. Tregs: Where we are and what comes next? *Front. Immunol.* **8**, 1578 (2017).
8. Badovinac, V. P. & Harty, J. T. Programming, demarcating, and manipulating CD8+ T-cell memory. *Immunol. Rev.* **211**, 67–80 (2006).
9. Ahmed, R. & Gray, D. Immunological memory and protective immunity: Understanding their relation. *Science (80-.).* **272**, 54–60 (1996).
10. Kaech, S. M. & Cui, W. Transcriptional control of effector and memory CD8+ T cell differentiation. *Nat. Rev. Immunol.* **12**, 749–761 (2012).
11. Sarkar, S. *et al.* Functional and genomic profiling of effector CD8 T cell subsets with distinct memory fates. *J. Exp. Med.* **205**, 625–640 (2008).
12. Joshi, N. S. *et al.* Inflammation Directs Memory Precursor and Short-Lived Effector CD8+ T Cell Fates via the Graded Expression of T-bet Transcription Factor. *Immunity* **27**, 281–295 (2007).
13. Lanzavecchia, A. & Sallusto, F. Progressive differentiation and selection of the fittest in the immune response. *Nat. Rev. Immunol.* **2**, 982–987 (2002).
14. Kaech, S. M. & Ahmed, R. Memory CD8+ T cell differentiation: Initial antigen encounter triggers a developmental program in naïve cells. *Nat. Immunol.* **2**, 415–422 (2001).
15. Langenkamp, A. *et al.* T cell priming by dendritic cells: thresholds for proliferation, differentiation and death and intraclonal functional diversification. *Eur. J. Immunol.* **32**, 2046 (2002).
16. Wherry, E. J. T cell exhaustion. *Nat. Immunol.* **12**, 492–499 (2011).
17. Virgin, H. W., Wherry, E. J. & Ahmed, R. Redefining Chronic Viral Infection. *Cell* **138**, 30–50 (2009).
18. Wherry, E. J., Blattman, J. N., Murali-Krishna, K., van der Most, R. & Ahmed, R. Viral persistence alters CD8 T-cell immunodominance and tissue distribution and results in distinct stages of functional impairment. *J. Virol.* **77**, 4911–27 (2003).
19. Fuller, M. J. & Zajac, A. J. Ablation of CD8 and CD4 T Cell Responses by High Viral Loads. *J. Immunol.* **170**, 477–486 (2003).
20. Zajac, A. J. *et al.* Viral immune evasion due to persistence of activated T cells without effector

function. *J. Exp. Med.* **188**, 2205–2213 (1998).

21. Chen, L. Co-inhibitory molecules of the B7-CD28 family in the control of T-cell immunity. *Nature Reviews Immunology* **4**, 336–347 (2004).

22. Sharpe, A. H., Wherry, E. J., Ahmed, R. & Freeman, G. J. The function of programmed cell death 1 and its ligands in regulating autoimmunity and infection. *Nature Immunology* **8**, 239–245 (2007).

23. Freeman, G. J. *et al.* Engagement of the PD-1 immunoinhibitory receptor by a novel B7 family member leads to negative regulation of lymphocyte activation. *J. Exp. Med.* **192**, 1027–1034 (2000).

24. Barber, D. L. *et al.* Restoring function in exhausted CD8 T cells during chronic viral infection. *Nature* **439**, 682–687 (2006).

25. Youngblood, B. *et al.* Chronic Virus Infection Enforces Demethylation of the Locus that Encodes PD-1 in Antigen-Specific CD8+ T Cells. *Immunity* **35**, 400–412 (2011).

26. Kuchroo, V. K., Umetsu, D. T., DeKruyff, R. H. & Freeman, G. J. The TIM gene family: Emerging roles in immunity and disease. *Nature Reviews Immunology* **3**, 454–462 (2003).

27. Monney, L. *et al.* Th1-specific cell surface protein Tim-3 regulates macrophage activation and severity of an autoimmune disease. *Nature* **415**, 536–541 (2002).

28. Rodriguez-Manzanet, R., DeKruyff, R., Kuchroo, V. K. & Umetsu, D. T. The costimulatory role of TIM molecules. *Immunol. Rev.* **229**, 259–270 (2009).

29. Jones, R. B. *et al.* Tim-3 expression defines a novel population of dysfunctional T cells with highly elevated frequencies in progressive HIV-1 infection. *J. Exp. Med.* **205**, 2763–2779 (2008).

30. Jin, H. T. *et al.* Cooperation of Tim-3 and PD-1 in CD8 T-cell exhaustion during chronic viral infection. *Proc. Natl. Acad. Sci. U. S. A.* **107**, 14733–14738 (2010).

31. Wherry, E. J. *et al.* Molecular Signature of CD8+ T Cell Exhaustion during Chronic Viral Infection. *Immunity* **27**, 670–684 (2007).

32. Blackburn, S. D. *et al.* Coregulation of CD8+ T cell exhaustion by multiple inhibitory receptors during chronic viral infection. *Nat. Immunol.* **10**, 29–37 (2009).

33. Maruhashi, T. *et al.* LAG-3 inhibits the activation of CD4 + T cells that recognize stable pMHCII through its conformation-dependent recognition of pMHCII. *Nat. Immunol.* **19**, 1415–1426 (2018).

34. Miller, B. C. *et al.* Subsets of exhausted CD8+ T cells differentially mediate tumor control and respond to checkpoint blockade. *Nat. Immunol. 2019 203* **20**, 326–336 (2019).

35. Yao, C. *et al.* Single-cell RNA-seq reveals TOX as a key regulator of CD8+ T cell persistence in chronic infection. *Nat. Immunol. 2019 207* **20**, 890–901 (2019).

36. Daniel, B. *et al.* Divergent clonal differentiation trajectories of T cell exhaustion. *Nat. Immunol. 2022 2311* **23**, 1614–1627 (2022).

37. Sekine, T. *et al.* TOX is expressed by exhausted and polyfunctional human effector memory CD8+ T cells. *Sci. Immunol.* **5**, (2020).

38. Zehn, D., Thimme, R., Lugli, E., de Almeida, G. P. & Oxenius, A. 'Stem-like' precursors are the fount to sustain persistent CD8+ T cell responses. *Nat. Immunol. 2022 236* **23**, 836–847 (2022).

39. Weber, B. N. *et al.* A critical role for TCF-1 in T-lineage specification and differentiation. *Nat. 2011 4767358* **476**, 63–68 (2011).

40. He, R. *et al.* Follicular CXCR5-expressing CD8+ T cells curtail chronic viral infection. *Nat. 2016 5377620* **537**, 412–416 (2016).

41. Utzschneider, D. T. *et al.* T Cell Factor 1-Expressing Memory-like CD8+ T Cells Sustain the Immune Response to Chronic Viral Infections. *Immunity* **45**, 415–427 (2016).

42. Im, S. J. *et al.* Defining CD8+ T cells that provide the proliferative burst after PD-1 therapy. *Nat. 2016 5377620* **537**, 417–421 (2016).

43. Li, Z. *et al.* In vivo labeling reveals continuous trafficking of TCF-1+ T cells between tumor and lymphoid tissue. *J. Exp. Med.* **219**, (2022).

44. Critchley-Thorne, R. J. *et al.* Impaired interferon signaling is a common immune defect in human cancer.

45. Im, S. J. *et al.* Defining CD8+ T cells that provide the proliferative burst after PD-1 therapy. *Nature* **537**, 417–421 (2016).

46. Hudson, W. H. *et al.* Proliferating Transitory T Cells with an Effector-like Transcriptional Signature Emerge from PD-1+ Stem-like CD8+ T Cells during Chronic Infection. *Immunity* **51**, 1043-1058.e4 (2019).

47. Thommen, D. S. & Schumacher, T. N. T Cell Dysfunction in Cancer. *Cancer Cell* **33**, 547–562 (2018).

48. Guo, L., Li, X., Liu, R., Chen, Y. & Ren, C. O R I G I N A L R E S E A R C H TOX correlates with prognosis, immune infiltration, and T cells exhaustion in lung adenocarcinoma. (2020). doi:10.1002/cam4.3324

49. Mlecnik, B. *et al.* Integrative Analyses of Colorectal Cancer Show Immunoscore Is a Stronger Predictor of Patient Survival Than Microsatellite Instability. *Immunity* **44**, 698–711 (2016).

50. Jiang, Y. *et al.* ImmunoScore Signature: A Prognostic and Predictive Tool in Gastric Cancer. *Ann. Surg.* **267**, 504–513 (2018).

51. Tawbi, H. A. *et al.* Relatlimab and Nivolumab versus Nivolumab in Untreated Advanced Melanoma. *N. Engl. J. Med.* **386**, 24–34 (2022).

52. Yang, R. *et al.* Galectin-9 interacts with PD-1 and TIM-3 to regulate T cell death and is a target for cancer immunotherapy. doi:10.1038/s41467-021-21099-2

53. Andreatta, M. *et al.* Interpretation of T cell states from single-cell transcriptomics data using reference atlases. doi:10.1038/s41467-021-23324-4

54. Sekine, T. *et al.* TOX is expressed by exhausted and polyfunctional human effector memory CD8 + T cells. *Sci. Immunol.* **5**, eaba7918 (2020).

55. Gide, T. N. *et al.* Distinct Immune Cell Populations Define Response to Anti-PD-1 Monotherapy and Anti-PD-1/Anti-CTLA-4 Combined Therapy. *Cancer Cell* **35**, 238-255.e6 (2019).

56. Sharpe, A. H. & Pauken, K. E. The diverse functions of the PD1 inhibitory pathway. *Nat. Rev. Immunol. 2017 183* **18**, 153–167 (2017).

57. Sharma, A. *et al.* Anti-CTLA-4 immunotherapy does not deplete Foxp3 þ regulatory T cells (Tregs) in human cancers. *Clin. Cancer Res.* **25**, 1233–1238 (2019).

58. Azarov, I., Helmlinger, G., Kosinsky, Y. & Peskov, K. Elaborating on anti CTLA-4 mechanisms of action using an agent-based modeling approach. *Front. Appl. Math. Stat.* **8**, 106 (2022).

59. Oliveira, G. *et al.* Phenotype, specificity and avidity of antitumour CD8+ T cells in melanoma. *Nat. 2021 5967870* **596**, 119–125 (2021).

60. Yost, K. E. *et al.* Clonal replacement of tumor-specific T cells following PD-1 blockade. *Nat. Med. 2019 258* **25**, 1251–1259 (2019).

61. Wu, T. D. *et al.* Peripheral T cell expansion predicts tumour infiltration and clinical response. *Nat. 2020 5797798* **579**, 274–278 (2020).

62. Royal, R. E. *et al.* Phase 2 trial of single agent ipilimumab (Anti-CTLA-4) for locally advanced or metastatic pancreatic adenocarcinoma. *J. Immunother.* **33**, 828–833 (2010).

63. Farren, M. R. *et al.* Systemic Immune Activity Predicts Overall Survival in Treatment-Naïve Patients with Metastatic Pancreatic Cancer. *Clin. Cancer Res.* **22**, 2565–74 (2016).

64. Hiraoka, N., Onozato, K., Kosuge, T. & Hirohashi, S. Prevalence of FOXP3+ regulatory T cells increases during the progression of pancreatic ductal adenocarcinoma and its premalignant lesions. *Clin. Cancer Res.* **12**, 5423–5434 (2006).

65. Tang, E. S. *et al.* Association of Immunologic Markers with Survival in Upfront Resectable Pancreatic Cancer. *JAMA Surgery* **153**, 1055–1057 (2018).

66. Muller, M. *et al.* The Immune Landscape of Human Pancreatic Ductal Carcinoma: Key Players, Clinical Implications, and Challenges. *Cancers (Basel).* **14**, (2022).

67. Goulart, M. R., Stasinos, K., Fincham, R. E. A., Delvecchio, F. R. & Kocher, H. M. T cells in pancreatic cancer stroma. *World J. Gastroenterol.* **27**, 7956–7968 (2021).

68. Goulart, M. R., Stasinos, K., Fincham, R. E. A., Delvecchio, F. R. & Kocher, H. M. T cells in pancreatic cancer stroma. *World J. Gastroenterol.* **27**, 7956–7968 (2021).

69. Yang, J. *et al.* Dynamic profiling of immune microenvironment during pancreatic cancer development suggests early intervention and combination strategy of immunotherapy. *eBioMedicine* **78**, 103958 (2022).

70. Jainarayanan, A. *et al.* Pseudotime dynamics of T cells in pancreatic ductal adenocarcinoma inform distinct functional states within the regulatory and cytotoxic T cells. *iScience* **26**, 106324 (2023).

71. Kaneda, M. M. *et al.* Macrophage PI3Kγ drives pancreatic ductal adenocarcinoma progression. *Cancer Discov.* **6**, 870 (2016).

72. Mariathasan, S. *et al.* TGFβ attenuates tumour response to PD-L1 blockade by contributing to exclusion of T cells. *Nature* **554**, 544–548 (2018).

73. Liyanage, U. K. *et al.* Prevalence of Regulatory T Cells Is Increased in Peripheral Blood and Tumor Microenvironment of Patients with Pancreas or Breast Adenocarcinoma. *J. Immunol.* **169**, 2756–2761 (2002).

74. Canè, S. *et al.* Neutralization of NET-associated human ARG1 enhances cancer immunotherapy. *Sci. Transl. Med.* **15**, (2023).

75. Ho, W. J., Jaffee, E. M. & Zheng, L. The tumour microenvironment in pancreatic cancer — clinical challenges and opportunities. *Nat. Rev. Clin. Oncol. 2020 179* **17**, 527–540 (2020).

76. Meng, Q. *et al.* Enhanced tumor-infiltrating lymphocytes (eTIL) for cellular therapy of patients with pancreatic cancer or glioblastoma. *J. Immunother. Cancer* **3**, P35 (2015).

77. Lim, Y. *et al.* Artificial intelligence (AI) –powered spatial analysis of tumor-infiltrating lymphocytes (TILs) for prediction of prognosis in resectable pancreatic adenocarcinoma (PDAC). *https://doi.org/10.1200/JCO.2023.41.16_suppl.4162* **41**, 4162–4162 (2023).

78. Miksch, R. C. *et al.* Prognostic Impact of Tumor-Infiltrating Lymphocytes and Neutrophils on Survival of Patients with Upfront Resection of Pancreatic Cancer. *Cancers (Basel).* **11**, (2019).

79. Jang, J. E. *et al.* Crosstalk between Regulatory T Cells and Tumor-Associated Dendritic Cells Negates Anti-tumor Immunity in Pancreatic Cancer. *Cell Rep.* **20**, 558–571 (2017).

80. Feig, C. *et al.* Targeting CXCL12 from FAP-expressing carcinoma-associated fibroblasts synergizes with anti-PD-L1 immunotherapy in pancreatic cancer. *Proc. Natl. Acad. Sci.* (2013). doi:10.1073/pnas.1320318110

81. Weisberg, S. P. *et al.* Tissue-Resident Memory T Cells Mediate Immune Homeostasis in the Human Pancreas through the PD-1/PD-L1 Pathway. *Cell Rep.* **29**, 3916-3932.e5 (2019).

82. Xu, Q., Chen, S., Hu, Y. & Huang, W. Single-cell RNA transcriptome reveals the intra-tumoral heterogeneity and regulators underlying tumor progression in metastatic pancreatic ductal adenocarcinoma. *Cell Death Discov. 2021 71* **7**, 1–16 (2021).

83. Raghavan, S. *et al.* Microenvironment drives cell state, plasticity, and drug response in pancreatic cancer. *Cell* **184**, 6119-6137.e26 (2021).

84. Meng, Q. *et al.* Empirical identification and validation of tumor-targeting T cell receptors from circulation using autologous pancreatic tumor organoids. *J. Immunother. Cancer* **9**, e003213 (2021).

85. Ali, A. I. *et al.* Genetic redirection of T cells for the treatment of pancreatic cancer. *Front. Oncol.* **9**, 56 (2019).

86. Meng, Q. *et al.* Empirical identification and validation of tumor-targeting T cell receptors from circulation using autologous pancreatic tumor organoids. *J. Immunother. Cancer* **9**, e003213 (2021).

87. Stromnes, I. M., Hulbert, A., Pierce, R. H., Greenberg, P. D. & Hingorani, S. R. T-cell localization, activation, and clonal expansion in human pancreatic ductal adenocarcinoma. *Cancer Immunol. Res.* **5**, 978 (2017).

88. Wang, H. *et al.* Analysis of T-cell receptor repertoire in peripheral blood of patients with pancreatic cancer and other pancreatic diseases. *J. Cell. Mol. Med.* **25**, 3991 (2021).

89. Pan, Y. *et al.* High-dimensional single-cell analysis unveils distinct immune signatures of peripheral blood in patients with pancreatic ductal adenocarcinoma. *Front. Endocrinol. (Lausanne).* **14**, 1181538 (2023).

90. Wherry, E. J. & Kurachi, M. Molecular and cellular insights into T cell exhaustion. *Nat. Rev. Immunol.* **15**, 486–499 (2015).

91. Hanahan, D. & Weinberg, R. A. Hallmarks of cancer: The next generation. *Cell* **144**, 646–674 (2011).

92. Blank, C. U. *et al.* Defining 'T cell exhaustion'. *Nat. Rev. Immunol.* (2019). doi:10.1038/s41577-019-0221-9

93. Cossarizza, A. *et al.* Guidelines for the use of flow cytometry and cell sorting in immunological studies. *Eur. J. Immunol.* **47**, 1584–1797 (2017).

94. Dunsford, L. S., Thoirs, R. H., Rathbone, E. & Patakas, A. A Human In Vitro T Cell Exhaustion Model for Assessing Immuno-Oncology Therapies. *Methods Pharmacol. Toxicol.* 89–101 (2020). doi:10.1007/978-1-0716-0171-6_6

95. Quah, B. J. C., Warren, H. S. & Parish, C. R. Monitoring lymphocyte proliferation in vitro and in vivo with the intracellular fluorescent dye carboxyfluorescein diacetate succinimidyl ester. *Nat. Protoc. 2007 29* **2**, 2049–2056 (2007).

96. Langmead, B. & Salzberg, S. L. Fast gapped-read alignment with Bowtie 2. *Nat. Methods 2012 94* **9**, 357–359 (2012).

97. Dobin, A. *et al.* STAR: ultrafast universal RNA-seq aligner. *Bioinformatics* **29**, 15–21 (2013).

98. Xing, Y. *et al.* An expectation-maximization algorithm for probabilistic reconstructions of full-length isoforms from splice graphs. *Nucleic Acids Res.* **34**, 3150–3160 (2006).

99. Love, M. I., Huber, W. & Anders, S. Moderated estimation of fold change and dispersion for RNA-seq data with DESeq2. *Genome Biol.* **15**, 1–21 (2014).

100. Vardhana, S. A. *et al.* Impaired mitochondrial oxidative phosphorylation limits the self-renewal of T cells exposed to persistent antigen. *Nat. Immunol. 2020 219* **21**, 1022–1033 (2020).

101. Zhao, M. *et al.* Rapid in vitro generation of bona fide exhausted CD8+ T cells is accompanied by Tcf7 promotor methylation. *PLOS Pathog.* **16**, e1008555 (2020).

102. Wang, H. *et al.* Analysis of T-cell receptor repertoire in peripheral blood of patients with pancreatic cancer and other pancreatic diseases. *J. Cell. Mol. Med.* **25**, 3991 (2021).

103. Bai, X. *et al.* Characteristics of Tumor Infiltrating Lymphocyte and Circulating Lymphocyte Repertoires in Pancreatic Cancer by the Sequencing of T Cell Receptors OPEN. (2015). doi:10.1038/srep13664

104. Link, J. M. *et al.* Ongoing Replication Stress Response and New Clonal T Cell Development Discriminate Between Liver and Lung Recurrence Sites and Patient Outcomes in Pancreatic Ductal Adenocarcinoma. *bioRxiv* 2022.05.04.490552 (2022). doi:10.1101/2022.05.04.490552

105. Avery, L., Filderman, J., Szymczak-Workman, A. L. & Kane, L. P. Tim-3 co-stimulation promotes short-lived effector T cells, restricts memory precursors, and is dispensable for T cell exhaustion. *Proc. Natl. Acad. Sci. U. S. A.* **115**, 2455–2460 (2018).

106. Lee, S. W. *et al.* CD8+ TILs in NSCLC differentiate into TEMRA via a bifurcated trajectory: deciphering immunogenicity of tumor antigens. *J. Immunother. Cancer* **9**, e002709 (2021).

107. Yang, D.-H. *et al.* Genomic Profiles and Subset Characterization of CD8+terminally Differentiated Effector Memory (TEMRA) Cells from Cancer Patients. *Blood* **134**, 2329–2329 (2019).

108. Mankor, J. M. *et al.* Efficacy of nivolumab and ipilimumab in patients with malignant pleural mesothelioma is related to a subtype of effector memory cytotoxic T cells: Translational evidence from two clinical trials. *EBioMedicine* **62**, 103040 (2020).

109. Tokumaru, Y. *et al.* Association of Th2 high tumors with aggressive features of breast cancer. *https://doi.org/10.1200/JCO.2020.38.15_suppl.e12584* **38**, e12584–e12584 (2020).

110. Piro, G. *et al.* A circulating TH2 cytokines profile predicts survival in patients with resectable pancreatic adenocarcinoma. *Oncoimmunology* **6**, (2017).

111. Clayton, K. L. *et al.* T cell Ig and mucin domain-containing protein 3 is recruited to the immune synapse, disrupts stable synapse formation, and associates with receptor phosphatases. *J. Immunol.* **192**, 782–791 (2014).

112. Wolf, Y., Anderson, A. C. & Kuchroo, V. K. TIM3 comes of age as an inhibitory receptor. *Nat. Rev. Immunol. 2019 203* **20**, 173–185 (2019).

113. Fourcade, J. *et al.* PD-1 and Tim-3 regulate the expansion of tumor antigen-specific $CD8^+$ T cells induced by melanoma vaccines. *Cancer Res.* **74**, 1045–1055 (2014).

114. Sakuishi, K. *et al.* Targeting Tim-3 and PD-1 pathways to reverse T cell exhaustion and restore anti-tumor immunity. *J. Exp. Med.* **207**, 2187–2194 (2010).

115. Jeannet, G. *et al.* Essential role of the Wnt pathway effector Tcf-1 for the establishment of functional CD8 T cell memory. *Proc. Natl. Acad. Sci. U. S. A.* **107**, 9777–9782 (2010).

116. Zhao, X., Shan, Q. & Xue, H.-H. TCF1 in T cell immunity: a broadened frontier. doi:10.1038/s41577-021-00563-6

117. Brummelman, J. *et al.* High-dimensional single cell analysis identifies stem-like cytotoxic CD8+ T cells infiltrating human tumors. *J. Exp. Med.* **215**, 2520–2535 (2018).

118. Avery, L., Filderman, J., Szymczak-Workman, A. L. & Kane, L. P. Tim-3 co-stimulation promotes short-lived effector T cells, restricts memory precursors, and is dispensable for T cell exhaustion. *Proc. Natl. Acad. Sci. U. S. A.* **115**, 2455–2460 (2018).

119. Sabins, N. C. *et al.* TIM-3 Engagement Promotes Effector Memory T Cell Differentiation of Human Antigen-Specific CD8 T Cells by Activating mTORC1. *J. Immunol.* **199**, 4091–4102 (2017).

120. Lee, J. *et al.* Phosphotyrosine-Dependent Coupling of Tim-3 to T-Cell Receptor Signaling Pathways. *Mol. Cell. Biol.* **31**, 3963–3974 (2011).

121. Ferris, R. L., Lu, B. & Kane, L. P. Too Much of a Good Thing? Tim-3 and TCR Signaling in T Cell Exhaustion. *J. Immunol.* **193**, 1525–1530 (2014).

122. Ju, Y. *et al.* Blockade of Tim-3 Pathway Ameliorates Interferon-γ Production from Hepatic CD8+ T Cells in a Mouse Model of Hepatitis B Virus Infection. *Cell. Mol. Immunol. 2009 61* **6**, 35–43 (2009).

123. Lu, C. *et al.* An Emerging Role of TIM3 Expression on T Cells in Chronic Kidney Inflammation. *Front. Immunol.* **12**, 5764 (2022).

124. Fourcade, J. *et al.* Upregulation of Tim-3 and PD-1 expression is associated with tumor antigen–specific CD8+ T cell dysfunction in melanoma patients. *J. Exp. Med.* **207**, 2175–2186 (2010).

125. Zeyu Chen, A. *et al.* TCF-1-Centered Transcriptional Network Drives an Effector versus Exhausted CD8 T Cell-Fate Decision. *Immunity* **51**, 840–855 (2019).

126. Utzschneider, D. T. *et al.* Early precursor T cells establish and propagate T cell exhaustion in chronic infection. *Nat. Immunol. 2020 2110* **21**, 1256–1266 (2020).

127. Miller, B. C. *et al.* Subsets of exhausted CD8+ T cells differentially mediate tumor control and respond to checkpoint blockade. *Nat. Immunol.* **20**, 326 (2019).

128. Power, D. *et al.* IFI44 suppresses HIV-1 LTR promoter activity and facilitates its latency. *Virology* **481**, 142–150 (2015).

129. Busse, D. C. *et al.* Interferon-Induced Protein 44 and Interferon-Induced Protein 44-Like Restrict Replication of Respiratory Syncytial Virus. *J. Virol.* **94**, (2020).

130. Pan, H. *et al.* Interferon-Induced Protein 44 Correlated With Immune Infiltration Serves as a Potential Prognostic Indicator in Head and Neck Squamous Cell Carcinoma. *Front. Oncol.* **10**, 1962 (2020).

131. EBI expression Atlas. Available at: https://www.ebi.ac.uk/gxa/experiments/E-MTAB-3827/Results?geneQuery=%5B%7B%22value%22%3A%22ENSG00000277586%22%7D%5D.

132. Zhou, X. *et al.* PMN-MDSCs accumulation induced by CXCL1 promotes CD8+ T cells exhaustion in gastric cancer. *Cancer Lett.* **532**, 215598 (2022).

133. Bianchi, A. *et al.* Cell-Autonomous Cxcl1 Sustains Tolerogenic Circuitries and Stromal Inflammation via Neutrophil-Derived TNF in Pancreatic Cancer. *Cancer Discov.* **13**, 1428–1453 (2023).

134. Chen, J. H. *et al.* Prostaglandin E2 and programmed cell death 1 signaling coordinately impair CTL function and survival during chronic viral infection. *Nat. Med. 2015 214* **21**, 327–334 (2015).

135. Wang, T. *et al.* PTGES/PGE2 signaling links immunosuppression and lung metastasis in Gprc5a-knockout mouse model. *Oncogene 2020 3915* **39**, 3179–3194 (2020).

136. Ma, K. *et al.* Th17 cells regulate the production of CXCL1 in breast cancer. *Int. Immunopharmacol.*

56, 320–329 (2018).

137. Somerville, T. D. D. *et al.* ZBED2 is an antagonist of interferon regulatory factor 1 and modifies cell identity in pancreatic cancer. *Proc. Natl. Acad. Sci. U. S. A.* **117**, 11471–11482 (2020).

138. Supino, D. *et al.* Negative Regulation of the IL-1 System by IL-1R2 and IL-1R8: Relevance in Pathophysiology and Disease. *Front. Immunol.* **13**, 14 (2022).

139. Chen, L. *et al.* IL1R2 increases regulatory T cell population in the tumor microenvironment by enhancing MHC-II expression on cancer-associated fibroblasts. *J. Immunother. Cancer* **10**, e004585 (2022).

140. Peters, V. A., Joesting, J. J. & Freund, G. G. IL-1 receptor 2 (IL-1R2) and its role in immune regulation. *Brain. Behav. Immun.* **32**, 1 (2013).

141. Chuang, Y.-T., Fang, L.-W., Lin-Feng, M.-H., Chen, R.-H. & Lai, M.-Z. The Tumor Suppressor Death-Associated Protein Kinase Targets to TCR-Stimulated NF-κB Activation. *J. Immunol.* **180**, 3238–3249 (2008).

142. Ni, X. *et al.* Death associated protein kinase 2 suppresses T-B interactions and GC formation. *Mol. Immunol.* **128**, 249–257 (2020).

143. Dysfunctional CD8 T Cells Form a Proliferative, Dynamically Regulated Compartment within Human Melanoma Graphical Abstract. doi:10.1016/j.cell.2018.11.043

144. Staton, T. L. *et al.* Dampening of death pathways by schnurri-2 is essential for T-cell development. *Nat. 2011 4727341* **472**, 105–109 (2011).

145. Nakayama, T. & Kimura, M. Y. Memory Th1/Th2 cell generation controlled by Schnurri-2. *Adv. Exp. Med. Biol.* **684**, 1–10 (2010).

146. Kimura, M. Y. *et al.* Regulation of T helper type 2 cell differentiation by murine Schnurri-2. *J. Exp. Med.* **201**, 397–408 (2005).

147. Weisshaar, N. *et al.* Rgs16 promotes antitumor CD8+ T cell exhaustion. *Sci. Immunol.* **7**, 1873 (2022).

148. Lippert, E. *et al.* Role of Regulator of G Protein Signaling 16 in Inflammation- Induced T Lymphocyte Migration and Activation. *J. Immunol.* **171**, 1542–1555 (2003).

149. Myers, L. M. *et al.* A functional subset of CD8+ T cells during chronic exhaustion is defined by SIRPα expression. *Nat. Commun. 2019 101* **10**, 1–15 (2019).

150. Miller, B. C. *et al.* Subsets of exhausted CD8+ T cells differentially mediate tumor control and respond to checkpoint blockade. *Nat. Immunol. 2019 203* **20**, 326–336 (2019).

151. Ataide, M. A. *et al.* BATF3 programs CD8+ T cell memory. *Nat. Immunol. 2020 2111* **21**, 1397–1407 (2020).

152. Qiu, Z., Khairallah, C., Romanov, G. & Sheridan, B. S. Cutting Edge: Batf3 Expression by CD8 T Cells Critically Regulates the Development of Memory Populations. *J. Immunol.* **205**, 901–906 (2020).

153. O'Neill, R. E. *et al.* T cell-derived CD70 delivers an immune checkpoint function in inflammatory T cell responses. *J. Immunol.* **199**, 3700 (2017).

154. Brugnoni, D. *et al.* CD70 expression on T-cell subpopulations: Study of normal individuals and patients with chronic immune activation. *Immunol. Lett.* **55**, 99–104 (1997).

155. Huang, L. *et al.* OX40L induces helper T cell differentiation during cell immunity of asthma through PI3K/AKT and P38 MAPK signaling pathway. *J. Transl. Med.* **16**, 1–10 (2018).

156. Mendel, I. & Shevach, E. M. Activated T cells express the OX40 ligand: requirements for induction and costimulatory function. *Immunology* **117**, 196–204 (2006).

157. Andreatta, M. *et al.* Interpretation of T cell states from single-cell transcriptomics data using reference atlases. *Nat. Commun. 2021 121* **12**, 1–19 (2021).

158. Ali, L. R. *et al.* PD-1 blockade and CDK4/6 inhibition augment nonoverlapping features of T cell activation in cancer. (2023). doi:10.1084/jem.20220729

159. Deng, J. *et al.* CDK4/6 Inhibition Augments Antitumor Immunity by Enhancing T-cell Activation. (2018). doi:10.1158/2159-8290.CD-17-0915

160. Lai, A. Y. *et al.* CDK4/6 inhibition enhances antitumor efficacy of chemotherapy and immune checkpoint inhibitor combinations in preclinical models and enhances T-cell activation in patients with SCLC receiving chemotherapy. *J. Immunother. Cancer* **8**, e000847 (2020).

161. Aasheim, H. C., Delabie, J. & Finne, E. F. Ephrin-A1 binding to CD4+ T lymphocytes stimulates migration and induces tyrosine phosphorylation of PYK2. *Blood* **105**, 2869–2876 (2005).

162. Hjorthaug, H. S. & Aasheim, H. C. Ephrin-A1 stimulates migration of CD8+CCR7+ T lymphocytes. *Eur. J. Immunol.* **37**, 2326–2336 (2007).

163. Wang, J. *et al.* CCR2/CCR5 inhibitor permits the radiation-induced effector T cell infiltration in pancreatic adenocarcinoma. *J. Exp. Med.* **219**, (2022).

164. Zhang, H. H. *et al.* CCR2 Identifies a Stable Population of Human Effector Memory CD4+ T Cells Equipped for Rapid Recall Response. *J. Immunol.* **185**, 6646–6663 (2010).

165. Bakos, E. *et al.* CCR2 Regulates the Immune Response by Modulating the Interconversion and Function of Effector and Regulatory T Cells. *J. Immunol.* **198**, 4659–4671 (2017).

166. Barrett, B. *et al.* SAMHD1 Promotes the Antiretroviral Adaptive Immune Response in Mice Exposed to Lipopolysaccharide. *J. Immunol.* **208**, 444–453 (2022).

167. Baldauf, H. M. *et al.* SAMHD1 restricts HIV-1 infection in resting CD4+ T cells. *Nat. Med. 2012 1811* **18**, 1682–1688 (2012).

168. Wang, C. *et al.* Actin-Bundling Protein L-Plastin Regulates T Cell Activation. *J. Immunol.* **185**, 7487–7497 (2010).

169. Lake, C. M. *et al.* TIM-3 drives temporal differences in restimulation-induced cell death sensitivity in effector CD8+ T cells in conjunction with CEACAM1. *Cell Death Dis. 2021 124* **12**, 1–17 (2021).

170. Avery, L., Filderman, J., Szymczak-Workman, A. L. & Kane, L. P. Tim-3 co-stimulation promotes short-lived effector T cells, restricts memory precursors, and is dispensable for T cell exhaustion. *Proc. Natl. Acad. Sci. U. S. A.* **115**, 2455–2460 (2018).

12 APPENDIX A

12.1 LIST OF ANTIBODIES & FLUOROCHROMES

Antibody	Fluorochrome	Clone
CD3	BUV395	UCHT1
CD4	PerCP/Cyanine5.5	RPA-T4
CD8	Alexa Fluor 700	RPA-T8
CD45RA	Brilliant Violet 711	HI100
CD45RO	Brilliant Violet 650	UCHL1
CCR7 (CD197)	BUV563	G043H7
CCR6 (CD196)	Brilliant Violet 510	G034E3
CXCR3 (CD183)	PE/Dazzle™ 594	G025H7
FOXP3	Alexa Fluor 488	259D
CD25	Brilliant Violet 785	BC96
TCF1	Alexa Fluor 647	7F11A10
PD1 (CD279)	Brilliant Violet 605	EH12.2H7
TIM3 (CD366)	Brilliant Violet 421	F38-2E2
CFSE	Biolegend	-
Zombie UV	Biolegend	-
Zombie NIR	Biolegend	

12.2 T EXHAUSTION PROTOCOL SCHEMATIC REPRESENTATION

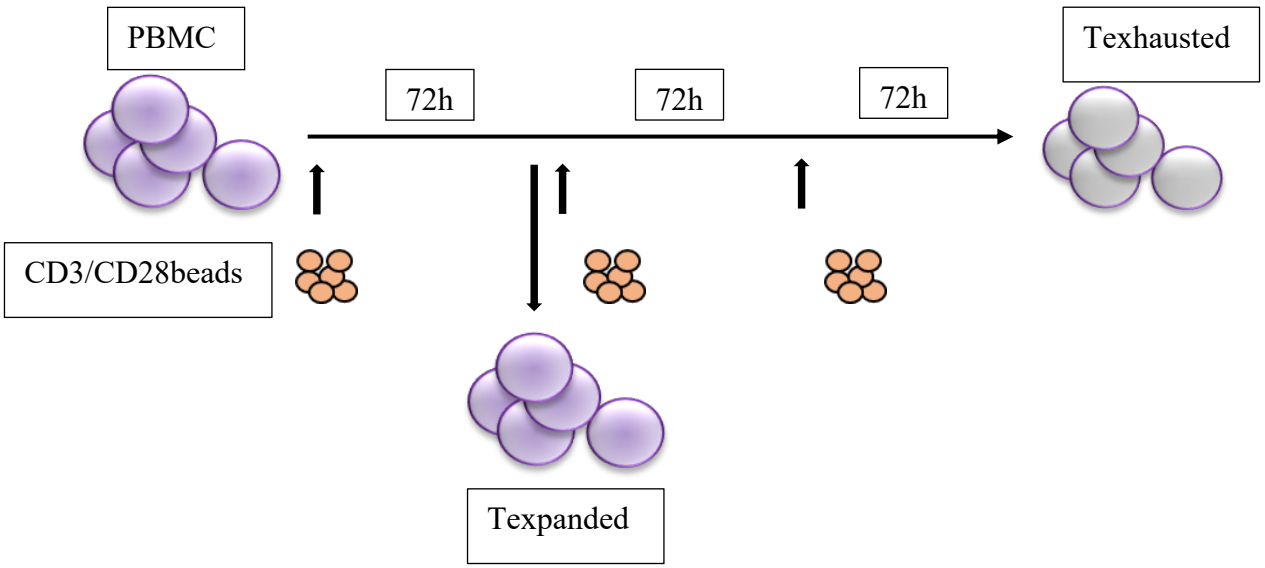

13 APPENDIX B

13.1 RNA EXTRACTION QUALITY METRICS

Sample ID	Nanodrop Conc (ng/uL)	260/280	260/230	Bioanalyser RIN score	Volume	Total yeild (ng)	Proceed with Library preparation ? Y/N/Maybe	
P846B	102.7	2.07	1.15	9.6	10	1027	y	
P850A	14.42	1.94	0.45	9.6	10	144.2	y	
P853B	59.65	2.12	0.5	10	10	596.5	y	
P855B	27.94	2.04	0.39	9.1	10	279.4	y	
P858B	30.82	2.18	0.45	8.7	10	308.2	y	
P859B	39.45	2.14	0.27	9.9	10	394.5	y	
P850BB	23.49	2.07	0.43	6.3	10	234.9	Y	
P850CB	36.37	2.06	0.68	9.5	10	363.7	y	
P850BA	16.26	2.36	0.11	8	10	162.6	y	
P850CA	82.52	2.07	1.25	10	10	825.2	y	
P866BB	17.17	2.01	0.66	10	10	171.7	y	
P866CB	48.34	1.96	0.81	9.4	10	483.4	y	
P866BA	8.296	2.71	0.16	9.8	10	82.96	Maybe	More template
P866CA	19.87	1.96	0.05	1.4	10	198.7	N	Replacement sample
P862BB	17.87	2.02	0.8	8.1	10	178.7	y	
P862CB	41.04	2.07	0.32	8.4	10	410.4	y	
P862BA	1.709	3.82	0.01	9.1	10	17.09	N	<50ng
P862CA	98.06	2.15	1.62	9.5	10	980.6	y	

Additional sample extraction

SampleID	Conc.	260/280	260/230	RIN	Bioanalyser Conc (ng/ul)	dil factor	Actual conc (ng/ul)
P866CA	7.207	1.96	0.02	10	0.88	2	1.76
P866BA	10.19	1.81	0.37	8.7	5.4	3	16.2
P866BB	16.08	2.78	1.21	8.7	14.8	3	44.4

Subject ID	Make up vol to 100ul RNAse-free water (ul)	Elution volume (uL)	Concentration (ng/uL)	260/280	260/230	RIN Score	Total yield (ug)
P866BA	78.5	14	5.295	1.66	0.17	9.4	63.5
P866BB	82.5	14	10.88	1.78	0.24	8.6	130.6

13.2 QUALITY METRICS FOR TRANSCRIPTOMICS – PRE-ALIGNMENT METRICS

Sample name	Sampling time	Total reads	Read length	Avg. read quality	% N	% GC
GC-KS-9916-P846B_S10	Preoperative	27352502	76	33.5942	0.00847	45.6
GC-KS-9916-P850A_S17	Preoperative	19884432	76	33.7122	0.00847	46.1931
GC-KS-9916-P850BA_S15	N/A	23811764	76	33.5772	0.008347	45.7324
GC-KS-9916-P850BB_S18	Preoperative	22224336	76	33.3694	0.008206	45.6274
GC-KS-9916-P850CA_S7	N/A	20401620	76	33.7188	0.008305	45.8894
GC-KS-9916-P850CB_S3	Postoperative	29893907	76	33.649	0.008716	45.8719
GC-KS-9916-P853B_S4	Preoperative	29995757	76	33.7534	0.008569	45.2323
GC-KS-9916-P855B_S14	Preoperative	21878375	76	33.6088	0.008434	45.7177
GC-KS-9916-P858B_S12	Preoperative	27946973	76	33.6184	0.008571	45.1459
GC-KS-9916-P859B_S16	Preoperative	23655034	76	33.0865	0.008367	47.0905
GC-KS-9916-P862BA_S11	N/A	13474315	76	32.9927	0.008322	45.5858
GC-KS-9916-P862BB_S8	Preope rative	20706481	76	33.5803	0.008536	47.2431
GC-KS-9916-P862CA_S9	N/A	25973948	76	33.7783	0.008548	46.0749
GC-KS-9916-P862CB_S5	Postoperative	27759085	76	33.5529	0.008472	45.9048
GC-KS-9916-P866BA_S2	N/A	26335296	76	33.6954	0.008525	45.8126
GC-KS-9916-P866BB_S13	Preoperative	24981166	76	33.4434	0.008611	46.6052

GC-KS-9916-P866CA_S6	N/A	19656125	76	33.6045	0.008413	46.0031
GC-KS-9916-P866CB_S1	Postoperative	24639282	76	33.6148	0.008439	45.7089

13.3 QUALITY METRICS FOR TRANSCRIPTOMICS – POST-ALIGNMENT METRICS

Sample name	Total alignments	Aligned	Total unaligned	Unaligned	Total unique paired	Unique pai	Total non-u	Non-uniqu	Coverage	Avg. cover	Avg. length	Avg. qualit	%GC
GC-KS-9916-P862BA_S11	20526562	68.65554204	4223451	31.34445796	8592298	63.76798	658566	4.887566	0.841722	58.4599	76	34.0132	45.7495
GC-KS-9916-P859B_S16	38368446	73.43427619	6284131	26.56572381	16307496	68.9388	1063407	4.495479	4.91443	18.7428	76	33.8952	46.8649
GC-KS-9916-P862BB_S8	39091752	79.20071015	4306801	20.79928985	14728031	71.12764	1671649	8.073071	4.88346	19.1722	76	34.0158	49.2371
GC-KS-9916-P866BB_S13	48902882	81.7488343	4559354	18.2511657	18283343	73.18851	2138469	8.560325	2.61927	44.8396	76	34.038	49.0085
GC-KS-9916-P862CA_S9	44954944	79.83656932	5237239	20.16343068	19583241	75.3957	1153468	4.440865	3.58446	30.0551	76	34.1421	46.3763
GC-KS-9916-P850A_S17	35530000	81.08203946	3761729	18.91796054	15150513	76.19284	972190	4.889202	4.41254	19.3322	76	34.1101	47.2648
GC-KS-9916-P850BB_S18	39339212	81.85685278	4032194	18.14314722	17253822	77.63481	938320	4.222038	4.6927	20.1333	76	33.8674	46.3242
GC-KS-9916-P858B_S12	49993312	82.1356753	4992538	17.8643247	21704884	77.66453	1249551	4.47115	6.69298	17.9615	76	34.1318	46.022
GC-KS-9916-P850CA_S7	36453122	82.64447137	3540809	17.35552863	15949120	78.17575	911691	4.468719	3.5653	24.531	76	34.0934	46.3278
GC-KS-9916-P855B_S14	40060040	83.3208225	3649133	16.6791775	17151697	78.39566	1077545	4.92516	4.27208	22.5263	76	34.0461	46.6092
GC-KS-9916-P866CA_S6	35592074	83.57089711	3229325	16.42910289	15515884	78.93664	910916	4.63426	1.9746	43.3198	76	34.0546	46.6483
GC-KS-9916-P866BA_S2	48706542	84.49887178	4082268	15.50112822	20868654	79.24215	1384374	5.256725	2.6133	44.78	76	34.0786	46.4556
GC-KS-9916-P846B_S10	49674326	84.06241228	4359329	15.93758772	21822077	79.78092	1171096	4.281495	4.33935	27.537	76	34.0616	46.449
GC-KS-9916-P862CB_S5	52700414	86.12966169	3850279	13.87033831	22448561	80.86924	1460245	5.260422	4.86835	26.0667	76	33.9928	47.1243
GC-KS-9916-P850CB_S3	55816124	86.05007703	4170177	13.94992297	24330998	81.39116	1392732	4.658916	4.55374	29.5132	76	34.0675	46.674
GC-KS-9916-P850BA_S15	44410274	86.21490621	3282474	13.78509379	19390083	81.43069	1139207	4.784219	3.67176	29.1629	76	34.0306	46.5981
GC-KS-9916-P853B_S4	55091164	86.08526533	4173830	13.91473467	24756208	82.53237	1065719	3.552899	7.2168	18.4021	76	34.1237	45.9549
GC-KS-9916-P866CB_S1	47327332	88.32166051	2877459	11.67833949	20631970	83.73608	1129853	4.585576	4.36573	26.1468	76	33.9947	46.6494

13.4 GENE ONTOLOGY T CELL SPECIFIC LIST USED ON QUIESCENT SAMPLE TRANSCRIPTOMICS

Ensemble ID	Gene name	Ensemble ID	Gene name
ENSG00000117335	CD46	ENSG00000125245	GPR18
ENSG00000124253	PCK1	ENSG00000113520	IL4
ENSG00000108691	CCL2	ENSG00000143842	SOX13
ENSG00000124343	XG	ENSG00000115966	ATF2
ENSG00000158769	F11R	ENSG00000158869	FCER1G
ENSG00000099942	CRKL	ENSG00000198435	NRARP
ENSG00000167193	CRK	ENSG00000198286	CARD11
ENSG00000002586	CD99	ENSG00000113916	BCL6
ENSG00000213047	DENND1B	ENSG00000153563	CD8A
ENSG00000196101		ENSG00000101882	NKAP
ENSG00000135341	MAP3K7	ENSG00000185650	ZFP36L1
ENSG00000172940	SLC22A13	ENSG00000117215	PLA2G2D
ENSG00000204642	HLA-F	ENSG00000127152	BCL11B
ENSG00000115594	IL1R1	ENSG00000109471	IL2
ENSG00000117090	SLAMF1	ENSG00000175097	RAG2
ENSG00000106546	AHR	ENSG00000172845	SP3

ENSG00000118520	ARG1	ENSG00000069667	RORA
ENSG00000131019	ULBP3	ENSG00000177628	GBA
ENSG00000073008	PVR	ENSG00000135046	ANXA1
ENSG00000112679	DUSP22	ENSG00000110719	TCIRG1
ENSG00000127191	TRAF2	ENSG00000104432	IL7
ENSG00000079385	CEACAM1	ENSG00000144802	NFKBIZ
ENSG00000175104	TRAF6	ENSG00000112658	SRF
ENSG00000196352	CD55	ENSG00000105810	CDK6
ENSG00000158477	CD1A	ENSG00000169884	WNT10B
ENSG00000188372	ZP3	ENSG00000116251	RPL22
ENSG00000196843	ARID5A	ENSG00000168036	CTNNB1
ENSG00000121807	CCR2	ENSG00000222028	PSMB11
ENSG00000143184	XCL1	ENSG00000122224	LY9
ENSG00000125538	IL1B	ENSG00000165699	TSC1
ENSG00000204267	TAP2	ENSG00000164690	SHH
ENSG00000072694	FCGR2B	ENSG00000182866	LCK
ENSG00000010704	HFE	ENSG00000116678	LEPR
ENSG00000111981	ULBP1	ENSG00000168685	IL7R
ENSG00000131015	ULBP2	ENSG00000166527	CLEC4D
ENSG00000130529	TRPM4	ENSG00000134321	RSAD2
ENSG00000164520	RAET1E	ENSG00000172673	THEMIS
ENSG00000167207	NOD2	ENSG00000115085	ZAP70
ENSG00000204305	AGER	ENSG00000134545	KLRC1
ENSG00000130202	NECTIN2	ENSG00000118046	STK11
ENSG00000168811	IL12A	ENSG00000165025	SYK
ENSG00000155918	RAET1L	ENSG00000182566	CLEC4G
ENSG00000028137	TNFRSF1B	ENSG00000135870	RC3H1
ENSG00000158485	CD1B	ENSG00000164136	IL15
ENSG00000079950	STX7	ENSG00000049768	FOXP3
ENSG00000104951	IL4I1	ENSG00000119919	NKX2-3
ENSG00000203722	RAET1G	ENSG00000120738	EGR1
ENSG00000145868	FBXO38	ENSG00000140691	ARMC5
ENSG00000153310	FAM49B	ENSG00000105647	PIK3R2
ENSG00000134539	KLRD1	ENSG00000139636	LMBR1L
ENSG00000204525	HLA-C	ENSG00000198846	TOX
ENSG00000158488	CD1E	ENSG00000160199	PKNOX1
ENSG00000234745	HLA-B	ENSG00000067560	RHOA
ENSG00000105205	CLC	ENSG00000179588	ZFPM1
ENSG00000131042	LILRB2	ENSG00000134516	DOCK2
ENSG00000081913	PHLPP1	ENSG00000166710	B2M
ENSG00000163513	TGFBR2	ENSG00000188092	GPR89B
ENSG00000204632	HLA-G	ENSG00000117461	PIK3R3
ENSG00000167604	NFKBID	ENSG00000141510	TP53
ENSG00000131759	RARA	ENSG00000125084	WNT1
ENSG00000114013	CD86	ENSG00000143365	RORC

ENSG00000183655	KLHL25	ENSG00000010610	CD4
ENSG00000121594	CD80	ENSG00000138684	IL21
ENSG00000150782	IL18	ENSG00000100105	PATZ1
ENSG00000107338	SHB	ENSG00000162552	WNT4
ENSG00000067606	PRKCZ	ENSG00000113263	ITK
ENSG00000111537	IFNG	ENSG00000107758	PPP3CB
ENSG00000162594	IL23R	ENSG00000171608	PIK3CD
ENSG00000096996	IL12RB1	ENSG00000173757	STAT5B
ENSG00000105639	JAK3	ENSG00000112486	CCR6
ENSG00000163874	ZC3H12A	ENSG00000070495	JMJD6
ENSG00000101665	SMAD7	ENSG00000135144	DTX1
ENSG00000115318	LOXL3	ENSG00000133895	MEN1
ENSG00000171150	SOCS5	ENSG00000197471	SPN
ENSG00000110651	CD81	ENSG00000124813	RUNX2
ENSG00000168961	LGALS9	ENSG00000147168	IL2RG
ENSG00000135077	HAVCR2	ENSG00000168421	RHOH
ENSG00000242574	HLA-DMB	ENSG00000174697	LEP
ENSG00000131981	LGALS3	ENSG00000081059	TCF7
ENSG00000122862	SRGN	ENSG00000131188	PRR7
ENSG00000186818	LILRB4	ENSG00000151694	ADAM17
ENSG00000123338	NCKAP1L	ENSG00000253729	PRKDC
ENSG00000067955	CBFB	ENSG00000081237	PTPRC
ENSG00000020633	RUNX3	ENSG00000138795	LEF1
ENSG00000159216	RUNX1	ENSG00000156127	BATF
ENSG00000164889	SLC4A2	ENSG00000104856	RELB
ENSG00000185338	SOCS1	ENSG00000113302	IL12B
ENSG00000114315	HES1	ENSG00000174405	LIG4
ENSG00000166949	SMAD3	ENSG00000106952	TNFSF8
ENSG00000163154	TNFAIP8L2	ENSG00000198018	ENTPD7
ENSG00000078747	ITCH	ENSG00000198851	CD3E
ENSG00000172575	RASGRP1	ENSG00000112149	CD83
ENSG00000197329	PELI1	ENSG00000196189	SEMA4A
ENSG00000018280	SLC11A1	ENSG00000025770	NCAPH2
ENSG00000125735	TNFSF14	ENSG00000196839	ADA
ENSG00000277807		ENSG00000104312	RIPK2
ENSG00000065675	PRKCQ	ENSG00000124766	SOX4
ENSG00000113811	SELENOK	ENSG00000180549	FUT7
ENSG00000109943	CRTAM	ENSG00000175354	PTPN2
ENSG00000064012	CASP8	ENSG00000160224	AIRE
ENSG00000162723	SLAMF9	ENSG00000143772	ITPKB
ENSG00000080815	PSEN1	ENSG00000145675	PIK3R1
ENSG00000088832	FKBP1A	ENSG00000161405	IKZF3
ENSG00000196684	HSH2D	ENSG00000117262	GPR89A
ENSG00000144381	HSPD1	ENSG00000073861	TBX21
ENSG00000197635	DPP4	ENSG00000066336	SPI1

ENSG00000066294	CD84	ENSG00000122122	SASH3
ENSG00000071051	NCK2	ENSG00000057663	ATG5
ENSG00000198821	CD247	ENSG00000118058	KMT2A
ENSG00000102524	TNFSF13B	ENSG00000168040	FADD
ENSG00000167815	PRDX2	ENSG00000171522	PTGER4
ENSG00000005844	ITGAL	ENSG00000128917	DLL4
ENSG00000064201	TSPAN32	ENSG00000189403	HMGB1
ENSG00000087088	BAX	ENSG00000077238	IL4R
ENSG00000114423	CBLB	ENSG00000105438	KDELR1
ENSG00000100345	MYH9	ENSG00000160685	ZBTB7B
ENSG00000117280	RAB29	ENSG00000160654	CD3G
ENSG00000112195	TREML2	ENSG00000187736	NHEJ1
ENSG00000026508	CD44	ENSG00000115604	IL18R1
ENSG00000128829	EIF2AK4	ENSG00000163251	FZD5
ENSG00000154639	CXADR	ENSG00000177283	FZD8
ENSG00000127951	FGL2	ENSG00000106003	LFNG
ENSG00000111729	CLEC4A	ENSG00000056586	RC3H2
ENSG00000112576	CCND3	ENSG00000158473	CD1D
ENSG00000172243	CLEC7A	ENSG00000173585	CCR9
ENSG00000077420	APBB1IP	ENSG00000124126	PREX1
ENSG00000089692	LAG3	ENSG00000153029	MR1
ENSG00000007129	CEACAM21	ENSG00000204592	HLA-E
ENSG00000147885	IFNA16	ENSG00000204287	HLA-DRA
ENSG00000236637	IFNA4	ENSG00000196126	HLA-DRB1
ENSG00000120235	IFNA6	ENSG00000131037	EPS8L1
ENSG00000177047	IFNW1	ENSG00000276557	TRBV18
ENSG00000105246	EBI3	ENSG00000211793	TRAV9-2
ENSG00000183214		ENSG00000211807	TRAV26-1
ENSG00000204516	MICB	ENSG00000211701	TRGV1
ENSG00000180900	SCRIB	ENSG00000211819	TRAV40
ENSG00000136167	LCP1	ENSG00000211802	TRAV22
ENSG00000158092	NCK1	ENSG00000211797	TRAV17
ENSG00000117586	TNFSF4	ENSG00000211800	TRAV20
ENSG00000147896	IFNK	ENSG00000211716	TRBV9
ENSG00000026950	BTN3A1	ENSG00000211697	TRGV5
ENSG00000134460	IL2RA	ENSG00000211785	TRAV12-1
ENSG00000205220	PSMB10	ENSG00000211777	TRAV3
ENSG00000131507	NDFIP1	ENSG00000211788	TRAV13-1
ENSG00000089041	P2RX7	ENSG00000211784	TRAV10
ENSG00000177697	CD151	ENSG00000211791	TRAV13-2
ENSG00000049130	KITLG	ENSG00000211776	TRAV2
ENSG00000149021	SCGB1A1	ENSG00000211767	TRBJ2-3
ENSG00000172724	CCL19	ENSG00000211786	TRAV8-2
ENSG00000010810	FYN	ENSG00000255569	TRAV1-1
ENSG00000110492	MDK	ENSG00000211779	TRAV5

ENSG00000105851	PIK3CG	ENSG00000211795	TRAV8-6
ENSG00000138735	PDE5A	ENSG00000211816	TRAV38-1
ENSG00000254647	INS	ENSG00000211812	TRAV26-2
ENSG00000186827	TNFRSF4	ENSG00000211820	TRAV41
ENSG00000119927	GPAM	ENSG00000211778	TRAV4
ENSG00000124215	CDH26	ENSG00000211794	TRAV12-3
ENSG00000174564	IL20RB	ENSG00000211805	TRAV24
ENSG00000102034	ELF4	ENSG00000211813	TRAV34
ENSG00000172116	CD8B	ENSG00000211806	TRAV25
ENSG00000228083	IFNA14	ENSG00000211801	TRAV21
ENSG00000214042	IFNA7	ENSG00000211699	TRGV3
ENSG00000197919	IFNA1	ENSG00000282780	TRBJ1-6
ENSG00000233816	IFNA13	ENSG00000277880	TRBV17
ENSG00000164251	F2RL1	ENSG00000282133	TRBJ1-3
ENSG00000037749	MFAP3	ENSG00000282420	TRBJ1-2
ENSG00000137077	CCL21	ENSG00000211790	TRAV8-4
ENSG00000116824	CD2	ENSG00000274752	TRBV12-3
ENSG00000160593	JAML	ENSG00000256553	TRAV1-2
ENSG00000206503	HLA-A	ENSG00000229769	TRBV10-2
ENSG00000184995	IFNE	ENSG00000275791	TRBV10-3
ENSG00000131203	IDO1	ENSG00000253291	TRBV7-7
ENSG00000162736	NCSTN	ENSG00000211706	TRBV6-1
ENSG00000147065	MSN	ENSG00000211752	TRBV27
ENSG00000119782	FKBP1B	ENSG00000211720	TRBV11-1
ENSG00000069974	RAB27A	ENSG00000237254	TRBV30
ENSG00000102879	CORO1A	ENSG00000211721	TRBV6-5
ENSG00000188379	IFNA2	ENSG00000211717	TRBV10-1
ENSG00000186803	IFNA10	ENSG00000211764	TRBJ2-1
ENSG00000137080	IFNA21	ENSG00000211771	TRBJ2-7
ENSG00000147873	IFNA5	ENSG00000163519	TRAT1
ENSG00000234829	IFNA17	ENSG00000283063	TRBV6-2
ENSG00000171855	IFNB1	ENSG00000282173	TRBJ1-5
ENSG00000165283	STOML2	ENSG00000276953	TRBV12-4
ENSG00000015285	WAS	ENSG00000211818	TRAV39
ENSG00000213658	LAT	ENSG00000259092	TRAV30
ENSG00000101082	SLA2	ENSG00000211749	TRBV23-1
ENSG00000244038	DDOST	ENSG00000211731	TRBV5-7
ENSG00000003137	CYP26B1	ENSG00000253188	TRBV6-7
ENSG00000197892	KIF13B	ENSG00000211715	TRBV5-3
ENSG00000171793	CTPS1	ENSG00000211694	TRGV10
ENSG00000075711	DLG1	ENSG00000211809	TRAV27
ENSG00000105374	NKG7	ENSG00000211825	TRDJ1
ENSG00000090339	ICAM1	ENSG00000282499	TRBV25-1
ENSG00000111679	PTPN6	ENSG00000211750	TRBV24-1
ENSG00000120337	TNFSF18	ENSG00000211747	TRBV20-1

ENSG00000120242	IFNA8	ENSG00000211746	TRBV19
ENSG00000182985	CADM1	ENSG00000211714	TRBV7-3
ENSG00000163512	AZI2	ENSG00000211693	TRGV11
ENSG00000110944	IL23A	ENSG00000282320	TRBJ1-1
ENSG00000158481	CD1C	ENSG00000211695	TRGV9
ENSG00000103855	CD276	ENSG00000276597	TRBV11-3
ENSG00000128815	WDFY4	ENSG00000256590	TRDV3
ENSG00000138814	PPP3CA	ENSG00000211821	TRDV2
ENSG00000090776	EFNB1	ENSG00000211817	TRAV38-2DV8
ENSG00000026751	SLAMF7	ENSG00000281958	TRBJ1-4
ENSG00000167984	NLRC3	ENSG00000211799	TRAV19
ENSG00000027869	SH2D2A	ENSG00000211796	TRAV16
ENSG00000173762	CD7	ENSG00000211707	TRBV7-1
ENSG00000107099	DOCK8	ENSG00000211782	TRAV8-1
ENSG00000160223	ICOSLG	ENSG00000211787	TRAV8-3
ENSG00000172175	MALT1	ENSG00000253534	TRBV6-8
ENSG00000136504	KAT7	ENSG00000211724	TRBV6-6
ENSG00000136244	IL6	ENSG00000211886	TRAJ3
ENSG00000141968	VAV1	ENSG00000276405	TRBV13
ENSG00000166523	CLEC4E	ENSG00000211798	TRAV18
ENSG00000135047	CTSL	ENSG00000211792	TRAV14DV4
ENSG00000168610	STAT3	ENSG00000211803	TRAV23DV6
ENSG00000114861	FOXP1	ENSG00000211815	TRAV36DV7
ENSG00000163508	EOMES	ENSG00000211781	TRAV7
ENSG00000103423	DNAJA3	ENSG00000211783	TRAV9-1
ENSG00000204103	MAFB	ENSG00000211780	TRAV6
ENSG00000198793	MTOR	ENSG00000211789	TRAV12-2
ENSG00000162739	SLAMF6	ENSG00000211690	TRGJ1
ENSG00000171791	BCL2	ENSG00000233306	TRGV2
ENSG00000155760	FZD7	ENSG00000275243	TRBV16
ENSG00000118513	MYB	ENSG00000211810	TRAV29DV5
ENSG00000136630	HLX	ENSG00000278030	TRBV7-9
ENSG00000134242	PTPN22	ENSG00000141293	SKAP1
ENSG00000126804	ZBTB1	ENSG00000230099	TRBV5-4
ENSG00000129465	RIPK3	ENSG00000211698	TRGV4
ENSG00000166349	RAG1	ENSG00000211696	TRGV8
ENSG00000137154	RPS6	ENSG00000253409	TRBV7-4
ENSG00000165240	ATP7A	ENSG00000223997	TRDD1
ENSG00000166888	STAT6	ENSG00000275158	TRBV12-5
ENSG00000125347	IRF1	ENSG00000226660	TRBV2
ENSG00000169508	GPR183	ENSG00000211804	TRDV1
ENSG00000126353	CCR7	ENSG00000211713	TRBV6-4
ENSG00000006042	TMEM98	ENSG00000211727	TRBV7-6
ENSG00000097007	ABL1	ENSG00000282431	TRBD1

ENSG00000069399	BCL3	ENSG00000232869	TRBV29-1
ENSG00000152518	ZFP36L2	ENSG00000211753	TRBV28
ENSG00000178562	CD28	ENSG00000275743	TRBV14
ENSG00000157404	KIT	ENSG00000211728	TRBV5-6
ENSG00000184916	JAG2	ENSG00000211725	TRBV5-5
ENSG00000106571	GLI3	ENSG00000211734	TRBV5-1
ENSG00000144840	RABL3	ENSG00000211710	TRBV4-1
ENSG00000160712	IL6R	ENSG00000237702	TRBV3-1
ENSG00000137265	IRF4	ENSG00000211745	TRBV4-2
ENSG00000135426	TESPA1	ENSG00000282939	TRBV7-2
ENSG00000109101	FOXN1	ENSG00000106829	TLE4
ENSG00000056972	TRAF3IP2	ENSG00000140332	TLE3
ENSG00000167286	CD3D	ENSG00000196781	TLE1
ENSG00000019582	CD74	ENSG00000116128	BCL9
ENSG00000157764	BRAF	ENSG00000198728	LDB1
ENSG00000141736	ERBB2	ENSG00000152284	TCF7L1
ENSG00000107485	GATA3	ENSG00000186174	BCL9L
ENSG00000171316	CHD7	ENSG00000148737	TCF7L2
ENSG00000196628	TCF4	ENSG00000163348	PYGO2
ENSG00000100453	GZMB		

13.5 GENE SET ENRICHMENT OF QUIESCENT SAMPLES

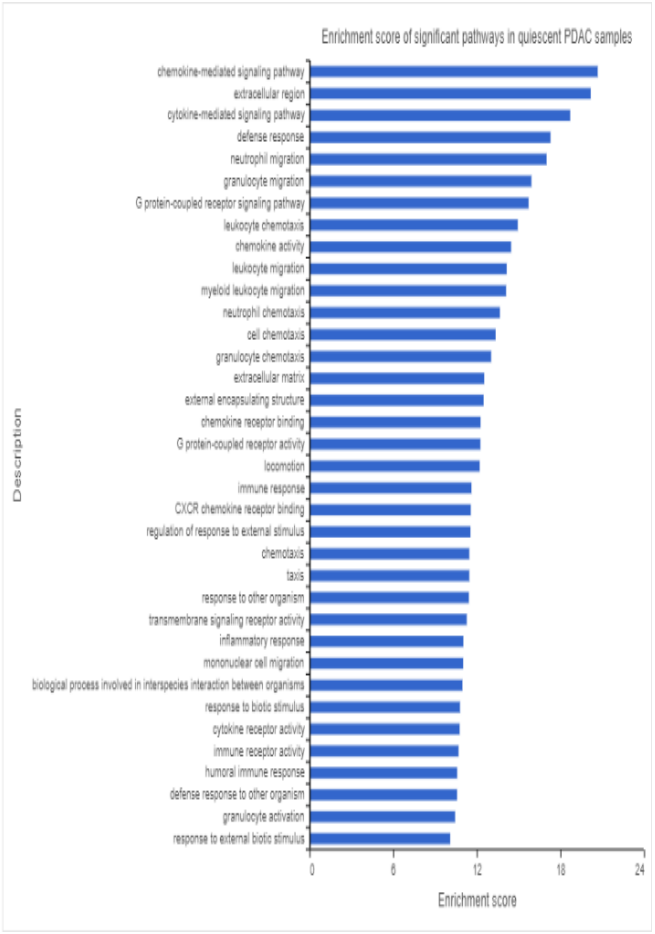

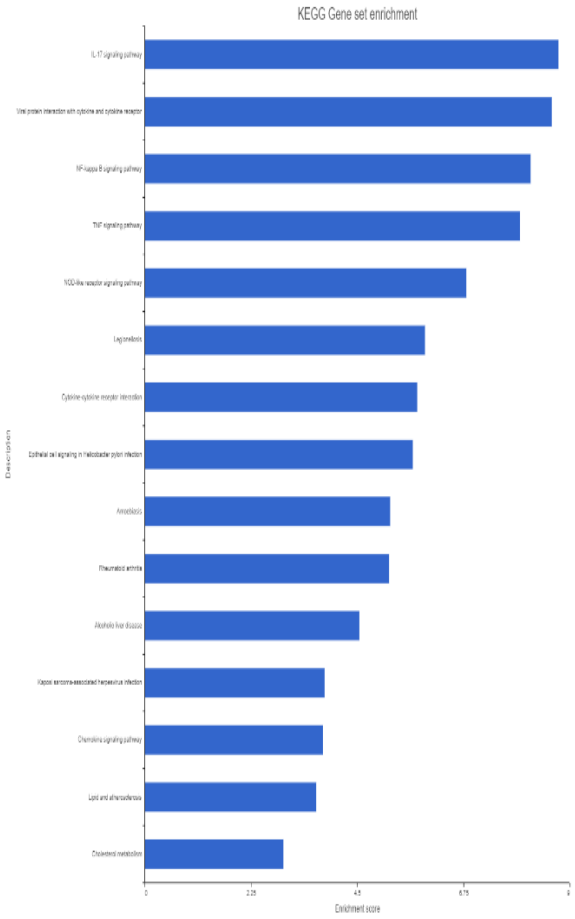

13.6 DIFFERENTIAL GENE EXPRESSION RESULTS OF PREOPERATIVE VS POSTOPERATIVE SAMPLES AT QUIESCENCE

Gene name	P-value (Postoperative vs Preoperative)	FDR step up (Postoperative vs Preoperative)	Ratio (Postoperative vs Preoperative)	Fold change (Postoperative vs Preoperative)	LSMean(Postoperative) (Postoperative vs Preoperative)	LSMean(Preoperative) (Postoperative vs Preoperative)
PHACTR1	3.03E-10	4.59E-06	4.51E-01	-2.22E+00	2.81E+02	6.23E+02
ACP6	1.49E-07	1.13E-03	3.64E-01	-2.75E+00	3.83E+01	1.05E+02
CXCL2	1.08E-06	4.99E-03	7.54E-02	-1.33E+01	1.54E+01	2.04E+02
PAN3-AS1	1.31E-06	4.99E-03	1.28E-01	-7.79E+00	6.30E+00	4.91E+01
SNED1	2.07E-06	6.29E-03	2.91E-01	-3.43E+00	1.38E+01	4.72E+01

CRAMP1	4.36E-06	8.53E-03	4.13E-01	-2.42E+00	7.64E+01	1.85E+02
---	4.50E-06	8.53E-03	2.86E-01	-3.49E+00	1.72E+01	6.00E+01
KNTC1	5.77E-06	9.73E-03	2.30E-01	-4.34E+00	1.55E+01	6.74E+01
---	6.49E-06	9.86E-03	1.09E-01	-9.19E+00	1.33E+01	1.22E+02
IFI44L	7.89E-06	1.01E-02	3.96E+00	3.96E+00	9.89E+02	2.50E+02
ZNF587B	8.32E-06	1.01E-02	3.50E-01	-2.86E+00	2.10E+01	6.00E+01
ZNF432	8.65E-06	1.01E-02	3.06E-01	-3.27E+00	3.27E+01	1.07E+02
---	9.39E-06	1.02E-02	2.23E-01	-4.48E+00	8.03E+00	3.60E+01
TRAF5	1.09E-05	1.10E-02	3.54E-01	-2.83E+00	1.74E+02	4.92E+02
HIPK1-AS1	1.16E-05	1.10E-02	2.46E-01	-4.07E+00	1.70E+01	6.91E+01
CMPK2	1.26E-05	1.13E-02	2.28E+00	2.28E+00	9.83E+02	4.31E+02
CABP4	1.57E-05	1.33E-02	2.61E-01	-3.83E+00	1.03E+01	3.96E+01
---	2.11E-05	1.51E-02	2.96E-01	-3.38E+00	5.73E+01	1.94E+02
PTGES	2.14E-05	1.51E-02	1.46E-01	-6.84E+00	1.14E+01	7.79E+01
IFI44	2.19E-05	1.51E-02	2.29E+00	2.29E+00	8.36E+02	3.65E+02
---	2.36E-05	1.56E-02	2.36E-01	-4.24E+00	8.52E+00	3.61E+01
LINC01138	2.67E-05	1.62E-02	4.82E-01	-2.08E+00	4.92E+01	1.02E+02
CXCL1	2.68E-05	1.62E-02	1.58E-01	-6.33E+00	1.99E+01	1.26E+02
NATD1	3.51E-05	2.05E-02	4.97E-01	-2.01E+00	1.40E+02	2.82E+02
GUSBP11	3.81E-05	2.08E-02	2.77E-01	-3.61E+00	1.37E+01	4.95E+01
MYEF2	3.84E-05	2.08E-02	2.30E-01	-4.34E+00	8.67E+00	3.77E+01
---	4.17E-05	2.18E-02	2.52E-01	-3.98E+00	1.72E+01	6.85E+01
---	5.75E-05	2.91E-02	1.94E-01	-5.16E+00	9.25E+00	4.77E+01
LINC01588	6.72E-05	3.12E-02	4.90E-01	-2.04E+00	6.37E+01	1.30E+02
NEFL	6.78E-05	3.12E-02	2.30E+00	2.30E+00	3.06E+02	1.33E+02
LYPD2	7.10E-05	3.17E-02	2.13E-01	-4.69E+00	3.33E+01	1.56E+02
NUP107-DT	7.86E-05	3.40E-02	2.35E-01	-4.25E+00	1.10E+01	4.67E+01
---	8.23E-05	3.40E-02	3.65E-01	-2.74E+00	1.98E+01	5.42E+01
SNTA1	1.17E-04	4.55E-02	4.98E-01	-2.01E+00	3.74E+01	7.51E+01
---	1.36E-04	4.69E-02	3.19E-01	-3.14E+00	7.50E+00	2.35E+01
LPL	1.39E-04	4.69E-02	1.45E-01	-6.90E+00	1.68E+01	1.16E+02
ACKR3	1.39E-04	4.69E-02	1.40E-01	-7.16E+00	1.44E+01	1.03E+02
PTBP2	1.45E-04	4.79E-02	2.80E-01	-3.57E+00	3.09E+01	1.11E+02
AP1S3	1.73E-04	5.60E-02	3.75E-01	-2.67E+00	3.09E+01	8.26E+01
APOBEC2	1.82E-04	5.65E-02	2.52E-01	-3.97E+00	5.49E+00	2.18E+01
CUTALP	1.97E-04	5.98E-02	3.71E-01	-2.70E+00	1.42E+02	3.82E+02
CASS4	2.09E-04	6.21E-02	2.93E-01	-3.42E+00	6.54E+01	2.23E+02
IFI6	2.27E-04	6.57E-02	2.45E+00	2.45E+00	2.98E+03	1.22E+03
LINC02980	2.30E-04	6.57E-02	3.38E-01	-2.96E+00	1.62E+01	4.79E+01
CXCL8	2.35E-04	6.60E-02	1.33E-01	-7.50E+00	4.63E+02	3.47E+03
RASD1	2.57E-04	7.08E-02	2.26E-01	-4.43E+00	1.91E+01	8.45E+01
IL1R2	2.77E-04	7.22E-02	5.80E-02	-1.73E+01	4.14E+01	7.15E+02
CCL4L2	2.80E-04	7.22E-02	2.53E-01	-3.96E+00	1.30E+02	5.13E+02

SNHG9	2.94E-04	7.43E-02	3.23E-01	-3.09E+00	2.12E+01	6.56E+01
ZNF250	3.09E-04	7.67E-02	4.32E-01	-2.31E+00	3.29E+01	7.61E+01
PBX4	3.15E-04	7.67E-02	4.07E-01	-2.45E+00	1.78E+01	4.37E+01
SLC12A5-AS1	3.24E-04	7.67E-02	1.23E-01	-8.11E+00	5.68E+00	4.61E+01
---	3.29E-04	7.67E-02	2.80E-01	-3.58E+00	2.31E+01	8.26E+01
---	3.33E-04	7.67E-02	3.95E-01	-2.53E+00	9.13E+01	2.31E+02
APOLD1	3.34E-04	7.67E-02	1.81E-01	-5.54E+00	4.15E+00	2.30E+01
SIGLEC1	3.53E-04	7.69E-02	3.78E+00	3.78E+00	3.35E+02	8.86E+01
SLX1A-SULT1A3	3.57E-04	7.69E-02	4.76E-01	-2.10E+00	7.23E+01	1.52E+02
ZFP28	3.59E-04	7.69E-02	2.04E-01	-4.90E+00	9.26E+00	4.54E+01
---	3.78E-04	7.69E-02	1.47E-01	-6.83E+00	1.24E+01	8.50E+01
OAS3	3.82E-04	7.69E-02	2.50E+00	2.50E+00	1.79E+03	7.17E+02
CD177	4.00E-04	7.69E-02	1.03E-01	-9.75E+00	2.80E+01	2.73E+02
GOLGA4-AS1	4.02E-04	7.69E-02	4.00E-01	-2.50E+00	1.67E+01	4.18E+01
ATF7IP2	4.04E-04	7.69E-02	4.52E-01	-2.21E+00	1.50E+02	3.31E+02
CLK1	4.13E-04	7.69E-02	4.20E-01	-2.38E+00	2.17E+02	5.18E+02
MX1	4.14E-04	7.69E-02	2.38E+00	2.38E+00	3.66E+03	1.54E+03
PDGFRA	4.24E-04	7.69E-02	2.69E-01	-3.72E+00	1.07E+01	3.99E+01
ZNF487	4.28E-04	7.69E-02	4.71E-01	-2.12E+00	7.25E+01	1.54E+02
PIM3	4.43E-04	7.69E-02	2.28E+00	2.28E+00	1.74E+03	7.61E+02
MATN1-AS1	4.54E-04	7.69E-02	3.12E-01	-3.20E+00	1.04E+01	3.32E+01
CXCL3	4.55E-04	7.69E-02	2.26E-01	-4.42E+00	1.95E+01	8.63E+01
JDP2-AS1	4.57E-04	7.69E-02	2.98E-01	-3.36E+00	2.32E+01	7.80E+01
TCTN1	4.62E-04	7.69E-02	4.05E-01	-2.47E+00	4.37E+01	1.08E+02
---	4.71E-04	7.69E-02	3.66E-01	-2.73E+00	1.29E+01	3.51E+01
ISG15	4.71E-04	7.69E-02	2.11E+00	2.11E+00	1.75E+03	8.28E+02
ZNF507	4.80E-04	7.75E-02	4.83E-01	-2.07E+00	6.17E+01	1.28E+02
XAF1	4.98E-04	7.86E-02	2.14E+00	2.14E+00	3.09E+03	1.44E+03
MMP9	5.05E-04	7.86E-02	1.02E-01	-9.78E+00	2.38E+02	2.33E+03
---	5.12E-04	7.86E-02	3.70E-01	-2.70E+00	1.68E+01	4.53E+01
TMEM167B-DT	5.31E-04	8.04E-02	2.89E-01	-3.46E+00	1.48E+01	5.11E+01
CCDC141	5.52E-04	8.19E-02	3.10E-01	-3.22E+00	2.57E+01	8.28E+01
OXER1	5.56E-04	8.19E-02	3.69E-01	-2.71E+00	3.50E+01	9.49E+01
ELAPOR2	5.98E-04	8.51E-02	3.29E-01	-3.04E+00	2.26E+01	6.87E+01
TPPP3	5.98E-04	8.51E-02	3.00E-01	-3.33E+00	1.24E+02	4.12E+02
BUB1	6.02E-04	8.51E-02	2.37E+00	2.37E+00	1.51E+02	6.35E+01
TMCC3	6.07E-04	8.51E-02	2.85E-01	-3.51E+00	2.33E+02	8.19E+02
NPIPB3	6.11E-04	8.51E-02	2.81E-01	-3.56E+00	3.27E+01	1.16E+02
---	6.24E-04	8.60E-02	2.74E-01	-3.66E+00	1.37E+01	4.99E+01
---	6.56E-04	8.95E-02	3.25E-01	-3.08E+00	7.85E+00	2.42E+01
OASL	6.64E-04	8.95E-02	2.33E+00	2.33E+00	9.72E+02	4.17E+02

PKP2	6.67E-04	8.95E-02	2.20E-01	-4.55E+00	4.25E+01	1.94E+02
IL18RAP	7.58E-04	1.00E-01	2.38E-01	-4.21E+00	8.88E+01	3.73E+02
TSPYL5	7.76E-04	1.02E-01	3.60E-01	-2.78E+00	2.56E+01	7.12E+01
---	8.59E-04	1.09E-01	2.06E-01	-4.86E+00	5.38E+00	2.62E+01
CABP5	8.59E-04	1.09E-01	2.97E-01	-3.37E+00	3.29E+01	1.11E+02
ZNF550	9.29E-04	1.13E-01	4.63E-01	-2.16E+00	5.36E+01	1.16E+02
AATK	9.39E-04	1.13E-01	2.71E-01	-3.69E+00	3.21E+01	1.19E+02
---	9.41E-04	1.13E-01	4.18E-01	-2.39E+00	3.12E+01	7.45E+01
ARMCX2	9.58E-04	1.13E-01	2.97E-01	-3.37E+00	8.21E+00	2.76E+01
CCND1	9.64E-04	1.13E-01	2.92E-01	-3.42E+00	6.67E+00	2.28E+01
PILRB	1.02E-03	1.18E-01	4.46E-01	-2.24E+00	1.42E+02	3.19E+02
---	1.02E-03	1.18E-01	2.78E-01	-3.60E+00	8.11E+00	2.92E+01
ABCA7	1.04E-03	1.19E-01	4.82E-01	-2.07E+00	1.30E+02	2.69E+02
AKAP1-DT	1.12E-03	1.26E-01	2.95E-01	-3.39E+00	8.63E+00	2.92E+01
PPIAP19	1.12E-03	1.26E-01	2.98E-01	-3.35E+00	6.18E+00	2.07E+01
RN7SK	1.13E-03	1.26E-01	2.42E+00	2.42E+00	4.62E+01	1.91E+01
DCAF4	1.15E-03	1.27E-01	4.29E-01	-2.33E+00	3.47E+01	8.08E+01
LINC01220	1.18E-03	1.30E-01	3.57E-01	-2.80E+00	2.68E+01	7.51E+01
CA4	1.29E-03	1.35E-01	1.39E-01	-7.22E+00	1.22E+01	8.83E+01
ZNF441	1.29E-03	1.35E-01	4.55E-01	-2.20E+00	5.99E+01	1.32E+02
USP18	1.31E-03	1.35E-01	2.47E+00	2.47E+00	2.53E+02	1.02E+02
RPS3AP47	1.31E-03	1.35E-01	4.86E-01	-2.06E+00	2.67E+01	5.50E+01
NPIPA1	1.32E-03	1.35E-01	2.03E-01	-4.92E+00	1.61E+01	7.90E+01
FMNL1-DT	1.41E-03	1.42E-01	3.46E-01	-2.89E+00	3.13E+01	9.06E+01
CETP	1.46E-03	1.45E-01	2.04E-01	-4.90E+00	8.13E+00	3.98E+01
ADGRG3	1.47E-03	1.45E-01	1.53E-01	-6.56E+00	9.13E+01	5.98E+02
ZCWPW2	1.47E-03	1.45E-01	3.72E-01	-2.69E+00	8.06E+00	2.17E+01
SLC4A4	1.52E-03	1.46E-01	3.02E-01	-3.31E+00	1.60E+01	5.30E+01
---	1.63E-03	1.51E-01	2.93E-01	-3.42E+00	7.64E+00	2.61E+01
NPIPB13	1.64E-03	1.51E-01	3.04E-01	-3.28E+00	5.73E+01	1.88E+02
PTPRS	1.65E-03	1.51E-01	3.66E-01	-2.73E+00	1.47E+01	4.01E+01
RBPMS2	1.66E-03	1.51E-01	2.16E-01	-4.64E+00	1.31E+01	6.08E+01
RPL21P28	1.67E-03	1.51E-01	3.71E-01	-2.69E+00	2.70E+01	7.29E+01
HSD3B7	1.67E-03	1.51E-01	3.19E+00	3.19E+00	8.66E+01	2.72E+01
ZNF433	1.76E-03	1.55E-01	2.76E-01	-3.63E+00	1.18E+01	4.28E+01
CCR1	1.79E-03	1.56E-01	2.48E+00	2.48E+00	4.44E+03	1.79E+03
CHST10	1.95E-03	1.65E-01	4.09E-01	-2.44E+00	1.93E+01	4.71E+01
MIR3945HG	2.03E-03	1.69E-01	2.37E-01	-4.21E+00	2.36E+01	9.93E+01
ZNF582-DT	2.04E-03	1.69E-01	4.09E-01	-2.44E+00	1.12E+01	2.75E+01
SLX1B-SULT1A4	2.05E-03	1.69E-01	2.87E-01	-3.49E+00	8.12E+00	2.83E+01
PRKAG2-AS1	2.06E-03	1.69E-01	4.22E-01	-2.37E+00	3.21E+01	7.62E+01
CCDC122	2.07E-03	1.69E-01	3.83E-01	-2.61E+00	1.94E+01	5.08E+01

ZNF337-AS1	2.11E-03	1.70E-01	2.90E-01	-3.45E+00	1.31E+01	4.50E+01
LAMP5	2.11E-03	1.70E-01	4.34E-01	-2.31E+00	2.87E+01	6.61E+01
TMEM191C	2.15E-03	1.73E-01	3.74E-01	-2.67E+00	9.92E+00	2.65E+01
CAMKK1	2.22E-03	1.75E-01	3.33E-01	-3.00E+00	2.34E+01	7.03E+01
ZMAT1	2.22E-03	1.75E-01	3.65E-01	-2.74E+00	2.64E+01	7.24E+01
DAPK2	2.23E-03	1.75E-01	3.26E-01	-3.06E+00	6.24E+01	1.91E+02
TEC	2.23E-03	1.75E-01	4.24E-01	-2.36E+00	1.77E+01	4.17E+01
KCNE1	2.23E-03	1.75E-01	3.24E-01	-3.08E+00	3.29E+01	1.01E+02
IGKV1D-33	2.30E-03	1.78E-01	1.75E-01	-5.71E+00	1.34E+01	7.64E+01
SNHG26	2.33E-03	1.79E-01	3.49E-01	-2.86E+00	1.28E+01	3.66E+01
RPL13AP25	2.35E-03	1.80E-01	4.37E-01	-2.29E+00	4.55E+01	1.04E+02
ORM1	2.39E-03	1.81E-01	3.46E-01	-2.89E+00	6.72E+01	1.94E+02
RAP2C-AS1	2.39E-03	1.81E-01	4.64E-01	-2.15E+00	2.40E+01	5.18E+01
MMP11	2.40E-03	1.81E-01	3.21E-01	-3.12E+00	1.03E+01	3.22E+01
ZNF345	2.41E-03	1.81E-01	4.05E-01	-2.47E+00	3.46E+01	8.54E+01
ROPN1L	2.43E-03	1.82E-01	3.25E-01	-3.08E+00	3.69E+01	1.14E+02
ADGRL1	2.44E-03	1.82E-01	3.84E-01	-2.61E+00	1.62E+01	4.21E+01
ZNF680	2.46E-03	1.82E-01	4.42E-01	-2.26E+00	5.63E+01	1.27E+02
ARG1	2.52E-03	1.82E-01	1.39E-01	-7.22E+00	1.04E+02	7.51E+02
AHSA2P	2.59E-03	1.85E-01	3.34E-01	-3.00E+00	6.82E+01	2.04E+02
TP53INP2	2.60E-03	1.85E-01	3.84E-01	-2.61E+00	2.49E+01	6.48E+01
COBLL1	2.60E-03	1.85E-01	4.50E-01	-2.22E+00	8.44E+01	1.87E+02
PPP1R17	2.69E-03	1.91E-01	3.08E-01	-3.25E+00	2.38E+01	7.74E+01
LGALS3BP	2.83E-03	1.97E-01	2.49E+00	2.49E+00	1.13E+03	4.53E+02
ZCWPW1	2.84E-03	1.97E-01	4.80E-01	-2.08E+00	3.16E+01	6.59E+01
RASAL2	2.85E-03	1.97E-01	1.75E-01	-5.72E+00	5.54E+00	3.17E+01
---	2.89E-03	1.98E-01	2.65E-01	-3.77E+00	5.62E+00	2.12E+01
---	2.92E-03	1.98E-01	2.29E-01	-4.36E+00	6.55E+00	2.86E+01
---	2.97E-03	2.00E-01	2.09E-01	-4.78E+00	6.34E+00	3.03E+01
FLVCR1-DT	2.99E-03	2.00E-01	2.37E-01	-4.22E+00	1.48E+01	6.26E+01
CHD1-DT	3.04E-03	2.03E-01	3.71E-01	-2.70E+00	2.53E+01	6.83E+01
LINC02207	3.06E-03	2.03E-01	2.19E-01	-4.56E+00	3.56E+01	1.62E+02
---	3.09E-03	2.04E-01	2.19E-01	-4.57E+00	1.47E+01	6.71E+01
TSPOAP1	3.15E-03	2.07E-01	2.55E-01	-3.93E+00	2.16E+01	8.47E+01
NIPSNAP3B	3.21E-03	2.10E-01	3.23E-01	-3.10E+00	1.34E+01	4.14E+01
WHAMMP2	3.30E-03	2.13E-01	3.76E-01	-2.66E+00	9.49E+01	2.53E+02
ZNF284	3.36E-03	2.15E-01	3.89E-01	-2.57E+00	1.65E+01	4.25E+01
LAMTOR5-AS1	3.53E-03	2.23E-01	3.62E-01	-2.76E+00	7.76E+00	2.15E+01
CCNJL	3.56E-03	2.23E-01	1.64E-01	-6.10E+00	3.33E+01	2.03E+02
SLC25A15	3.56E-03	2.23E-01	4.94E-01	-2.03E+00	5.78E+01	1.17E+02
LINC02352	3.58E-03	2.23E-01	3.13E-01	-3.19E+00	6.38E+00	2.04E+01
TREML2	3.58E-03	2.23E-01	3.79E-01	-2.64E+00	9.62E+01	2.54E+02

FLT3	3.59E-03	2.23E-01	4.71E-01	-2.12E+00	1.23E+02	2.62E+02
---	3.71E-03	2.25E-01	2.83E-01	-3.53E+00	1.90E+01	6.73E+01
PLAGL2	3.79E-03	2.25E-01	2.03E+00	2.03E+00	6.65E+02	3.27E+02
MAP3K2-DT	3.79E-03	2.25E-01	4.27E-01	-2.34E+00	1.98E+01	4.64E+01
GASAL1	3.80E-03	2.25E-01	3.98E-01	-2.52E+00	1.19E+01	3.00E+01
ZNF8	3.80E-03	2.25E-01	4.98E-01	-2.01E+00	2.56E+01	5.14E+01
MME	3.81E-03	2.25E-01	1.18E-01	-8.47E+00	1.18E+02	9.99E+02
TTC16	3.83E-03	2.25E-01	3.45E-01	-2.90E+00	1.57E+01	4.55E+01
---	3.84E-03	2.25E-01	4.33E-01	-2.31E+00	1.24E+01	2.87E+01
---	3.86E-03	2.25E-01	2.54E-01	-3.94E+00	1.43E+01	5.64E+01
FCGR1A	3.97E-03	2.30E-01	2.36E+00	2.36E+00	1.44E+03	6.12E+02
PITPNA-AS1	3.97E-03	2.30E-01	3.16E-01	-3.17E+00	9.81E+00	3.11E+01
IL4I1	4.02E-03	2.32E-01	2.99E+00	2.99E+00	1.07E+02	3.57E+01
C1QB	4.06E-03	2.33E-01	2.37E+00	2.37E+00	4.14E+02	1.75E+02
RAMP1	4.13E-03	2.35E-01	3.57E-01	-2.80E+00	1.81E+01	5.06E+01
ALOX15B	4.15E-03	2.35E-01	1.35E-01	-7.42E+00	1.84E+01	1.36E+02
---	4.17E-03	2.35E-01	2.30E-01	-4.35E+00	2.35E+01	1.02E+02
---	4.26E-03	2.36E-01	2.80E-01	-3.57E+00	2.52E+01	8.99E+01
---	4.27E-03	2.36E-01	2.33E-01	-4.29E+00	8.01E+00	3.43E+01
---	4.27E-03	2.36E-01	3.28E-01	-3.05E+00	8.06E+00	2.46E+01
---	4.28E-03	2.36E-01	4.21E-01	-2.37E+00	3.58E+01	8.50E+01
ZNF439	4.37E-03	2.40E-01	3.50E-01	-2.85E+00	2.49E+01	7.12E+01
SERPING1	4.37E-03	2.40E-01	2.64E+00	2.64E+00	8.12E+02	3.08E+02
CCL3	4.49E-03	2.43E-01	1.29E-01	-7.76E+00	1.97E+02	1.53E+03
SCML1	4.53E-03	2.44E-01	3.59E-01	-2.79E+00	1.80E+01	5.02E+01
MTCO1P2	4.54E-03	2.44E-01	4.10E-01	-2.44E+00	1.44E+01	3.51E+01
---	4.57E-03	2.44E-01	3.86E-01	-2.59E+00	4.22E+01	1.09E+02
RUBCNL	4.64E-03	2.46E-01	4.85E-01	-2.06E+00	1.83E+02	3.77E+02
---	4.75E-03	2.49E-01	2.54E-01	-3.93E+00	6.47E+00	2.55E+01
---	4.92E-03	2.55E-01	3.38E-01	-2.96E+00	7.99E+00	2.36E+01
ZNF517	4.99E-03	2.55E-01	4.56E-01	-2.19E+00	1.07E+01	2.35E+01
MANSC1	5.07E-03	2.56E-01	1.93E-01	-5.18E+00	6.25E+01	3.23E+02
RPL9P32	5.08E-03	2.56E-01	2.95E-01	-3.40E+00	4.48E+00	1.52E+01
ARHGAP27P1-BPTFP1-KPNA2P3	5.11E-03	2.56E-01	2.51E-01	-3.99E+00	4.91E+00	1.96E+01
ALPL	5.12E-03	2.56E-01	9.93E-02	-1.01E+01	5.56E+01	5.60E+02
CXCL10	5.14E-03	2.56E-01	3.08E+00	3.08E+00	3.25E+02	1.05E+02
---	5.17E-03	2.56E-01	3.89E-01	-2.57E+00	1.55E+01	3.99E+01
CCL3L1	5.25E-03	2.56E-01	1.28E-01	-7.81E+00	6.59E+01	5.15E+02
---	5.27E-03	2.56E-01	3.10E-01	-3.23E+00	1.10E+01	3.55E+01
---	5.29E-03	2.56E-01	2.36E-01	-4.24E+00	1.72E+01	7.27E+01
ANKS3	5.29E-03	2.56E-01	4.76E-01	-2.10E+00	1.96E+01	4.12E+01

MTND5P11	5.45E-03	2.61E-01	4.99E-01	-2.00E+00	3.28E+01	6.58E+01
CHI3L1	5.48E-03	2.61E-01	1.66E-01	-6.01E+00	1.26E+02	7.55E+02
RPL11P3	5.52E-03	2.62E-01	3.92E-01	-2.55E+00	1.57E+01	4.02E+01
SLC20A1-DT	5.57E-03	2.63E-01	4.80E-01	-2.08E+00	1.36E+01	2.83E+01
IDI2-AS1	5.60E-03	2.63E-01	3.76E-01	-2.66E+00	1.11E+01	2.95E+01
CCDC30	5.65E-03	2.64E-01	3.89E-01	-2.57E+00	1.28E+01	3.30E+01
WWTR1	5.86E-03	2.72E-01	3.03E-01	-3.30E+00	4.49E+00	1.48E+01
CHKB-DT	5.91E-03	2.73E-01	3.90E-01	-2.57E+00	1.50E+01	3.85E+01
---	5.98E-03	2.74E-01	3.01E+00	3.01E+00	2.02E+01	6.70E+00
MTND6P4	6.02E-03	2.75E-01	4.90E-01	-2.04E+00	3.56E+01	7.28E+01
---	6.20E-03	2.81E-01	3.49E-01	-2.86E+00	1.16E+01	3.32E+01
LINC00239	6.26E-03	2.82E-01	3.36E-01	-2.97E+00	9.40E+00	2.80E+01
LILRA4	6.33E-03	2.82E-01	4.65E-01	-2.15E+00	1.48E+02	3.19E+02
MCF2L	6.33E-03	2.82E-01	3.39E-01	-2.95E+00	1.59E+01	4.68E+01
---	6.35E-03	2.82E-01	4.53E-01	-2.21E+00	8.23E+00	1.82E+01
---	6.54E-03	2.88E-01	2.40E+00	2.40E+00	3.30E+01	1.38E+01
RPSAP19	6.60E-03	2.89E-01	3.67E-01	-2.72E+00	2.38E+01	6.47E+01
ZNF607	6.62E-03	2.89E-01	4.28E-01	-2.34E+00	2.12E+01	4.95E+01
---	6.62E-03	2.89E-01	2.58E-01	-3.87E+00	1.45E+01	5.62E+01
PHOSPHO1	6.68E-03	2.90E-01	2.07E-01	-4.83E+00	7.56E+01	3.65E+02
PLGLB1	6.73E-03	2.90E-01	2.72E-01	-3.67E+00	8.87E+00	3.26E+01
GTF2IP20	6.76E-03	2.91E-01	2.27E-01	-4.40E+00	4.01E+00	1.76E+01
PGGHG	6.78E-03	2.91E-01	4.51E-01	-2.22E+00	6.10E+01	1.35E+02
VNN3P	6.80E-03	2.91E-01	2.88E-01	-3.48E+00	4.84E+01	1.68E+02
PDZD2	6.82E-03	2.91E-01	2.43E-01	-4.11E+00	6.27E+00	2.58E+01
GPR34	6.84E-03	2.91E-01	4.79E-01	-2.09E+00	1.06E+02	2.21E+02
FCGR3B	6.91E-03	2.93E-01	1.37E-01	-7.31E+00	7.74E+02	5.66E+03
CCDC13	6.97E-03	2.94E-01	3.86E-01	-2.59E+00	9.87E+00	2.56E+01
AMY2B	7.00E-03	2.94E-01	4.63E-01	-2.16E+00	1.99E+01	4.28E+01
ZNF425	7.03E-03	2.94E-01	2.44E-01	-4.10E+00	6.67E+00	2.73E+01
PIK3C2B	7.13E-03	2.97E-01	4.62E-01	-2.17E+00	2.07E+01	4.48E+01
ZNF155	7.17E-03	2.98E-01	3.78E-01	-2.65E+00	2.56E+01	6.78E+01
STXBP5-AS1	7.31E-03	3.02E-01	2.97E-01	-3.36E+00	1.73E+01	5.81E+01
MEGF6	7.35E-03	3.03E-01	3.81E-01	-2.62E+00	1.96E+01	5.13E+01
RPL9P7	7.42E-03	3.03E-01	2.73E-01	-3.66E+00	3.92E+00	1.43E+01
---	7.51E-03	3.04E-01	4.23E-01	-2.36E+00	2.67E+01	6.30E+01
NPIPP1	7.60E-03	3.04E-01	2.61E-01	-3.84E+00	7.42E+00	2.85E+01
---	7.66E-03	3.04E-01	2.08E-01	-4.80E+00	9.82E+00	4.72E+01
H2BC15	7.68E-03	3.04E-01	4.41E-01	-2.27E+00	2.22E+01	5.04E+01
ZNF37BP	7.70E-03	3.04E-01	4.31E-01	-2.32E+00	4.41E+01	1.02E+02
---	7.90E-03	3.08E-01	4.91E-01	-2.04E+00	1.46E+01	2.97E+01
PRMT5-AS1	8.14E-03	3.13E-01	3.32E-01	-3.01E+00	8.17E+00	2.46E+01
HJURP	8.34E-03	3.16E-01	3.22E-01	-3.10E+00	1.09E+01	3.38E+01

PMS2CL	8.45E-03	3.19E-01	3.30E-01	-3.03E+00	2.58E+01	7.81E+01
RASL11A	8.47E-03	3.19E-01	2.94E-01	-3.41E+00	4.91E+00	1.67E+01
ENHO	8.49E-03	3.19E-01	2.97E-01	-3.37E+00	2.12E+01	7.14E+01
---	8.55E-03	3.20E-01	3.75E-01	-2.67E+00	1.95E+01	5.20E+01
CMTM2	8.58E-03	3.20E-01	1.73E-01	-5.77E+00	1.58E+02	9.14E+02
EFHD2-AS1	8.60E-03	3.20E-01	3.60E-01	-2.78E+00	8.40E+00	2.33E+01
PPP4R3B-DT	8.69E-03	3.21E-01	4.83E-01	-2.07E+00	1.54E+01	3.18E+01
TOLLIP-DT	8.94E-03	3.29E-01	4.78E-01	-2.09E+00	2.39E+01	4.99E+01
ZNF552	9.06E-03	3.31E-01	4.49E-01	-2.23E+00	6.57E+01	1.46E+02
VPS13B-DT	9.14E-03	3.31E-01	4.29E-01	-2.33E+00	1.47E+01	3.43E+01
---	9.18E-03	3.31E-01	4.54E-01	-2.20E+00	3.25E+01	7.15E+01
---	9.21E-03	3.31E-01	4.77E-01	-2.09E+00	1.12E+02	2.35E+02
HERC5	9.26E-03	3.31E-01	2.10E+00	2.10E+00	6.26E+02	2.98E+02
NBPF10	9.42E-03	3.33E-01	4.90E-01	-2.04E+00	5.00E+01	1.02E+02
MRNIP-DT	9.45E-03	3.33E-01	3.63E-01	-2.76E+00	9.28E+00	2.56E+01
THBS1	9.47E-03	3.33E-01	1.85E-01	-5.41E+00	8.85E+02	4.79E+03
FZD6	9.57E-03	3.35E-01	4.51E-01	-2.22E+00	3.83E+01	8.50E+01
H3P13	9.70E-03	3.36E-01	4.01E-01	-2.49E+00	7.32E+00	1.82E+01
CDHR3	9.71E-03	3.36E-01	4.50E-01	-2.22E+00	1.24E+01	2.76E+01
SESN1	9.81E-03	3.36E-01	3.74E-01	-2.68E+00	2.55E+02	6.82E+02
CYP51A1P1	9.98E-03	3.38E-01	2.41E+00	2.41E+00	3.46E+01	1.44E+01
RNF227	9.99E-03	3.38E-01	4.99E-01	-2.00E+00	3.79E+01	7.60E+01
S100P	1.00E-02	3.38E-01	1.70E-01	-5.87E+00	1.36E+02	8.00E+02
RP9P	1.01E-02	3.38E-01	4.86E-01	-2.06E+00	1.20E+01	2.47E+01
---	1.02E-02	3.40E-01	2.11E-01	-4.74E+00	1.36E+01	6.42E+01
RGS5	1.02E-02	3.41E-01	3.50E-01	-2.85E+00	5.89E+00	1.68E+01
CXCR1	1.03E-02	3.43E-01	2.12E-01	-4.72E+00	3.06E+02	1.44E+03
---	1.04E-02	3.43E-01	2.82E-01	-3.55E+00	4.94E+00	1.75E+01
---	1.04E-02	3.43E-01	3.20E-01	-3.12E+00	3.73E+00	1.16E+01
KAZN	1.04E-02	3.43E-01	2.12E-01	-4.73E+00	5.77E+00	2.73E+01
CYP4F3	1.05E-02	3.44E-01	1.92E-01	-5.22E+00	1.02E+02	5.32E+02
RPL5P24	1.05E-02	3.45E-01	4.36E-01	-2.29E+00	1.15E+01	2.64E+01
L2HGDH	1.08E-02	3.49E-01	3.94E-01	-2.54E+00	1.99E+01	5.06E+01
XCL1	1.08E-02	3.49E-01	3.25E-01	-3.08E+00	1.66E+01	5.11E+01
FOXP1-IT1	1.09E-02	3.49E-01	2.95E-01	-3.39E+00	1.21E+01	4.09E+01
TNFRSF21	1.09E-02	3.50E-01	3.48E-01	-2.87E+00	4.32E+01	1.24E+02
SNORD3A	1.10E-02	3.50E-01	2.98E-01	-3.35E+00	3.27E+01	1.10E+02
SLC16A1-AS1	1.11E-02	3.53E-01	3.61E-01	-2.77E+00	2.07E+01	5.73E+01
---	1.11E-02	3.53E-01	4.61E-01	-2.17E+00	2.95E+01	6.39E+01
MTCO2P12	1.13E-02	3.55E-01	4.57E-01	-2.19E+00	1.03E+02	2.25E+02
---	1.15E-02	3.62E-01	2.82E-01	-3.54E+00	7.30E+00	2.59E+01
HLA-K	1.15E-02	3.62E-01	3.47E-01	-2.88E+00	5.39E+00	1.55E+01
---	1.16E-02	3.62E-01	4.68E-01	-2.14E+00	3.35E+02	7.16E+02

FAM21FP	1.16E-02	3.62E-01	4.41E-01	-2.27E+00	7.36E+00	1.67E+01
NSUN5P2	1.17E-02	3.62E-01	4.96E-01	-2.02E+00	2.22E+01	4.48E+01
RPL7P32	1.18E-02	3.66E-01	4.92E-01	-2.03E+00	1.68E+01	3.42E+01
MTCO2P2	1.19E-02	3.68E-01	4.83E-01	-2.07E+00	3.30E+01	6.83E+01
ZC3H12D	1.22E-02	3.73E-01	4.73E-01	-2.11E+00	3.20E+01	6.76E+01
MYL6P3	1.22E-02	3.73E-01	4.60E-01	-2.18E+00	1.76E+01	3.82E+01
PRLR	1.22E-02	3.73E-01	2.55E-01	-3.93E+00	6.01E+00	2.36E+01
CXCR2	1.24E-02	3.77E-01	2.21E-01	-4.52E+00	7.45E+02	3.37E+03
TWF2-DT	1.25E-02	3.77E-01	4.00E-01	-2.50E+00	8.65E+00	2.16E+01
MT-TS1	1.25E-02	3.77E-01	4.58E-01	-2.18E+00	3.28E+01	7.17E+01
WDR35	1.26E-02	3.79E-01	3.22E-01	-3.11E+00	2.71E+01	8.42E+01
ANKRD18EP	1.26E-02	3.79E-01	4.75E-01	-2.11E+00	2.40E+01	5.05E+01
ARHGAP11B-DT	1.28E-02	3.79E-01	4.07E-01	-2.46E+00	6.66E+00	1.64E+01
MEOX1	1.28E-02	3.80E-01	4.69E-01	-2.13E+00	2.24E+01	4.77E+01
LINC01135	1.30E-02	3.81E-01	3.67E-01	-2.72E+00	1.32E+01	3.59E+01
UFD1-AS1	1.31E-02	3.83E-01	3.08E-01	-3.25E+00	9.22E+00	3.00E+01
GUSBP2	1.32E-02	3.83E-01	3.65E-01	-2.74E+00	4.75E+00	1.30E+01
---	1.32E-02	3.83E-01	4.88E-01	-2.05E+00	2.03E+01	4.17E+01
POLG2	1.32E-02	3.84E-01	4.90E-01	-2.04E+00	3.38E+01	6.90E+01
PRAL	1.34E-02	3.88E-01	2.55E+00	2.55E+00	8.75E+01	3.43E+01
CKB	1.35E-02	3.88E-01	4.59E-01	-2.18E+00	6.10E+01	1.33E+02
---	1.35E-02	3.88E-01	3.23E-01	-3.09E+00	1.69E+01	5.23E+01
PDGFD	1.37E-02	3.90E-01	4.21E-01	-2.37E+00	1.29E+02	3.07E+02
GPR153	1.39E-02	3.94E-01	3.87E-01	-2.58E+00	1.89E+01	4.89E+01
SAP30-DT	1.39E-02	3.94E-01	4.47E-01	-2.24E+00	4.47E+01	1.00E+02
ITPKC	1.40E-02	3.95E-01	4.99E-01	-2.01E+00	1.02E+02	2.05E+02
PPM1H	1.40E-02	3.95E-01	4.38E-01	-2.28E+00	2.48E+01	5.66E+01
---	1.40E-02	3.95E-01	4.54E-01	-2.20E+00	2.15E+01	4.72E+01
---	1.41E-02	3.95E-01	3.51E-01	-2.85E+00	9.20E+00	2.62E+01
MISP3	1.45E-02	4.03E-01	4.88E-01	-2.05E+00	3.18E+01	6.52E+01
MIR23AHG	1.46E-02	4.04E-01	4.49E-01	-2.23E+00	1.99E+02	4.43E+02
PGLYRP1	1.48E-02	4.05E-01	2.31E-01	-4.33E+00	1.75E+02	7.56E+02
---	1.49E-02	4.05E-01	3.89E-01	-2.57E+00	8.74E+00	2.24E+01
DDX50P2	1.49E-02	4.05E-01	4.16E-01	-2.40E+00	6.63E+00	1.59E+01
THAP9	1.52E-02	4.11E-01	4.35E-01	-2.30E+00	1.71E+01	3.94E+01
---	1.52E-02	4.11E-01	2.85E-01	-3.51E+00	2.25E+01	7.89E+01
EEF1A1P8	1.53E-02	4.12E-01	4.10E-01	-2.44E+00	7.81E+00	1.90E+01
SPRY1	1.54E-02	4.12E-01	1.86E-01	-5.38E+00	2.38E+01	1.28E+02
RANBP20P	1.55E-02	4.12E-01	3.76E-01	-2.66E+00	4.76E+00	1.27E+01
RNF144B	1.55E-02	4.12E-01	4.10E-01	-2.44E+00	5.97E+02	1.46E+03
ADGRE3	1.55E-02	4.12E-01	4.76E-01	-2.10E+00	2.16E+02	4.55E+02
PRDM11	1.56E-02	4.13E-01	4.04E-01	-2.47E+00	1.40E+01	3.45E+01

PXYLP1	1.58E-02	4.15E-01	4.62E-01	-2.16E+00	9.40E+01	2.03E+02
TLR7	1.59E-02	4.17E-01	2.25E+00	2.25E+00	1.05E+03	4.67E+02
LINC01126	1.60E-02	4.17E-01	3.09E-01	-3.24E+00	6.51E+00	2.11E+01
KLHL17	1.60E-02	4.17E-01	4.02E-01	-2.49E+00	1.12E+01	2.80E+01
TIGD3	1.60E-02	4.17E-01	4.24E-01	-2.36E+00	2.66E+01	6.28E+01
---	1.60E-02	4.17E-01	3.74E-01	-2.67E+00	8.97E+00	2.40E+01
YES1	1.61E-02	4.17E-01	4.15E-01	-2.41E+00	2.82E+01	6.79E+01
SERPINE2	1.62E-02	4.19E-01	4.20E-01	-2.38E+00	3.94E+01	9.38E+01
COL9A2	1.64E-02	4.21E-01	4.89E-01	-2.04E+00	2.79E+01	5.69E+01
BACE2	1.65E-02	4.22E-01	3.96E-01	-2.52E+00	6.51E+01	1.64E+02
TAMALIN	1.65E-02	4.22E-01	3.51E-01	-2.85E+00	3.97E+01	1.13E+02
NRBF2P4	1.66E-02	4.22E-01	4.14E-01	-2.42E+00	7.73E+00	1.87E+01
SMG1P1	1.66E-02	4.23E-01	4.10E-01	-2.44E+00	8.44E+01	2.06E+02
PHC2	1.66E-02	4.23E-01	4.41E-01	-2.27E+00	1.73E+03	3.93E+03
---	1.69E-02	4.27E-01	2.74E-01	-3.65E+00	7.46E+00	2.72E+01
PFKFB2	1.71E-02	4.28E-01	3.77E-01	-2.65E+00	6.66E+01	1.76E+02
NBPF19	1.71E-02	4.28E-01	3.77E-01	-2.65E+00	7.66E+01	2.03E+02
ZNF837	1.72E-02	4.28E-01	4.73E-01	-2.11E+00	2.56E+01	5.41E+01
ECHDC3	1.73E-02	4.29E-01	3.52E-01	-2.84E+00	9.21E+01	2.61E+02
ZNF205	1.73E-02	4.29E-01	2.47E+00	2.47E+00	1.98E+01	8.02E+00
MMP25	1.74E-02	4.30E-01	3.43E-01	-2.92E+00	1.49E+02	4.36E+02
DNAJC3-DT	1.75E-02	4.32E-01	3.98E-01	-2.51E+00	3.14E+01	7.88E+01
CTSK	1.76E-02	4.32E-01	4.14E-01	-2.41E+00	1.80E+01	4.34E+01
KLRC4-KLRK1	1.76E-02	4.32E-01	4.32E-01	-2.31E+00	6.23E+01	1.44E+02
RPL3P6	1.77E-02	4.32E-01	4.35E-01	-2.30E+00	9.04E+00	2.08E+01
SEMA3F-AS1	1.77E-02	4.32E-01	3.62E-01	-2.76E+00	1.09E+01	3.02E+01
FAM157C	1.79E-02	4.33E-01	4.70E-01	-2.13E+00	2.79E+01	5.93E+01
AK1	1.79E-02	4.33E-01	3.32E-01	-3.01E+00	5.14E+00	1.55E+01
---	1.79E-02	4.33E-01	2.40E+00	2.40E+00	3.85E+01	1.61E+01
RPS4XP17	1.81E-02	4.34E-01	3.91E-01	-2.55E+00	8.00E+00	2.04E+01
RPL9P3	1.81E-02	4.34E-01	4.04E-01	-2.47E+00	8.31E+00	2.06E+01
DSC1	1.82E-02	4.35E-01	2.84E-01	-3.52E+00	1.80E+01	6.34E+01
---	1.82E-02	4.35E-01	3.58E-01	-2.79E+00	1.34E+01	3.75E+01
---	1.83E-02	4.36E-01	3.84E-01	-2.60E+00	1.70E+01	4.42E+01
PI4KAP2	1.85E-02	4.37E-01	4.90E-01	-2.04E+00	3.47E+01	7.09E+01
RPL23AP3	1.85E-02	4.37E-01	4.98E-01	-2.01E+00	1.30E+01	2.60E+01
NPIPA9	1.87E-02	4.38E-01	4.65E-01	-2.15E+00	3.07E+01	6.60E+01
---	1.88E-02	4.39E-01	3.66E-01	-2.73E+00	2.04E+01	5.57E+01
NUDT16-DT	1.89E-02	4.39E-01	2.70E-01	-3.70E+00	5.68E+00	2.10E+01
TBC1D16	1.90E-02	4.41E-01	4.01E-01	-2.50E+00	1.00E+01	2.50E+01
---	1.91E-02	4.41E-01	4.82E-01	-2.08E+00	1.59E+01	3.31E+01
SAP30	1.92E-02	4.41E-01	3.80E-01	-2.63E+00	5.45E+02	1.43E+03
TNFRSF14-	1.95E-02	4.43E-01	4.02E-01	-2.49E+00	1.33E+01	3.31E+01

AS1						
CEP250-AS1	1.96E-02	4.43E-01	4.40E-01	-2.27E+00	1.60E+01	3.64E+01
ZNF577	1.97E-02	4.44E-01	4.17E-01	-2.40E+00	2.56E+01	6.14E+01
FBXO36	1.98E-02	4.44E-01	3.13E-01	-3.19E+00	1.19E+01	3.79E+01
---	1.98E-02	4.44E-01	4.66E-01	-2.15E+00	1.33E+02	2.85E+02
SETD9	1.98E-02	4.44E-01	4.78E-01	-2.09E+00	4.69E+01	9.81E+01
H4-16	2.00E-02	4.46E-01	4.53E-01	-2.21E+00	1.97E+01	4.34E+01
RPL21P120	2.03E-02	4.51E-01	4.46E-01	-2.24E+00	1.58E+01	3.55E+01
HSPA4L	2.04E-02	4.51E-01	3.87E-01	-2.58E+00	6.29E+00	1.62E+01
LINC00957	2.04E-02	4.51E-01	4.73E-01	-2.11E+00	3.29E+01	6.96E+01
ZIK1	2.05E-02	4.51E-01	4.74E-01	-2.11E+00	3.68E+01	7.77E+01
MKKS	2.06E-02	4.51E-01	4.43E-01	-2.26E+00	8.41E+01	1.90E+02
ZNF665	2.07E-02	4.52E-01	4.56E-01	-2.19E+00	1.89E+01	4.14E+01
---	2.07E-02	4.52E-01	3.95E-01	-2.53E+00	1.10E+01	2.79E+01
GSTO2	2.08E-02	4.53E-01	4.22E-01	-2.37E+00	7.63E+00	1.81E+01
IFIT1	2.10E-02	4.55E-01	2.21E+00	2.21E+00	9.54E+02	4.31E+02
FBLN2	2.14E-02	4.59E-01	4.51E-01	-2.22E+00	1.14E+01	2.52E+01
---	2.14E-02	4.60E-01	4.60E-01	-2.18E+00	4.20E+01	9.13E+01
ZNF542P	2.15E-02	4.60E-01	4.65E-01	-2.15E+00	1.10E+02	2.38E+02
EFHC1	2.16E-02	4.61E-01	4.57E-01	-2.19E+00	3.26E+01	7.12E+01
SPINK2	2.16E-02	4.61E-01	3.42E-01	-2.93E+00	8.37E+00	2.45E+01
LIPC	2.16E-02	4.61E-01	4.46E-01	-2.24E+00	1.50E+01	3.36E+01
NRSN2	2.17E-02	4.62E-01	3.30E-01	-3.03E+00	1.17E+01	3.53E+01
PBX1	2.19E-02	4.63E-01	4.87E-01	-2.06E+00	6.80E+01	1.40E+02
LINC02432	2.20E-02	4.63E-01	4.83E-01	-2.07E+00	1.02E+02	2.11E+02
MCM10	2.21E-02	4.63E-01	2.62E+00	2.62E+00	6.59E+01	2.51E+01
HECW2	2.21E-02	4.63E-01	3.55E-01	-2.82E+00	1.83E+01	5.15E+01
---	2.24E-02	4.65E-01	3.55E-01	-2.82E+00	9.45E+00	2.66E+01
RPL18AP16	2.24E-02	4.65E-01	3.75E-01	-2.67E+00	6.20E+00	1.66E+01
KRT23	2.26E-02	4.67E-01	2.15E-01	-4.65E+00	5.15E+01	2.40E+02
SDHAP1	2.27E-02	4.67E-01	4.77E-01	-2.09E+00	3.56E+01	7.46E+01
NPIPB5	2.27E-02	4.67E-01	4.57E-01	-2.19E+00	1.89E+02	4.12E+02
CHIC1	2.28E-02	4.67E-01	4.48E-01	-2.23E+00	3.29E+01	7.35E+01
APBB3	2.29E-02	4.68E-01	4.57E-01	-2.19E+00	3.02E+01	6.61E+01
---	2.30E-02	4.69E-01	3.07E-01	-3.25E+00	2.26E+01	7.36E+01
GRAMD2B	2.31E-02	4.69E-01	4.81E-01	-2.08E+00	5.88E+01	1.22E+02
PRTN3	2.32E-02	4.70E-01	2.26E-01	-4.42E+00	4.21E+01	1.86E+02
KRT8P12	2.33E-02	4.71E-01	4.73E-01	-2.11E+00	1.76E+01	3.72E+01
RPL31P2	2.34E-02	4.72E-01	4.40E-01	-2.27E+00	2.09E+01	4.76E+01
AGAP1	2.34E-02	4.72E-01	3.42E-01	-2.93E+00	1.52E+01	4.44E+01
FAM157A	2.36E-02	4.72E-01	2.41E-01	-4.15E+00	9.30E+00	3.87E+01
PTGFRN	2.36E-02	4.72E-01	2.52E+00	2.52E+00	4.73E+01	1.88E+01
---	2.37E-02	4.73E-01	3.77E-01	-2.65E+00	6.01E+00	1.59E+01

CPLANE1	2.40E-02	4.78E-01	4.79E-01	-2.09E+00	3.75E+01	7.83E+01
GVQW3	2.42E-02	4.79E-01	3.85E-01	-2.60E+00	1.06E+01	2.76E+01
PDCD6P1	2.43E-02	4.80E-01	4.22E-01	-2.37E+00	9.95E+01	2.36E+02
TPT1P6	2.46E-02	4.81E-01	4.96E-01	-2.02E+00	1.58E+01	3.18E+01
---	2.52E-02	4.90E-01	3.59E-01	-2.79E+00	4.41E+00	1.23E+01
APLF	2.56E-02	4.95E-01	4.44E-01	-2.25E+00	4.46E+01	1.00E+02
---	2.57E-02	4.95E-01	4.35E-01	-2.30E+00	2.99E+01	6.89E+01
---	2.58E-02	4.96E-01	4.51E-01	-2.22E+00	6.24E+00	1.38E+01
---	2.59E-02	4.97E-01	4.73E-01	-2.11E+00	3.84E+01	8.12E+01
PARD6B	2.59E-02	4.97E-01	3.40E-01	-2.94E+00	1.70E+01	5.00E+01
CCR5	2.60E-02	4.98E-01	2.02E+00	2.02E+00	2.44E+02	1.21E+02
ITGA6-AS1	2.63E-02	4.99E-01	4.46E-01	-2.24E+00	1.27E+01	2.85E+01
ITLN1	2.66E-02	5.00E-01	3.78E-01	-2.64E+00	1.20E+01	3.16E+01
---	2.66E-02	5.00E-01	4.03E-01	-2.48E+00	4.66E+00	1.16E+01
---	2.66E-02	5.00E-01	4.76E-01	-2.10E+00	1.30E+01	2.72E+01
RPL14P3	2.67E-02	5.00E-01	4.88E-01	-2.05E+00	1.47E+01	3.02E+01
C1R	2.72E-02	5.06E-01	4.53E-01	-2.21E+00	1.24E+01	2.74E+01
SORL1-AS1	2.76E-02	5.07E-01	3.92E-01	-2.55E+00	6.93E+00	1.77E+01
---	2.78E-02	5.07E-01	3.57E-01	-2.80E+00	1.43E+01	3.99E+01
---	2.78E-02	5.07E-01	4.40E-01	-2.27E+00	1.25E+01	2.83E+01
---	2.79E-02	5.07E-01	3.42E-01	-2.93E+00	4.20E+00	1.23E+01
PTPN13	2.79E-02	5.07E-01	4.07E-01	-2.46E+00	1.41E+01	3.46E+01
HILPDA	2.80E-02	5.07E-01	4.19E-01	-2.39E+00	2.00E+01	4.78E+01
ZNRF2P1	2.81E-02	5.07E-01	3.06E-01	-3.27E+00	3.33E+00	1.09E+01
---	2.82E-02	5.07E-01	3.51E-01	-2.85E+00	3.01E+01	8.58E+01
DTHD1	2.83E-02	5.07E-01	4.29E-01	-2.33E+00	6.10E+01	1.42E+02
MTCO1P40	2.85E-02	5.07E-01	4.99E-01	-2.00E+00	5.47E+01	1.10E+02
CCDC157	2.85E-02	5.07E-01	3.66E-01	-2.73E+00	1.07E+01	2.91E+01
LTBP2	2.85E-02	5.07E-01	4.58E-01	-2.19E+00	9.54E+00	2.09E+01
CALCRL	2.85E-02	5.07E-01	3.49E-01	-2.87E+00	4.02E+01	1.15E+02
IFI27	2.91E-02	5.11E-01	4.74E+00	4.74E+00	1.57E+02	3.30E+01
RPL7P26	2.91E-02	5.11E-01	4.04E-01	-2.47E+00	7.04E+00	1.74E+01
ZNF773	2.95E-02	5.13E-01	4.76E-01	-2.10E+00	4.69E+01	9.85E+01
---	2.95E-02	5.13E-01	1.14E-01	-8.75E+00	5.38E+02	4.71E+03
LOH12CR2	2.96E-02	5.13E-01	4.95E-01	-2.02E+00	1.11E+01	2.24E+01
---	2.96E-02	5.13E-01	3.37E-01	-2.97E+00	9.65E+00	2.86E+01
RPL23AP18	2.96E-02	5.13E-01	4.87E-01	-2.06E+00	1.03E+01	2.13E+01
MCPH1-AS1	2.97E-02	5.13E-01	4.77E-01	-2.10E+00	2.89E+01	6.06E+01
KCNJ2-AS1	2.97E-02	5.13E-01	4.20E-01	-2.38E+00	1.73E+01	4.13E+01
LINC00211	2.97E-02	5.13E-01	4.24E-01	-2.36E+00	3.05E+01	7.18E+01
---	2.99E-02	5.14E-01	4.57E-01	-2.19E+00	3.67E+01	8.02E+01
TNFRSF10C	3.00E-02	5.15E-01	2.97E-01	-3.36E+00	3.22E+02	1.08E+03
LINC01004	3.00E-02	5.15E-01	4.67E-01	-2.14E+00	3.61E+01	7.73E+01

IGHV4-4	3.02E-02	5.16E-01	3.45E-01	-2.89E+00	3.68E+01	1.07E+02
ANXA3	3.02E-02	5.16E-01	3.04E-01	-3.28E+00	3.26E+02	1.07E+03
---	3.07E-02	5.20E-01	4.33E-01	-2.31E+00	3.65E+01	8.44E+01
RPL10P12	3.10E-02	5.20E-01	4.94E-01	-2.02E+00	1.01E+01	2.05E+01
KNDC1	3.11E-02	5.20E-01	3.27E-01	-3.06E+00	1.04E+01	3.19E+01
OLR1	3.11E-02	5.20E-01	1.80E-01	-5.56E+00	3.24E+01	1.80E+02
---	3.13E-02	5.20E-01	4.42E-01	-2.26E+00	3.09E+01	7.01E+01
TMSB4Y	3.13E-02	5.20E-01	3.11E-01	-3.21E+00	2.71E+01	8.72E+01
---	3.14E-02	5.20E-01	4.40E-01	-2.27E+00	1.04E+02	2.37E+02
---	3.15E-02	5.22E-01	4.65E-01	-2.15E+00	7.66E+00	1.65E+01
RHEBP2	3.19E-02	5.24E-01	4.74E-01	-2.11E+00	3.94E+01	8.32E+01
NBPF25P	3.19E-02	5.24E-01	3.87E-01	-2.59E+00	5.12E+00	1.32E+01
ZNF66	3.21E-02	5.24E-01	4.97E-01	-2.01E+00	2.21E+01	4.46E+01
DOCK9-DT	3.21E-02	5.24E-01	3.82E-01	-2.62E+00	9.20E+00	2.41E+01
GPRC5C	3.21E-02	5.24E-01	3.74E-01	-2.68E+00	6.27E+00	1.68E+01
RFX2	3.21E-02	5.24E-01	4.93E-01	-2.03E+00	7.05E+01	1.43E+02
SMPD4BP	3.22E-02	5.24E-01	4.17E-01	-2.40E+00	3.59E+01	8.60E+01
H3P43	3.22E-02	5.24E-01	3.59E-01	-2.79E+00	4.99E+00	1.39E+01
---	3.24E-02	5.25E-01	4.15E-01	-2.41E+00	8.01E+00	1.93E+01
---	3.26E-02	5.25E-01	4.72E-01	-2.12E+00	1.52E+01	3.22E+01
---	3.26E-02	5.25E-01	4.44E-01	-2.25E+00	1.39E+01	3.14E+01
SLC30A6-DT	3.30E-02	5.25E-01	3.92E-01	-2.55E+00	8.01E+00	2.04E+01
LINC01150	3.30E-02	5.25E-01	4.06E-01	-2.46E+00	6.67E+00	1.64E+01
DRAXIN	3.31E-02	5.25E-01	4.13E-01	-2.42E+00	1.80E+01	4.36E+01
---	3.35E-02	5.28E-01	3.72E-01	-2.68E+00	9.52E+00	2.56E+01
CDK5R1	3.37E-02	5.30E-01	4.00E-01	-2.50E+00	1.02E+02	2.56E+02
EPN2	3.38E-02	5.31E-01	4.52E-01	-2.21E+00	1.34E+01	2.95E+01
NBPF8	3.39E-02	5.32E-01	4.91E-01	-2.03E+00	4.99E+01	1.01E+02
ZNF781	3.42E-02	5.35E-01	5.00E-01	-2.00E+00	1.99E+01	3.98E+01
---	3.49E-02	5.42E-01	3.95E-01	-2.53E+00	2.41E+01	6.09E+01
IFITM3P9	3.49E-02	5.42E-01	3.42E-01	-2.93E+00	5.64E+00	1.65E+01
GPR150	3.49E-02	5.42E-01	4.22E-01	-2.37E+00	1.80E+01	4.26E+01
BMERB1	3.50E-02	5.43E-01	4.46E-01	-2.24E+00	2.19E+01	4.91E+01
PVALB	3.52E-02	5.43E-01	3.15E-01	-3.18E+00	2.75E+01	8.73E+01
DAGLA	3.52E-02	5.43E-01	4.25E-01	-2.35E+00	1.41E+01	3.31E+01
RPS6P26	3.53E-02	5.43E-01	4.84E-01	-2.07E+00	8.94E+00	1.85E+01
OBSCN	3.54E-02	5.43E-01	4.07E-01	-2.46E+00	2.07E+01	5.08E+01
---	3.56E-02	5.44E-01	4.02E-01	-2.49E+00	4.97E+00	1.24E+01
---	3.56E-02	5.44E-01	4.02E-01	-2.49E+00	4.97E+00	1.24E+01
KLF9	3.57E-02	5.45E-01	4.55E-01	-2.20E+00	1.77E+02	3.89E+02
---	3.58E-02	5.45E-01	4.84E-01	-2.06E+00	2.82E+01	5.82E+01
TOX2	3.58E-02	5.45E-01	4.66E-01	-2.14E+00	2.03E+01	4.36E+01
TEX54	3.64E-02	5.46E-01	3.93E-01	-2.54E+00	6.93E+00	1.76E+01

NPIPB4	3.66E-02	5.46E-01	3.92E-01	-2.55E+00	1.91E+01	4.86E+01
CTSG	3.69E-02	5.46E-01	2.44E-01	-4.10E+00	8.43E+01	3.45E+02
POU6F1	3.70E-02	5.46E-01	4.48E-01	-2.23E+00	1.79E+01	4.00E+01
---	3.70E-02	5.46E-01	4.35E-01	-2.30E+00	6.98E+00	1.60E+01
FRG1DP	3.71E-02	5.46E-01	3.96E-01	-2.53E+00	3.92E+00	9.92E+00
NR6A1	3.72E-02	5.46E-01	3.77E-01	-2.65E+00	4.91E+00	1.30E+01
NLRP6	3.76E-02	5.49E-01	3.80E-01	-2.63E+00	2.45E+01	6.46E+01
H2BC4	3.82E-02	5.54E-01	4.83E-01	-2.07E+00	1.14E+02	2.36E+02
LINC00513	3.87E-02	5.58E-01	3.28E-01	-3.05E+00	6.68E+00	2.04E+01
TPI1P2	3.87E-02	5.58E-01	4.56E-01	-2.19E+00	8.35E+00	1.83E+01
HS3ST1	3.94E-02	5.61E-01	3.62E-01	-2.76E+00	1.02E+01	2.83E+01
TPSB2	3.99E-02	5.65E-01	3.62E-01	-2.76E+00	6.97E+00	1.92E+01
CRISP3	3.99E-02	5.65E-01	2.42E-01	-4.12E+00	2.43E+02	1.00E+03
TMEM263-DT	4.05E-02	5.68E-01	4.47E-01	-2.24E+00	1.22E+01	2.73E+01
ANKRD36BP2	4.05E-02	5.68E-01	3.88E-01	-2.58E+00	2.07E+01	5.34E+01
KLRC4	4.11E-02	5.71E-01	4.33E-01	-2.31E+00	2.23E+01	5.15E+01
FOXM1	4.12E-02	5.71E-01	2.04E+00	2.04E+00	5.17E+01	2.54E+01
ANKDD1B	4.13E-02	5.71E-01	3.24E-01	-3.09E+00	7.05E+00	2.17E+01
GOLM2P1	4.14E-02	5.71E-01	4.27E-01	-2.34E+00	5.82E+00	1.36E+01
CLDN5	4.15E-02	5.71E-01	4.80E-01	-2.08E+00	1.83E+02	3.81E+02
SCOC-AS1	4.20E-02	5.72E-01	4.30E-01	-2.33E+00	7.28E+00	1.69E+01
IGHV3-73	4.21E-02	5.72E-01	4.63E-01	-2.16E+00	4.64E+01	1.00E+02
---	4.24E-02	5.75E-01	4.72E-01	-2.12E+00	1.68E+01	3.57E+01
SLC25A6P2	4.26E-02	5.76E-01	4.69E-01	-2.13E+00	6.94E+00	1.48E+01
ZEB2-AS1	4.28E-02	5.76E-01	4.69E-01	-2.13E+00	4.22E+01	8.99E+01
XPC-AS1	4.28E-02	5.76E-01	4.13E-01	-2.42E+00	7.83E+00	1.89E+01
NCR1	4.34E-02	5.79E-01	4.63E-01	-2.16E+00	7.02E+01	1.52E+02
BDNF-AS	4.35E-02	5.79E-01	4.87E-01	-2.05E+00	1.05E+01	2.15E+01
KLRC3	4.35E-02	5.79E-01	3.72E-01	-2.69E+00	3.96E+01	1.07E+02
RSKR	4.37E-02	5.80E-01	3.69E-01	-2.71E+00	6.47E+00	1.75E+01
LGR6	4.41E-02	5.83E-01	4.83E-01	-2.07E+00	7.76E+01	1.61E+02
TPM2	4.45E-02	5.86E-01	4.99E-01	-2.00E+00	1.84E+01	3.68E+01
TRABD-AS1	4.49E-02	5.87E-01	3.54E-01	-2.82E+00	3.97E+00	1.12E+01
MTND6P22	4.55E-02	5.90E-01	4.70E-01	-2.13E+00	7.52E+00	1.60E+01
NFYC-AS1	4.59E-02	5.91E-01	4.79E-01	-2.09E+00	1.41E+01	2.94E+01
CCDC163	4.60E-02	5.91E-01	4.45E-01	-2.25E+00	2.17E+01	4.88E+01
TXNP5	4.63E-02	5.93E-01	4.45E-01	-2.25E+00	6.53E+00	1.47E+01
ZNF687-AS1	4.65E-02	5.94E-01	4.47E-01	-2.24E+00	7.90E+00	1.77E+01
---	4.66E-02	5.95E-01	2.99E-01	-3.34E+00	8.49E+00	2.84E+01
MGAM	4.68E-02	5.96E-01	3.22E-01	-3.11E+00	1.33E+02	4.12E+02
---	4.68E-02	5.96E-01	4.60E-01	-2.18E+00	2.56E+01	5.57E+01

ZFP30	4.68E-02	5.96E-01	3.86E-01	-2.59E+00	1.28E+01	3.30E+01
CBR3-AS1	4.70E-02	5.97E-01	4.52E-01	-2.21E+00	1.81E+01	4.00E+01
---	4.71E-02	5.97E-01	4.58E-01	-2.19E+00	2.18E+01	4.77E+01
---	4.79E-02	6.03E-01	3.90E-01	-2.56E+00	1.45E+01	3.71E+01
SERPINF2	4.79E-02	6.03E-01	4.34E-01	-2.30E+00	1.58E+01	3.65E+01
EFNA5	4.87E-02	6.07E-01	3.05E-01	-3.28E+00	6.51E+00	2.14E+01
---	4.92E-02	6.07E-01	3.25E-01	-3.08E+00	6.78E+00	2.09E+01
RSAD2	4.92E-02	6.07E-01	2.17E+00	2.17E+00	7.64E+02	3.51E+02
HCAR3	4.97E-02	6.09E-01	4.12E-01	-2.43E+00	1.20E+02	2.91E+02

13.7 DIFFERENTIAL GENE EXPRESSION OF T CELL SPECIFIC GENES

Gene name	P-value (Postoperative vs Preoperative)	FDR step up (Postoperative vs Preoperative)	Ratio (Postoperative vs Preoperative)	Fold change (Postoperative vs Preoperative)	LSMean(Postoperative) (Postoperative vs Preoperative)	LSMean(Preoperative) (Postoperative vs Preoperative)
GPR89A	1.37E-04	4.69E-02	5.87E-01	-1.70E+00	1.79E+02	3.06E+02
FBXO38	1.87E-03	1.60E-01	6.44E-01	-1.55E+00	2.67E+02	4.14E+02
ARG1	2.52E-03	1.82E-01	1.39E-01	-7.22E+00	1.04E+02	7.51E+02
TREML2	3.58E-03	2.23E-01	3.79E-01	-2.64E+00	9.62E+01	2.54E+02
IL4I1	4.02E-03	2.32E-01	2.99E+00	2.99E+00	1.07E+02	3.57E+01
CD1C	4.12E-03	2.35E-01	5.36E-01	-1.87E+00	3.13E+02	5.85E+02
CASP8	7.58E-03	3.04E-01	7.36E-01	-1.36E+00	1.24E+03	1.69E+03
XCL1	1.08E-02	3.49E-01	3.25E-01	-3.08E+00	1.66E+01	5.11E+01
LGALS9	1.84E-02	4.37E-01	1.33E+00	1.33E+00	2.06E+03	1.55E+03
CCR2	2.46E-02	4.81E-01	1.81E+00	1.81E+00	3.85E+03	2.12E+03
ARID5A	2.62E-02	4.99E-01	6.72E-01	-1.49E+00	8.41E+02	1.25E+03
ZFPM1	2.81E-02	5.07E-01	6.32E-01	-1.58E+00	4.75E+01	7.51E+01
ARMC5	3.65E-02	5.46E-01	7.22E-01	-1.39E+00	9.97E+01	1.38E+02
CD55	4.02E-02	5.67E-01	6.45E-01	-1.55E+00	2.77E+03	4.30E+03
ERBB2	4.14E-02	5.71E-01	5.58E-01	-1.79E+00	7.34E+01	1.32E+02
CBLB	4.28E-02	5.76E-01	6.34E-01	-1.58E+00	4.15E+02	6.55E+02
SLC11A1	4.32E-02	5.78E-01	7.34E-01	-1.36E+00	1.68E+03	2.29E+03
RC3H2	4.36E-02	5.79E-01	8.01E-01	-1.25E+00	6.44E+02	8.03E+02
TNFSF13B	4.59E-02	5.91E-01	1.33E+00	1.33E+00	4.26E+03	3.20E+03
BCL3	4.71E-02	5.97E-01	1.72E+00	1.72E+00	1.07E+03	6.21E+02
RSAD2	4.92E-02	6.07E-01	2.17E+00	2.17E+00	7.64E+02	3.51E+02
SOX4	5.05E-02	6.14E-01	7.24E-01	-1.38E+00	4.65E+02	6.43E+02
ZFP36L2	5.29E-02	6.22E-01	6.44E-01	-1.55E+00	1.50E+04	2.32E+04

HSPD1	5.37E-02	6.22E-01	1.25E+00	1.25E+00	1.84E+03	1.48E+03
IL18R1	6.19E-02	6.50E-01	5.81E-01	-1.72E+00	2.01E+02	3.45E+02
NCKAP1L	6.20E-02	6.50E-01	1.23E+00	1.23E+00	4.02E+03	3.27E+03
FGL2	6.23E-02	6.52E-01	1.50E+00	1.50E+00	1.74E+04	1.16E+04
JAK3	6.96E-02	6.69E-01	1.40E+00	1.40E+00	1.98E+03	1.42E+03
KLRD1	7.37E-02	6.76E-01	5.66E-01	-1.77E+00	2.36E+03	4.17E+03
TNFRSF4	7.54E-02	6.81E-01	1.46E+00	1.46E+00	8.32E+01	5.69E+01
EOMES	7.72E-02	6.82E-01	6.24E-01	-1.60E+00	4.84E+02	7.77E+02
FADD	8.40E-02	6.94E-01	7.30E-01	-1.37E+00	2.90E+02	3.97E+02
CTNNB1	9.25E-02	7.09E-01	1.29E+00	1.29E+00	1.57E+03	1.22E+03
TLE1	9.49E-02	7.11E-01	5.11E-01	-1.96E+00	2.64E+02	5.17E+02
TOX	1.01E-01	7.20E-01	6.67E-01	-1.50E+00	2.69E+02	4.03E+02
EIF2AK4	1.09E-01	7.34E-01	8.05E-01	-1.24E+00	4.41E+02	5.47E+02
CD28	1.16E-01	7.50E-01	1.39E+00	1.39E+00	6.13E+02	4.42E+02
HLA-DRB1	1.23E-01	7.56E-01	1.38E+00	1.38E+00	2.24E+04	1.62E+04
TRGV9	1.28E-01	7.56E-01	5.50E-01	-1.82E+00	8.69E+01	1.58E+02
AZI2	1.29E-01	7.57E-01	1.16E+00	1.16E+00	1.46E+03	1.25E+03
CCR7	1.29E-01	7.57E-01	6.16E-01	-1.62E+00	2.91E+03	4.73E+03
ICAM1	1.31E-01	7.62E-01	1.51E+00	1.51E+00	1.16E+03	7.72E+02
RELB	1.33E-01	7.66E-01	1.36E+00	1.36E+00	4.97E+02	3.66E+02
ZFP36L1	1.36E-01	7.69E-01	1.53E+00	1.53E+00	4.19E+03	2.74E+03
GZMB	1.36E-01	7.69E-01	6.11E-01	-1.64E+00	2.40E+03	3.93E+03
CEACAM1	1.41E-01	7.70E-01	5.81E-01	-1.72E+00	1.60E+02	2.75E+02
CHD7	1.45E-01	7.76E-01	6.77E-01	-1.48E+00	3.12E+02	4.61E+02
TBX21	1.58E-01	7.85E-01	6.31E-01	-1.59E+00	8.04E+02	1.28E+03
TRAV8-1	1.59E-01	7.87E-01	1.47E+00	1.47E+00	4.99E+01	3.40E+01
MICB	1.61E-01	7.89E-01	1.43E+00	1.43E+00	3.69E+02	2.58E+02
ZAP70	1.62E-01	7.90E-01	7.46E-01	-1.34E+00	9.61E+02	1.29E+03
TRBV28	1.68E-01	7.97E-01	1.49E+00	1.49E+00	1.66E+02	1.11E+02
TRAV25	1.72E-01	8.04E-01	5.53E-01	-1.81E+00	1.00E+01	1.81E+01
TRBV10-3	1.78E-01	8.07E-01	1.37E+00	1.37E+00	5.28E+01	3.86E+01
RABL3	1.88E-01	8.12E-01	1.19E+00	1.19E+00	6.49E+02	5.44E+02
GPAM	1.88E-01	8.12E-01	5.96E-01	-1.68E+00	2.95E+01	4.95E+01
TRAV8-6	1.90E-01	8.15E-01	1.42E+00	1.42E+00	7.01E+01	4.92E+01
TRAV8-4	1.96E-01	8.23E-01	1.49E+00	1.49E+00	8.17E+01	5.49E+01
FCER1G	2.04E-01	8.30E-01	1.24E+00	1.24E+00	1.86E+04	1.51E+04
CLEC4E	2.11E-01	8.34E-01	6.41E-01	-1.56E+00	1.41E+03	2.20E+03
TRDV1	2.12E-01	8.34E-01	4.43E-01	-2.26E+00	2.96E+01	6.68E+01
IRF1	2.14E-01	8.35E-01	1.38E+00	1.38E+00	6.17E+03	4.47E+03
PTPN2	2.17E-01	8.37E-01	1.17E+00	1.17E+00	1.52E+03	1.30E+03

TRAV1-2	2.19E-01	8.39E-01	1.47E+00	1.47E+00	4.14E+01	2.80E+01
STX7	2.21E-01	8.39E-01	1.18E+00	1.18E+00	1.94E+03	1.65E+03
SMAD3	2.23E-01	8.39E-01	1.19E+00	1.19E+00	5.34E+02	4.47E+02
TRAV5	2.23E-01	8.39E-01	1.41E+00	1.41E+00	4.76E+01	3.38E+01
CD99	2.24E-01	8.41E-01	8.49E-01	-1.18E+00	4.67E+03	5.50E+03
PTGER4	2.24E-01	8.41E-01	7.90E-01	-1.27E+00	9.77E+02	1.24E+03
CRTAM	2.24E-01	8.41E-01	6.85E-01	-1.46E+00	1.91E+02	2.79E+02
KDELR1	2.27E-01	8.44E-01	1.18E+00	1.18E+00	8.62E+02	7.33E+02
CD83	2.29E-01	8.45E-01	1.42E+00	1.42E+00	5.01E+02	3.53E+02
TRBV27	2.31E-01	8.46E-01	1.48E+00	1.48E+00	1.43E+02	9.64E+01
ENTPD7	2.31E-01	8.46E-01	7.79E-01	-1.28E+00	7.71E+01	9.90E+01
CD4	2.34E-01	8.48E-01	1.21E+00	1.21E+00	6.46E+03	5.33E+03
SEMA4A	2.37E-01	8.50E-01	1.16E+00	1.16E+00	2.72E+03	2.34E+03
IL2RA	2.38E-01	8.51E-01	6.75E-01	-1.48E+00	1.25E+02	1.85E+02
RARA	2.41E-01	8.52E-01	1.20E+00	1.20E+00	9.02E+02	7.51E+02
NCK2	2.41E-01	8.52E-01	7.64E-01	-1.31E+00	1.42E+03	1.86E+03
CBFB	2.44E-01	8.52E-01	1.11E+00	1.11E+00	3.57E+03	3.22E+03
CD44	2.50E-01	8.55E-01	1.17E+00	1.17E+00	1.50E+04	1.28E+04
ITK	2.51E-01	8.55E-01	6.90E-01	-1.45E+00	1.24E+03	1.80E+03
CD151	2.54E-01	8.61E-01	1.28E+00	1.28E+00	9.42E+02	7.38E+02
TRAV13-2	2.56E-01	8.62E-01	1.35E+00	1.35E+00	6.48E+01	4.79E+01
TRAF2	2.66E-01	8.68E-01	7.99E-01	-1.25E+00	1.44E+02	1.80E+02
SRGN	2.67E-01	8.68E-01	8.34E-01	-1.20E+00	3.19E+04	3.83E+04
SKAP1	2.67E-01	8.68E-01	8.43E-01	-1.19E+00	9.54E+02	1.13E+03
ICOSLG	2.68E-01	8.68E-01	7.27E-01	-1.37E+00	4.58E+01	6.30E+01
CLEC7A	2.69E-01	8.68E-01	1.18E+00	1.18E+00	2.40E+03	2.04E+03
PREX1	2.69E-01	8.68E-01	8.24E-01	-1.21E+00	2.46E+03	2.98E+03
PRKCZ	2.72E-01	8.71E-01	8.32E-01	-1.20E+00	7.88E+01	9.48E+01
IRF4	2.73E-01	8.71E-01	8.10E-01	-1.23E+00	3.64E+02	4.50E+02
TNFAIP8L2	2.75E-01	8.72E-01	1.28E+00	1.28E+00	8.06E+02	6.29E+02
ATG5	2.75E-01	8.72E-01	1.12E+00	1.12E+00	9.39E+02	8.40E+02
HLA-DMB	2.75E-01	8.72E-01	1.23E+00	1.23E+00	4.22E+03	3.45E+03
BCL9	2.78E-01	8.73E-01	1.42E+00	1.42E+00	9.77E+01	6.87E+01
CD247	2.78E-01	8.74E-01	7.67E-01	-1.30E+00	2.52E+03	3.28E+03
RUNX1	2.83E-01	8.77E-01	1.27E+00	1.27E+00	9.60E+02	7.59E+02
TNFSF4	2.90E-01	8.80E-01	7.56E-01	-1.32E+00	1.81E+02	2.39E+02
NCAPH2	2.94E-01	8.84E-01	1.14E+00	1.14E+00	3.77E+02	3.31E+02
PRKDC	2.96E-01	8.84E-01	8.73E-01	-1.15E+00	9.40E+02	1.08E+03
LIG4	2.96E-01	8.84E-01	1.18E+00	1.18E+00	2.97E+02	2.51E+02
TRBV20-1	3.04E-01	8.86E-01	1.25E+00	1.25E+00	2.57E+02	2.05E+02

TRBV4-1	3.06E-01	8.87E-01	1.35E+00	1.35E+00	9.26E+01	6.86E+01
RHOA	3.07E-01	8.87E-01	1.09E+00	1.09E+00	2.48E+04	2.28E+04
FKBP1A	3.09E-01	8.87E-01	1.13E+00	1.13E+00	3.43E+03	3.04E+03
TRBV14	3.12E-01	8.89E-01	1.38E+00	1.38E+00	3.43E+01	2.48E+01
TRAV8-3	3.13E-01	8.89E-01	1.24E+00	1.24E+00	4.31E+01	3.48E+01
THEMIS	3.16E-01	8.93E-01	1.38E+00	1.38E+00	9.25E+02	6.72E+02
TRAV1-1	3.19E-01	8.95E-01	1.49E+00	1.49E+00	1.58E+01	1.06E+01
RIPK3	3.20E-01	8.95E-01	1.15E+00	1.15E+00	2.67E+02	2.32E+02
RUNX3	3.24E-01	8.96E-01	7.81E-01	-1.28E+00	2.71E+03	3.48E+03
TCF4	3.27E-01	8.99E-01	7.84E-01	-1.28E+00	7.43E+02	9.48E+02
TRBV2	3.29E-01	9.00E-01	1.25E+00	1.25E+00	8.72E+01	7.00E+01
TRBV6-4	3.31E-01	9.00E-01	6.36E-01	-1.57E+00	5.11E+00	8.04E+00
LCP1	3.33E-01	9.00E-01	1.13E+00	1.13E+00	4.91E+04	4.34E+04
TRAV27	3.34E-01	9.00E-01	1.41E+00	1.41E+00	4.21E+01	2.98E+01
DUSP22	3.35E-01	9.00E-01	8.52E-01	-1.17E+00	1.04E+03	1.22E+03
ZBTB7B	3.36E-01	9.00E-01	1.17E+00	1.17E+00	4.97E+02	4.24E+02
ATP7A	3.41E-01	9.04E-01	8.31E-01	-1.20E+00	2.03E+02	2.44E+02
STAT3	3.41E-01	9.04E-01	1.12E+00	1.12E+00	5.01E+03	4.47E+03
PRKCQ	3.44E-01	9.04E-01	8.80E-01	-1.14E+00	4.91E+02	5.58E+02
PIK3CG	3.44E-01	9.05E-01	8.90E-01	-1.12E+00	1.45E+03	1.63E+03
TRAV8-2	3.44E-01	9.05E-01	1.33E+00	1.33E+00	4.91E+01	3.69E+01
CD86	3.47E-01	9.06E-01	1.18E+00	1.18E+00	2.60E+03	2.20E+03
CD7	3.48E-01	9.06E-01	8.22E-01	-1.22E+00	1.17E+03	1.42E+03
CARD11	3.49E-01	9.06E-01	7.79E-01	-1.28E+00	4.08E+02	5.23E+02
HFE	3.49E-01	9.06E-01	1.19E+00	1.19E+00	1.44E+02	1.21E+02
NFKBIZ	3.53E-01	9.06E-01	6.95E-01	-1.44E+00	1.61E+03	2.31E+03
LILRB4	3.54E-01	9.06E-01	1.17E+00	1.17E+00	6.83E+02	5.83E+02
AHR	3.56E-01	9.07E-01	1.22E+00	1.22E+00	1.31E+03	1.08E+03
HMGB1	3.59E-01	9.07E-01	9.00E-01	-1.11E+00	7.27E+03	8.08E+03
HLA-F	3.62E-01	9.07E-01	8.88E-01	-1.13E+00	2.99E+03	3.37E+03
DLG1	3.62E-01	9.07E-01	8.39E-01	-1.19E+00	3.88E+02	4.62E+02
EGR1	3.63E-01	9.07E-01	1.88E+00	1.88E+00	3.41E+03	1.81E+03
MAFB	3.65E-01	9.07E-01	1.33E+00	1.33E+00	5.10E+03	3.85E+03
IL18	3.67E-01	9.08E-01	8.47E-01	-1.18E+00	1.22E+02	1.44E+02
PKNOX1	3.70E-01	9.08E-01	8.64E-01	-1.16E+00	2.77E+02	3.21E+02
FZD5	3.70E-01	9.08E-01	1.35E+00	1.35E+00	2.73E+01	2.02E+01
PSEN1	3.71E-01	9.08E-01	1.10E+00	1.10E+00	2.37E+03	2.16E+03
VAV1	3.75E-01	9.09E-01	1.16E+00	1.16E+00	6.55E+02	5.67E+02
IL1R1	3.75E-01	9.09E-01	7.12E-01	-1.40E+00	4.99E+01	7.00E+01
SOCS1	3.77E-01	9.09E-01	6.07E-01	-1.65E+00	2.03E+02	3.35E+02
TRAV3	3.77E-01	9.09E-01	1.29E+00	1.29E+00	8.95E+01	6.94E+01
IL15	3.77E-01	9.09E-01	1.17E+00	1.17E+00	3.81E+02	3.27E+02
TP53	3.78E-01	9.09E-01	1.11E+00	1.11E+00	7.25E+02	6.54E+02

TLE4	3.78E-01	9.09E-01	9.16E-01	-1.09E+00	1.21E+03	1.32E+03
ADAM17	3.80E-01	9.09E-01	1.12E+00	1.12E+00	8.39E+02	7.50E+02
RAB27A	3.83E-01	9.09E-01	1.12E+00	1.12E+00	3.27E+03	2.93E+03
ABL1	3.85E-01	9.10E-01	8.75E-01	-1.14E+00	2.43E+02	2.78E+02
KLRC1	3.87E-01	9.10E-01	7.57E-01	-1.32E+00	2.57E+02	3.40E+02
HLA-E	3.89E-01	9.10E-01	9.07E-01	-1.10E+00	4.96E+04	5.47E+04
PRR7	3.91E-01	9.10E-01	8.19E-01	-1.22E+00	7.67E+01	9.36E+01
SLC4A2	3.94E-01	9.10E-01	1.22E+00	1.22E+00	3.94E+02	3.23E+02
PSMB10	3.95E-01	9.11E-01	1.10E+00	1.10E+00	3.55E+03	3.23E+03
HSH2D	4.00E-01	9.12E-01	8.24E-01	-1.21E+00	5.84E+02	7.10E+02
SH2D2A	4.02E-01	9.13E-01	7.89E-01	-1.27E+00	3.91E+02	4.95E+02
P2RX7	4.02E-01	9.13E-01	1.22E+00	1.22E+00	5.37E+02	4.41E+02
TRBV6-5	4.04E-01	9.13E-01	1.21E+00	1.21E+00	6.96E+01	5.75E+01
TRAV2	4.11E-01	9.15E-01	1.39E+00	1.39E+00	5.01E+01	3.62E+01
FYN	4.15E-01	9.16E-01	8.81E-01	-1.13E+00	4.71E+03	5.35E+03
HLA-DRA	4.18E-01	9.16E-01	1.15E+00	1.15E+00	4.39E+04	3.81E+04
HLX	4.22E-01	9.17E-01	1.17E+00	1.17E+00	3.73E+02	3.19E+02
TRAV13-1	4.33E-01	9.19E-01	1.15E+00	1.15E+00	1.27E+02	1.10E+02
BCL9L	4.33E-01	9.19E-01	1.32E+00	1.32E+00	6.75E+01	5.12E+01
ZP3	4.34E-01	9.19E-01	8.20E-01	-1.22E+00	4.91E+01	5.99E+01
JAML	4.44E-01	9.22E-01	1.14E+00	1.14E+00	7.55E+03	6.63E+03
NKG7	4.48E-01	9.22E-01	8.13E-01	-1.23E+00	4.91E+03	6.04E+03
SPN	4.53E-01	9.22E-01	1.10E+00	1.10E+00	3.04E+03	2.75E+03
EBI3	4.57E-01	9.22E-01	1.39E+00	1.39E+00	2.66E+01	1.91E+01
TRAT1	4.60E-01	9.22E-01	1.21E+00	1.21E+00	1.24E+03	1.02E+03
STAT5B	4.61E-01	9.22E-01	8.89E-01	-1.12E+00	2.08E+03	2.33E+03
TRBV11-3	4.62E-01	9.22E-01	6.89E-01	-1.45E+00	6.38E+00	9.25E+00
CORO1A	4.63E-01	9.22E-01	1.07E+00	1.07E+00	1.67E+04	1.56E+04
TRBV12-5	4.64E-01	9.22E-01	6.80E-01	-1.47E+00	4.37E+00	6.43E+00
WDFY4	4.65E-01	9.22E-01	8.74E-01	-1.14E+00	3.35E+02	3.84E+02
TRAV23DV6	4.72E-01	9.24E-01	1.33E+00	1.33E+00	6.44E+01	4.85E+01
TRBV5-5	4.79E-01	9.26E-01	7.46E-01	-1.34E+00	1.94E+01	2.60E+01
CRK	4.84E-01	9.27E-01	1.10E+00	1.10E+00	7.72E+02	6.99E+02
SRF	4.87E-01	9.27E-01	1.10E+00	1.10E+00	2.83E+02	2.57E+02
CD46	4.89E-01	9.27E-01	9.06E-01	-1.10E+00	4.26E+03	4.70E+03
CCR9	4.93E-01	9.29E-01	7.11E-01	-1.41E+00	6.14E+01	8.64E+01
RUNX2	4.95E-01	9.30E-01	8.65E-01	-1.16E+00	3.29E+02	3.80E+02
TNFRSF1B	4.98E-01	9.32E-01	1.11E+00	1.11E+00	1.34E+04	1.21E+04
HES1	5.02E-01	9.33E-01	7.99E-01	-1.25E+00	1.77E+01	2.21E+01

PPP3CA	5.05E-01	9.33E-01	9.36E-01	-1.07E+00	8.51E+02	9.09E+02
TRBV7-6	5.06E-01	9.33E-01	7.79E-01	-1.28E+00	1.95E+01	2.51E+01
LILRB2	5.08E-01	9.33E-01	1.08E+00	1.08E+00	3.49E+03	3.24E+03
MEN1	5.11E-01	9.33E-01	1.08E+00	1.08E+00	4.90E+02	4.53E+02
CLEC4D	5.12E-01	9.33E-01	1.11E+00	1.11E+00	8.56E+02	7.69E+02
STOML2	5.12E-01	9.33E-01	1.10E+00	1.10E+00	6.72E+02	6.13E+02
IKZF3	5.14E-01	9.34E-01	8.87E-01	-1.13E+00	1.33E+03	1.50E+03
CRKL	5.14E-01	9.34E-01	1.08E+00	1.08E+00	1.67E+03	1.54E+03
HAVCR2	5.16E-01	9.34E-01	8.98E-01	-1.11E+00	8.52E+02	9.49E+02
LY9	5.16E-01	9.34E-01	9.04E-01	-1.11E+00	7.79E+02	8.62E+02
MSN	5.17E-01	9.34E-01	1.07E+00	1.07E+00	2.10E+04	1.95E+04
IL4R	5.17E-01	9.34E-01	8.75E-01	-1.14E+00	1.12E+03	1.28E+03
TRAV6	5.19E-01	9.35E-01	1.23E+00	1.23E+00	4.11E+01	3.33E+01
WAS	5.21E-01	9.36E-01	1.07E+00	1.07E+00	1.29E+03	1.20E+03
TGFBR2	5.30E-01	9.39E-01	9.07E-01	-1.10E+00	2.53E+03	2.79E+03
BTN3A1	5.39E-01	9.43E-01	1.14E+00	1.14E+00	1.33E+03	1.16E+03
RAB29	5.43E-01	9.43E-01	9.27E-01	-1.08E+00	1.62E+03	1.75E+03
TRAV24	5.50E-01	9.45E-01	1.39E+00	1.39E+00	4.14E+01	2.97E+01
TRBV5-4	5.54E-01	9.46E-01	1.20E+00	1.20E+00	6.83E+01	5.71E+01
PATZ1	5.55E-01	9.46E-01	1.13E+00	1.13E+00	3.19E+02	2.83E+02
F11R	5.56E-01	9.47E-01	1.09E+00	1.09E+00	1.49E+03	1.36E+03
TRAV12-1	5.59E-01	9.47E-01	1.20E+00	1.20E+00	4.15E+01	3.45E+01
STAT6	5.59E-01	9.47E-01	1.07E+00	1.07E+00	2.95E+03	2.75E+03
CD1A	5.63E-01	9.47E-01	8.44E-01	-1.18E+00	6.00E+01	7.10E+01
DDOST	5.64E-01	9.47E-01	1.05E+00	1.05E+00	3.96E+03	3.79E+03
CLEC4A	5.65E-01	9.47E-01	1.13E+00	1.13E+00	1.32E+03	1.18E+03
PVR	5.67E-01	9.47E-01	8.92E-01	-1.12E+00	1.37E+02	1.54E+02
ATF2	5.67E-01	9.48E-01	1.10E+00	1.10E+00	7.99E+02	7.29E+02
PELI1	5.68E-01	9.48E-01	8.51E-01	-1.18E+00	1.29E+03	1.51E+03
NLRC3	5.70E-01	9.48E-01	8.43E-01	-1.19E+00	3.28E+02	3.89E+02
TRAV38-2DV8	5.71E-01	9.48E-01	7.86E-01	-1.27E+00	4.92E+01	6.26E+01
EFNB1	5.71E-01	9.48E-01	8.84E-01	-1.13E+00	1.33E+02	1.50E+02
IL23A	5.73E-01	9.48E-01	8.40E-01	-1.19E+00	3.85E+01	4.58E+01
CADM1	5.77E-01	9.48E-01	8.65E-01	-1.16E+00	6.34E+01	7.33E+01
TRAV22	5.77E-01	9.48E-01	7.83E-01	-1.28E+00	2.26E+01	2.89E+01
TRPM4	5.83E-01	9.50E-01	8.48E-01	-1.18E+00	3.19E+01	3.77E+01
TRAV19	5.91E-01	9.50E-01	1.22E+00	1.22E+00	3.49E+01	2.86E+01
ZC3H12A	5.91E-01	9.50E-01	1.19E+00	1.19E+00	2.28E+02	1.92E+02
NOD2	5.97E-01	9.50E-01	1.14E+00	1.14E+00	5.29E+02	4.65E+02
TRAV26-1	6.01E-01	9.52E-01	8.47E-01	-1.18E+00	4.36E+01	5.15E+01

SLA2	6.03E-01	9.53E-01	9.09E-01	-1.10E+00	3.74E+02	4.12E+02
RHOH	6.04E-01	9.53E-01	9.22E-01	-1.08E+00	1.38E+03	1.50E+03
CD3G	6.04E-01	9.53E-01	1.11E+00	1.11E+00	3.31E+03	2.99E+03
TRBV19	6.08E-01	9.54E-01	8.57E-01	-1.17E+00	1.77E+02	2.07E+02
TNFSF14	6.10E-01	9.55E-01	8.49E-01	-1.18E+00	1.53E+02	1.80E+02
TRBV24-1	6.11E-01	9.55E-01	8.59E-01	-1.16E+00	4.15E+01	4.83E+01
TRAV4	6.12E-01	9.55E-01	8.88E-01	-1.13E+00	5.91E+01	6.66E+01
TRAV29DV5	6.12E-01	9.55E-01	1.17E+00	1.17E+00	1.32E+02	1.13E+02
CTSL	6.12E-01	9.55E-01	1.10E+00	1.10E+00	7.06E+02	6.44E+02
TRBV7-2	6.15E-01	9.55E-01	8.66E-01	-1.16E+00	1.64E+02	1.89E+02
BCL6	6.18E-01	9.56E-01	1.09E+00	1.09E+00	8.60E+02	7.91E+02
TRAV10	6.22E-01	9.56E-01	8.44E-01	-1.19E+00	2.34E+01	2.78E+01
TRBV7-3	6.27E-01	9.56E-01	8.36E-01	-1.20E+00	3.33E+01	3.99E+01
APBB1IP	6.28E-01	9.56E-01	1.07E+00	1.07E+00	1.98E+03	1.86E+03
TRAV21	6.28E-01	9.56E-01	1.21E+00	1.21E+00	1.01E+02	8.39E+01
RPS6	6.28E-01	9.56E-01	9.12E-01	-1.10E+00	1.26E+04	1.38E+04
SLAMF6	6.29E-01	9.56E-01	8.91E-01	-1.12E+00	1.41E+03	1.59E+03
KIF13B	6.38E-01	9.56E-01	1.08E+00	1.08E+00	1.83E+02	1.69E+02
TRGV10	6.38E-01	9.56E-01	8.16E-01	-1.23E+00	3.56E+01	4.37E+01
TNFSF8	6.38E-01	9.56E-01	8.82E-01	-1.13E+00	1.12E+03	1.27E+03
TRGV2	6.38E-01	9.56E-01	1.28E+00	1.28E+00	8.06E+01	6.32E+01
SLAMF7	6.40E-01	9.56E-01	1.12E+00	1.12E+00	2.00E+03	1.78E+03
MFAP3	6.43E-01	9.57E-01	9.15E-01	-1.09E+00	1.97E+02	2.15E+02
KAT7	6.44E-01	9.57E-01	1.07E+00	1.07E+00	8.52E+02	7.97E+02
TRGV3	6.46E-01	9.58E-01	1.20E+00	1.20E+00	4.12E+01	3.43E+01
DOCK8	6.47E-01	9.58E-01	1.07E+00	1.07E+00	3.24E+03	3.01E+03
NFKBID	6.49E-01	9.58E-01	8.60E-01	-1.16E+00	8.95E+01	1.04E+02
TRAV12-2	6.49E-01	9.58E-01	1.14E+00	1.14E+00	1.02E+02	8.91E+01
TRBV6-2	6.54E-01	9.59E-01	8.56E-01	-1.17E+00	5.99E+01	7.00E+01
LGALS3	6.58E-01	9.60E-01	1.10E+00	1.10E+00	3.61E+03	3.29E+03
RORA	6.59E-01	9.61E-01	8.97E-01	-1.11E+00	5.04E+02	5.62E+02
MYB	6.62E-01	9.61E-01	8.66E-01	-1.15E+00	1.03E+02	1.19E+02
DPP4	6.66E-01	9.61E-01	1.13E+00	1.13E+00	6.16E+02	5.47E+02
LOXL3	6.68E-01	9.61E-01	9.11E-01	-1.10E+00	1.99E+02	2.19E+02
CCR6	6.70E-01	9.61E-01	1.07E+00	1.07E+00	4.56E+02	4.27E+02
CD2	6.70E-01	9.61E-01	1.08E+00	1.08E+00	3.12E+03	2.87E+03
TRBV4-2	6.71E-01	9.61E-01	1.20E+00	1.20E+00	9.92E+01	8.28E+01
CCND3	6.71E-01	9.61E-01	9.39E-01	-1.06E+00	7.80E+03	8.31E+03
TAP2	6.76E-01	9.62E-01	9.51E-01	-1.05E+00	7.66E+02	8.06E+02
LCK	6.76E-01	9.62E-01	1.08E+00	1.08E+00	4.20E+03	3.89E+03

RC3H1	6.78E-01	9.63E-01	9.14E-01	-1.09E+00	8.18E+02	8.96E+02
DOCK2	6.78E-01	9.63E-01	9.41E-01	-1.06E+00	2.89E+03	3.07E+03
SCRIB	6.86E-01	9.65E-01	1.08E+00	1.08E+00	7.12E+01	6.59E+01
SOX13	6.88E-01	9.66E-01	8.54E-01	-1.17E+00	2.90E+01	3.40E+01
HLA-A	6.95E-01	9.69E-01	1.05E+00	1.05E+00	4.89E+04	4.67E+04
MYH9	6.98E-01	9.69E-01	1.07E+00	1.07E+00	8.69E+03	8.15E+03
CLEC4G	7.00E-01	9.70E-01	1.14E+00	1.14E+00	5.25E+01	4.62E+01
NHEJ1	7.04E-01	9.70E-01	9.35E-01	-1.07E+00	3.12E+02	3.34E+02
RASGRP 1	7.05E-01	9.70E-01	1.08E+00	1.08E+00	1.03E+03	9.58E+02
FOXP3	7.07E-01	9.70E-01	1.11E+00	1.11E+00	1.13E+02	1.02E+02
SOCS5	7.11E-01	9.70E-01	9.17E-01	-1.09E+00	1.49E+02	1.62E+02
TRBV9	7.12E-01	9.70E-01	1.12E+00	1.12E+00	9.47E+01	8.47E+01
LFNG	7.16E-01	9.71E-01	9.19E-01	-1.09E+00	2.93E+02	3.19E+02
FCGR2B	7.17E-01	9.71E-01	9.19E-01	-1.09E+00	6.04E+02	6.57E+02
RIPK2	7.21E-01	9.73E-01	9.23E-01	-1.08E+00	6.64E+02	7.20E+02
CD1D	7.22E-01	9.73E-01	9.33E-01	-1.07E+00	1.69E+03	1.81E+03
F2RL1	7.22E-01	9.73E-01	9.04E-01	-1.11E+00	2.73E+02	3.02E+02
B2M	7.25E-01	9.73E-01	1.05E+00	1.05E+00	4.73E+05	4.52E+05
MALT1	7.27E-01	9.74E-01	9.49E-01	-1.05E+00	1.12E+03	1.18E+03
PTPRC	7.27E-01	9.74E-01	1.05E+00	1.05E+00	2.92E+04	2.78E+04
NDFIP1	7.29E-01	9.74E-01	9.51E-01	-1.05E+00	2.72E+03	2.86E+03
CD84	7.31E-01	9.75E-01	1.05E+00	1.05E+00	1.07E+03	1.02E+03
TCF7L2	7.32E-01	9.75E-01	9.28E-01	-1.08E+00	4.46E+02	4.80E+02
SYK	7.32E-01	9.75E-01	1.04E+00	1.04E+00	4.84E+03	4.64E+03
FOXP1	7.35E-01	9.76E-01	9.34E-01	-1.07E+00	3.94E+03	4.21E+03
IL12RB1	7.36E-01	9.76E-01	9.53E-01	-1.05E+00	5.13E+02	5.38E+02
BATF	7.39E-01	9.76E-01	1.06E+00	1.06E+00	2.69E+02	2.53E+02
HLA-B	7.39E-01	9.76E-01	9.49E-01	-1.05E+00	8.13E+04	8.56E+04
PRDX2	7.42E-01	9.76E-01	1.09E+00	1.09E+00	1.57E+03	1.44E+03
HLA-G	7.42E-01	9.76E-01	1.11E+00	1.11E+00	1.88E+02	1.69E+02
GPR89B	7.46E-01	9.76E-01	9.40E-01	-1.06E+00	1.37E+02	1.46E+02
ANXA1	7.46E-01	9.76E-01	9.47E-01	-1.06E+00	1.34E+04	1.42E+04
CD74	7.47E-01	9.76E-01	1.05E+00	1.05E+00	9.65E+04	9.17E+04
TRBV18	7.47E-01	9.76E-01	9.27E-01	-1.08E+00	7.28E+01	7.85E+01
TRGV8	7.48E-01	9.76E-01	8.57E-01	-1.17E+00	1.99E+01	2.32E+01
IL2RG	7.53E-01	9.76E-01	1.05E+00	1.05E+00	9.82E+03	9.38E+03
TRBV7-9	7.53E-01	9.76E-01	1.09E+00	1.09E+00	1.26E+02	1.16E+02
RORC	7.53E-01	9.76E-01	1.13E+00	1.13E+00	6.28E+01	5.56E+01
GBA	7.55E-01	9.76E-01	1.04E+00	1.04E+00	9.02E+02	8.70E+02
SLAMF1	7.55E-01	9.76E-01	9.31E-01	-1.07E+00	1.78E+02	1.91E+02
SASH3	7.59E-01	9.76E-01	1.03E+00	1.03E+00	4.43E+03	4.29E+03
LEPR	7.65E-01	9.77E-01	9.29E-01	-1.08E+00	1.45E+02	1.56E+02

TRBV3-1	7.65E-01	9.77E-01	9.14E-01	-1.09E+00	9.31E+01	1.02E+02
GATA3	7.67E-01	9.77E-01	9.37E-01	-1.07E+00	7.29E+02	7.78E+02
CD8B	7.71E-01	9.78E-01	1.06E+00	1.06E+00	1.24E+03	1.17E+03
PYGO2	7.75E-01	9.79E-01	1.04E+00	1.04E+00	6.01E+02	5.77E+02
MTOR	7.81E-01	9.82E-01	9.55E-01	-1.05E+00	2.47E+02	2.59E+02
CD8A	7.82E-01	9.82E-01	9.45E-01	-1.06E+00	1.89E+03	2.00E+03
NECTIN2	7.83E-01	9.82E-01	8.94E-01	-1.12E+00	1.55E+02	1.73E+02
GPR18	7.85E-01	9.82E-01	1.07E+00	1.07E+00	1.91E+02	1.78E+02
PIK3R2	7.87E-01	9.82E-01	1.04E+00	1.04E+00	2.42E+02	2.32E+02
FKBP1B	7.91E-01	9.83E-01	9.26E-01	-1.08E+00	9.41E+01	1.02E+02
TRBV29-1	7.91E-01	9.83E-01	1.07E+00	1.07E+00	5.07E+01	4.75E+01
TRBV13	7.95E-01	9.83E-01	8.79E-01	-1.14E+00	1.28E+01	1.45E+01
ELF4	7.98E-01	9.83E-01	1.04E+00	1.04E+00	7.63E+02	7.32E+02
IL7	8.01E-01	9.83E-01	1.09E+00	1.09E+00	6.66E+01	6.13E+01
CEACAM21	8.02E-01	9.83E-01	9.41E-01	-1.06E+00	2.04E+02	2.17E+02
TRAF6	8.02E-01	9.83E-01	9.53E-01	-1.05E+00	2.58E+02	2.71E+02
SMAD7	8.03E-01	9.83E-01	9.25E-01	-1.08E+00	1.38E+02	1.49E+02
ZBTB1	8.03E-01	9.83E-01	1.04E+00	1.04E+00	1.07E+03	1.03E+03
SP3	8.14E-01	9.85E-01	9.75E-01	-1.03E+00	1.66E+03	1.70E+03
FUT7	8.16E-01	9.85E-01	9.52E-01	-1.05E+00	3.19E+02	3.35E+02
CYRIB	8.19E-01	9.85E-01	1.03E+00	1.03E+00	6.47E+03	6.30E+03
TRBV6-1	8.19E-01	9.85E-01	1.08E+00	1.08E+00	4.68E+01	4.35E+01
PTPN6	8.22E-01	9.85E-01	1.03E+00	1.03E+00	6.66E+03	6.49E+03
TCF7	8.23E-01	9.85E-01	1.06E+00	1.06E+00	3.66E+03	3.46E+03
BRAF	8.25E-01	9.85E-01	9.69E-01	-1.03E+00	3.32E+02	3.42E+02
MAP3K7	8.25E-01	9.85E-01	1.03E+00	1.03E+00	9.58E+02	9.28E+02
STK11	8.26E-01	9.85E-01	1.02E+00	1.02E+00	8.55E+02	8.35E+02
SHB	8.31E-01	9.85E-01	9.13E-01	-1.10E+00	1.01E+01	1.11E+01
TRBV5-1	8.31E-01	9.85E-01	1.04E+00	1.04E+00	1.72E+02	1.65E+02
BCL11B	8.32E-01	9.85E-01	1.05E+00	1.05E+00	8.63E+02	8.21E+02
PDE5A	8.33E-01	9.85E-01	9.28E-01	-1.08E+00	3.10E+02	3.34E+02
NCK1	8.33E-01	9.85E-01	1.03E+00	1.03E+00	1.01E+03	9.76E+02
IFNG	8.37E-01	9.86E-01	9.08E-01	-1.10E+00	2.96E+01	3.26E+01
TCIRG1	8.39E-01	9.86E-01	1.02E+00	1.02E+00	2.69E+03	2.64E+03
SPI1	8.40E-01	9.86E-01	1.03E+00	1.03E+00	4.18E+03	4.07E+03
TRBV12-4	8.41E-01	9.86E-01	9.06E-01	-1.10E+00	1.17E+02	1.29E+02
DENND1B	8.45E-01	9.86E-01	9.72E-01	-1.03E+00	4.49E+02	4.62E+02
ITCH	8.46E-01	9.86E-01	1.04E+00	1.04E+00	5.99E+02	5.77E+02
KMT2A	8.49E-01	9.88E-01	1.03E+00	1.03E+00	1.22E+03	1.19E+03
CDK6	8.51E-01	9.88E-01	1.03E+00	1.03E+00	3.97E+02	3.84E+02

GPR183	8.52E-01	9.88E-01	1.04E+00	1.04E+00	3.02E+03	2.92E+03
TRAV9-2	8.53E-01	9.88E-01	1.05E+00	1.05E+00	6.49E+01	6.16E+01
HLA-C	8.55E-01	9.88E-01	9.73E-01	-1.03E+00	4.97E+04	5.11E+04
JMJD6	8.56E-01	9.88E-01	1.03E+00	1.03E+00	4.61E+02	4.49E+02
CD3E	8.56E-01	9.88E-01	1.04E+00	1.04E+00	4.14E+03	3.99E+03
LEF1	8.63E-01	9.89E-01	1.05E+00	1.05E+00	2.91E+03	2.77E+03
TRAV14DV4	8.65E-01	9.89E-01	1.05E+00	1.05E+00	4.64E+01	4.41E+01
LAG3	8.67E-01	9.90E-01	1.07E+00	1.07E+00	2.06E+02	1.93E+02
NCSTN	8.68E-01	9.90E-01	1.02E+00	1.02E+00	2.48E+03	2.42E+03
TRBV12-3	8.73E-01	9.91E-01	1.04E+00	1.04E+00	1.27E+02	1.22E+02
TRAV41	8.73E-01	9.91E-01	9.39E-01	-1.06E+00	2.36E+01	2.52E+01
CD3D	8.77E-01	9.92E-01	9.68E-01	-1.03E+00	2.63E+03	2.71E+03
TRAF3IP2	8.78E-01	9.92E-01	9.65E-01	-1.04E+00	1.27E+02	1.32E+02
NKAP	8.79E-01	9.92E-01	1.02E+00	1.02E+00	4.28E+02	4.21E+02
PPP3CB	8.85E-01	9.92E-01	1.02E+00	1.02E+00	4.71E+02	4.61E+02
LAT	8.91E-01	9.92E-01	1.02E+00	1.02E+00	1.58E+03	1.55E+03
ADA	8.94E-01	9.93E-01	9.78E-01	-1.02E+00	5.97E+02	6.10E+02
LMBR1L	8.96E-01	9.93E-01	9.79E-01	-1.02E+00	3.73E+02	3.81E+02
RPL22	8.98E-01	9.93E-01	9.80E-01	-1.02E+00	2.19E+03	2.24E+03
CTPS1	9.00E-01	9.93E-01	9.77E-01	-1.02E+00	1.80E+02	1.84E+02
EPS8L1	9.00E-01	9.93E-01	1.06E+00	1.06E+00	1.75E+01	1.65E+01
TRAV26-2	9.01E-01	9.93E-01	1.06E+00	1.06E+00	1.87E+01	1.77E+01
MR1	9.01E-01	9.93E-01	1.02E+00	1.02E+00	1.12E+03	1.10E+03
SELENOK	9.04E-01	9.93E-01	1.02E+00	1.02E+00	1.45E+03	1.42E+03
DTX1	9.07E-01	9.93E-01	9.71E-01	-1.03E+00	5.89E+01	6.07E+01
ITPKB	9.10E-01	9.94E-01	9.78E-01	-1.02E+00	8.05E+02	8.23E+02
PIK3R1	9.10E-01	9.94E-01	1.03E+00	1.03E+00	1.88E+03	1.82E+03
TRBV5-6	9.10E-01	9.94E-01	9.63E-01	-1.04E+00	3.48E+01	3.62E+01
BCL2	9.14E-01	9.94E-01	1.03E+00	1.03E+00	8.01E+02	7.74E+02
DNAJA3	9.16E-01	9.94E-01	9.85E-01	-1.02E+00	4.42E+02	4.49E+02
IL7R	9.19E-01	9.95E-01	1.03E+00	1.03E+00	5.36E+03	5.20E+03
TRBV25-1	9.21E-01	9.95E-01	1.05E+00	1.05E+00	2.27E+01	2.17E+01
TRAV12-3	9.30E-01	9.96E-01	1.04E+00	1.04E+00	5.96E+01	5.74E+01
TRAV20	9.32E-01	9.96E-01	1.03E+00	1.03E+00	4.42E+01	4.30E+01
IL1B	9.40E-01	9.96E-01	9.54E-01	-1.05E+00	6.58E+02	6.90E+02
PIK3CD	9.45E-01	9.96E-01	9.87E-01	-1.01E+00	2.32E+03	2.35E+03
TSPAN32	9.56E-01	9.97E-01	9.89E-01	-1.01E+00	2.94E+02	2.97E+02

TSC1	9.59E-01	9.97E-01	9.85E-01	-1.02E+00	2.08E+02	2.11E+02
ITGAL	9.62E-01	9.97E-01	9.91E-01	-1.01E+00	3.46E+03	3.49E+03
IL6R	9.66E-01	9.97E-01	1.01E+00	1.01E+00	2.21E+03	2.19E+03
CD81	9.66E-01	9.97E-01	1.01E+00	1.01E+00	1.33E+03	1.32E+03
IDO1	9.67E-01	9.97E-01	9.84E-01	-1.02E+00	5.50E+01	5.59E+01
TRBV6-6	9.78E-01	9.98E-01	1.01E+00	1.01E+00	3.44E+01	3.42E+01
TLE3	9.78E-01	9.99E-01	1.00E+00	1.00E+00	8.34E+02	8.30E+02
TRAV39	9.79E-01	9.99E-01	1.01E+00	1.01E+00	1.10E+01	1.09E+01
LDB1	9.79E-01	9.99E-01	9.97E-01	-1.00E+00	3.63E+02	3.64E+02
CLC	9.85E-01	9.99E-01	1.01E+00	1.01E+00	1.02E+03	1.01E+03
TRAV17	9.92E-01	9.99E-01	1.00E+00	1.00E+00	9.79E+01	9.77E+01
TESPA1	9.94E-01	9.99E-01	1.00E+00	1.00E+00	8.40E+02	8.38E+02
TRAV16	9.95E-01	1.00E+00	9.97E-01	-1.00E+00	1.73E+01	1.73E+01
PTPN22	9.97E-01	1.00E+00	9.99E-01	-1.00E+00	9.96E+02	9.96E+02
BAX	9.98E-01	1.00E+00	1.00E+00	1.00E+00	1.03E+03	1.03E+03

13.8 DIFFERENTIAL GENE EXPRESSION BASED ON STIMULATION AND OPERATION STATUS

Gene name	P-value (Post-stimulation ,Postoperative vs Post-stimulation ,Preoperative)	FDR step up (Post-stimulation ,Postoperative vs Post-stimulation ,Preoperative)	Ratio (Post-stimulation ,Postoperative vs Post-stimulation ,Preoperative)	Fold change (Post-stimulation ,Postoperative vs Post-stimulation ,Preoperative)	LSMean(Post-stimulation, Postoperative) (Post-stimulation, Postoperative vs Post-stimulation, Preoperative)	LSMean(Post-stimulation ,Preoperative) (Post-stimulation ,Postoperative vs Post-stimulation ,Preoperative)	Shrunken Log2(Ratio) (Post-stimulation ,Postoperative vs Post-stimulation ,Preoperative)
CORO7	6.95E-09	5.82E-05	2.33E+00	2.33E+00	1.01E+03	4.32E+02	1.07E+00
CPB2-AS1	7.80E-09	5.82E-05	2.36E+00	2.36E+00	5.00E+02	2.12E+02	1.08E+00
LCP1	1.98E-08	9.85E-05	1.87E+00	1.87E+00	4.25E+04	2.28E+04	7.00E-01
SLC36A1	7.57E-08	2.38E-04	3.70E+00	3.70E+00	1.30E+02	3.52E+01	1.62E+00
KDM	7.97E-08	2.38E-04	2.74E+00	2.74E+00	5.67E+02	2.07E+02	1.24E+00

3A							
CDKN2B	6.31E-07	1.57E-03	1.22E+01	1.22E+01	4.20E+01	3.45E+00	2.48E+00
ARHGEF6	7.36E-07	1.57E-03	1.83E+00	1.83E+00	2.38E+03	1.30E+03	6.08E-01
NRBP2	1.25E-06	1.73E-03	7.54E+00	7.54E+00	4.13E+01	5.47E+00	2.10E+00
SCCPDH	1.30E-06	1.73E-03	4.24E-01	-2.36E+00	3.52E+02	8.31E+02	-8.93E-01
LIME1	1.33E-06	1.73E-03	2.03E+00	2.03E+00	1.27E+03	6.27E+02	6.99E-01
MSNP1	1.34E-06	1.73E-03	2.81E+00	2.81E+00	2.47E+02	8.79E+01	1.12E+00
CCR2	1.39E-06	1.73E-03	5.97E+00	5.97E+00	8.55E+02	1.43E+02	1.91E+00
TRAPPC11	1.71E-06	1.97E-03	2.59E+00	2.59E+00	4.94E+02	1.91E+02	9.97E-01
IATPR	2.38E-06	2.53E-03	1.32E+01	1.32E+01	5.18E+01	3.93E+00	2.10E+00
PELI2	2.85E-06	2.83E-03	5.85E+00	5.85E+00	3.58E+01	6.12E+00	1.76E+00
ZDHHC14	4.83E-06	4.23E-03	3.41E-01	-2.94E+00	4.59E+01	1.35E+02	-1.05E+00
BATF3	5.28E-06	4.23E-03	3.78E-01	-2.64E+00	5.49E+02	1.45E+03	-9.29E-01
CD70	5.30E-06	4.23E-03	3.97E-01	-2.52E+00	3.09E+02	7.79E+02	-8.75E-01
SEC31A	5.41E-06	4.23E-03	1.65E+00	1.65E+00	1.90E+03	1.16E+03	4.85E-01
SAMHD1	5.67E-06	4.23E-03	2.12E+00	2.12E+00	4.66E+03	2.20E+03	6.79E-01
GLG1	5.99E-06	4.25E-03	1.90E+00	1.90E+00	2.02E+03	1.06E+03	5.79E-01
RGS16	7.04E-06	4.77E-03	2.57E-01	-3.89E+00	1.26E+02	4.90E+02	-1.27E+00
PALLD	8.84E-06	5.74E-03	1.32E-01	-7.58E+00	1.68E+01	1.28E+02	-1.57E+00
---	1.08E-05	6.29E-03	3.10E-01	-3.23E+00	8.82E+01	2.84E+02	-1.04E+00
TRIB2	1.09E-05	6.29E-03	3.79E+00	3.79E+00	3.12E+02	8.25E+01	1.17E+00
NNT	1.10E-05	6.29E-03	1.92E+00	1.92E+00	1.55E+03	8.07E+02	5.65E-01
---	1.51E-05	7.99E-03	4.02E+00	4.02E+00	4.23E+01	1.05E+01	1.14E+00
MAP3K5	1.54E-05	7.99E-03	2.29E+00	2.29E+00	5.65E+02	2.47E+02	6.86E-01

VOPP1	1.55E-05	7.99E-03	5.95E-01	-1.68E+00	9.85E+02	1.66E+03	-4.74E-01
RPS6KA3	1.68E-05	8.36E-03	1.78E+00	1.78E+00	1.81E+03	1.02E+03	5.03E-01
ZNF554	1.85E-05	8.91E-03	5.67E+00	5.67E+00	5.33E+01	9.39E+00	1.25E+00
MSN	2.39E-05	1.10E-02	1.79E+00	1.79E+00	1.22E+04	6.82E+03	4.94E-01
TRAF4	2.44E-05	1.10E-02	3.87E-01	-2.59E+00	2.31E+02	5.97E+02	-7.46E-01
SREBF1	2.64E-05	1.16E-02	2.17E+00	2.17E+00	7.76E+02	3.58E+02	6.06E-01
ACTBP2	2.75E-05	1.17E-02	1.68E+00	1.68E+00	7.13E+03	4.25E+03	4.60E-01
MLST8	2.83E-05	1.17E-02	5.33E-01	-1.88E+00	5.38E+02	1.01E+03	-5.13E-01
RBL2	3.29E-05	1.33E-02	2.20E+00	2.20E+00	2.19E+03	9.93E+02	6.01E-01
SELL	3.56E-05	1.40E-02	2.13E+00	2.13E+00	1.65E+04	7.73E+03	5.75E-01
POTEE	3.76E-05	1.42E-02	1.88E+00	1.88E+00	2.85E+03	1.52E+03	5.01E-01
MTMM1	3.80E-05	1.42E-02	1.71E+00	1.71E+00	8.84E+02	5.17E+02	4.59E-01
SPTBN1	3.98E-05	1.45E-02	1.74E+00	1.74E+00	1.91E+03	1.10E+03	4.64E-01
LBR	4.44E-05	1.58E-02	1.98E+00	1.98E+00	7.29E+03	3.68E+03	5.21E-01
FBLN5	5.67E-05	1.97E-02	2.63E+00	2.63E+00	1.88E+02	7.16E+01	6.60E-01
KLF3	5.97E-05	2.02E-02	2.14E+00	2.14E+00	4.72E+02	2.20E+02	5.44E-01
ADAM10	6.14E-05	2.04E-02	1.86E+00	1.86E+00	1.91E+03	1.03E+03	4.78E-01
---	7.03E-05	2.28E-02	7.65E-02	-1.31E+01	9.54E+00	1.25E+02	-6.61E-01
ZNF836	7.62E-05	2.42E-02	3.24E+00	3.24E+00	1.43E+02	4.42E+01	7.12E-01
UBR5-DT	8.05E-05	2.42E-02	1.35E-01	-7.40E+00	6.52E+00	4.83E+01	-7.68E-01
EIF4E3	8.08E-05	2.42E-02	2.00E+00	2.00E+00	2.17E+03	1.08E+03	4.95E-01
EPHA1	8.11E-05	2.42E-02	7.91E+00	7.91E+00	9.12E+01	1.15E+01	7.54E-01
VCL	9.10E-05	2.66E-02	2.49E+00	2.49E+00	4.60E+02	1.84E+02	5.81E-01
TNFSF4	1.19E-04	3.33E-02	3.65E-01	-2.74E+00	1.01E+02	2.77E+02	-5.86E-01
---	1.21E-04	3.33E-02	2.64E+00	2.64E+00	4.87E+01	1.84E+01	5.72E-01
ZBTB10	1.21E-04	3.33E-02	3.48E+00	3.48E+00	9.23E+01	2.65E+01	6.49E-01

ADD3	1.23E-04	3.33E-02	1.92E+00	1.92E+00	3.14E+03	1.64E+03	4.58E-01
NKAP	1.26E-04	3.35E-02	6.22E-01	-1.61E+00	3.48E+02	5.59E+02	-4.05E-01
---	1.33E-04	3.47E-02	2.22E+01	2.22E+01	1.72E+01	7.75E-01	3.66E-01
DGKA	1.39E-04	3.57E-02	1.96E+00	1.96E+00	2.27E+03	1.16E+03	4.60E-01
S1PR1	1.43E-04	3.61E-02	1.70E+00	1.70E+00	2.88E+03	1.70E+03	4.17E-01
ZNF337	1.52E-04	3.73E-02	2.49E+00	2.49E+00	9.94E+01	3.98E+01	5.28E-01
ZBTB14	1.56E-04	3.73E-02	1.82E+00	1.82E+00	4.77E+02	2.63E+02	4.32E-01
TMEM131L	1.57E-04	3.73E-02	2.16E+00	2.16E+00	1.15E+03	5.31E+02	4.81E-01
DHFR2	1.58E-04	3.73E-02	2.04E+00	2.04E+00	2.49E+02	1.22E+02	4.64E-01
ZNF518B	1.76E-04	4.12E-02	2.66E+00	2.66E+00	2.48E+02	9.32E+01	5.31E-01
GZMB	1.91E-04	4.38E-02	2.31E-01	-4.32E+00	3.27E+03	1.41E+04	-5.84E-01
PXN	2.00E-04	4.53E-02	2.18E+00	2.18E+00	9.75E+02	4.48E+02	4.66E-01